UNIVERSITÀ DEGLI STUDI DI PADOVA

UNIVERSITÀ DEGLI STUDI DI PADOVA

SEDE AMMINISTRATIVA: Università degli Studi di Padova

DIPARTIMENTO DI ASTRONOMIA

SCUOLA DI DOTTORATO DI RICERCA IN ASTRONOMIA

Ciclo XXII

Overluminous Core-Collapse Supernovae

Direttore della Scuola: Prof. Giampaolo PIOTTO

Supervisori: Dott. Stefano BENETTI
Dott. Luca ZAMPIERI

Dottoranda:
Irene AGNOLETTO

1 Febbraio 2010

Abstract

This Thesis is focused on a photometric and spectroscopic study of four Type IIn supernovae (i.e. SN 2006gy, 2007bt, 2007bw and 2008fz), which are among the brightest supernovae (SNe) ever detected. They belong to the sample of overluminous or *Very Luminous SuperNovae* (VLSNe) which currently includes other 3-4 well studied events. Their absolute luminosity at maximum, $M_V < -20$ is much higher than any other previous supernovae, either core-collapse and or thermonuclear. Their huge brightness ($> 10^{51}$erg are emitted in the first $\sim$200 days) link these events to massive or supermassive progenitors, which experienced extreme mass-losses during their last stages of evolution. However, other explosion mechanisms or sources of energy are being investigated; the debate on their nature is still open.

The first object discussed in this Thesis is SN 2006gy, which is one the most debated supernovae ever. Contrary to typical IIn SNe, this event did dot show any strong x-rays or radio emission near the epoch of maximum. This has lead to consider other feasible non-standard sources of energy beyond interaction. In this thesis, the evolution of multiband light curves, the pseudo-bolometric (BVRI) light curve and an extended spectral sequence are presented and used to derive constraints on the origin and evolution of the nature of the SN.

Its light curve is characterized by a broad, bright ($M_R \sim -21.7$ at about 70 days) peak, followed by a rapid luminosity fading which turns into a slower decline by day $\sim$180. At late phases (> 237 days), because of the large luminosity drop (> 3 mag), only upper visibility limits are obtained in the B, R and I bands. In the near-infrared, two K-band detections on days 411 and 510 possibly indicate dust formation or IR echoes scenarios. At all epochs the spectra are characterized a multicomponent Hα profile, without any P-Cygni.

By means of a semi-analytical code, the light curve in the first 170 days is found to be consistent with the explosion of a compact progenitor ($R \sim 6 - 8 \times 10^{12}$ cm, $M_{ej} \sim 5 - 14 M_{\odot}$), whose ejecta collided with massive ($6 - 10 M_{\odot}$), opaque clumps of previously ejected material. These clumps do not completely obscure the SN photosphere, so that at its peak the luminosity is due both to the decay of ^{56}Ni and to interaction with the circumstellar medium (CSM).

After 170 days spectroscopic and photometric similarities are found between SN 2006gy and bright, interaction-dominated SNe (e.g. SN 1997cy, SN 1999E and SN 2002ic). This suggests that ejecta-CSM interaction plays a key role in SN 2006gy about 6 to 8 months after maximum, sustaining the late-time-light curve. Alternatively, the late luminosity may be related to the radioactive decay of $\sim 3 M_{\odot}$ of ^{56}Ni.

In this scenario, a supermassive star is not required to explain the observational data, nor is an extra-ordinarily large explosion energy.

For the SNe 2007bt, 2007bw and 2008fz UBVRI light curves and an extended spectral sequence are also presented. Analogies and differences are highlighted, both among each other and with respect to the sample of VLSNe from the literature.

Photometrically, it is shown that the light curves of SNe 2007bt and 2007bw are substantially different from that of SN 2008fz, evolving more slowly, being redder at the earlier phases and decaying with a rate consistent with that predicted by the radioactive decay of ^{56}Co. On the contrary, the photometric evolution of SN 2008fz is reminiscent to the light curves of IIL SNe, showing a short peak followed by a steep decline.

Spectroscopically the three events are characterized by high-velocity (up to $\sim 12000\,\mathrm{km\,s^{-1}}$), slowly-decelerating emission lines. The spectra of the SNe 2007bt and 2007bw are dominated by Balmer lines, overimposed on a relatively flat continuum ($T_{BB} \sim 6000 - 7000\,\mathrm{K}$); an asymmetry in the early profile of Hα is observed, slowly disappearing with time. Measurements of the narrow components of Hα in SN 2007bt indicate CSM speed of 320 $\mathrm{km\,s^{-1}}$, which are only consistent with the winds surrounding luminous blue variable (LBV) stars. The early spectra of SN 2008fz are found to be similar to SN 2006gy; however, they show higher temperatures ($T_{BB} \sim 14000\,\mathrm{K}$) and a more rapid evolution.

For the three events, the energetic, luminosity, initial radius ($> 10^{15}$cm) and the kinematic derived from the analysis of the light curves and spectra could be reproduced by the conversion of kinetic energy into radiation by a clumpy CSM which is hit by the energetic SN ejecta, similarly to what was proposed for SN 2006gy. For SNe 2007bt and 2007bw the asymmetry in the Hα line can be

explained if a massive (>10 $M_\odot$) clumpy CSM lies face-on in the direction of the observer. The asymmetry in the CSM distribution around the star could be due by a binarity effect in the progenitor system, or asymmetric mass ejection of a single star.

For SN 2008fz the rapid expansion of the black-body radius favor a less massive CSM ($\sim 1\,M_\odot$), which is efficiently warmed up and accelerated by the high-velocity SN ejecta. Because of the relatively small mass in the CSM/shell, the photon diffusion time is smaller than that calculated for SN 2006gy, and the radiated energy plummets rapidly as the light curve.

As for the case of SN 2006gy, these scenarios have the advantage that they do not involve any exotic explosion mechanism for these VLSNe. However, other scenarios could be consistent with their photometric evolution. Among these, the possibility of a pair-instability explosion cannot be excluded. This and other likely hypothesis proposed by other authors are discussed.

Riassunto

Questa Tesi si incentra sullo studio fotometrico e spettroscopico di quattro supernovae (SNe) di tipo IIn (cioè SN 2006gy, 2007bt, 2007bw e 2008fz), che sono tra le supernovae più brillanti mai scoperte. Infatti appartengono alla classe delle SNe iperluminose o *Very Luminous SuperNovae* (VLSNe, supernovae molto brillanti), che al momento include altri 3-4 oggetti ben studiati. La loro luminosità assoluta all'epoca del massimo, $M_V < -20$, è superiore rispetto a qualsiasi altro evento, sia di natura termonucleare che di collasso del core. L'enorme luminosità emessa ($> 10^{51}$erg nei primi $\sim$200 giorni) associa questi eventi a progenitori massicci o supermassicci, che hanno subito fenomeni di perdita di massa estremi durante le loro fasi evolutive finali. Comunque, al momento si stanno studiando anche altri meccanismi o possibili fonti di energia, e il dibattito sulla natura di questi eventi è tuttora aperto.

Il primo oggetto discusso è la SN 2006gy, che è una delle supernovae pi dibattute in assoluto. Contrariamente alle tipiche IIn, essa non mostrava alcuna emissione X o radio all'epoca del massimo di luminosità. Questo ha portato a considerare altre possibili sorgenti di energia oltre all'interazione. In questa Tesi, l'evoluzione delle curve di luce multibanda, la curva di luce pseudobolometrica e una sequenza di spettri vengono studiati per ricavare delle informazioni sull'evoluzione e sulla natura della supernova e del progenitore.

La curva di luce è caratterizzata da un picco ampio e luminoso ($M_R \sim -21.7$ a circa 70 giorni), seguito da un declino di luminosità veloce, il quale si assesta su un declino più lento, a circa 180 giorni. A fasi avanzate (>237 giorni), a causa del forte indebolimento della luminosità (>3 mag) vengono ricavati solo dei limiti ottici nelle bande B, R ed I. Nel vicino infrarosso, due *detection* nella banda K' indicano una possibile presenza di regioni di formazione

di polvere, o eventualmente di echi infrarossi. A tutte le epoche gli spettri sono caratterizzati dalla presenza di profili di righe a multi-componente, senza però alcun profilo P-Cygni. ramite un codice semi-analitico si trova che la curva di luce nei primi 170 giorni è consistente con l'esplosione di un progenitore compatto ($R \sim 6 - 8 \times 10^{12}$cm, $M_{ej} \sim 5 - 14 M_{\odot}$), le cui ejecta collidono con dei *clumps* massicci ($6 - 10 M_{\odot}$) e opachi di materiale espulso precedentemente. Tali *clumps* non oscurano completamente la fotosfera della supernova, cosicché all'epoca del picco la luminosità è dovuta sia al decadimento radioattivo del ^{56}Ni che all'interazione con il mezzo circumstellare.

Vengono inoltre evidenziate, a partire da circa 170 giorni, delle analogie fotometriche e spettroscopiche tra la SN 2006gy e un gruppo di supernovae interagenti (cio SN 1997cy, 1999E e 2002ic). Ciò suggerisce che l'interazione tra ejecta e CSM gioca un ruolo importante anche nella SN 2006gy a circa 6-8 mesi dal massimo, sostenendo la curva di luce a fasi avanzate. In alternativa, la luminosità a queste fasi potrebbe essere dovuta al decadimento radioattivo di $\sim 3 M_{\odot}$ di ^{56}Ni.

Questo scenario non richiede la presenza di una stella supermassiccia o di un'energia straordinariamente grande per spiegare i dati osservativi.

Anche per le supernovae 2007bt, 2007bw e 2008fz vengono presentate delle curve di luce UBVRI e una sequenza di spettri estesa. Vengono messe in luce analogie e differenze tra tali supernovae e tra le VLSNe in letteratura. Dal punto di vista fotometrico si mostra che le curve di luce delle SNe 2007bt e 2007bw differiscono sostanzialmente da quella della SN 2008fz, poich evolvono più lentamente, sono più rosse a fasi iniziali e decadono ad un tasso consistente con quello predetto dal decadimento del ^{56}Co.

Spettroscopicamente i tre eventi sono caratterizzati da righe di emissione ad alte velocità, fino a 12000 $\mathrm{km\,s^{-1}}$. Gli spettri delle supernovae 2007bt e 2007bw sono dominati dalle righe di Balmer su un continuo relativamente piatto ($T_{BB} \sim 6000 - 7000\,\mathrm{K}$). Inoltre viene osservata un'asimmetria nel profilo iniziale di Hα, che però si indebolisce col tempo. Dalla misura della componente strette di Hα nella SN 2007bt si ricavano velocità di 320 $\mathrm{km\,s^{-1}}$, le quali sono consistenti solo con i venti di stelle LBV (luminose, blu, variabili). Si trova inoltre che i primi spettri della SN 2008fz sono consistenti con quelli della SN 2006gy; tuttavia, essi indicano temperature maggiori ($T_{BB} \sim 14000\,\mathrm{K}$) ed un'espansione più rapida.

Per i tre eventi, l'energia in gioco, la luminosità, il raggio iniziale ($> 10^{15}$cm) e la cinematica derivati dall'analisi delle curve di luce e degli spettri potrebbe essere riprodotta dalla conversione di energia cinetica in radiazione da parte di un mezzo circumstellare ricco di *clumps*, il quale viene raggiunto dalle ejecta energetiche della supernova, similmente a quanto supposto per SN 2006gy.

Per le SNe 2007bt e 2007bw l'asimmetria del profilo di Hα può essere spiegata se un mezzo massiccio (>10 $M_\odot$) ricco di *clumps* si trova esattamente davanti all'osservatore, perpendicolarmente alla linea di vista. L'asimmetria nella distribuzione del mezzo circumstellare potrebbe essere dovuta ad effetti di binarietà del sistema del progenitore, o ad espulsioni di materiale asimmetriche in una stella singola.

Per la SN 2008fz la rapida espansione del raggio iniziale di corpo nero tende a favorire un mezzo meno massiccio ($\sim 1\,M_\odot$), il quale viene riscaldato ed accelerato efficientemente dalle ejecta ad alta velocità. A causa della massa relativamente piccola del mezzo, il tempo di diffusione dei fotoni inferiore di quanto calcolato per la SN 2006gy, cosicché l'energia radiativa diminuisce rapidamente, come la curva di luce.

Come nel caso della SN 2006gy, il vantaggio di questi scenari è che non involvono alcun meccanismo di esplosione esotico. Tuttavia, la loro evoluzione fotometrica puà essere consistente anche con altri scenari. Tra questi, anche l'esplosione di una supernova di instabilit di coppia non può essere esclusa. Questi ed altri scenari vengono discussi nel capitolo conclusivo.

Contents

List of Tables

List of Figures

CHAPTER 1

Introduction

In this chapter I will give an introductive overview of supernovae in general. I will explain how they were discovered in their history and how they were classified. Then I will describe the current models for the explosion (i.e. thermonuclear or core-collapse). Finally, for each supernova type I will briefly list the characterizing observational properties, both from the photometric and from the spectroscopic point of view.

Supernovae (SNe hereafter) are among the most energetic and spectacular events in the Universe. Throughout history they have fascinated mankind, unexpectedly appearing as new, bright stars in the sky.

Now it is known that SNe are powerful explosions that mark the fate of massive single stars or compact stars in a binary system. The star explodes so violently that for a few weeks it outshine its parent galaxy. In our own Galaxy, the Milky Way, a supernova may even be visible in daylight. Still, only one part in 10000 of the released energy is emitted in visible light. In core collapse supernovae the major part of the energy, $\sim$99%, is emitted as neutrinos. About 1% of the energy is spent to eject the matter at a speed of $\sim$10000 $\mathrm{km\,s^{-1}}$. Since SNe can be observed at large distances, they have become increasingly interesting

Date/Year	Constellation	AR - Dec	Mag	Notes
185	Cen	14:43.1-62:28	-2	SNR: G135.4-2.3
393/396	Sco	17:14-39.8	-3	3 Remnant as radio sources
Apr 30, 1006	Lup	15:02.8 -41:57	-9^{+1}_{-1}	...
Jul 4, 1054	Tau	05:34.5 +22:01	-6	SNR: M1 (Crab Nebula)
Aug 6, 1181	Cas	02:05.6 +64:49	-1	...
Nov 6, 1572	Cas	00:25.3 +64:09	-4	...
Oct 9, 1604	Oph	17:30.6 -21:29	-3	Kepler SN
1680?1667?	Cas	23:23.4 +58:50	6?	SNR: Cassiopea

Table 1.1— Some historical supernovae.

for cosmology, as probes of the evolution of the early Universe.
But supernovae are not merely fireworks in the sky. They constitute an important part of the life cycle of stars and play a major role in the chemical enrichment of the Universe, releasing into the space the products of the progenitor star and of their own explosion nucleosynthesis. The SN shocks can eventually compress dense molecular clouds and trigger vigorous bursts of stars, which will be enriched in heavy elements. SNe can be used in numerous theoretical fields, such as probes of the stellar evolution theory, or, in the case of Galactic core-collapse explosions (CCSNe hereafter), the standard model of particle physics, through the study of the strong neutrino emission. SNe are among the best tools also in the study of the star formation history out to a redshift $z > 1$ and, to date, the most precise distance indicators. Finally, the association of long-duration γ-ray bursts (GRBs) with some core-collapse SNe can be the key for understanding the nature of these puzzling events. Hence the progress in a number of fields in astrophysics and cosmology depends on our understanding of SN phenomenon, boosting numerous and strong efforts in their searches.

1.1 Supernovae in the history

Temporary stars, comets and novae, as well as occasional supernovae, were fairly frequently recorded in East Asian history (cf. Table 1.1). One of the first discoveries well documented by the Chinese and Japanese chronicles, is dated 1006 a.D. (Green & Stephenson 2003). Also the historical documents reporting the appearance of a bright supernova in 1054 a.D. have to be attributed to the Chinese astronomers. The transient remained visible for about one month. This SN gave origin to the famous SN remnant which is called "Crab Nebula"

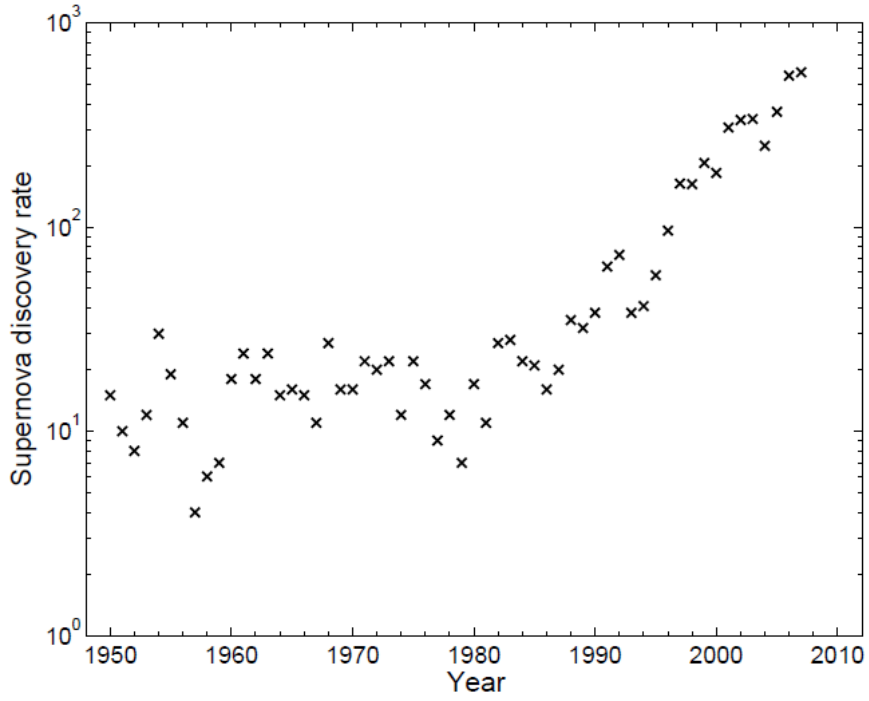

Figure 1.1— Supernova discovery rates, as collected from http://www.cfa.-harvard.edu/iau/lists/Supernovae.html. Note the sharp increase from year 1988 to 2007.

(M31 in the Messier Catalogue),

In 1572 d.c the Danish astronomer Tycho Brahe reported a new SN event in the Cassiopea constellation and computed several distance estimated. In the essay "*De nova et nullius evi memoria prius visa stella*", he concluded that the object did not show any relative motion, being nothing but a "fixed star". He denoted it "nova". From that moment the interest towards novae increases noticeably in Europe, also thanks to the diffusion of the first telescopes; the observations became more and more frequent.

In 1604 the appearance of a new bright "nova" led Johannes Kepler to deepen the study of the luminosity evolution of the transient, whose position and variability was reported in the work *"De stella nova in Pede Serpentari"*. This object was observed also in Padova by Galileo Galileo, who thus began to be interested in the astronomical observation.

3 centuries later, i.e. in 1920, Lundmark realized that there was a particular

class of very bright novae. But only after the extragalactic nebulae were placed at their actual distances by Edwin Hubble, it was understood that the novae occurring in these nebulae were more distant and therefore more luminous than the Galactic novae.

In 1938 Baade and Zwicky finally defined them as supernovae; using the Palomar 18-inch Schmidt telescope they started the first systematic SN search, discoverying 19 SNe. During this same period, the convention was introduced of cataloguing the SNe by identifying them with the discovery year followed by a letter of the alphabet which indicates the chronological order of discovery.

In the following years, a few SNe of a different kind were discovered, and Minkowski (1941) provisionally divided SNe into Type I and II, distinguished by the lack or presence of Hydrogen lines in their early spectra, respectively. The improvement of the instrumentation, the construction of new telescopes and also the significant progresses in the understanding of the stellar evolution, stimulated the research and cataloguing of the SNe. With this aim, in 1957 several Schmidt telescopes were devoted to SN searches (in Zimmerwald, Switzerland by P. Wild; in Asiago, Italy by L. Rosino; in Tonantzintla, Mexico by G. Haro and E. Chavira). In 1958, the Palomar 48- inch Schmidt telescope began another deeper SN search.

In the Sixties, thanks to international SN searches coordinated by Zwicky, $\sim$100 SNe were discovered and three other SN types were added (III, IV and V). All these SNe had peculiar light curves and evidence of hydrogen (H) in the spectra. Now we believe that the Type V objects are likely not genuine SNe, but superficial outbursts resembling η Carinae. Also in 1968 the first SN discovered by an amateur was reported (SN 1968L discovered by J. Bennet).
In the Eighties, with the introduction of the CCD and the construction of telescopes of increasing diameter and relatively large field of view, the number of SNe observed grew and it became possible also to obtain spectra with better resolution and to study the evolution of the luminosity of the SNe for longer times. The SNe classification became consequently more complex due mainly to more careful comparisons among the SNe types.

The technological advances also allowed to extend the search to a higher redshift (z=0.2 – 0.4) and to broaden the observations wavelength range, namely in the IR bands, radio, ultraviolet (UV) and X-ray bands. In 1987, the explosion of the SN 1987A in the Large Magellanic Cloud (LMC), the closest extragalactic SN observed in modern times (i.e. 50 kpc) made possible to detect the SN progenitor (in pre-explosion images) and the neutrino flux produced during the explosion.

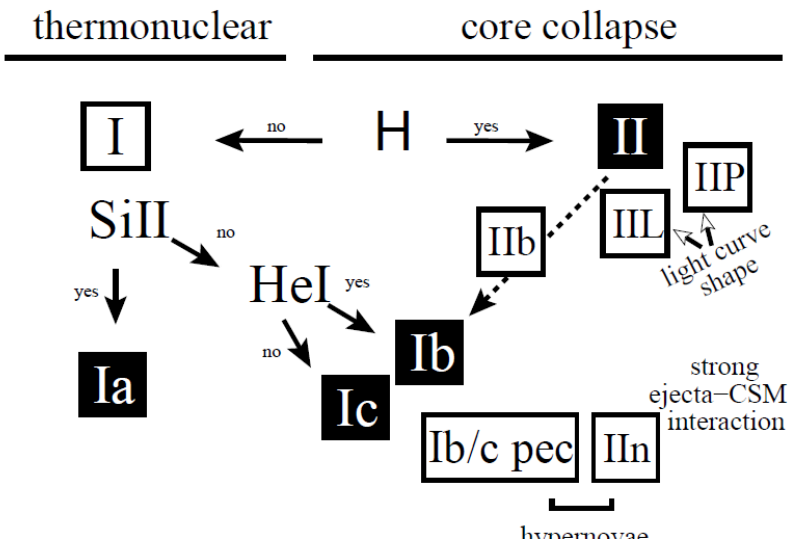

Figure 1.2— General classification scheme of supernovae (Turatto et al. 2003).

Fig.1.1 shows the discovery rates of SNe from year 1950 to year 2007. Until 1987, the discoveries were in the range of ∼10-30 per year. However, after SN 1987A and onwards, the discovery rate has increased almost exponentially: today, about two SNe are discovered per day, using the visual and automated methods of research. Nevertheless, if one only considers the bright events, i.e. brighter than magnitude 15, such increase in the discovery rate is less defined, staying roughly constant at about 10 events per year (Cappellaro 2003). This is due to the fact that nearly all bright, nearby SNe are discovered.

This trend has been modified only in the last few years, with the advent of the several deep supernovae searches (cf. Sect. 9.1), which are daily scanning large areas of the sky even at high distances, thus constantly providing new, interesting detections, like the luminous supernovae that will be discussed in this thesis.

1.2 Classification

As seen before, the first fundamental classification was given by Minkowski (1941) who distinguished the SNe in two different classes based on the lack (SNe I) or presence (SNe II) of H lines in their early spectra. Since SNe may be very different observationally in terms of chemical composition, physical condi-

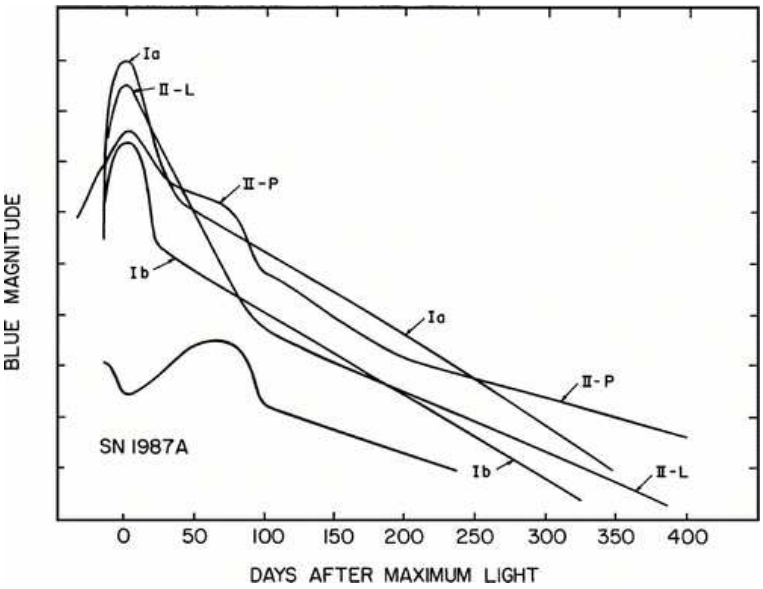

Figure 1.3— Schematic representation of the most frequent light curves (Filippenko et al. 1997).

tions, photometry, time evolution, radio and X-ray properties etc, in the 1980's new subclasses were introduced. The types Ib, Ic, IIn, II-L, II-P, IIb were related to characteristics of their spectra (small letter) or to the evolution of the light curves (capital letter).
In Fig.1.2 a sketch of the classification system is shown, which highlights the main characteristics used to differentiate between the various types and subtypes and their relation to each other. The SNe of type I are subdivided in three subclasses, depending on the presence or lack of Si II and He I in the spectra. Type Ia SNe present a strong line of Si II at ∼6150 Å in their spectra (recognized to be due to the doublet of Si II at 6355 Å), while the spectra of the SNe Ib do not have this feature but are characterized by pronounced lines of He I, as that at 5876 Å. Finally, the SNe Ic do not present Si II nor He I lines (or He I is very weak).
The class of the SNe II is formed by four main subclasses and their spectra are dominated by H lines at all epochs. The SNe IIP and SNe IIL constitute the most numerous subclasses and are characterized by the shape of the light curve, but they do not show deep spectral differences. After a luminosity declines which last a few days, the light curve of SNe IIP shows a relatively constant luminosity, or plateau, with a duration of approximately 2-3 months (Fig.1.3). The light curve of SNe IIL shows a linear decline starting shortly past maximum. The SNe IIn (narrow emission lines) present spectra in which the Balmer emission lines are formed by several components that evolve in the time in various ways. The spectrum of the SNe IIb, finally, is similar, during maximum light, to that of the SNe IIP and IIL, i.e. it has strong lines of H, but in the following week it metamorphoses to that of SNe Ib, thus pointing out a physical link between these two classes. This classification, based on early phase spectra, is normally used in the CBET Telegrams when a new SN candidate is confirmed, but it is not always accurate, as it is not related to the physical characteristics of the objects but only to their spectral and photometric appearance soon after the explosion. Note that in many cases the appearance of a SN can change in time due to the characteristics of the progenitor or to those of the circumstellar material. Therefore, it is preferable to divide SNe according to the physical character of the explosion rather than the morphology of the spectra or light curves. Nowadays we divide supernovae in two categories which are based only on the physics of the explosion, which may occur via *core-collapse* or via *thermonuclear explosions*. A more detailed description will be given in the next Sections.

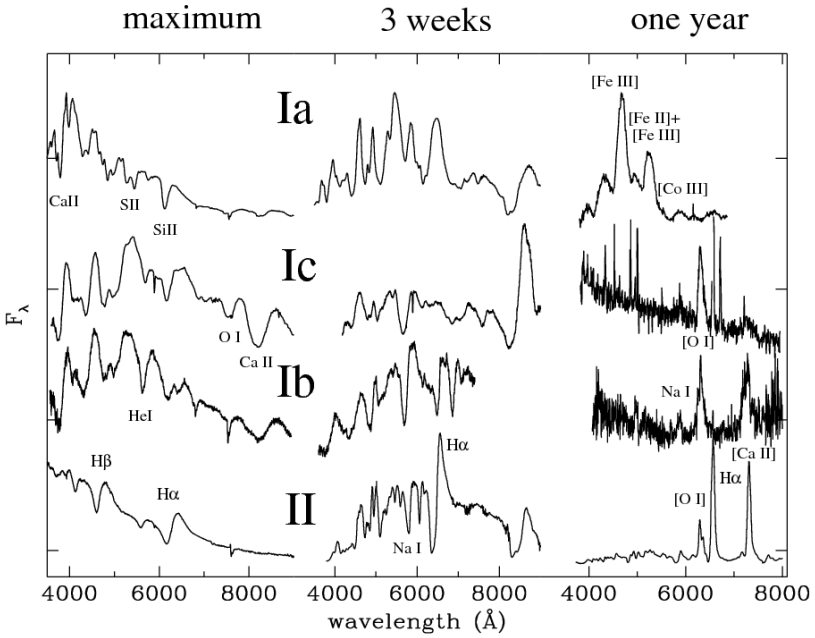

Figure 1.4— Typical spectra of the principal SN types, at maximum, three weeks and one year after explosion (Turatto et al. 2003).

1.3 The evolution of a supernova

Regardless of which supernova type, at the time of explosion a large quantity of material, called *ejecta*, is expelled with high velocity into the circumstellar medium (CSM). The ejecta are compact, dense and opaque and their chemical composition depends on the SN progenitor nature. Their expansion occurs with a velocity directly proportional to the distance from the center of the explosion *(homologous expansion)*, while their density and temperature decrease. At the very early phases the high density of the ejecta determines the formation of a *photosphere*, which emits a black body spectrum (typical early temperatures are in the order of ∼10000-20000 K). The optical spectrum is characterized by lines with P-Cygni profiles over a blue continuum. These epochs are called "photospheric".

With the expansion, the visible surface, where the observed light is emitted from the photosphere, recedes and completely disappears a few months later, when the optical depth of the expelled matter becomes very low and even the innermost regions are exposed. As the expansion proceeds further, the

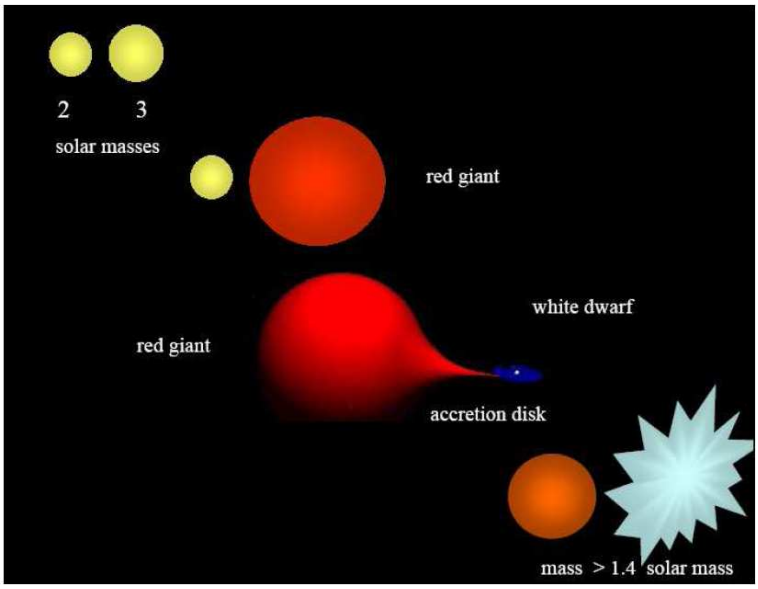

Figure 1.5— Single-Degenerate (SD) scenario schematic evolution.

photosphere and the region of the line formation recede more deeply in the ejecta and the P-Cygni width decreases. The spectral energy distribution is shifted redwards as a consequence of the temperature decrease and the ratio between the emission lines and the continuum grows in favor to the former.

At these phases the energy is completely supplied by the radioactive decay of ^{56}Ni , which represent a fundamental source of energy in general during all the SN evolution. In fact, the ^{56}Ni synthesized during the explosion decays into ^{56}Co, which in turn decays into ^{56}Fe. The first reaction, having an half-life of 6.1 days, influences the first phases of the SN evolution, while the second one with an half-life of 77.1 days determines the SN display on longer temporal scales. At very late epochs (>1000 days) the contributions of the decays of ^{57}Co and of ^{44}Ti may also become important.

In the "nebular" phase the most interior part of the SN is exposed. The spectra show only emission lines; the density is so low that even forbidden lines appear.

This scenario is common to each SN type, both thermonuclear and core-collapse. Through the study of the light curves and spectra it is possible to

reconstruct the SN evolution in time until the moment of the explosion, possibly deriving constraints also on the nature of the SN progenitor.

In the next Sections I will review the basic evolution scenario and the observational properties of the main supernova types.

1.4 Thermonuclear supernovae

Type Ia supernovae are believed to originate from the thermonuclear disruption of electron-degenerate white dwarf (WD) stars (Hoyle et al. 1960), when they have accreted enough matter from a binary companion to reach the so-called "Chandrasekhar limit", i.e. $M_{Ch} \sim 1.4\,M_{\odot}$ (Livio et al. 2000; Nomoto et al. 2000). As proof of their compact, evolved progenitors, light curves of Ia SNe show a rapid (<20 days, Hayden et al. 2010) rise in luminosity to maximum [246, 4], and a fast post-maximum decline. The lack of H and He in their spectra, and the appearance of SN Ia in all morphological types of galaxies (including early-type, elliptical galaxies; Cappellaro et al. 1999), hint at the association of SN Ia progenitors with old stellar populations. However, it appears that the less luminous SN Ia preferentially occur in elliptical galaxies, and the more luminous ones in late-type or blue spiral galaxies (Hamuy et al. 2000). This could be due to a decrease in the progenitor WD C/O ratio with lookback time, according to (Hoflich et al. 1998; Umeda et al. 1999). The composition of the exploding white dwarf is still subject to uncertainties, though C+O WDs are preferred for their allowed range of masses ($0.8-1.2\ M_{\odot}$) and accretion rates ($10^{-8} - 10^{-6} M_{\odot}\,yr^{-1}$), favoring the occurrence of a SN Ia event upon reaching the Chandrasekhar limit.

While it is accepted that WD must accrete matter from a binary companion to become unstable, the nature of this "donor" star is still very much debated. Currently, two scenarios are accepted: *(i)* the "*double-degenerate*" (DD) scenario results from the merging of two C/O WDs in a close (orbital separation $\sim 10\,R_{\odot}$; see Iben et al. 1991) binary system, where the two components are progressively brought together via emission of gravitational waves; *(ii)* the "*single-degenerate*" (SD) scenario in which the WD accretes H- or He-rich matter from a non-degenerate subgiant/giant star (Whelon & Iben 1973).

The DD scenario requires a binary WD system in which the total mass exceeds the Chandrasekhar mass, and with short enough orbital periods (<10 hours), to let the merger event occur within the Hubble time. Although such short-period WD binary systems have been detected, only two systems has been found with a total mass within 10% of the Chandrasekhar limit. Moreover,

the outcome of the merger is still uncertain and collapse to a NS seems more likely in such a scenario (Livio et al. 2000). Recently, the definite detection of H emission in the spectrum of SNe 2002ic (Hamuy et al. 2003, but see also Benetti et al. 2006 for an alternative scenario) has brought a fatal blow to the DD scenario.

The favored progenitor scenario thus appears to be the SD scenario. Still, it remains uncertain whether a WD can reach the Chandrasekhar limit by accretion of H. Binary systems in which the WD stably accretes H at a high rate ($< 10^{-7} M_{\odot} yr^{-1}$) from a subgiant companion have been identified, and are known as Supersoft X-ray Sources (Van den Heuvel et al. 1992). Thus, despite the existence of a "preferred" progenitor model for SN Ia, several theoretical uncertainties remain.

1.4.1 Explosion models

The mechanisms by which SN Ia explode, and in particular the ignition of the burning in the accreting WD, continues to be uncertain.

As for the progenitor systems, two distinct classes of models are proposed for the onset of thermonuclear burning. In one model, C is ignited at the WD center, when the latter reaches the Chandrasekhar limit. Variations within this model are associated with the propagation of the burning front: *pure detonations* (supersonic) have been discarded due to their overproduction of Fe-group elements, and excessively high expansion velocities (Woosley et al. 1986); *pure deflagration* (subsonic) models, such as the W7 model of Nomoto et al. [211], have been more successful in reproducing the ejecta composition and expansion velocities as derived from spectral synthesis calculations (e.g., Mazzali et al. 1993), although the propagation speed of the deflagration wave in this model is parametric. An alternative solution is for the burning front to start as a deflagration and change to a detonation at a given transition density. Such models are referred to as *delayed detonation* (DDT) models (Khoklov et al. 1993), and have been shown to reproduce some of the observations (Hoflich et al. 1995).

In a second set of models, applicable to sub-Chandrasekhar mass WDs, the He detonates at the WD surface, near the bottom of the accreted helium layer (see Livio & Arnett 1995). The resulting inward-propagating pressure wave compresses the C/O core which ignites offcenter. Although such models would in principle explain the sub-luminous SN Ia events, the high-velocity ejecta tend to have the wrong composition (He and ^{56}Ni dominate).

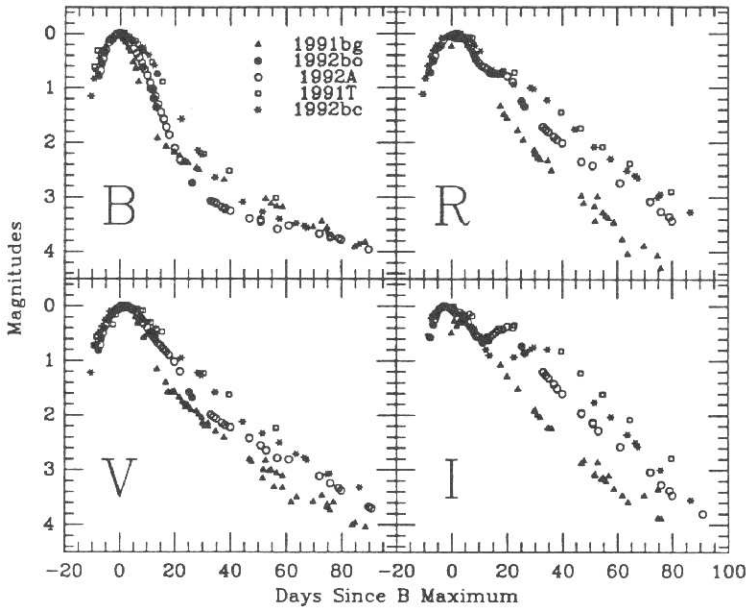

Figure 1.6— Light curves of a normal SN Ia (SN 1992A) and of a few peculiar ones (from Suntzeff 1996).

1.4.2 Light curves

Examples of SN Ia light curves in various bands are visible in Fig. 1.6.

With initial radii of $\sim 10^4$ km (corresponding to a white dwarf radius) and typical expansion velocities of $\sim 10^4$ km s^{-1} (as determined from blueshifted absorption features in SN Ia spectra), admitting the photon emission though adiabatic cooling would be problematic. Indeed, it has been suggested that in thermonuclear supernovae the observed light curve is entirely powered by the radioactive decay of ^{56}Ni synthesized during the explosion (Colgate and McKee). Typically $\sim$0.4$-$0.8 M$_\odot$ of radioactive ^{56}Ni is synthesized during the explosion, and the peak luminosity of the SN Ia event scales with the ^{56}Ni mass (Arnett et al. 1985). The decay to ^{56}Co proceeds via electron capture, then through electron capture and $\beta+$ decay to stable ^{56}Fe. Each of these decays produces γ-ray photons, which scatter and diffuse out at longer wavelengths, where the opacity in the ejecta is lower. Typically, roughly 80% of the radiative flux is emitted at optical and near-infrared wavelengths (Suntzeff 2003).

Although the luminosities vary by a factor of 10 at peak, SN Ia light curves share fundamental properties. At the earliest times, the ejecta is so opaque that

the radioactive energy input is converted into kinetic energy of the expansion. As the supernova expands, the time for thermalised photons to diffuse out shortens, and the luminosity increases. This, combined with the exponentially decreasing rate of energy input from ^{56}Ni decay, causes a maximum in the light curve, at which time the luminosity equals the instantaneous energy deposition rate (under the assumption of constant opacity) referred to as "Arnetts rule" (Arnett 1982). After a rapid post-maximum decline in luminosity, the light curves display an exponential tail after ∼40 days past maximum. At these phases, the ejecta is optically thin: a large fraction of γ-rays escape conversion to optical photons, and the decline in luminosity is faster than the ^{56}Co $\longrightarrow^{56}$ Fe decay rate.

The near-infrared (IJHK) light curves of SN Ia display a secondary maximum at ∼20 - 40 days past B maximum light, which appear as a shoulder in the V and R light curves. Though the mechanisms leading to this secondary maximum are unclear, Pinto and Eastman (2000) have suggested that it could be explained by a decrease in the opacity in the outer layers of the SN Ia ejecta.

As a consequence of the standardization of their light curve, following the work of Philips 1993 and Hamuy et al. 1995 (among many others) which ricalibrated the SN absolute luminosity according to the shape of the (B) light curve, thermonuclear SNe are very good distance indicators. Moreover, the potential of type Ia in the cosmology field has been largely proved by successful projects aimed at determining the dynamic of the Universe, (SCP, Perlmutter et al. 1998, 1999; the High z SuperNova Search, Riess et al. 1998; ESSENCE, Wood-Vasey et al. 2007).

1.4.3 Spectra

As seen before, the spectra of SNe Ia are characterized at every phase by the absence of the emission lines of H (Fig.1.7). The very early phase spectra of SNe Ia (about 2 weeks before maximum light) show broad lines with the characteristic P-Cygni profiles, produced in the expanding atmosphere. The wide features at a velocity of about $25-30000$ km s^{-1} are due to intermediate mass elements such as Ca, Si, S or Mg. At a phase earlier than -14 days from maximum light, lines are difficult to identify due to heavy blanketing effect, although the H and K lines of Ca II and, at a slower velocity, C II could be visible in some cases. Later on lines become easier to identify, and they are mostly due to Ca II, Si II and Si III, S II and Mg II. The Si II line at 6355 Å is always evident and characterizes the spectra of SNe Ia for over one month. Si II expands at around 15000 km s^{-1} at maximum light, and later on its velocity decreases at a slower rate than the photosphere, indicating that the Si layer

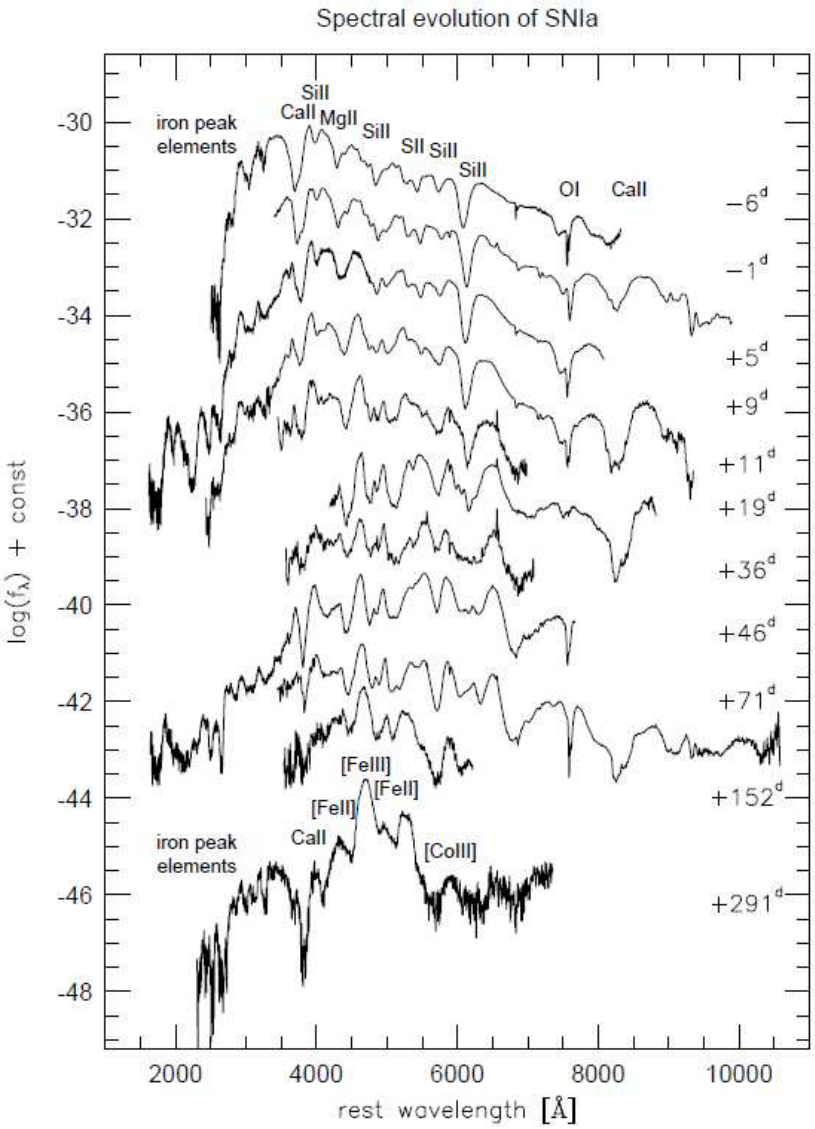

Figure 1.7— Spectral evolution of a typical SN Ia from 6 days before maximum to about 300 days after (from Wheeler & Benetti 2000).

is detached. At about two weeks after maximum light, Ni-Co-Fe lines from the core start to appear, as the photosphere is retreating towards the inner regions of the expanding envelope. Eventually, at ∼3 weeks after maximum light, Fe lines dominate the entire spectrum with some leftover Si and, a couple of months after maximum light, with Co, Cr II and Na I.

1.5 Core-Collapse Supernovae

Since CCSNe are the outcome of the explosion of luminous, massive stars, in the last years it has been possible to identify the progenitors of the closest SN explosions (mainly of type IIP) on archival pre-discovery images, publicly available to the community (Smartt et al. 2009). This has allowed to determine the SN progenitor mass and main features (evolutionary stage, luminosity, temperature etc.). This work has allowed to constrain the lower limit for the star mass to initiate the collapse, which is fixed at $8^{+1}_{-1.5}M_{\odot}$.
However, observationally CCSNe are extremely heterogeneous (Fig.1.10), due to different configurations of the progenitor star at the moment of explosion, its energetics and, possibly, angular momentum (Turatto 2003). Peculiar objects with unexpected observational features are becoming more and more frequent, thus enriching the zoo of classes and subclasses and eventually adding more crucial parameters to the current SN evolution scenario.

Indeed, one of the aims of the study of CCSNe is understanding what is driving the progenitors along different paths to the various CCSNe subtypes and determining the amount of material locked into the compact remnant and that ejected in the ISM.

In the next Sections I will briefly describe the physics of the collapse and present the main photometric and spectroscopic features of the principal SNe types. However, a more detailed description of the possible evolution of the massive stars producing different SN displays, and of its dependency to the parameters like metallicity or rotation will be given in Chapter 2.

1.5.1 The physics of the core-collapse

Conventionally, the life of a star begins when it starts burning H to He in the main sequence (MS), where it spends the largest fraction of its lifetime. Once a He core is formed, H continues to burn in a shell around the core and the stellar radius increases, becoming 100-1000 times that of the Sun. At this stage the star becomes a red giant (RG) or, for the most luminous, a red supergiant (RSG). Massive stars undergo further burning stages: He burns to form C and

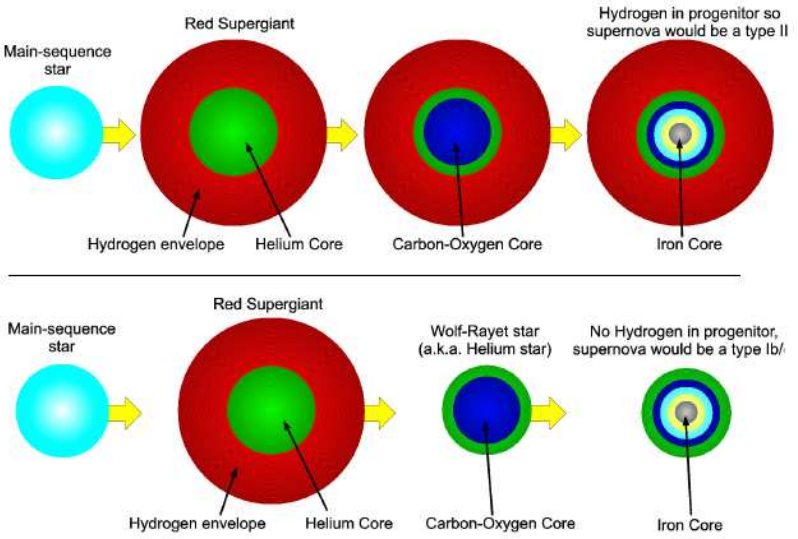

Figure 1.8— Pre-SN evolution of massive stars until the collapse. In the first case *(upper panel)* the star does not lose the H envelope before the explosion, and therefore produces a SN display of the type IIP (cfr. Sect. 1.2 and 1.5.3). In the second case the progenitor is affected by mass loss phenomena which completely deplet the H envelope. The star evolves to a Wolf Rayet before exploding as a type Ic SN (Eldridge et al. 2008).

O and then progressively heavier elements burning prevents stellar collapse until an Fe core is formed. At this stage the star has an "onion structure" (Fig.1.8), with a heavy Fe core surrounded by shells of lighter element until the original H atmosphere.

The mass of the Fe core will continue to grow until it approximately reaches the Chandrasekhar mass. At this mass, electron degeneracy pressure can no longer withstand the gravitational forces and, consequently, the Fe core starts to contract. Due to electron captures in the Fe core, $e^- + p \rightarrow n + \nu_e$, the number of electrons decreases and the pressure reduces accordingly. Furthermore, energetic photons in the core start to photodisintegrate Fe into α particles and baryons. This process is endothermic and lowers the thermal energy and leads to a lower pressure support. This makes the Fe core contract faster, and the increasing core density leads to higher rates of electron captures, which again reduces the degeneracy pressure. Hence, these processes will trigger a gravitational collapse of the core.

Once the collapse is underway, the inner part of the core collapses subsonically and homologously ($v \propto r$), while the outer part collapses supersonically and can reach speeds of about 25% of the speed of light. Because of the high temperature and density, most of the energy release is in the form of neutrinos during the core collapse. The neutrinos that are produced, are scattered by both free and bound neutrons and protons. For a core density exceeding $\sim 10^{12} \mathrm{g\,cm^{-3}}$, the diffusion time of the neutrinos is much longer than the dynamical time scale of the collapse. Hence, the neutrinos will be trapped and the collapse will proceed almost adiabatically. The collapse of the inner core continues until the density exceeds nuclear density ($2 \times 10^{14} \mathrm{g\,cm^{-3}}$). At this stage, the repulsive nuclear forces start to counteract the collapse and the equation of state becomes very stiff in a short period of time. This causes the infalling matter to bounce back and a shock wave is sent outwards through the infalling material.

As the shock plows through the infalling material of the iron core, it disintegrates the iron nuclei into protons and neutrons. This endothermic process effectively reduces the shock energy. Once protons become available, they capture electrons which, in turn, produce neutrinos. These neutrinos will further drain the shock from its energy. Simulations indicate that, in most cases, this drain of energy will cause the shock to stall after some time after the bounce (10−20 ms) and at a relatively small radius (∼100 km) (e.g., Janka et al. 2008). Thus, an accretion shock will be set up at constant radius inside the iron core as the infall of matter continues. Hence, in most simulations, it has turned out that this so called prompt explosion scenario is not able to generate an explosion of the star (e.g., Baron et al. 1985; Woosley & Janka 2005). Thus, an additional source of energy is needed to re-accelerate the shock and make a succesful SN explosion.

Since the bulk of the released gravitational binding energy is carried away by neutrinos, a natural extra energy source would be the deposition of energy of the neutrinos in layers behind the accretion shock. Such a mechanism was first proposed by Colgate & White (1966). In this scenario, the neutrinos emerging from the neutrinosphere in the inner core, heat the post-shock gas through the reactions $\nu_\mathrm{e} + \mathrm{e} \rightarrow \mathrm{p} + \mathrm{e}^-$ and $\nu_\mathrm{e} + \mathrm{p} \rightarrow \mathrm{n} + \mathrm{e}^-$. This heating will increase linearly with the density, whereas the cooling rate of the gas (by the inverse of these reactions) will scale with the density squared. Since the density scales with the radius as $\rho \propto 10^{-3}$, it follows that beyond some radius there will be a net neutrino heating of the gas. Hence, if the neutrinos could deposit a fraction ($\sim$ 10%, Janka et al. 2008) of their total energy into this region behind the

stalled shock, pressure could build up and ultimately lead to an explosion of the star. This scenario is often referred to as the delayed explosion mechanism. However, since both the mass accretion rate and the neutrino flux decrease with time, there will be a time window of a possible explosion, streching from a few tenths of a second to a few seconds.

Even though this delayed explosion mechanism is considered to be a plausible scenario, many details in the mechanism are uncertain. Nevertheless, it is believed that convection of the gas behind the accreation shock should play an important role for making the neutrino heating more efficient. Such convective motions would dredge up hot material from deeper regions and at the same time transport cooler gas close to the shock into deeper layers where it can be re-heated. However, detailed calculations of the neutrino transport indicates that the convection mechanism is not as efficient as was prevoiusly believed (Janka et al. 2008) and hence, it may not be strong enough to push the stalled shock further out. Relatively recently, another type of hydrodynamic instability has been discovered (Blondin et al. 2003). This is the so-called standing accretion shock instability (SASI), which is able to grow efficiently, independent of convective motions. Due to the SASI, the accreted gas can stay longer in the heating layer interior of the shock, and is thus able to more efficiently absorb energy from the neutrino flux. Another consequence of this instability is a global asymmetry of the shock front. Such an asymmetry in the explosion can give the remnant a kick sufficiently large to explain the observed pulsar velocities of several hundred kilometers per second (Janka et al. 2008). In addition, this instability may also explain the spin of the pulsars without the need of introducing rotation of the progenitor star (Blondin & Mezzacappa 2007; Blondin & Shaw 2007).

Once the outgoing shock escapes the Fe core, the density decreases and the shock will therefore suffer much less from energy losses. Hence, at this stage, the shock will be able to propagate through the whole star within hours. While the shock propagates through the star it will either accelerate or decelerate depending on changes in the quantity ρr^{-3}, which is a measure of the swept-up mass. Hence, if the density declines at a slower rate than r^{-3}, the shock will decelerate and leave behind a region of Rayleigh-Taylor instabilities. Such instabilities will introduce mixing of the different burning zones. This kind of mixing is an important ingredient in order to explain the shapes of the observed SN light curves and spectral features (Woosley et al.2002).

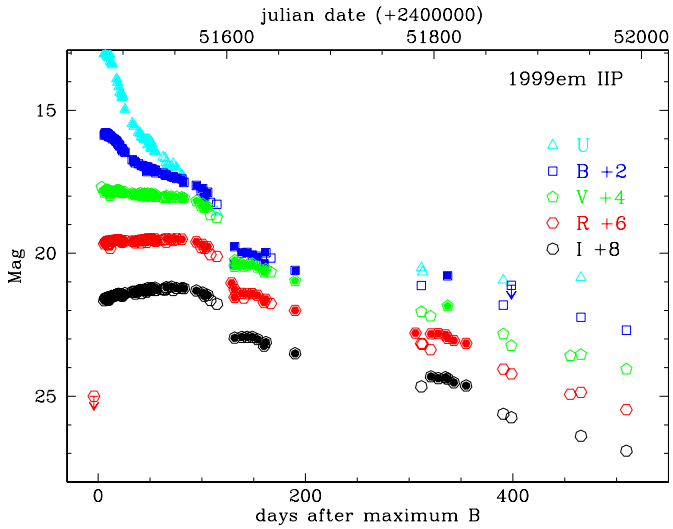

Figure 1.9— UBVRI light curve of type IIP SN 1999em, one of the most studied SNe and the prototype of IIP SNe (Elmhamdi et al. 2003; Leonard et al. 2003).

1.5.2 Light curves of core-collapse SNe

A core-collapse SN starts to be visible at the shock breakout, i.e. when the shock wave produced by the core collapse reaches the surface. This phenomenon occurs about three hours from core-collapse and it is bright especially in the UV, thus creating a spike in the bolometric light curve.

After the shock breakout the adiabatic expansion of the outer envelope causes a rapid decline of temperature and luminosity. At this point the diffusion of the internal energy from the bluk of the envelope and the radioactive energy of the ^{56}Ni synthetized at the passage of the shock wave start to be important. This increases the luminosity, and the SN reaches the maximum phase.

As the SN expands and cools the ionized matter starts to recombine. A recombination wave moves inward in mass throughout the ejecta, recombining the H. The opacity decreases and the residual internal energy can be released. Depending on the envelope mass and explosion energy, this phase may be particularly long-lasting ($\sim$100 days), creating the typical "luminosity plateau" which is seen in type IIP SNe. During this phase the temperature stays nearly constant. On the contrary, if the envelope is less massive only a short (20$-$30 days) peak is observed followed by a linear luminosity decline. In this case the

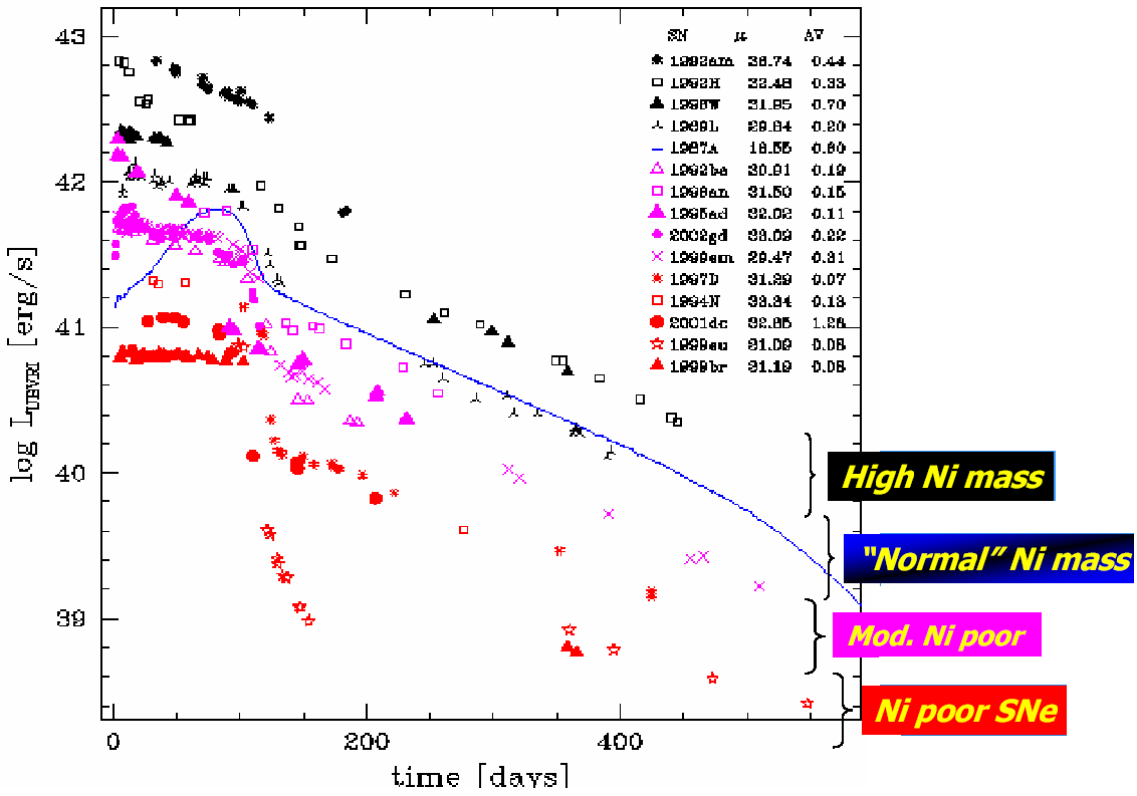

Figure 1.10— Light curves of a sample of 14 CCSNe (Pastorello et al. 2003). This figure shows an evident dispersion both in the photospheric and in the nebular luminosity; the dispersion at nebular phases denotes a variety in the mass of the ejected ^{56}Ni .

light curve resembles the IIL type.

Once the H is recombined the SN light curve settles into the exponential tail, during which the radioactive decay of ^{56}Co represent the main energy source, and the luminosity decline is 0.098 mag/day as predicted by the decay.

At nebular epochs the observed decline rate can be modified by two effect. The first one is the dust formation within the ejecta. The light at optical wavelengths is absorbed by newly formed dust grains and re-emitted in the near infra-red (NIR). This makes the opacity increase, and thus the luminosity decrease faster. A second effect may be caused by the presence of high density circumstellar medium (CSM): if the SN environment is rich of material, this may interact with the fast ejecta, providing additional energy to the luminosity. This effect can occur even at earlier phases. In that case, the SN is denoted as "IIn".

1.5.3 Spectra of core-collapse SNe

In the previous sections it was mentioned that the term "core-collapse supernovae" denotes a class of SNe with a large variety of observational properties. From the spectroscopic point of view, CCSNe may or may not show H, depending on the level of stripping of the outer star's envelopes at the time of explosion. Therefore core-collapse SNe may be either of the type I or of the type II. The main properties of each subclasses are here listed:

- **SNe Ib/c** are thought to be produced by the core collapse of very massive stars which have been stripped, before explosion, by their envelope of H (Type Ib) and both H and He (Type Ic). Therefore, at some epoch of their evolution, the Ib/c SNe are expected to interact with the interstellar material lost by the progenitor stars.

  For both types the Si II line may be present, even if much weaker than in type Ia SNe. Other prominent lines in photospheric spectra are: Ca II, O I, Na I, Fe II, Ti II (e.g. Matheson et al. 2001a; Branch et al. 2002; Millard et al. 1999). The nebular spectra are dominated by [O I] and [Ca II], but also Na I and Ca II lines are visible (Fig.1.11).

  Peculiar cases of Type Ib/c SNe are the so-calles "Hypernovae", whose prototype is SN 1998bw. The latter was a very energetic event ($\sim 10^{52}$erg) with exceptionally high expansion velocities (>30000 km s^{-1}) and very luminous light curves (Iwamoto et al., 1998; Sollerman et al., 2000; Patat et al., 2001). Hypernovae have deserved a large attention because of their connection to the long-duration Gamma Ray Bursts (GRBs).

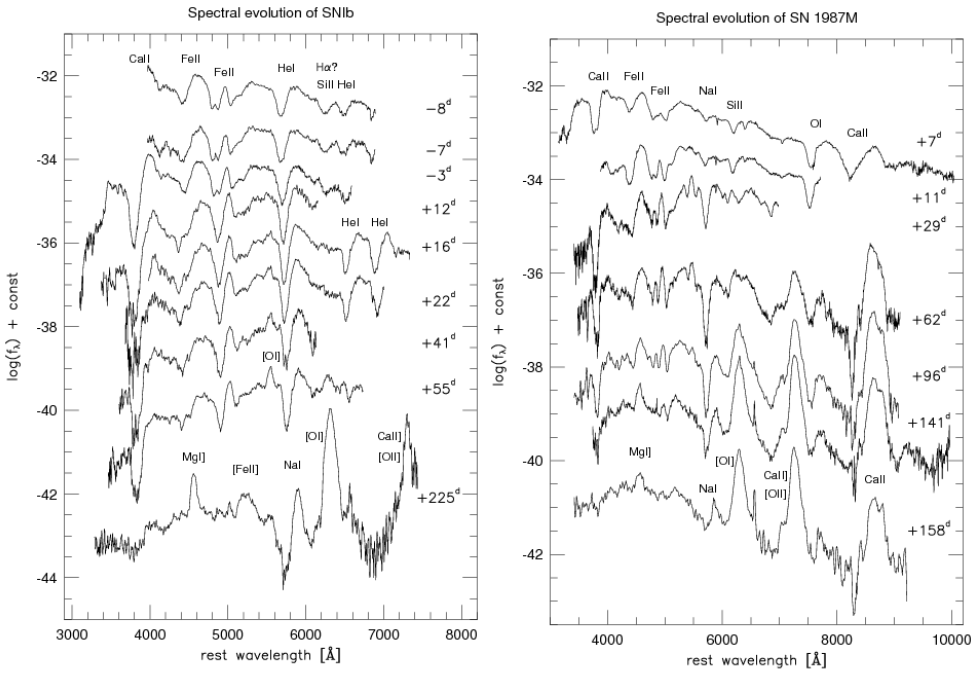

Figure 1.11— Spectroscopic evolution of type Ib SN 1984L (Harkness et al., 1987, *left*) and of type Ic SN 1987M (Filippenko et al., 1990).

Current models predict that these transient are the outcome of very energetic BH forming explosions of very massive stars (30-50 $M_{\odot}$) which eject large amounts of ^{56}Ni (0.3-0.5 $M_{\odot}$). Direct evidences of aspherical explosions come from the late-time observations of Type Ic SNe (Mazzali et al. 2005), as well as from the large measured polarization (Leonard et al. 2005), giving an important role to the asymmetries in the explosions. Interestingly, not all broad-lined Ic are accompanied by a GRB (e.g. SNe 2002ap Mazzali et al. 2002, or SN 2003jd Valenti et al. 2007). These SNe have smaller luminosity, mass of the ejecta and explosion energy than the GRB-SNe, but it is not clear whether the non-detection of the GRB is a geometric effect due to the asymmetries or an intrinsic properties of the explosion/progenitor.

- **SNe IIb** belong to a class that denotes a spectroscopic transition from the type II to the type Ib: at early time spectra show prominent H lines,

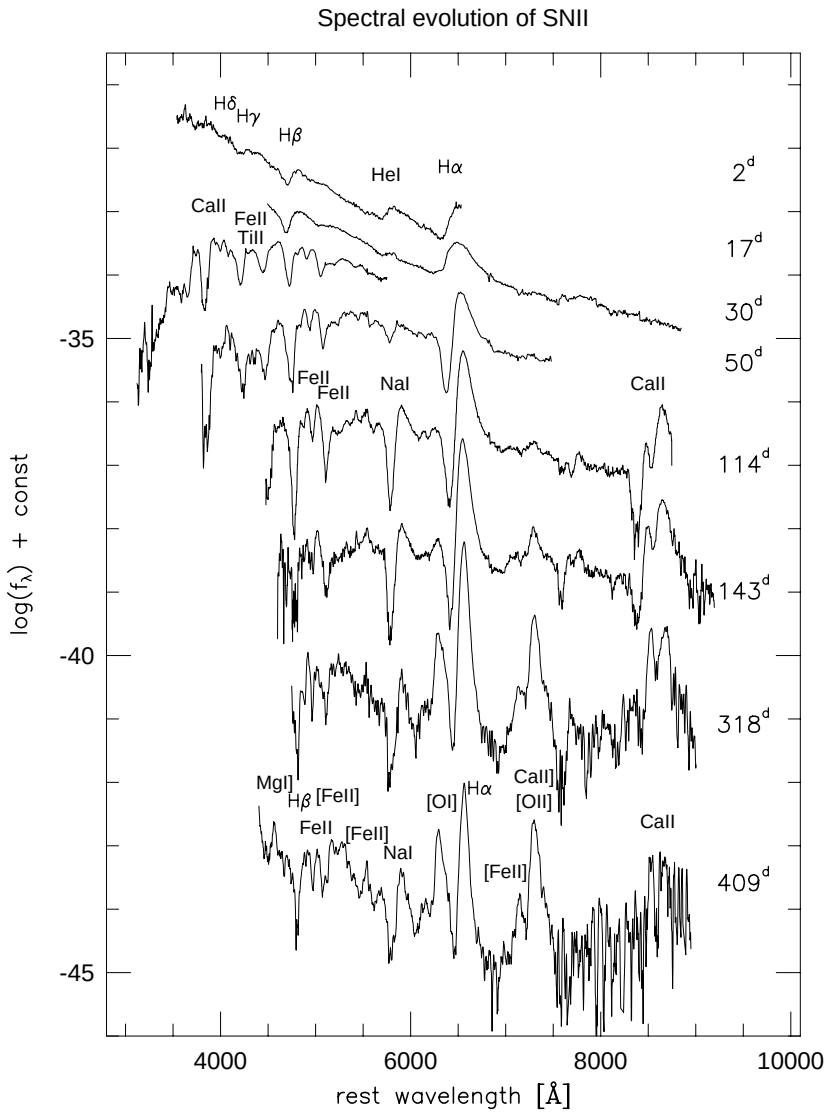

Figure 1.12— Spectroscopic evolution IIP SN 1992H (Clocchiatti et al., 1996).

but these disappear with time, while stronger He I $\lambda\lambda$ 5876, 6678 and 7065 lines develop. The progenitor stars of SNe IIb are expected to have lost most of their mass before explosion; however, the released H-rich CSM lies in the proximity of the exploding star. An important representative supernova of this class SN 1993J in M31, which is the best studied SNe ever (Barbon et al. 1995; Matheson et al. 2000a)

- **SNe II** do show H in the spectra. For this reason they are commonly associated with late-type galaxies and recent star formation regions. As it will be shown in the next Chapter, the progenitors of CCSNe may span a large range of masses. The precursors of type **IIP SNe** are supposed to have not suffer significant mass loss phenomena before the explosion, and therefore no ejecta-interaction signatures are reveled by the spectra even at late-times (Fig. 1.12). On the contrary, stars exploding as **IIL SNe** are thought to have their H envelope partially removed by the winds (still, less than IIb SNe). In this case the nebular spectra may show hints of interaction [e.g. SN 1979C, Montes et al. (2000)]. The other extreme is represented by the SNe of the IIn type, for which the interaction is dominant during the whole evolution, so that it is reasonable to assume that the progenitor was a very massive star that suffered copious mass-loss (cf. Chapter 2).

  Besides the Balmer lines, in SNe IIP/IIL also He I lines are visible for a few days after the explosion. Then other lines (e.g. Na I, Ca II, Fe II, Sc II, Ti II, Ba II, Sr II) become prominent during the late photospheric phase. At nebular phases, all CCSNe types appear similar. The spectra show strong H I (for type II), [O I], Ca II, [Ca II] and [Fe II] emission lines. **IIn** SNe are characterized by a slow spectral evolution, dominated by strong Balmer emission lines without the characteristic broad absorptions or P-Cygni. The early time continua are very blue, He I emission is often present and, in some cases, narrow Balmer and Na I absorptions are visible corresponding to expansion velocities of about 1000 km s^{-1} (Pastorello et al., 2002). Unresolved forbidden lines of [OI], [OIII], and of highly ionized elements such as [FeVII], [FeX], and [AX] are sometimes present.

1.6 Interacting supernovae

Interacting SNe deserve a special mention, since the SNe that will be discussed in this thesis were also classified as "IIn", though they present other peculiar properties. In general, latetime signatures of interaction with a CSM are frequent also among other SN types and they are detectable when the other

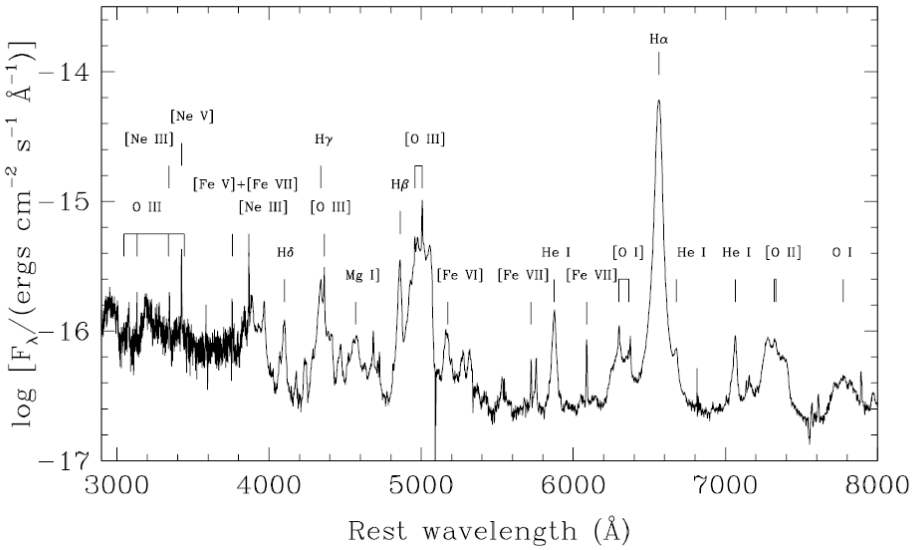

Figure 1.13— Combined HST and Keck spectra of SN 1995N at a phase of 943 days (Fransson et al. 2002, ApJ, 572, 350). The strongest emission lines are identified. Through spectral modeling, 3 distinct kinematic components could be identified, likely powered by the X-rays from the interaction of the ejecta and the circumstellar medium of the progenitor. While the narrow lines come from unshocked circumstellar gas and the intermediate-velocity component from processed ejecta, the high-velocity are related to an either clumpy or asymmetric CSM.

sources of energy powering the SN fade (Pastorello et al. 2003). As mentioned, this may occur more frequently in SNe IIL and, occasionally, also in SNe IIP. An example is SN 1987A which, from HST images, shows unequivocal evidences of interaction with the circumstellar rings (Groningsson et al. 2003).

Especially for the subclass of type IIn SNe, mass loss during the progenitor pre-explosion phase is a key parameter. In fact, the CSM structure, density and kinematics strongly affect both the SN spectroscopic and the photometric evolution. Typical mass loss rate are in the order of $10^{-6} - 10^{-5}\,\mathrm{M}_\odot\,\mathrm{yr}^{-1}$, but this value may change significantly, as we will see in Chapter 2, depending on several factors. The density profile and the distance of the CSM play also a major role.

Soon after explosion, the spectra of SNe IIn are characterized by the presence of strong, narrow Balmer emission lines on top of broader emission lines (Fig. 1.13). It is generally believed that narrow lines of SNe IIn originate from the reprocessing of radiation generated when the high velocity SN ejecta vio-

lently impact on a relatively dense, surrounding gas released by the progenitor star. The collision causes the conversion of part of the ejecta kinetic energy into radiation. This interaction generates forward and reverse shock waves which bound the shock wind and SN ejecta (Chevalier & Fransson 1994, Fig.1.14). Sometimes the pressure and temperature behind the shock are sufficiently high that the post-shock ejecta and CSM may become powerful X-rays emitters. At the same time synchrotron radiation is generated by electrons accelerated up to relativistic energies at the shock front. The forward shock produces a very hot shell ($\sim 10^9$K), while the reverse shock produces a denser, cooler ($\sim 10^7$K) shell with much higher emission measure, from which the X-rays emission arises.
Despite the apparently complicated CSM configuration, precious information on the SN environment can be derived from optical spectra, whose most intense line in emission is Hα : by studying its multi-component profile it is possible to reconstruct the kinematic and structure of the gas surrounding the star both in pre- and post-explosion phase. Its intermediate component traces the kinematic of the slower, smaller radiating layer, having a velocity of a few hundreds of km s^{-1} . The broadest component has a velocity of a few thousand of km s^{-1} and it is normally associated to the SN ejecta, which achieve radii of 10^{13}cm a few weeks after explosion; a broad component is seen also in the emission lines intermediate mass elements, as OIII and CaII, which lie in the inner part of the ejecta.

The very narrow feature on top of Hαline, which sometimes shows a P-Cygni absorption, is indicative of the kinematics of the unperturbed CSM shed by the progenitor. Its velocity spans from a few tens to a few hundred of km s^{-1} , and typically increases with progenitor star mass, being about 10-20 km s^{-1} , 20-40 km s^{-1} and 100-200 km s^{-1} for AGB, RSG and LBV winds, respectively (Smith et al. 2007). Very narrow emission lines can be recognized also in Fe group lines (Salamanca et al. 2002) , likely being caused by the photoionization of the CSM by the UV and X-ray photons produced during the initial supernova flash.
Depending on the CSM density distribution, the strong CSM-ejecta interaction may last for months (e.g., SN 1994W) to years (e.g., SN 1988Z, SN 1995N, SN 1995G). In fact, if the mass of the CSM is of the same order of the ejecta mass, the outer material can cause a significant deceleration of the ejecta, with a very efficient conversion of kinetic energy into internal and radiative energy. This explains the photometrically slow evolution, especially at early phases. Of course, more-luminous SNe require progenitors with higher mass-loss rates or slower wind speeds. To account for some of the most-luminous SNe IIn detected (SN 2005ap, Quimby et al. 2007; SN 2006gy, Smith et al. 2007, 2008, Agnoletto et al. 2008; SN2006tf, Smith et al. 2008b), inferred progenitor mass-loss rates

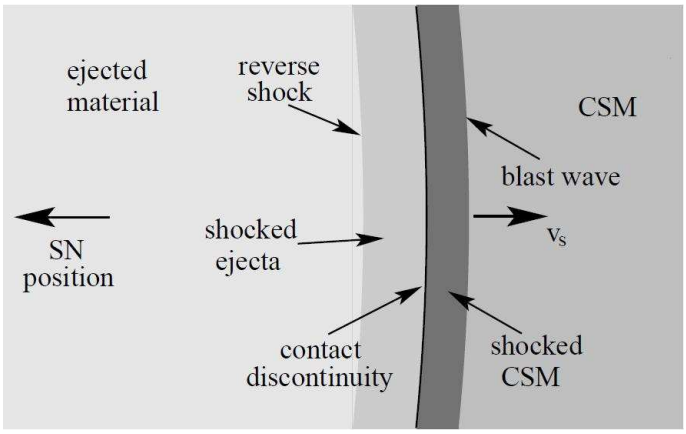

Figure 1.14— Schematic view of the circumstellar environment of a massive star, at the time of SN ejecta impact. The collision generates a forward and a reverse shock, which may emit at X and radio wavelengths. Optical emission is mostly concentrated at Hα line, and its profile reflects the kinematic of the different emitting layers. The intermediate component originate from the shocked CSM. The broadest one is attributed to the SN ejecta. The narrowest component forms in the outer zones, where the stellar wind (CSM) is still unperturbed.

need to be much higher, i.e. in the order of $0.1\,M_{\odot}yr^{-1}$ or higher (Chugai et al. 2004, Smith et al. 2008). Such rates have to be assumed also for the so-called "SNe impostors" (SN 1999bw, Filippenko et al., 1999a; SN 2002kg, Schwartz et al. 2001; SN 2003gm, Patat et al., 2003). These objects show spectra with narrow Balmer emission lines resembling those of typical SNe IIn (Filippenko, 2000), but they are underluminous and show very peculiar and unforeseeable photometric evolution. They are thought to be not genuine SN explosions, but luminous outbursts of the external shells of massive stars, similar to η Carinae, because the progenitor star likely survives to the burst.

The prototype SN of the IIn type is SN 1988Z (Stathakis and Sadler, 1991; Turatto et al., 1993b; Aretxaga et al., 1999). The luminosity of this SN was powered by the interaction ejectaCSM for a long time, and the evolution of this objects was followed at all wavelengths for about 10 years after discovery (Aretxaga et al., 1999). However, because of the large number of possible initial configurations of the star+CSM system, type SNe IIn are observationally very heterogeneous. This includes ejecta mass, explosion energy, mass loss rates and synthetized ^{56}Ni mass. Nevertheless, through the combination of light curves and spectral analysis, SNe IIn offer us the rare opportunity to determine the

composition, structure and kinematics of the SN environment, as it was successfully done for SN 1987A (Groningsson et al. 2008).

CHAPTER 2

Massive and Very Massive Stars

2.1 Evolution and fate of massive stars

Massive stars started forming about 400 millions years after the Big Bang and ended the dark ages by re-ionizing the Universe. They therefore played a key role in the early evolution of the Universe. Understanding the properties and the evolution of the first stellar generations allows to determine the feedback they had on the formation of the first cosmic structures.

The evolution of stars is governed by three main parameters, which are the initial mass, metallicity (Z) and rotation rate. The evolution is also influenced by the presence of magnetic fields and by a close binary companion. For massive stars around solar metallicity, mass loss plays a crucial role, in some cases leaving only a 10-20 $M_{\odot}$ envelope.

To clarify the role of these parameters, precious information can be derived through the study of core-collapse supernovae which, as seen in Chapter 1, mark the fate of stars more massive than 8 $M_{\odot}$. Once the relationship between massive star evolution and the type of SN observed is established, CCSNe can become our best probe of mass loss, circumstellar structure, stellar evolution, rotation and star formation rates throughout cosmic time.

Although the fate and evolution of stars depend on several factors (e.g. binarity, mass loss, metallicity, rotation), a rough classification scheme may be based on the initial mass or main sequence mass, as follows:

2.1.1 Stars with mass $8\,M_\odot < M < 35\,M_\odot$

According to the most recent estimates, based on the mass calculations of SN progenitors identificated in the pre-explosion images [44, 46, 54], the minimum mass that can produce a core-collapse is $8^{+1}_{-1.5}M_\odot$.

Once the star has formed, its center generally evolves to increasing central density and temperature. This overall contraction is interrupted by phases of nuclear fusion of H to He, He to C and O, then C, Ne, O and Si, until finally Fe is produced and the core collapses. Each fuel burns first in the center, then in a shell. The time scale for He burning is much shorter than that of H burning, mostly because of the lower energy release per unit mass. However, the time scale of the burning stages beyond central helium-burning is radically reduced by thermal neutrino losses that dissipate energy, instead of transporting it to the stellar surface. These losses increase with temperature, roughly proportionally to T^9. When the star has built up a large enough Fe core, exceeding its Chandrasekhar mass, it collapses to form a neutron star (NS) or a black hole (BH). A SN explosion or a GRB explosion may result.

Except for the pair-instability supernovae regime (cf. Sect. 2.1.3), the explosion of massive stars leave behind compact remnants (see Fig.2.1 for the IMF and SN remnant at Z=0, from Heger et al. [22]). Up to an initial mass of 20-25 $M_\odot$ typically neutron stars (NS) result [14]. The layers above the NS are ejected, consisting of the ashes of the preceding hydrostatic stellar burning phases and explosive burning products. At higher masses a large fraction of the core can fall back onto the NS after the explosion has first driven the matter outward [15]. If the resulting remnant mass exceeds the maximum mass for a NS, it collapses to a BH (Zampieri et al. [60] and reference therein).

2.1.2 Stars with mass $35\,M_\odot < M < 100\,M_\odot$

Above 20-40 $M_\odot$ the role of mass loss, due to stellar winds, is non negligible [39] and it may become so strong that, after the RSG stage, the entire H envelope is lost prior to explosion of the star. The exact mass for when this happens depends on several factors, e.g., the mass loss rates and the initial stellar rotation.

Once massive stars have lost their H envelope, they become He stars or Wolf-Rayet (WR) stars. Also at this stage the mass loss is known to be large, but its rate is again quite uncertain. Wolf-Rayet stars can release products of central He burning, like C and O, by stellar winds before explosion or even if they do not explode. Such objects are denoted as WC and WO stars, respectively.

For a 60 $M_\odot$ star, we expect that the evolutionary sequence is

O→BSG→RSG→WR. However, the most massive stars may lose mass so fast that they never evolve to the RSG stage, but instead evolve as luminous blue variable (LBVs) and then directly to the WR stage, in the sequence O→LBV→WR. This issue will be discussed more in detail in Sect. 2.2.

Concerning their fate, for masses above 35 $M_\odot$ the fate of these stars is similar to that of less massive stars except that the mass at core continues increasing. Massive stars may form NS or BHs by fall-back. However, as the He core mass at core collapse increases depending on the metallicity, eventually a successful supernova shock cannot be launched due to ram pressure caused by the early strong infall of the increasingly larger O and Si core masses. A BH forms directly and no supernova explosion should occur [22].

2.1.3 Stars with with mass $100\,M_\odot < M < 140\,M_\odot$

Above a He core mass of ∼60 $M_\odot$, nuclear-powered and opacity-driven pulsations occur, with the effect of increasing the mass loss (the so called "k" and "ϵ" mechanisms, [22]). However, such mechanisms are apparently suppressed on extreme Population III stars [5]. Therefore, it is reasonable to assume that at sufficiently low metallicity ($Z/Z_\odot \sim Z^{-4}$) very massive stars do retain most of their mass through the end of central He burning, forming a massive He core. Zero-metallicity stars above 100 $M_\odot$ are radiation-pressure-dominated; for temperatures in excess of 10^9 K, a large amount of thermal energy goes into making the masses of an increasing abundance of electronpositron pairs in the core rather than providing pressure. This can decrease the adiabatic index below 4/3 and destabilize the core [28](Fig. 2.2, right). As a consequence, for stars with an initial mass above ∼140 $M_\odot$, rapid contraction may occur, followed by a thermonuclear explosion. Such explosions are denoted as "*pair-creation supernovae*" (PCSNe) or "*pair-instabilities supernovae*" (PISNe). However, for masses in the range $100<M_\odot<140$ the energy released by the explosive burning is inadequate to unbind the entire star [22, 58]. It suffices, however, violently to eject many solar masses of surface material, including all that is left of H envelope, in a series of giant "pulses". Each pulse may result in a SN display [58], which is then called "*pulsational pair instability supernova*". The typical binding energy for the H envelope of such massive stars is only ∼0.1 to 1×10^{49} erg, whereas the energy of a pulse is $\sim 110 \times 10^{49}$ erg, so that the envelope is easily ejected in the first pulse.

The outer layers, the H envelope and possibly part of the He and CO core (especially at the high-mass end of the regime) are ejected. These pulsations continue until the star has lost so much mass or decreased in central entropy

that it no longer encounters the pair instability before forming a Fe core in hydrostatic equilibrium. Since the Fe core mass is large and the entropy high, such a star probably finally make BHs. These stars will not have a H envelope at the time of collapse, but the ejecta may still be close by [21, 58].

2.1.4 Stars with mass $140\,M_\odot < M < 260\,M_\odot$

For initial masses from 140-260 $M_\odot$ (corresponding to an He core mass of $64-133$ $M_\odot$) the explosion energy of the first pulse is already sufficient to entirely disrupt the star. A PISN occurs. In this case no remnant remains and all the metals are ejected. These SNe release energies ranging from 3×10^{51} erg (i.e. 64 $M_\odot$ He core) up to almost 100×10^{51} erg (i.e. 133 $M_\odot$ He core, [25]) - enough to disrupt a small proto-galaxy. More than 50 $M_\odot$ of radioactive ^{56}Ni may be ejected. These are the most powerful thermonuclear explosions in the universe [**?**].

Since stars of lower mass (<140 $M_\odot$) or higher mass (> 260 $M_\odot$) collapse into BHs without significant heavy element creation, pair-instability SNe may be considered a "clean" source of nucleosynthesis in the sense that neighboring mass ranges do not "pollute" the sample [24].

PISNe are supposed to be particularly frequent at very high redshift; at z = 20, the rate of pair-creation supernovae is calculated by Heger et al. [24] as $\sim$0.16 events per second, i.e., $3.9 \times 10-6$ events per second per square degree. The photometric evolution of these objects has been modeled by Scannapieco et al. [43], which have predicted a very bright, broad peak, followed by a luminosity decay which follows the decay of ^{56}Co into ^{56}Fe, due to high amount of ^{56}Ni produced in the explosion. Heger et al. [22] have calculated that, at z = 20, the first peak of the light curve (from the shock breakout) would last for about a month; the second, broad peak (plateau), probably brighter in the far infrared, would last for about 10 yr. Statistically, at any time there should be about a dozen of these supernovae per square degree at the peak of the light curve, and more than 1000 in the plateau phase of the light curve.

For this reason, we may expect that PISNe will be primary targets for the next generations telescopes. Apparently, signals of PISNe have already been detected at to z = 2 [8].

2.1.5 Stars with mass $M > 260\,M_\odot$

Above initial masses of 260 $M_\odot$ photo-disintegration of alpha-particles (which themselves are already the result of photo-disintegration of Fe group elements which were made in Si burning) reduces the pressure enough that the collapse

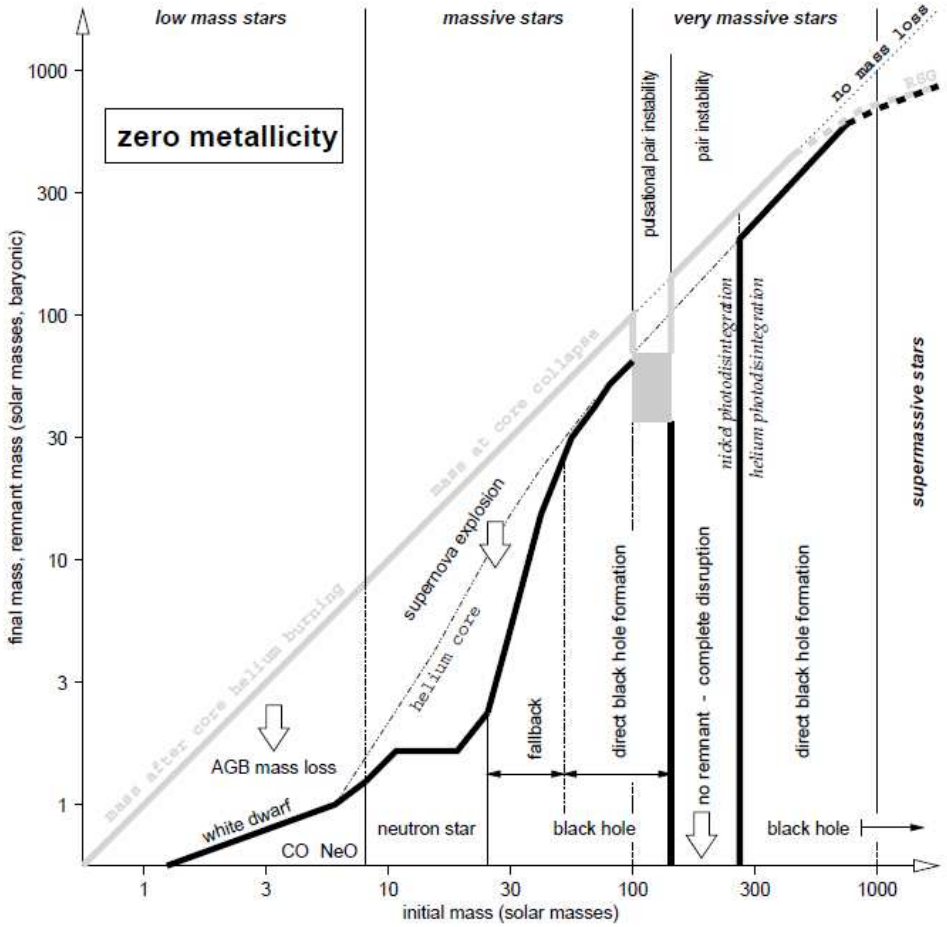

Figure 2.1— Expected initial mass function for "Population III" stars [24]. The thick black curve denotes the final mass and the mass of the compact remnant. The thick gray line refers to the mass of the star before producing the remnant. Since at Z = 0 no mass loss is expected (except for the pair-instability regime), the grey curve is approximately the same as the no-mass-loss-line, traced with a dotted line. The effects of rotations are not taken into account in this scheme.

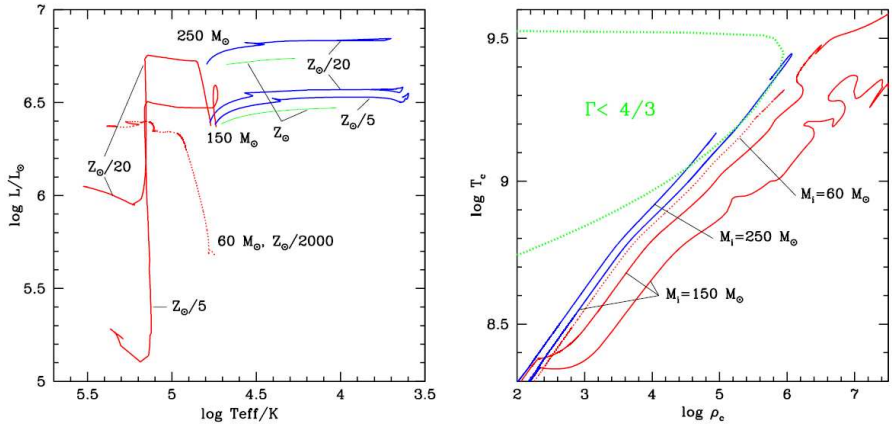

Figure 2.2— *Left*: Stellar evolutionary tracks computed by Langer et al. [31], from main sequence to pre-SN. The red lines denote stars that rotate rapidly and evolve quasi-chemically homogeneously until the Fe collapse. Blue lines represent slow rotators, which become yellow hypergiants after the main sequence evolution. Furthermore, solar metallicity tracks for 150 $M_\odot$ and 250 $M_\odot$ are shown with green lines; they end during core H burning, when their surfaces become unstable.

of the star is not turned around but directly continues into a BH [22].

2.2 Mass-loss

As we have seen, mass loss plays an important role in the evolution of massive stars, especially in the regime beyond 25 $M_\odot$. Not only does it reduce the mass of the star, but also affects its convective core size, temperature, angular momentum and its luminosity. Hence, the amount of mass loss affects the star's evolutionary track and its time on the main-sequence phase [50]. The mass of the H envelope is crucial for the light curve of the SN. An understanding of the mass loss processes is therefore central for the SN taxonomy.

Because mass loss increases with luminosity and mass, $\dot{M} \propto L \propto M^{-2,-3}$ [39], the effects are most important for the most massive stars. Moreover, the properties of the winds that shed the outer stars' envelopes vary dramatically between the different evolutionary stages. In particular, the wind velocity scales roughly with the escape velocity of the star, which varies by a factor of about a hundred between the BSG, RSG, and WR phases.

In the blue supergiant (BSG) MS phase the winds are radiatively driven through momentum deposition from absorption of the photospheric radiation

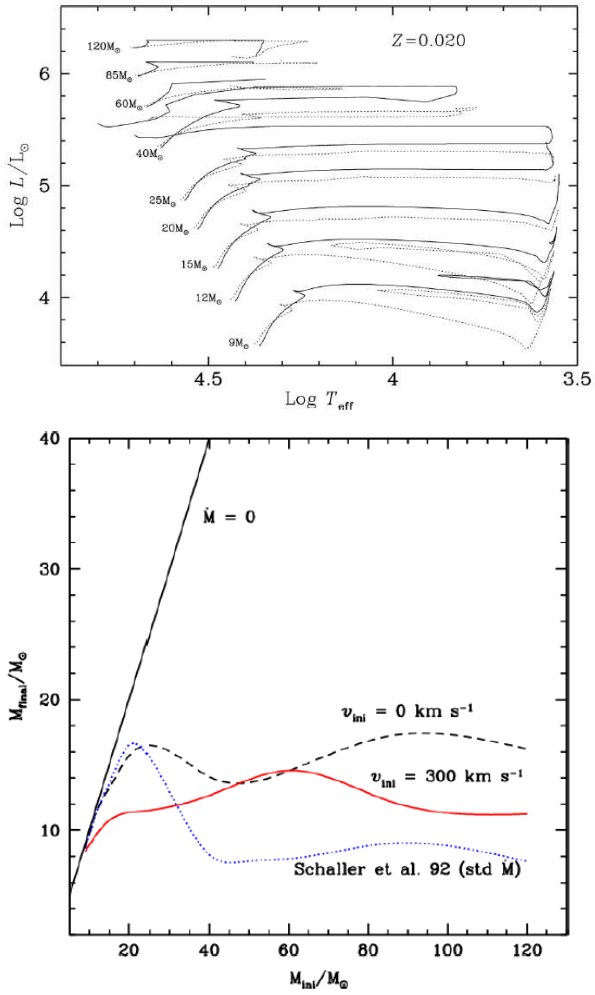

Figure 2.3— *Top*: The effects of rotation and mass loss on the final mass of massive stars at solar metallicity. The solid line gives the final mass for a ZAMS rotational velocity of 300 $\mathrm{km\,s^{-1}}$, while the dashed line gives the zero velocity result, only including mass loss [37]. *Bottom*: Evolutionary tracks for stars more massive than 9 M with (solid lines) and without rotation. [37].

by the many resonance lines in especially the UV and far-UV. This is a fairly well understood process both theoretically and observationally. The mass loss rates of BSGs are in the order of $10^{-6} - 10^{-7}\,\mathrm{M_\odot\,yr^{-1}}$. In addition, since the wind velocity is roughly the same as the star escape velocity, the winds from these relatively compact objects are very fast with velocities in the range of 1000-3000 $\mathrm{km\,s^{-1}}$.

The driving mechanisms behind the winds during the post-MS phases are less well understood. In red supergiants (RSG) the absorption of the radiation by dust is believed to account for most of the momentum input. What initiates the wind (e.g., photospheric shocks connected to pulsations) is, however, not known. The formation of the dust probably takes place in a similar way as in lower mass AGB stars.

Further, it is likely that the star experiences a superwind phase, lasting $\sim 10^4$ years, in the very last phases of the RSG stage. What drives this superwind is somewhat unclear, but pulsational instabilities may be particularly important [23]. Typical mass loss rates are in the general RSG phase of the order of $10^{-6}\,\mathrm{M_\odot\,yr^{-1}}$ [33]. In the superwind phase mass loss rates are as high $10^{-4} - 10^{-3}\,\mathrm{M_\odot\,yr^{-1}}$ [6]. The duration of this phase must obviously be only of the order of a few times 10^4 yrs. Because of their large extension, and hence low escape velocity, the winds are slow with velocities of only 10-50 $\mathrm{km\,s^{-1}}$. As it will be discussed in Sect. 2.5, LBV stars suffer the stringest mass-loss rates, which reach $0.1 - 1\,\mathrm{M_\odot\,yr^{-1}}$ [50]; the winds have velocity in the order of 100-200 $\mathrm{km\,s^{-1}}$.

Finally, in the Wolf-Rayet (WR) phase the wind velocities increase to 2000-5000 $\mathrm{km\,s^{-1}}$, while the mass loss rate is $10^{-5}\,\mathrm{M_\odot\,yr^{-1}}$. The driving of the wind is here to a large extent radiation on resonance lines, as in the OB star case. The initiation of the wind is, however, not clear, and pulsations may be important for this.

Observationally, clumping of the wind is important, with a typical clumping factor of about two [16, 20] .

2.3 Rotation

Observationally, it is known that massive stars on the main sequence are rotating rapidly. Typical surface velocities are $\sim$200 $\mathrm{km\,s^{-1}}$. Because of convection, rigid rotation is likely to be established on the main sequence; thanks to the convection and the Eddington-Sweet circulation in radiative layers, angular momentum can be transported outwards [41].

Rotation affects the evolution in several ways.

First, rotation induces circulation and mixing of the stellar interior in a way resembling that of increased convection: nuclear burning products may become visible at the surface already in the H and He burning stages. This is most apparent from the presence of CNO burning products already on the main sequence and He burning stages. For the more efficient mixing, in a rotating model products of the CNO processing (^{14}N) will be visible already in the BSG stage. Such stars are expected to evolve and collapse as Wolf-Rayet WC star, with a large ^{12}C abundance from He-burning in the rotating case. As a consequence of the increase in the abundance of the products of the CNO cycle in the outer layers, the opacity, and therefore the mass loss, will grow.

The second effect of rotation concerns the change in the star form. In fact, because of the centrifugal force the rotating star becomes oblate. The larger radius in the equatorial plane leads to a lower effective temperature and flux compared to the polar direction. Therefore, in the latter direction the luminosity and the mass loss will be higher.

For the conservation of angular momentum this implies that during the evolution to the RSG stage the angular velocity decreases dramatically. The core, however, increases its angular velocity because of contraction, and may end up rotating close to the critical velocity. Angular momentum may, however, be lost in especially the RSG and in the WR phase due to mass loss. The efficiency of this depends sensitively on the magnetic field [36].

In Fig. 2.3 the evolutionary tracks in the HR diagram with and without rotation are shown. It is evident that especially for the most massive stars the late evolution is substantially altered by rotation. For non-rotating stars the lower mass limit to evolve to a WR-star is 37 $M_\odot$. With rotation, even a 22$M_\odot$ star evolves all the way to the WR stage, rather than ending its life as a RSG. This is also the case for stars more massive than this. Thanks to rotation the most massive stars with M $>$ 60 $M_\odot$ may skip even the LBV phase, and evolve directly from the MS to the WR phase. Because of the increased mass loss rate in the rotational case, the final masses of the stars at the beginning of C burning will in general be smaller than in the non-rotational case. The life time in the WR phase will also increase by a factor of about two. For a non-rotating 60 $M_\odot$ star the total life time is 4.0 Myrs, of which 0.37 Myrs are spent as a Wolf-Rayet star. The corresponding numbers for a star with main sequence rotational velocity of 300 km s^{-1} are 4.67 Myrs and 0.75 Myrs, respectively.

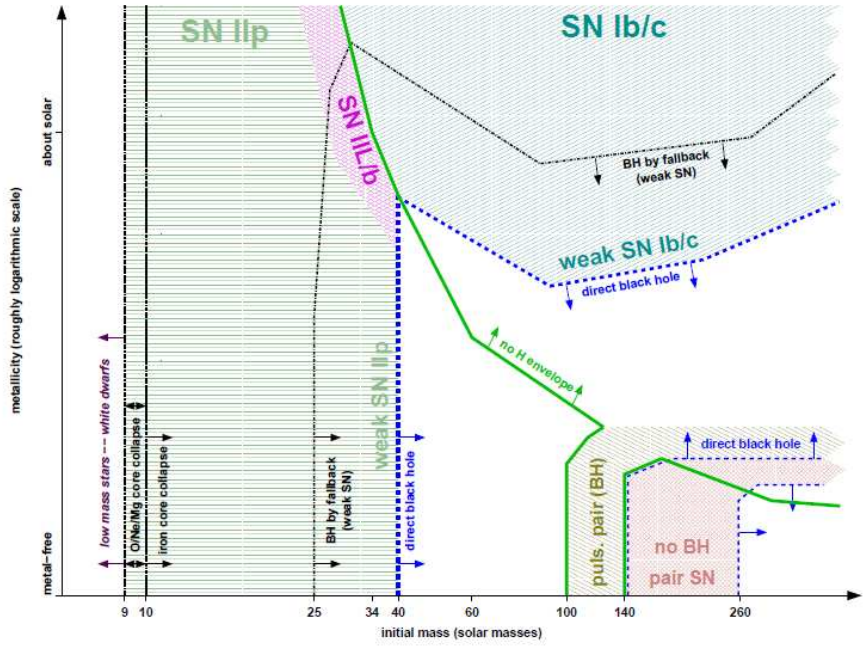

Figure 2.4— Supernova population diagram showing the evolution of massive stars as a function of initial mass and metallicity [22].

2.4 Metallicity, mass-loss, rotation & the supernova display

Wind driven mass loss is also found to be dependent on the metallicity. The exact scaling of mass loss with the metallicity is likely to depend on the evolutionary stage of the star, but is normally assumed to follow $\dot{M} \sim Z^{(0.5-0.7)}$ [30] Thus, stars with low metallicity suffer to a lower extent from mass loss and have therefore larger He cores and H envelopes at the end of their lives. The opposite is true for high-metallicity stars, where the radiation pressure in the envelope is higher.

A schematic view which illustrates the different SN outcome with varying metallicity is shown in Fig. 2.4.

In SNe of type II the mass of the star He core governs the evolution and fate, whereas the H envelope determines much of the SN spectral features and the shape of the light curves. Stars that end their lives as moderate mass RSGs (up

to 25 $M_\odot$) with a massive H envelope (>2 $M_\odot$), will result in a type IIP [45]. If, however, the metallicity is low enough, type IIP SNe are also possible in the mass range of 25−40 $M_\odot$. Such events are expected to be faint because of the fallback of the inner layers of the core (see Fig.2.4).

Stars with a less massive H envelope (<2 $M_\odot$) will end their lives either as a type IIL or as a type IIb SN. Since the mass loss needs to be strong enough to remove a substantial part of the H envelope in order to produce Type IIL/b, a single star with at least a moderate metallicity as well as a high initial mass (<25-40 $M_\odot$) is needed. According to the predictions of Heger et al. [22], the majority (∼90%) of the massive single stars are, forming SNe of type II and out of these, the majority will produce normal type IIP. Only a minority (< 10%) of the Type II events will, depending on the metallicity, either produce scaled down type IIP or type IIL/b SNe.

For type Ib/c SNe the entire H envelope is removed prior to explosion, making the observational features sensitive to the He core mass of the progenitor. Clearly, a single star resulting in a type Ib/c must meet the conditions of having both a high metallicity and a high initial mass. For a non-rotating star with solar metallicity, the mass has been estimated to be <34 $M_\odot$ [59].

Instead, for subsolar metallicities, many of the Ib/c SNe would leave behind a BH by later fallback and are therefore expected to be sub-luminous, as is the case of type IIL/b.

To reduce the He core enough for luminous type IIL/b to be formed from a non-rotating single star, the metallicity would have to exceed solar. Bright type Ib/c could, however, also be formed for a metallicity slightly less than solar if the progenitor's initial mass exceeds 60 $M_\odot$. One would therefore expect that these types of SNe are in most cases likely to be produced in binary systems were mass transfer through Roche lobe overflow occurs. In fact, this is a well-known channel to form Wolf-Rayet stars which, in turn, are the progenitors of type Ib/c events. Notice however, that fast rotating stars the mass loss is enhanced, therefore the metallicity needed in order to produce type IIL/b and type Ib/c is reduced: for stars with rotation and solar metallicity, a lower mass limit of 22 $M_\odot$ has been estimated [36]. As a result, one would expect more of these types of SNe to be strong explosions and fewer of these events to produce BH from fallback.

Only at extremely low metallicities, where the cooling processes that govern star formation are greatly reduced and the effects of magnetic field and turbu-

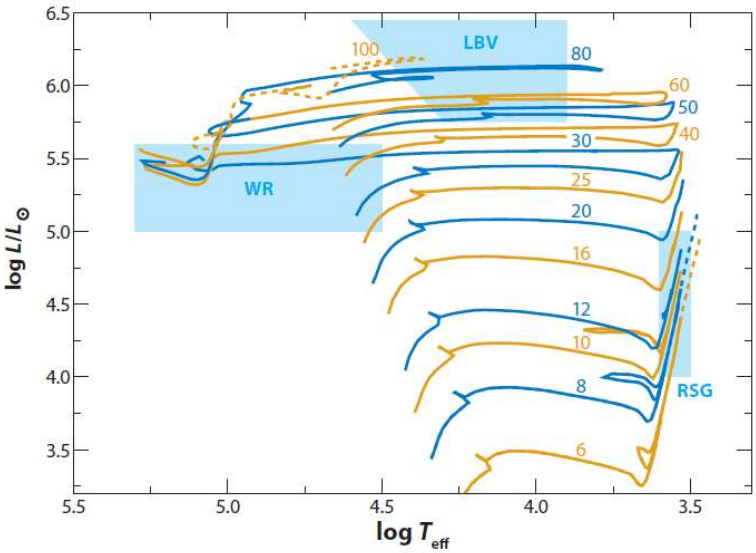

Figure 2.5— The Hertzsprung-Russell diagram of the STARS evolutionary tracks [11]. The blue, upper region denote the expected location of the LBV stars according to the predictions of Smith, Vink & De Koter (2004). The position of the WR and RSG stars is also marked.

lence are less important, stars are expected to evolve to masses larger than 100 $M_\odot$ without experiencing heavy mass losses. As seen in Sect. 2.1.3, these stars produce pairs inside the core and may experience giant pulsations. The kinetic energy of the pulses is of the order of or even more than a normal SN but they will be less bright since they lack any radioactive material to power the light curve. However the collisions between shells of material can eventually produce a SN display [58].

The exact thresholds of metallicities below which stars may undergo such instabilities have been recently investigated by Langer et al. [31]. Due to rotation, two possible channels for the precursors of PISNe are evidenced. According to their calculation, slowly rotating massive stars produce PISNe for initial masses in the range 140 $M_\odot$ to 260 $M_\odot$ in the yellow supergiant phase (Heger & Woosley 2002) and for $Z/Z_\odot \sim 1/3$; rapid, chemically evolved [59] rotators do so for initial masses above 80 $M_\odot$ and for $Z/Z_\odot < 10^{-3}$. I will come back to this in Chapter 6.

2.5 LBVs and the problem of mass loss in supermassive stars

Though an observational evidence is still lacking, the presence of extremely massive stars (even $\gg$200 $M_\odot$) is theoretically predicted in the primordial Universe at Z=0, where the Jeans mass may have been as great as $\sim$1000 $M_\odot$ [32] and where the initial mass function (IMF) either peaks at 100 $M_\odot$ [2] or is bimodal [38].

In the local Universe the most massive stars known are the Luminous Blue Variables stars (LBVs, cf. Fig.2.5), which have masses in the range 80$-$120 $M_\odot$. LBVs, also known as *S Doradus* variables, are very bright ($5.5 < \log(L/L_\odot) < 6.0$, [27]), blue, hypergiant variable stars named after S Doradus (SD), the brightest star of the LMC. They exhibit periodic changes in brightness, punctuated by occasional outbursts of substantial mass loss. Their types of variability that can be divided into three categories: *(i)* small-amplitude ($\sim$0.1 mag) "micro" variability, which is common amongst BSGs; *(ii)* "moderate" S Doradus variations of $\sim$1-2 mag (SD phases), and *(iii)* truly "giant" eruptions, of which P-Cyg and Eta Car are the best-known examples. The timescales for the SD-phases are either of <10 years ("short" SD phase) or > 20 years ("long" SD phase, [57]).

Stellar evolutionary theory predicts that LBVs have the largest allowed mass by gravity: if they were any larger, gravity would be insufficient to balance the radiation pressure and they would blow away the excess mass through stellar wind. As they are, they barely maintain hydrostatic equilibrium because their stellar wind constantly ejects matter. For this reason there are usually nebulae around such stars, created by these outbursts; Eta Carinae is the nearest and best-studied example [19, 34]. As explained in Sect. 2.1.2, after having completely shed their outer envelope, LBVs are supposed to become WR stars and eventually explode as Ib/c SNe. Note on this point that while the maximum initial mass is thought to be $\sim$150 [1], WR stars do not have masses in exceed of 20 $M_\odot$ [9]. Thus, very massive stars are supposed to remove a burden of 30$-$130 $M_\odot$ during their lifetime before the WR phase. This would mean that the mass-loss must be especially efficient during these late-evolutionary stages. Alternatively, one could tentatively assume that LBVs may somehow be able to explode as supernovae *before* having completely depleted their outer H envelope.

Indeed, the latter possibility was invoked by several authors in the last few years: the properties that were inferred to some CCSN progenitors do have

features which are commonly attributed to LBV stars (e.g. wind velocity, CSM density or structure).

As an example, Kotak & Vink [29] have analyzed the quasi-periodic deviations, from the expected power-law decline, reported for about a dozen of typee II and Ibc SNe [52]. They have interpreted the deviations of the SNe 2001ig and 2003bg as due to the ejecta interaction with the progenitor star's surrounding gas shells, which were ejected in a S-Doradus type variability. This would imply that the progenitor experienced a LBV phase immediately before the collapse.

For the type Ib SN 2006jc the progenitor was claimed to be a WC or WO star embedded in a He-rich CSM [13, 42], which underwent a heavy outburst about two years before the explosion. Interestingly, an outburst had been never associated to a WR before. In this sense, SN 2006jc may represent the first observed example of a star transitioning from the LBV phase to the WR through sporadic mass ejections, and may confirm the presence of big gaps in our knowledge of the mass-loss physics of evolved stars.

Also for SN 2005gj the analysis of the spectroscopic data led Trundle et al. [53] to suggest a LBV progenitor, in order to explain the multiple components in the absorption trough of Hα . Furthermore, for SN 1997eg, the properties of the dual-axis environment derived by Hoffman et al. [26] are found to be consistent with the CSM of stars in the LBV stage.

More recently, a SN progenitor with a luminosity consistent only with that of LBVs, i.e. $L/L_{\odot} \sim 10^6$, was serendipitously detected in archival HST images by Gal-Yam et al. [17]. Indeed, the IIn SN 2005gl showed spectroscopical evidence of ejecta-interaction with a circumstellar shell, as well as of high-velocity winds (~ 450 km s^{-1}), which are too fast if compared with the standard RSGs environments.

These features were also unequivocally detected in the spectra of the ultraluminous IIn supernovae like 2006gy [49] and 2006tf [48] (cf. Chapter 4 and 5). Such events, whose number has remarkably increased in the last 4-5 years, have lead to reconsider the problematic of winds and mass-loss surrounding massive stars. One important clue is that several lines of evidence point to the fact that winds of hot stars may be highly clumped, as several calculations had shown [12, 41]. This, in turn, means that mass-loss rates derived from density-squared diagnostics like Hα and radio continuum emission have severely (by a factor 3-10) overestimated the mass loss rates.

Therefore, as argued by Smith & Owocki [51], metallicity dependent line-driven winds of O stars do not shed enough mass in a stars lifetime and cannot account for the stripping of H envelopes that harkens the formation of WR stars.

On the other hand, the observations of stars like Eta Car prove empirically that in LBV the continuum driven eruptions are able to shed 10 $M_{\odot}$ or more in a single event. In some objects there is evidence for multiple shell ejections in timescales of 10^3 years. The extreme mass-loss rates of these LBV bursts imply that line opacity is too saturated to drive them, so they must instead be either continuum-driven super-Eddington winds [40] or hydrodynamic explosions [4]. Unlike steady winds driven by lines, the driving in these eruptions may be largely independent of metallicity, and might play a role in the mass loss of massive metal-poor stars.

Although LBV eruptions are rare, a number of extragalactic Eta Car analogs or "supernova impostors" have been observed , and some events seen as type IIn supernovae [35, 55, 56]. Furthermore, massive circumstellar shells have also been inferred to exist around supernovae and gamma-ray bursts (GRBs). Also for many radio bright IIn SNe a massive shell has been inferred (e.g. SN 1998Z, [3]; SN 1994W, [7]; SN1998S, [18]. These outbursts and the existence of massive circumstellar nebulae could indicate that giant eruptions like that of η Carinae may represent a common rite of passage in the late evolution of the most massive stars.

However, we cannot forget the possibility of *binary systems*; though more than 50% of the stars is supposed to have a companion, the effects of binarity are often forgotten by SN models. Eldridge et al. [10] have calculated that about 2−5% of WR stars will have companions in the LBV phase. Indeed, an explosion of a WR in a medium enriched by the outburst of a giant, erupting companion star would avoid inconsistencies with the current stellar evolutionary models. Though this rate is fairly low and could not be invoked for *all* the known IIn SNe (as argued by Smith [47]), at least the brightest IIn events could be explained (cf. Chapter 6). Note that the WR+LBV solution was also the preferred scenario by Pastorello et al. [42] for SN 2006jc.

In general, to determine the role and dynamics of winds in massive (and possibly binary) stars should be considered of the utmost importance. If confirmed, the existence of metallicity-independent phenomena would significantly affect not only the stellar evolution theory, but also the IMF at very high redshift, the enrichment of the ISM and the nature and rate of compact remnants, thus revolutioning our current picture of the primordial universe.

To this aim, the study of the properties of the most luminous IIn supernovae, directly linked to the supermassive stars can be extremely helpful.

Bibliography

[1]

[2] T. Abel, G. L. Bryan, and M. L. Norman. The Formation and Fragmentation of Primordial Molecular Clouds. *Apj*, 540:39–44, September 2000.

[3] I. Aretxaga, S. Benetti, R. J. Terlevich, A. C. Fabian, E. Cappellaro, M. Turatto, and M. della Valle. SN 1988Z: spectro-photometric catalogue and energy estimates. *Mnras*, 309:343–354, October 1999.

[4] D. Arnett, P. Young, K. A. Knierman, and J. R. Rigby. Boundary Conditions for Stellar Convection (invited review). In C. Charbonnel, D. Schaerer, & G. Meynet, editor, *Astronomical Society of the Pacific Conference Series*, volume 304 of *Astronomical Society of the Pacific Conference Series*, pages 342–+, 2003.

[5] I. Baraffe, A. Heger, and S. E. Woosley. On the Stability of Very Massive Primordial Stars. *Apj*, 550:890–896, April 2001.

[6] S. I. Blinnikov and O. S. Bartunov. Non-Equilibrium Radiative Transfer in Supernova Theory - Models of Linear Type-II Supernovae. *Aap*, 273:106–+, June 1993.

[7] N. N. Chugai, S. I. Blinnikov, R. J. Cumming, P. Lundqvist, A. Bragaglia, A. V. Filippenko, D. C. Leonard, T. Matheson, and J. Sollerman. The Type IIn supernova 1994W: evidence for the explosive ejection of a circumstellar envelope. *Mnras*, 352:1213–1231, August 2004.

[8] J. Cooke, M. Sullivan, E. J. Barton, J. S. Bullock, R. G. Carlberg, A. Gal-Yam, and E. Tollerud. Type IIn supernovae at redshift z˜2 from archival data. *Nature*, 460:237–239, July 2009.

[9] P. A. Crowther. Observed Metallicity Dependence of Winds from WR stars. In H. J. G. L. M. Lamers, N. Langer, T. Nugis, & K. Annuk, editor, *Stellar Evolution at Low Metallicity: Mass Loss, Explosions, Cosmology*, volume 353 of *Astronomical Society of the Pacific Conference Series*, pages 157–+, December 2006.

[10] J. J. Eldridge, R. G. Izzard, and C. A. Tout. The Effect of Massive Binaries on Stellar Populations and Supernova Progenitors. In F. Bresolin, P. A. Crowther, & J. Puls, editor, *IAU Symposium*, volume 250 of *IAU Symposium*, pages 179–184, June 2008.

[11] J. J. Eldridge and C. A. Tout. Exploring the divisions and overlap between AGB and super-AGB stars and supernovae. *Memorie della Societa Astronomica Italiana*, 75:694–+, 2004.

[12] A. Feldmeier, J. Puls, C. Reile, A. W. A. Pauldrach, R. P. Kudritzki, and S. P. Owocki. Shocks and Shells in Hot Star Winds. *Apss*, 233:293–299, November 1995.

[13] R. J. Foley, N. Smith, M. Ganeshalingam, W. Li, R. Chornock, and A. V. Filippenko. SN 2006jc: A Wolf-Rayet Star Exploding in a Dense He-rich Circumstellar Medium. *Apjl*, 657:L105–L108, March 2007.

[14] C. Fryer and S. Woosley. Astronomy: A new twist on neutron stars. *Nature*, 411:31–34, May 2001.

[15] C. L. Fryer, S. E. Woosley, and D. H. Hartmann. Formation Rates of Black Hole Accretion Disk Gamma-Ray Bursts. *Apj*, 526:152–177, November 1999.

[16] A. W. Fullerton, D. L. Massa, and R. K. Prinja. The Discordance of Mass-Loss Estimates for Galactic O-Type Stars. *Apj*, 637:1025–1039, February 2006.

[17] A. Gal-Yam and D. C. Leonard. A massive hypergiant star as the progenitor of the supernova SN 2005gl. *Nature*, 458:865–867, April 2009.

[18] C. L. Gerardy, R. A. Fesen, P. Höflich, and J. C. Wheeler. Detection of CO and Dust Emission in Near-Infrared Spectra of SN 1998S. *Aj*, 119:2968–2981, June 2000.

[19] K. Hamaguchi, M. F. Corcoran, T. Gull, K. Ishibashi, J. M. Pittard, D. J. Hillier, A. Damineli, K. Davidson, K. E. Nielsen, and G. V. Kober. X-Ray Spectral Variation of η Carinae through the 2003 X-Ray Minimum. *Apj*, 663:522–542, July 2007.

[20] W.-R. Hamann and L. Koesterke. Spectrum formation in clumped stellar winds: consequences for the analyses of Wolf-Rayet spectra. *Aap*, 335:1003–1008, July 1998.

[21] A. Heger, I. Baraffe, C. L. Fryer, and S. E. Woosley. Evolution and nucleosynthesis of very massive primordial stars. *Nuclear Physics A*, 688:197–200, May 2001.

[22] A. Heger, C. L. Fryer, S. E. Woosley, N. Langer, and D. H. Hartmann. How Massive Single Stars End Their Life. *Apj*, 591:288–300, July 2003.

[23] A. Heger, L. Jeannin, N. Langer, and I. Baraffe. Pulsations in red supergiants with high L/M ratio. Implications for the stellar and circumstellar structure of supernova progenitors. *Aap*, 327:224–230, November 1997.

[24] A. Heger, S. Woosley, I. Baraffe, and T. Abel. Evolution and Explosion of Very Massive Primordial Stars. In M. Gilfanov, R. Sunyeav, & E. Churazov, editor, *Lighthouses of the Universe: The Most Luminous Celestial Objects and Their Use for Cosmology*, pages 369–+, 2002.

[25] A. Heger and S. E. Woosley. The Nucleosynthetic Signature of Population III. *Apj*, 567:532–543, March 2002.

[26] J. L. Hoffman, D. C. Leonard, R. Chornock, A. V. Filippenko, A. J. Barth, and T. Matheson. The Dual-Axis Circumstellar Environment of the Type IIn Supernova 1997eg. *Apj*, 688:1186–1209, December 2008.

[27] R. M. Humphreys and K. Davidson. The luminous blue variables: Astrophysical geysers. *Pasp*, 106:1025–1051, October 1994.

[28] R. Kippenhahn and A. Weigert. *Stellar Structure and Evolution*. 1990.

[29] R. Kotak and J. S. Vink. Luminous blue variables as the progenitors of supernovae with quasi-periodic radio modulations. *Aap*, 460:L5–L8, December 2006.

[30] R. P. Kudritzki, A. Pauldrach, J. Puls, and D. C. Abbott. Radiation-driven winds of hot stars. VI - Analytical solutions for wind models including the finite cone angle effect. *Aap*, 219:205–218, July 1989.

[31] N. Langer, C. A. Norman, A. de Koter, J. S. Vink, M. Cantiello, and S.-C. Yoon. Pair creation supernovae at low and high redshift. *Aap*, 475:L19–L23, November 2007.

[32] R. B. Larson. Early star formation and the evolution of the stellar initial mass function in galaxies. *Mnras*, 301:569–581, December 1998.

[33] A. Maeder. The most massive stars evolving to red supergiants - Evolution with mass loss, WR stars as post-red supergiants and pre-supernovae. *Aap*, 99:97–107, June 1981.

[34] J. C. Martin, K. Davidson, R. M. Humphreys, D. J. Hillier, and K. Ishibashi. On the He II Emission in η Carinae and the Origin of Its Spectroscopic Events. *Apj*, 640:474–490, March 2006.

[35] J. R. Maund, S. J. Smartt, R.-P. Kudritzki, A. Pastorello, G. Nelemans, F. Bresolin, F. Patat, G. F. Gilmore, and C. R. Benn. Faint supernovae and supernova impostors: case studies of SN 2002kg/NGC 2403-V37 and SN 2003gm. *Mnras*, 369:390–406, June 2006.

[36] G. Meynet, R. Hirschi, and A. Maeder. Effects of Rotation on Pre-supernova Models. In M. Turatto, S. Benetti, L. Zampieri, & W. Shea, editor, *1604-2004: Supernovae as Cosmological Lighthouses*, volume 342 of *Astronomical Society of the Pacific Conference Series*, pages 99–+, December 2005.

[37] G. Meynet and A. Maeder. Stellar evolution with rotation. X. Wolf-Rayet star populations at solar metallicity. *Aap*, 404:975–990, June 2003.

[38] F. Nakamura and M. Umemura. Fragmentation of Primordial Gas Clouds: On the Mass of the First Stars. In A. Weiss, T. G. Abel, & V. Hill, editor, *The First Stars*, pages 263–+, 2000.

[39] H. Nieuwenhuijzen and C. de Jager. Atmospheric accelerations and the stability of dynamic supergiant atmospheres. *Aap*, 302:811–+, October 1995.

[40] S. P. Owocki. Rotation and Mass Ejection: the Launching of Be-Star Disks (Invited Review). In A. Maeder & P. Eenens, editor, *Stellar Rotation*, volume 215 of *IAU Symposium*, pages 515–+, June 2004.

[41] S. P. Owocki and J. Puls. Line-driven Stellar Winds: The Dynamical Role of Diffuse Radiation Gradients and Limitations to the Sobolev Approach. *Apj*, 510:355–368, January 1999.

[42] A. Pastorello, S. J. Smartt, S. Mattila, J. J. Eldridge, D. Young, K. Itagaki, H. Yamaoka, H. Navasardyan, S. Valenti, F. Patat, I. Agnoletto, T. Augusteijn, S. Benetti, E. Cappellaro, T. Boles, J.-M. Bonnet-Bidaud, M. T. Botticella, F. Bufano, C. Cao, J. Deng, M. Dennefeld, N. Elias-Rosa, A. Harutyunyan, F. P. Keenan, T. Iijima, V. Lorenzi, P. A. Mazzali, X. Meng, S. Nakano, T. B. Nielsen, J. V. Smoker, V. Stanishev, M. Turatto, D. Xu, and L. Zampieri. A giant outburst two years before the core-collapse of a massive star. *Nature*, 447:829–832, June 2007.

[43] E. Scannapieco, P. Madau, S. Woosley, A. Heger, and A. Ferrara. The Detectability of Pair-Production Supernovae at z = 6. *Apj*, 633:1031–1041, November 2005.

[44] S. J. Smartt, J. J. Eldridge, R. M. Crockett, and J. R. Maund. The death of massive stars - I. Observational constraints on the progenitors of Type II-P supernovae. *Mnras*, 395:1409–1437, May 2009.

[45] S. J. Smartt, J. R. Maund, G. F. Gilmore, C. A. Tout, D. Kilkenny, and S. Benetti. Mass limits for the progenitor star of supernova 2001du and other Type II-P supernovae. *Mnras*, 343:735–749, August 2003.

[46] S. J. Smartt, J. R. Maund, M. A. Hendry, C. A. Tout, G. F. Gilmore, S. Mattila, and C. R. Benn. Detection of a Red Supergiant Progenitor Star of a Type II-Plateau Supernova. *Science*, 303:499–503, January 2004.

[47] N. Smith. Episodic Mass Loss and Pre-SN Circumstellar Envelopes. In F. Bresolin, P. A. Crowther, & J. Puls, editor, *IAU Symposium*, volume 250 of *IAU Symposium*, pages 193–200, June 2008.

[48] N. Smith, R. Chornock, W. Li, M. Ganeshalingam, J. M. Silverman, R. J. Foley, A. V. Filippenko, and A. J. Barth. SN 2006tf: Precursor Eruptions and the Optically Thick Regime of Extremely Luminous Type IIn Supernovae. *Apj*, 686:467–484, October 2008.

[49] N. Smith, W. Li, R. J. Foley, J. C. Wheeler, D. Pooley, R. Chornock, A. V. Filippenko, J. M. Silverman, R. Quimby, J. S. Bloom, and C. Hansen. SN 2006gy: Discovery of the Most Luminous Supernova Ever Recorded, Powered by the Death of an Extremely Massive Star like η Carinae. *Apj*, 666:1116–1128, September 2007.

[50] N. Smith and S. P. Owocki. On the Role of Continuum-driven Eruptions in the Evolution of Very Massive Stars and Population III Stars. *Apjl*, 645:L45–L48, July 2006.

[51] N. Smith and S. P. Owocki. On the Role of Continuum-driven Eruptions in the Evolution of Very Massive Stars and Population III Stars. *Apjl*, 645:L45–L48, July 2006.

[52] A. M. Soderberg, S. R. Kulkarni, E. Berger, R. A. Chevalier, D. A. Frail, D. B. Fox, and R. C. Walker. The Radio and X-Ray-Luminous Type Ibc Supernova 2003L. *Apj*, 621:908–920, March 2005.

[53] C. Trundle, R. Kotak, J. S. Vink, and W. P. S. Meikle. SN 2005 gj: evidence for LBV supernovae progenitors? *Aap*, 483:L47–L50, June 2008.

[54] S. D. van Dyk, W. Li, and A. V. Filippenko. Core-Collapse Supernova Progenitors in Hubble Space Telescope Images. In W. Hillebrandt & B. Leibundgut, editor, *From Twilight to Highlight: The Physics of Supernovae*, pages 33–+, 2003.

[55] S. D. Van Dyk, W. Li, A. V. Filippenko, R. M. Humphreys, R. Chornock, R. Foley, and P. M. Challis. The Type IIn Supernova 2002kg: The Outburst of a Luminous Blue Variable Star in NGC 2403. *ArXiv Astrophysics e-prints*, March 2006.

[56] S. D. Van Dyk, C. Y. Peng, J. Y. King, A. V. Filippenko, R. R. Treffers, W. Li, and M. W. Richmond. SN 1997bs in M66: Another Extragalactic η Carinae Analog? *Pasp*, 112:1532–1541, December 2000.

[57] A. M. van Genderen. S Doradus variables in the Galaxy and the Magellanic Clouds. *Aap*, 366:508–531, February 2001.

[58] S. E. Woosley, S. Blinnikov, and A. Heger. Pulsational pair instability as an explanation for the most luminous supernovae. *Nature*, 450:390–392, November 2007.

[59] S. E. Woosley, A. Heger, and T. A. Weaver. The evolution and explosion of massive stars. *Reviews of Modern Physics*, 74:1015–1071, November 2002.

[60] L. Zampieri. Black hole formation in supernovae: prospects of unveiling fallback emission. In R. Cianci, R. Collina, M. Francaviglia, & P. Fré, editor, *Recent Developments in General Relativity*, pages 301–315, 2002.

CHAPTER 3

Observations and data processing

In this Chapter I will shortly describe the most important technical characteristics of the different instrumental configurations used to observe the SNe discussed in this thesis. Then I will also describe the adopted techniques for the reduction of optical and IR photometry and of optical spectroscopy.

3.1 Data Acquisition

The four supernovae discussed in this thesis were observed by the Padova-Asiago Supernovae Group in the course of my PhD.

Being targets of the Padova-Asiago Supernova Follow-up, their finding charts, coordinates and an updated observing log is reported at the webpage *http://web.oapd.inaf.it/supern/followup/* (cf. Fig.3.1), which I have designed and updated during my second year.

As a general rule, the observation campaign is started as soon as possible after discovery, for every peculiar or nearby SN event which is recognized to be caught early after the explosion. An alert group composed by members of the Group has the task to select, among the possible candidates, the suitable targets the follow-up on the base of the features described in their discovery of classification circulars. The scheduling of the observations depends on the visibility period of the SN and on its type, and is planned at the beginning of a follow-up (taking into account the availability of each telescope). For particularly interesting targets like the over-luminous SNe which I am going to presents in the next Chapters, an European or even world-wide collaboration is started

with other research institutions to guarantee the high-frequency sampling of the photometric and spectroscopic data, as well as a suitable instrumental set-up for the specific features of the SN.

For two of the four IIn SNe discussed in this thesis, i.e. SNe 2006gy and 2008fz, the classification was correctly accomplished by members of the group, i.e. Harutyunyan et al. (2006) [6] and Benetti et al. (2008) [2] also thanks to GELATO (GEneric cLAssification TOol[1]), an online classification software for the automatic comparison of SN spectra. The follow-up of was organized by the Padova-Asiago Supernova Group, on behalf of a larger collaboration with other SN groups from Belfast, (UK), Munich (Germany), Stockholm (Sweden) and Los Angeles (USA); the observations were performed by me and by members of the collaboration in Service or in Visitor mode.

Since interacting SNe are very blue at early phases, the optical range samples most of their Spectral Energy Distribution. Therefore, only optical instrumentation covering the UBVRI range, was used for the observations. In fact, for IIn SNe the NIR emission become important at the nebular phases, i.e. when the peak of SED shifts toward redder wavelength ranges or when the emission by eventual dust in the ejecta becomes not negligible. Indeed NIR photometric observations in the J, H and K' bands were performed at late epochs for SN 2006gy; for SN 2008fz NIR observations are foreseen for the next runs at NTT.

Spectra were acquired mostly at low-resolution, which is sufficient to trace the kinematic of the high velocity expanding SN layers and to detect the most important optical lines, such as H, He, Ca and O. High-resolution spectrographs, which are generally useful to sample the typical narrow emission lines of IIn SNe, could be used only for the SNe 2007bt and 2007bw.

The observations were stopped during Solar occultation or when the SNe became too faint for the available instrumentation.

3.2 Instrumental set-up

In the following, I will briefly describe the main technical characteristics of the different instrumental configurations used for the observations of the SNe presented in this thesis:

- **Asiago-Ekar 1.82m Copernico Telescope + AFOSC**

  The Copernico Telescope is located in the top of Mount Ekar, near Asiago (Italy). The instrument AFOSC *(Asiago Faint Object Spectrograph*

[1] https : //gelato.tng.iac.es/login.cgi

Figure 3.1— View of the online webpage of the Padova-Asiago Supernova follow-up, which was created to keep track on the observing logs regarding the current and past targets, and to support the observers during the observation with practical information concerning the target, the observing schedule or the weather.

and Camera) was equipped with a Tektronix TK1024 Thinned Back Illuminated CCD, 1024x1024, with pixel size 24 μm, pixel scale 0.473 arcsec/pixel, and a field of view is 8'.14 x 8'.14. The estimated Conversion Factor (CF) and the Read Out Noise (RON) of the detector are 1.86 e^-/ADU and 9.6 e^-. For photometry the Johnson U, B, V, R and Gunn i filter were adopted. For spectroscopy, we used the grism ♯2 (wavelength region 3720-10200 Å, dispersion 15.67 Å/pixel and resolution 38 Å with the 2".1slit and the grism ♯4 (wavelength region 3500-8450 Å, dispersion 4.99 Å/pixel and resolution 22 Å with the 2".1slit.

webpage: http://www.oapd.inaf.it/asiago/2000.html

- **Asiago-Pennar 1.22m Galilei Telescope + B&C**

  This is another telescope located in Asiago, and it is ruled by the Department of Astronomy of the Padova University. The *Boller and Chivens* (B&C) spectrograph has been equipped with the Dioptric Blue Galileo Camera. There are five gratings available for the B&C spectrograph. The 300 tr mm^{-1} grooves grating was usually used to get spectra with a dispersion of 4.06 Å/pixel. The scale of the CCD along the slit is 1.11 arcsec/pixel.

webpage: http://www.oapd.inaf.it/asiago/4000.html

- **Calar Alto 2.2m + CAFOS**

  The 2.2m Calar Alto telescope, located in Sierra de Los Filabres, Andalucia (Spain) was equipped with CAFOS *(Calar Alto Faint Object Spectrograph)*, a 2048x2048 SITe ♯1d CCD (pixel size 24 μm, image scale 0.53 arcsec/pixel, total field 18' x 18', CF = 2.3 e^-/ADU and RON = 5.060 e^-). For photometry the Johnson U, B, V, R, I filters were used; for spectroscopy the grism B-200 (range 3200-7000 Å with spectral resolution 13 Å), and the grism R-200 (range 6300-11000 Å) were adopted.

  webpage: http://w3.caha.es/alises/cafos/cafos.html

- **JKT+AGBX**

  The Jakobus Kapteyn Telescope is a 1m telescope located at La Palma (Spain), and it belongs to the Isaac Newton Group of Telescopes. AGBX was the instrument mounted at the telescope during the years 1991 and 1996, i.e. when the B, R and I observations (with Johnson filters) of the field of SN 2006gy were acquired. We downloaded these images from the online archive and used them as templates for the SN photometry. The detector used is a EEV5 CCD with 1152x1242 sensitive pixels with dimension 22 μm.

  webpage: http://www.ing.iac.es/Astronomy/telescopes/jkt/

- **LT + RATCAM**

  We obtained photometric data with the optical RATCAM CCD Camera of the 2m robotic Liverpool Telescope (LT) at La Palma (Spain). The CCD is a 2048x2048 pixel EEV CCD42-40, with pixel size 13.5 μm, pixel scale 0.135 arcsec/pixel and field of view 4'.6 x 4'.6. The CF is 2.72 e^-/ADU and the RON is 5 e^-. The photometry was obtained using the Sloan *u*, *r*, *i*, and the Bessell B, V filters.

  webpage: http://telescope.livjm.ac.uk/

- **NOT + ALFOSC**

  The detector that was used for the ALFOSC (*Andalucia Faint Object Spectrograph and Camera*) instrument mounted at the 2.5m Nordic Optical Telescope (NOT) in La Palma (Spain) is a EEV42-40 2Kx2K Manufacturer (CCD42−40) back illuminated, a 2048x2048 chip of pixel size 13.5 μm and 0.19 arcsec/pixel. The CF has been estimated to be 0.726 e^-/ADU and the RON = 5.3 e^-. For the photometry we used Bessel U,

B, V, R and I filters and for the spectroscopy we used the grism ♯4 (low resolution visual grism, range 3200-9100 and dispersion 3.0 Å/pixel) and the grism ♯5 (low resolution red grism, range 5000-10250 Å and dispersion 3.1 Å/pixel).

webpage:http://www.not.iac.es/instruments/alfosc/

- **NTT+EFOSC2** EFOSC2, or the *ESO Faint Object Spectrograph and Camera* is the new ESO instrument mounted on the 3.6m New Generation Telescope at La Silla (Chile). Despite its multi mode capabilities EFOSC2 is especially suitable for low resolution photometry and spectroscopy. The CCD ♯40, which is particularly sensitive to UV photons, is a Loral/Lesser, thinned, AR coated, UV flooded, MPP chip controlled by ESO-FIERA. It is composed by 2048 x 2048 pixel; the pixel size and pixel scale are 15μm and 0".157 arcsec/pixel, respectively. The field of view is 5'.2 x 5'.2. The CF and RON in slow mode are 1.3 e^-/ADU and 10.2 e^-. At this telescope only Bessel VR and Gunn i photometry of SN 2008fz were acquired.

  webpage: http://www.eso.org/sci/facilities/lasilla/instruments/efosc-3p6/Instrument-Overview.html

- **Observatorio de Cantabria Telescope**

  This telescope is located in Cantabria (Spain); its scientific activity is ruled by the University of Cantabria. The telescope has a mirror aperture of 40.64 cm. At the Cassegrain focus there is a ST-8XE CCD with 1530 1020 pxels with dimension 9 μm. The telescope field of view is 11.82' 7.88' and the pixel scale is 0.46 arcsec/pixel. The estimated RON is 15 e^-. The photometry acquired at this telescope is in the Johnson V, R and I filters.

  webpage: http : //venus.ifca.unican.es/oac/index$_o$bs.html

- **Palomar 60"**

  This telescope, which has a primary mirror of 1.5 m, is one of the 5 telescopes located at the Palomar Observatory (San Diego, CA, USA). These are owned and operated by the California Institute of Technologies. Recently it has been upgraded to work remotely and automatically with a dedicated CCD to monitor transient sources. The detector is a 2048x2048 pixel CCD, with field of view 11" x 11" and pixel-scale 0.378 arcsec/pixel. The CF is 2.2 e^-/ADU and the RON is 2.4 e^-. Photometry with the Johnson UBV and Kron RI filters was obtained for SN 2008fz at this telescope.

webpage: http://www.astro.caltech.edu/palomar/60inch/dfox/status.html

- **Schmidt Telescope**

  With a main mirror diameter of 1.5m, the Schmidt telescope is the biggest telescope at the Kiso Observatory in Japan. The detector is a SITe 2048x2048 pixel TK2048E CCD, with pixel size 24μm. The field of view is 50'x50'. The CF and RON of the CCD are 3.4 e^-/ADU and 23 e^-, respectively.

  At this telescope an image of the host of SN 2006gy, i.e. NGC 1260, was acquired in February, 12th, 2003 with the Johnson V filter. I have download this image from the archive and used it as a template for the SN photometry.

  webpage: http://www.ioa.s.u-tokyo.ac.jp/kisohp/top-e.html

- **TNG + Dolores**

  The *Device Optimized for the LOw RESolution* is installed at the Nasmyth B focus of the TNG (Telescopio Nazionale Galileo) in La Palma (Spain). The detector is a Loral thinned and back illuminated 2048x2048 CCD. The scale is 0.275 arcsec/pixel (μm 15), which yields a field of view of about 9'.4 x 9'.4. The CF is 0.97 e^-/ADU and the RON 2 e^-. We used the Johnson filters U, B, V, and Cousins R, I; for the spectroscopy we used LR-B (wavelength range 3000-8800 Å, dispersion 2.8 Å/pixel and resolution 11 Å with a 1" slit) and LR-R (wavelength range 4470-10360 Å, dispersion 2.9 Å/pixel and resolution 11 Å with a 1" slit).

  webpage: http://www.tng.iac.es/instruments/lrs/

- **TNG+NICS** NICS

  The *Near Infrared Camera Spectrometer* is the TNG infrared (0.9-2.5 μm) multimode instrument which is based on a HgCdTe Hawaii 1024 x 1024 pixel CCD. The latter has a pixel scale of 0.25 arcsec/pixel. The field of view is 4'.2 x 4'.2. The filters used for the observation of SN 2006gy are the Ocli J, H and K'.

  webpage: http://www.tng.iac.es/instruments/nics/imaging.html

- **Taurus Hill Observatory**

  The Taurus Hill Observatory is owned by an amateur astronomical association and it is located on the top of Hill Härkämäki, near Kangaslampi, Finland. The telescope that was used for the observation of SN 2008fz is the Meade 12" LX200 OTA Schmidt-Cassegrain telescope (focal length

3048 mm), which has as detector a CCD SBIG ST-8XME with 567 x 532 pixels. The pixel-scale is 0.609 arcsec/pix. Images were acquired without filters.

webpage: http://english.taurushill.net/

- **WHT + ISIS**

  WHT is the William Herschel 4.2m Telescope (WHT) at La Palma (Spain) equipped with ISIS (*Intermediate dispersion Spectrograph and Imaging System*), on which the CCD EEV12 (2148x4200 pixels, pixel size 13.5 μm, scale 0.19 arcsec/pixel) was mounted. The blue arm used the R158B grating (with dispersion 1.62 Å/pixel) and R300B grating (with dispersion 0.86 Å/pixel). At the red arm the grating R158R (with dispersion 1.81 Å/pixel) was adopted. ISIS has a CF of 2.3 e^-/ADU and RON 6 e^-.

  webpage: http://www.ing.iac.es/Astronomy/telescopes/wht/index.html

3.3 Data reduction

The SNe observations in the optical and NIR were processed using the IRAF routines. For photometry a collection of tasks developed in the IRAF environment by the Padova-Asiago SN Group was used.

Let us review in this Section the main steps of the whole photometry reduction procedure.

3.3.1 Pre-reduction

Before the measurement, it is important to remove any peculiar instrumental signature due to the detector and the instrument. This step, called pre-reduction, is briefly described as follows:

Bias subtraction. The bias level is an electronic offset added to the signal from the CCD to make sure that the Analogue-to-Digital Converter (ADC) always receives a positive value. The ADC samples the charge accumulated in a CCD pixel and returns a digital value. This value is proportional to the actual number of electrons detected in the pixel and is measured in Analogue-to-Digital Units (ADUs). The relation between ADU and the number of photons (charge) is a scale factor known as the gain. It is common practice to create a master bias image from the median of several (>10) bias images (frames obtained with exposure time of 0 seconds and closed shutter) in order to reduce the RON and to get rid of cosmic rays.

Overscan correction. In principle the bias level is constant, but it can slightly change during the night because of external factors (like temperature variations). To monitor this effect, the bias level of each image is measured in the "overscan" region (a stripe of a few columns/row at the edge of the CCDs, which is not exposed to the light) and removed from the whole frame, before the bias images combination. Indeed, after the overscan correction, the combined master-bias will have a mean value around zero, and will be removed from each scientific frame.

Trimming. After use, the overscan region can be cut off trimming the images. With this action, it is also possible to cut off the edge of the images, often affected by irregular response and degraded, and to delimit the useful area for the scientific analysis.

Flat-fielding. Due to construction faults and to variation of transmissivity of the CCD coating, and to dust contamination, the CCD response to the incident light is not uniform and can shows variation on different scales from that of the whole frame to pixel-to-pixel. So, it is necessary to divide the data by a sensitivity map (flat-field) created from calibration exposures. Usually, a flat-field is obtained by imaging a uniformly illuminated screen inside the telescope dome (dome-flats) or, better, the sky at twilight/dawn (sky-flat). Since the detector sensitivity changes with the wavelength, flat exposures are required in all the bands used for the scientific frames. In order to have a better statistic, to reduce the poisson statistics and to get rid of cosmics, a number of flats are averaged to obtain a master-flat.

For the spectroscopic master-flats another process has to be addes, i.e. their normalization along the dispersion axis.

For the IR magnitudes, additional reduction steps are required. Particular care has to be devoted to the sky subtraction from all science frames due to the rapid variation in the IR and to image coaddition due to very short integration time of each exposure.

Once the pre-reduction is concluded, it is possible to proceed with the measurement of the SN magnitudes or with the extraction of the spectrum.

3.4 Photometry

The photometric observations of the objects discussed in this theis were obtained with a number of instruments equipped with broadband UBVRI (and eventually JHK) filters. The observations consist of short exposures at early times and dithered multiple exposures at late epochs. In the latter case, the images in each filter were first geometrically aligned (registered) and then combined to produce a single deep image. A major complication in supernovae photometry is separating the light from the SN itself from the underlying galaxy contribution at the SN position. The importance of the galaxy contribution change from event to event, it depends on the SN position (close or far from the nucleus or HII regions of the host galaxy) but also on the phase of the SN and the distance of the galaxy. In order to have a good background subtraction, we measure the SN flux applying a PSF-fitting technique. This method consists in performing the fit of stellar profile and subtract the background galaxy contamination at the SN position, reconstructed with a polynominal surface, using as input the background just outside the SN PSF area. For this purpose the Padova team developed *SNOoPY* (SuperNOvaPhotometrY), a package originally designed by F. Patat and later implemented in IRAF by E. Cappellaro. It is based on DAOPHOT which allows to fit the SN profile with a PSF obtained from a set of local, unsaturated stars.

In Fig.3.2 is shown an example of the application of this method in the case of SN 2007bt when the SN was around the maximum light. The so obtained instrumental magnitudes must be scaled to a reference exposure time (e.g. 1 sec.) and corrected for the atmospheric extinction via

$$m_\lambda = m'_\lambda + 2.5 \log t_{exp} - K_\lambda \times \text{airmass}$$

where m_λ is the instrumental magnitude, t_{exp} the exposure time and K the atmospheric extinction coefficient which depend from the observing site and season. Since SNe are variable objects each observation is unique and non re- producible. For this reason an effort is done to use all available data, even those obtained under non ideal conditions. In order to calibrate the photometry obtained in non-photometric nights we make use of a set of local standards in each SN field. These stars are chosen among the isolated stars in the field in order to avoid the contamination by nearby objects. Also, they should be non-variable star and neither too bright to saturate during the long exposures at late phases nor too faint to be dominated by the photon noise. In turn, the local stars are a posteriori calibrated by mean of observations of standard stars during a subset of photometric nights. The observation of standard stars allows also to determinate the color terms for the various instrumental setups. To this

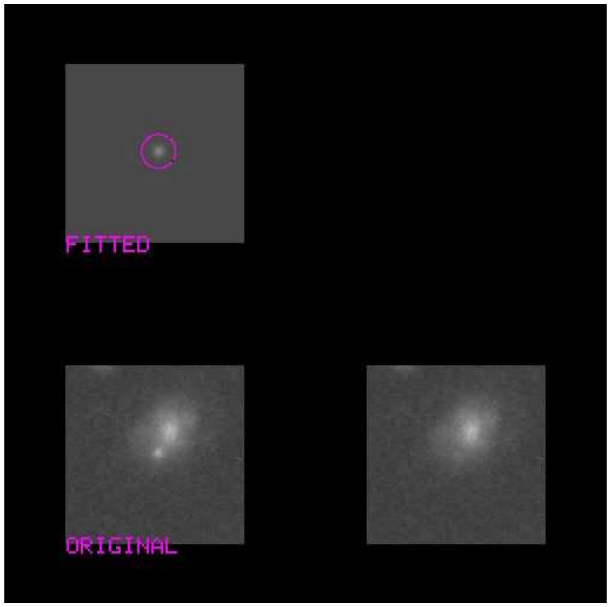

Figure 3.2— PSF-fitting technique applied to the case of SN 2007bt: original image of the SN region (bottom-left); SN contribution (fitted star), obtained after that the background at the SN position has been estimated fitting the region with a bidimensional polynomial of fixed degree (upper-left); and residual background (bottom-right).

aim we observe standard Landolt fields [7] on the photometric nights. In detail, for each night and instrumental configuration, the observation of the Landolt stars provide a system of color equations of the form:

$$\Delta m_\lambda = M_\lambda - m_\lambda = a_\lambda + b_\lambda \times (color)_\lambda$$

where M_λ is the standard magnitude of each star, M_λ is its instrumental measurement normalized at 1 second exposure time and corrected for atmospheric extinction. a_λ and b_λ characterize the instrumental configuration. a usually called the zero point and b is the color term. Solving the system of equations, we obtain a_λ and b_λ for all filters and we can determinate the standard magnitude M_λ, for the SN and the local standard stars for all bands. Finally a check of the photometric quality of each of the observing nights was performed on the local sequence. If Δm_λ represents the mean difference between the magnitude of the sequence stars in a non-photometric night and those of the photometric ones, a correction was applied to the a terms of the color

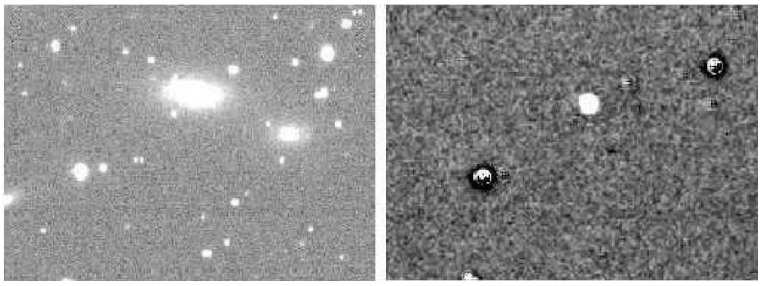

Figure 3.3— Left : portion of image displaying the galaxy NGC 1260, acquired on October 29th, 2006 at Ekar Observatory. The 1.82m telescope was equipped with AFOSC and a Bessel R filter. Right: Result of the photometric subtraction of SNOoPY and SVSUB. The image was obtained subtracting the left image containing the target SN 2006gy, and an archive image of NGC 1260 taken on December, 1st 1991 at Jakobus Kapteyn Telescope with R filter. SN 2006gy is clearly visible in the field. Around it, some residuals of saturated field stars are also present.

equations. The new values of the constant terms allow to estimate the final calibrated magnitude M_λ, of the object.

Uncertainties in the instrumental photometry were estimated by placing artificial stars with the same magnitude and profile as the SN, at positions close (within a few arcsec) to that of the SN, and then computing the deviations of the artificial star magnitudes. For the calibration error we adopted the r.m.s. of the observed magnitudes of the local sequence stars obtained during photometric nights only. The final errors are computed as the square root of the quadratic sum of instrumental and calibration errors.

3.5 Template subtraction

This technique is mandatory when the SN explode in a complex background area e.g. close to the galactic nucleus, H II region, spiral arms, and in general when the SN is faint. It consists in removing the host galaxy contribution, by subtracting its emission in an image acquired when the supernova was not present. The procedure makes use of the ISIS template subtraction program [1] and runs in the IRAF environment. For the application of this technique it is necessary to have a reference image of the host galaxy taken in each passband and obtained before or long after the SN explosion, when the SN luminosity has faded away, and this is often a limitation for the application of the method. Ideally, the templates should be obtained with the same telescope and with similar seeing as the scientific image containing the SN. Since this is not typi-

cally the case, a number of preliminary operation are required. The first step is the geometrical and photometrical registration of both images in order to correct for different instrumental pixel scales (*image stretching*), spatial orientation and position (*frame rotation and shifting*). After that, the image with better-seeing is degraded to that with poorer one and both images are scaled to the same intensity. Finally the reference (*template*) image is subtracted from the SN image. The resulting frame is flat in the ideal case, except for variable objects in the field (SN, variable galactic nuclei, variable star), accidental bodies (asteroids, meteors, artificial satellites, and so on). But in real case, a number of blemishes show up (saturated stars, cosmic rays, hot pixels and bad columns). At this point, the instrumental magnitude of the SN can be measured using the aperture photometry (e.g. IRAF task *imexamine*) or the PSF-fitting photometry (SNOoPY package) on the image obtained from the subtraction (without the host galaxy). An example of the results of this method is shown for the same SN in Fig.3.3.

3.5.1 IR photometry

For the IR magnitudes, additional reduction steps were required. Particular care was devoted to sky subtraction from all science frames due to the rapid variation in the IR and to image coaddition due to very short integration time of each exposure to improve the signal-to-noise. As for the optical photometry, the IR magnitudes were obtained using PSF fitting. For night-to-night calibration we also used a local sequence. However, as the number of IR standard fields observed each night was small, we adopted average color terms provided by the telescope teams. It is necessary to notice that the Ks band filter used in observation with SofI had a transmission curve slightly different from that of a standard K filter. Following Lidman (2002) we have transformed the Ks magnitudes to K by mean of the relation $K - K_s = -0.005 \times (J - K)$.

3.5.2 K-correction

In order to compare the intrinsic properties of objects at different redshift, one has to apply the so called K-correction, which accounts for the fact that the photometric bands sample different parts of the emitted spectrum because of the Doppler shift[2]. The value of the K-correction, which was applied to the photometry of the SNe with redshift >0.1, was calculated as the difference

[2]Because of Doppler effect, redshift occurs when the visible light from an object is shifted towards the red end of the spectrum. For visible light, red is the color with the longest wavelength. The corresponding shift to shorter wavelengths produced by a motion toward the observer, is called blueshift.

between the spectrophotometric magnitudes extrapolated from the observed and rest-frame spectra. Given the limited extension of the available spectra, the K-correction was computed only for the B, V and R bands.

3.5.3 Calculation of limits

When the SN luminosity fades, deep imaging at the available telescope may not be sufficient to detect the SN. In the cases when the SN is invisible in the image, it is worthy to establish at least the maximum threshold of the SN luminosity, i.e. un *upper limit* on the magnitude. This was done for SN 2006gy both in optical bands B and R, as well as in the NIR bands J and H. This was accomplished with an artificial, simple trick. First it was created an artificial star using the PSF of the sequence stars present in the field; secondly, the star was manually added in the image at the SN position. Then its luminosity is rescaled by a factor <1, until it becomes barely visible. At this point its magnitude corresponds to the desired upper limit of the SN luminosity.

3.5.4 Spectroscopy

The optical spectra were reduced using standard IRAF tasks from the *ctioslit* package after the preliminary removal of detector signatures which includes bias, overscan (only for the optical spectra) and flat field correction as mentioned in Section 3.3.

Then, the one-dimensional spectrum of the SN is extracted and the galaxy contribution along with the night sky lines are subtracted via a polynomial fit. The observation of lamp spectra (usually He-Ne, He-Ar, Hg-Cd lamps), obtained with the same instrumental configuration, allows the wavelength calibration of the SN spectrum. The identification of the lines allow us to match pixel to wavelength coordinates through a WCS (World Coordinate System) transformation. As we have said, the spectrum of a calibration lamp is usually taken at the position of the supernova, in order to compensate for the bending of the instrument. The accuracy of the wavelength calibration is verified against the position of the background sky lines in the spectra and is in general 1- 2 Å.

The following step is the flux calibration.

The response curve of the instrumental configuration is obtained observing spectroscopic standard stars from the lists of Oke [8], Hamuy et al. [5], Hamuy et al. [4]. This response curve is obtained by comparing the observed standard star spectrum to the flux tabulated for that star. The flux calibration is typically accurate within 20%.

Errors can be produced because the supernova and/or the flux standard

star have been observed under poor photometric conditions or when the object has not been perfectly centered in the slit.

Broad telluric absorptions contaminate the SN spectra which can be removed if a spectrum of a standard star obtained with the same resolution is available. Telluric absorptions are identified and removed from the observed spectrum which is then divided by the original one. The resulting spectrum (equal to 1 everywhere, except in coincidence with the telluric bands) is multiplied by the object spectrum. For the atmospheric extinction correction, we used the average extinction curves available for each site. To obtain full wavelength coverage in the optical region, we combined the spectra obtained using different grating/grisms. The absolute flux calibration of the spectra is checked against photometry and when necessary, the flux scale is adjusted to match the photometry. To this, we use the Pogson formula

$$\Delta \mathrm{I_i} = 10^{-0.4(\mathrm{M_{i,phot}} - \mathrm{M_{i,spec}})}$$

where $\Delta \mathrm{I_i}$ is the factor needed to scale the original spectrum. It is important to point out that most spectra were obtained with the slit oriented along the parallactic angle in order to minimize differential losses due to atmospheric refraction [3].

Additional processing required for the analysis of SN spectra are the correction for redshift of the host galaxy (it is necessary to identify the spectral lines and to estimate the expansion velocities) and the correction for interstellar extinction (it is necessary to compute the continuum temperature and obtain accurate measures).

Bibliography

[1] C. Alard. Image subtraction using a space-varying kernel. *Aaps*, 144:363–370, June 2000.

[2] S. Benetti, A. Harutyunyan, I. Agnoletto, S. Valenti, A. Pastorello, and V. Lorenzi. Supernova 2008fz. *Central Bureau Electronic Telegrams*, 1533:1–+, October 2008.

[3] A. V. Filippenko. The importance of atmospheric differential refraction in spectrophotometry. *Pasp*, 94:715–721, August 1982.

[4] M. Hamuy, N. B. Suntzeff, S. R. Heathcote, A. R. Walker, P. Gigoux, and M. M. Phillips. Southern spectrophotometric standards, 2. *Pasp*, 106:566–589, June 1994.

[5] M. Hamuy, A. R. Walker, N. B. Suntzeff, P. Gigoux, S. R. Heathcote, and M. M. Phillips. Southern spectrophotometric standards. *Pasp*, 104:533–552, July 1992.

[6] A. Harutyunyan, S. Benetti, M. Turatto, E. Cappellaro, N. Elias-Rosa, and G. Andreuzzi. Supernova 2006gy in NGC 1260. *Central Bureau Electronic Telegrams*, 647:1–+, September 2006.

[7] A. U. Landolt. Broadband UBVRI photometry of the Baldwin-Stone Southern Hemisphere spectrophotometric standards. *Aj*, 104:372–376, July 1992.

[8] J. B. Oke. Faint spectrophotometric standard stars. *Aj*, 99:1621–1631, May 1990.

CHAPTER 4

A new evolution scenario for the luminous SN 2006gy

The interest on energetic events started in 2006 with the discovery of the luminous supernova 2006gy, whose nature was long-debated. In this chapter I will first present the early observational data by Smith et al. [45] and review the several theories which were proposed concerning the origin of this peculiar transient. Then I will present the new evolution scenario that was proposed by Agnoletto et al. [1], based on original photometric and spectroscopic data. Finally I will briefly discuss the recent works of Kawabata et al. [21], Miller et al. [30] and Smith et al. [43] about SN 2006gy at late times.

4.1 An extra-ordinary discovery

On September 18.3 UT, 2006 an apparent supernova in NGC 1260 was identified by Quimby [39] on an image acquired with the ROTSE/IIb telescope at the Mc Donald Observatory, on the course of the Texas Supernova Search (TSS). On September 26.0 UT Harutyunyan et al. [19] obtained a spectrum and classified the event as a type II supernova, reporting the presence of a three-component Hα emission. Shortly thereafter Prieto et al. [37] argued that the position of the transient in the host-galaxy made it more likely to be an eruption of an Active Galactic Nucleus (AGN). However, Foley et al. [14] measured an offset of 2" from the host-galaxy nucleus and definitely classified the event as a type IIn supernova.

About two months past discovery the SN reached the maximum luminosity. The estimated absolute luminosity at peak, for the redshift z = 0.019, was

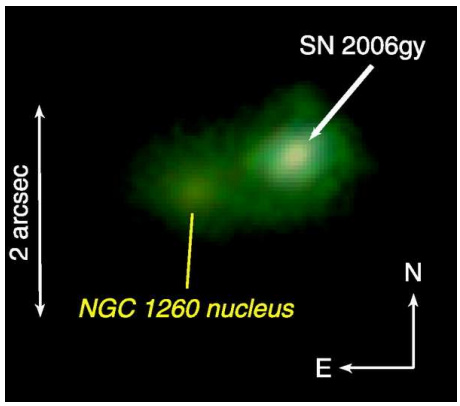

Figure 4.1— Laser guide adaptive optics image of SN 2006gy and the nucleus of NGC 1260.

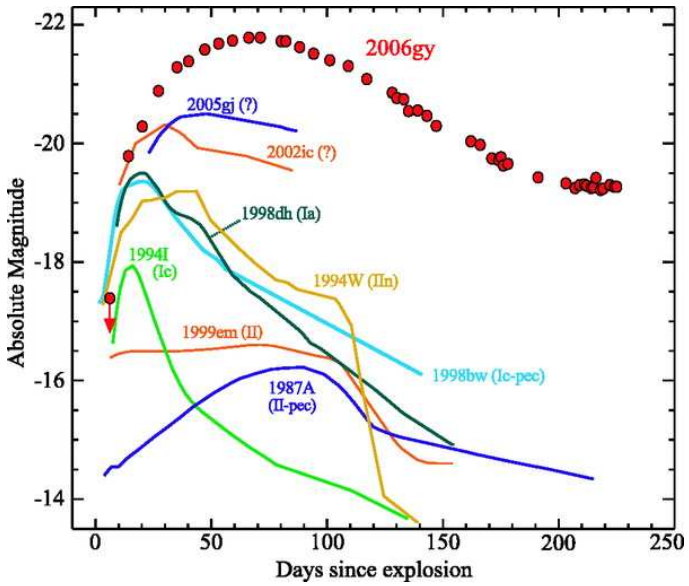

Figure 4.2— Light curve of SN 2006gy in the R-band compared to an heterogeneous sample of core-collapse supernovae (both figures from Smith et al. [45]).

$M_R \sim -22$ [43]. SN 2006gy was immediately recognized as the most luminous supernova ever discovered, raising much interest among the scientific community -and not only. In 2007, the *Time* newspaper reputed the discovery of SN 2006gy as one of the ten best discovery of the year[1].

4.1.1 Early photometry

Despite the explosion site, very close to the host-galaxy nucleus (Fig. 4.1), after discovery the optical emission of SN 2006gy could be well distinguished, and its luminosity was rising.

In 2007 Ofek et al. [32] first presented an early-times r and i light curve, as well as some low-resolution spectra. Shortly afterwards, Smith et al. [45] published a photometric study of the first $\sim$ 230 days (Fig. 4.2) and two spectra (Fig. 4.3), one of which is an excellent high-resolution spectrum acquired at Keck telescope. It was definitely shown that, though presenting the spectroscopic standard features of IIn SNe in the spectra, SN 2006gy was evolving photometrically with no precedent. A broad, bright peak characterized its light curve. After deriving the explosion epoch through a backward extrapolation of the early R-band light curve, Smith et al. [45] calculated that the maximum brightness had been reached only by day $\sim$70 after explosion. They also showed that, after maximum, the light curve had declined quite fast, until it had reached a phase of very low luminosity decay rate, between day $\sim$150 and $\sim$230. It was estimated that during the first 200 days the total luminosity *radiated* by SN 2006gy was huge: about 10^{51}erg.

4.1.2 Early spectroscopy

Spectroscopically, SN 2006gy showed the typical features of interacting SNe, like narrow emission lines, but their velocity was peculiar. In the high-resolution spectrum, Smith et al. [45]) showed that the profile of Hα presented a narrow component (FWHM$\sim$100 km s^{-1}), with an associated P-Cygni absorption feature that indicated outflow speeds between 130 km s^{-1} and 260 km s^{-1} (Fig. 4.3). As seen in Chapter 2, such velocities are far too fast both for the winds of red supergiant stars (RSG), but also one magnitude too slow for the winds of O-type supergiants, O-rich WN or for Wolf Rayet stars. Instead, they are consistent with those of LBVs (cfr. Section 2.5).

A velocity of $\sim$4000 km s^{-1} and of $\pm$6000 km s^{-1} were measured for the intermediate component and for the broad wings of Hα , respectively. Smith et al. [45] attributed the velocity of the intermediate component to the shock

[1] http : //www.time.com/time/specials/2007/top10/article/0, 30583, 1686204$_1$686252$_1$690931, 00.html

wave, and the fastest velocity of the broad component to the SN ejecta. Compared to the apparently huge energy of the explosion, a shock velocity of ∼4000 $\mathrm{km\,s^{-1}}$ by day 96 was considered unexpectedly slow.

4.1.3 Environment

The host of SN 2006gy, NGC 1260, is a S0/Sa peculiar galaxy within the Perseus cluster of galaxies. Its Heliocentric recession velocity is $5760\mathrm{km\,s^{-1}}$ and its velocity dispersion is $201\pm12\mathrm{km\,s^{-1}}$ [55]. Due to dust, NGC 1260 is infrared-bright, and was detected by the *InfraRed Astronomical Satellite* (IRAS). An infrared luminosity of $\log(\mathrm{L_{IR}/L_\odot}) = 9.85$ was calculated by Meusinger, Bruzendorf & Krieg [28], which, according to Kennicutt [22], implies a star-formation rate of $1.2\mathrm{M_\odot\,yr^{-1}}$. Ofek et al. [32] detected a dust lane passing about 300 pc from the SN location. Indeed, in the 2D Keck spectrum Smith et al. [45], detected an extended emission from gas that follows the rotation curve of the host galaxy. These emission lines, having intensity ratios typical of H II regions, are indicative of current star formation and are absent in nonstar-forming galaxies.

The $\mathrm{Mg_2}$ index of this galaxy was measured by Ofek et al. [32] as 0.240.27 mag [55]. This value, along with the synthetic spectral models of Vazdekis [54], suggests that the metallicity of NGC 1260 is not low, $[\mathrm{Fe/H}] \geq 0.2$.

Through a laser guide adaptive optics near-infrared image of SN 2006gy and the nucleus of NGC 1260 (Fig. 4.2), Smith et al. [45] measured an offset from the centroid of the galactic nucleus of 0".941 West, and 0".363 North.

4.2 First hypothesis on the origin of SN 2006gy

The intense debate the nature of SN 2006gy started as soon as *Swift* and *Chandra* detected only weak and soft X–ray emission close to the epoch of the optical maximum [45].

In type IIn SNe, the X-ray and radio bands emission are supposed to be produced from the interaction between the steady CSM and the high-velocity ejecta (cf. Sect.1.6). In the case of SN 2006gy, though the appearance of spectra unequivocally showed evidence of interaction phenomena, the weakness of the X-ray flux demonstrated that *the energy produced by CSM-interaction could not be the only source of the SN luminosity at maximum.* The absorption-corrected, absolute X-ray luminosity in the band $0.65 - 2\,\mathrm{keV}$ was only $1.65 \times 10^{39}\,\mathrm{erg\,s^{-1}}$ [45]. Additional energy mechanisms were investigated.

The H recombination and thermal radiation from the SN ejecta could be a valid source. However, based on the SN luminosity, this hypothesis would require an unlikely massive ejecta, in the order of ∼100 $\mathrm{M_\odot}$. Moreover, at a

photospheric temperature defined by the recombination front, the luminosity and relatively slow expansion of the shock blast would require an extremely large emitting radius, which results in a far-too-long peak in the light curve, or a very rapid ejecta deceleration at early times. This idea was soon rejected [45].

Could SN 2006gy have been a thermonuclear explosion, or one of the "type IIa" ? According to the first version of the paper of Ofek et al. [32] this hypothesis could not be excluded, given the evidence of Si lines in the spectra. In the context of type Ia supernovae, a massive CSM could be the result of a common-envelope phase in a binary system [48]. However, this scenario requires that the matter ejection from the progenitor shortly precedes the SN explosion. Moreover, the total kinetic energy of type Ia events is limited to 1.2×10^{51}erg, and it can get up to 2.5×10^{51}erg for super-Chandrasekhar models, which is in not consistent with the total radiative energy of SN 2006gy. Furthermore, the fast velocity derived by Smith et al. [45] for the unperturbed CSM and the luminosity at the same epochs were suggestive of extreme values of the progenitor mass-loss rate, in the order of 0.5 $M_\odot\,yr^{-1}$, only compatible with massive stars. Last but not least, an argument against the type Ia hypothesis concerned the slow deceleration of the ejecta: given that the ejecta decelerate by only 10% after discovery, then only 20% of the kinetic energy is transformed into radiation during that time. The huge radiative energy of SN 2006gy would then require a SN with energy $\geq 10^{51}$erg, which is too demanding for a type Ia [45].

Of course, a strong contribution to the overall luminosity might come from the *radioactive decay* of ^{56}Ni into ^{56}Co and ^{56}Fe, via γ and e^+ deposition. Typically, for H-rich, core-collapse SNe the ejected ^{56}Ni mass spans spans a wide range of values, $0.005 < M_{^{56}Ni} < 0.3M_\odot$ (Zampieri et al., in preparation), but is typically smaller than in SNe Ia and energetic Ib/c. In the case of SN 2006gy, the peak brightness of the event required an amount of ^{56}Ni of the order of 22 $M_\odot$ according to Smith et al. (2007) [45]. This quantity is far too much for being created by any known "standard" supernova event, both of the core-collapse and of the thermonuclear type.

In general, given the early-times observational data presented by Smith et al. [45] and by Ofek et al. [32] it was clear that the nature of SN 2006gy dealt with the explosion of a massive star, but the energetic of the events lead to consider either non-standard explosion mechanisms or alternative sources of energy.

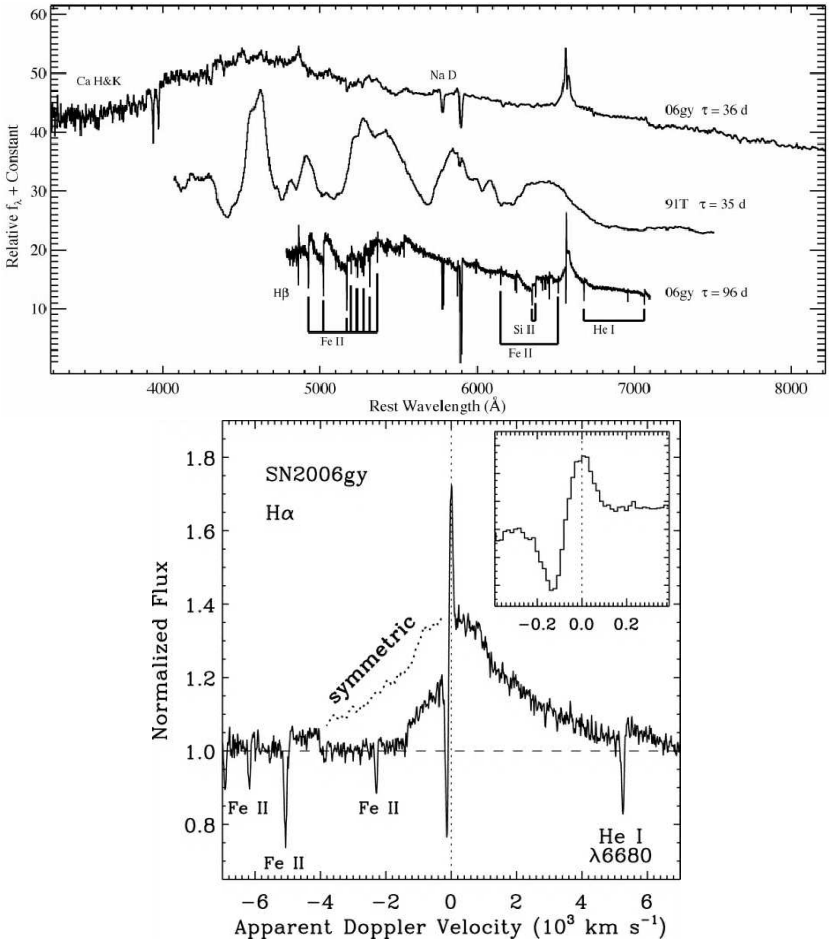

Figure 4.3— *Top*: Spectra from Smith et al. [45] compared to SN 1991T, one obtained at the telescope of the Lick Observatory (+ KAST spectrograph), and one obtained at the Keck II (+DEIMOS). The spectrum on day 96 clearly shows a quite red continuum and an asymmetric profile of Hα presenting a narrow emission. Several other absorption features by other elements, likely Fe II and Si II (as pointed out by Ofek et al. [32] are also evident). *Bottom*: Zoom on Hα line from the Keck+DEIMOS spectrum, from Smith et al. [45]. The blueshifted narrow absorption has a minimum at $\sim$130 km s^{-1} , reaching 260 km s^{-1} at its blue edge. Part of the emission of the intermediate component is "cut" by the blueshifted absorption; if symmetrically reflected on the blue side, the intermediate component extends to 4000 km s^{-1} , and it is supposed to trace the SN shock wave. The upper-right inset shows a closer view of the P-Cygni line profile associated to the narrow emission, tracing the wind velocity.

4.3 A long-debated event

Given the peculiarity of the event, in the last three years many groups have worked on the data of Smith et al. [45] to interpret the evolution of SN 2006gy and to constrain the nature of its progenitor. From the most common to the most exotic ones, several possible scenarios were proposed. Some of them were excluded, as recent, new, late-times observational data were published [21, 30]. However, a list and brief explanation of all proposed theories about the SN explosion mechanism and evolution will help to better comprehend the scenario suggested by Agnoletto et al. [1], which is partly based on the work of Smith & Mc Cray [46].

According to various authors, the origin of SN 2006gy could deal with:

i) **A supernova explosion via Pair Production (Ofek et al. [32]; Smith et al. [45])**.

As discussed above, an involved ^{56}Ni quantity of $\sim$22M$_\odot$ is far too large for any thermonuclear or core-collapse supernova, but it is not for a *pair instability supernova* (PISN, cfr. Sect. 2.1.4). From the observational point of view, in the models of Scannapieco et al. (2005) [41] for non-rotating, zero metallicity stars with no pre-mass-loss, the light curve of a PISN shows an initial, small, short, and a long rise to maximum powered by the decay of ^{56}Ni and ^{56}Co. Also, they predict relatively slow velocities (in the order of 5000 km s^{-1}) and the presence of H in the spectra. According to Smith et al. [45] both features are consistent with the data of SN 2006gy, as it is also the form of the light curve, assuming that the initial small peak is avoided due to the adiabatic cooling of an initially small radius.

Nevertheless, an argument against this hypothesis is that such phenomena are expected to occur among the primordial, metal-poor stars of the universe, whereas it is evident that NGC 1260 is metal-rich (Section 4.1.3). It is known that in a metal-rich environment, the line-driven winds are more efficient and massive stars lose very quickly their H envelope. On this point Smith et al. [45] argued that assuming an LBV progenitor for SN 2006gy would favor the presence of the much more efficient continuum-driven eruptions, instead of line-driven winds. Contrary to the latter (as seen in Sect. 2.5), such eruptions do not depend on metallicity.

According to Ofek et al. [32], also the merging of two massive stars could avoid the problem of the non-zero metallicity of NGC 1260. This could also explain the heavy mass-loss derived by the appearance and the velocity of the spectral lines.

As we will see in Section 4.10.2, the PISN hypothesis turned out to be inconsistent with the late-times NIR-detections of Miller et al. [30].

ii) **A pulsational pair instability supernova (Woosley et al. [57])**

As seen in Sect. 2.4, the collision between shells of matter released during subsequent outbursts by pulsational pair-instability SNe can produce a SN display, radiating 10^{50} erg of light, about a factor of ten more than an ordinary supernova. Depending on the initial He core mass and temperature, a newly-formed instability in the star can cause multiple matter ejections, even on short timescales (decades to days). Later ejections have lower mass, because the envelope is expelled in the first pulse, but have higher energy.

As an example, a 110 $M_\odot$ star with solar composition ends its life as a red supergiant (RSG) with a total mass of 74.6 $M_\odot$ and a He core of 49.9 solar masses. When central He and C is burnt and $T > 10^9$ K the instability takes place. The core contracts and gets hotter until it explodes, releasing an energy of 10^{51}erg. However, 10% of this energy is spent to eject $\sim$24.5 $M_\odot$ of the envelope. in a supernova-like display with a luminosity $\sim 4 \times 10^{41}\mathrm{erg\,s^{-1}}$ for 200 days. What is left behind is a 50.7 $M_\odot$ remnant that once again contracts and grows hotter. 6.8 years later, it encounters the pair instability for the second time. This time the pulse is stronger, and $6.0 \times 10^{50}\mathrm{erg\,s^{-1}}$ is shared by a smaller ejected mass of 5.1 $M_\odot$. The collision of this high-velocity shell with the larger mass ejected earlier produces a very bright light curve. Nine years later, the star finishes the final phase of contraction and gently starts silicon burning at its centre, making an iron core that collapses. Of course, many parameters like rotation, magnetic field, opacity etc. can affect the outcome of the last collapse, which lead to different types of compact objects (magnetar, collpsar, or BH).

According to the STELLA models of Woosley et al. [57] the 110 $M_\odot$ star-model can best reproduce the light curve of SN 2006gy (see Fig. 4.4). It should be noted that this scenario does not require an extremely high ^{56}Ni quantity, and also accounts for the weakness of the X-ray and radio emission (given that it does not involve phenomena of standard ejecta-CSM interaction), as well as for the high-velocity features in the spectra.

iii) **A runaway collision in a young starcluster (Portegies Zwart & Van den Heuvel, [35])**

The authors of this scenario want to overcome the inconsistency with the

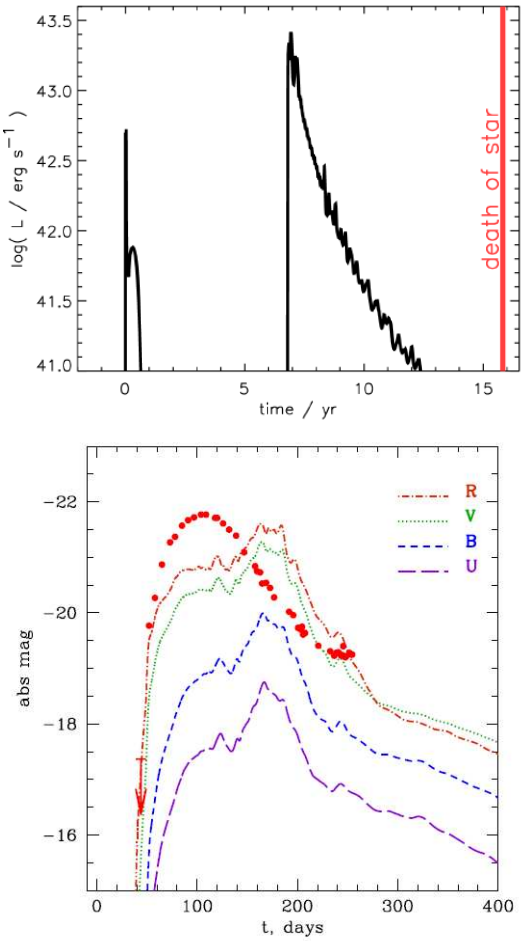

Figure 4.4— *Top*: Cumulative light curve obtained in the model for a 110M$_\odot$ star, from Woosley et al. [57]. The first major eruption ejects about 25 solar masses of hydrogenhelium envelope and makes a transient with luminosity $\sim 6 \times 10^{41}$erg s^{-1} lasting 200 days. Then 6.9 years later a second eruption produces a brilliant event as the fast-moving ejecta collide with the debris of the first supernova . 9 years after that, the star forms a 2.2-solar-mass iron core that collapses to a rapidly rotating neutron star or black hole. A third bright event, possibly a gamma-ray burst, might then occur. *Bottom*: modeled color magnitudes obtained by Woosley et al. [57], compared to the R-band observed light curve by Smith et al. [45]. The models refer to a star of 110M$_\odot$, in which the density of the pulses is multiplied by two. As a consequence, also the kinetic energy and the ejected mass is doubled.

theoretical assumption that, contrary to what observed in the spectra of SN 2006gy, a star with M>100 $M_\odot$ loses its H envelope several hundreds of years before the explosion. Instead, they claim that a merger between a very massive hydrogen-depleted star that already had a core in an advanced phase of helium burning, with a H-rich MS star of 10 to 40 $M_\odot$, 10^4 to 10^5 years prior to the supernova explosion may explain the unusual brightness of SN 2006gy, the presence of the H both in the interstellar medium and in the supernova itself. Phenomena of runaway collisions are supposed to occur frequently in young, dense, starclusters, where the subsequent bombardment results in a net increase in the stellar mass. Given the observational properties of SN 2006gy and of its environment, Portegies Zwart & Van den Heuvel [35] find likely that a young ($< 5\,\mathrm{Myr}$), dense and massive ($10^4 M_\odot \leq m_{cl} \leq 10^5 M_\odot$) star cluster is present at the location of the supernova. After calculating the tidal radius, the stellar mass function and the rate of mass accretion of the cluster, the authors use a King model to reproduce extremely massive stars (until 920 $M_\odot$) via collision runaway.

They conclude that a collision of a ∼20 $M_\odot$ main-sequence star with a supermassive star ($> 100\,M_\odot$) $\sim 10^5$ years before the supernova could conveniently explain the observational data of the bright event.

iiii) **A shell-shocked diffusion model (Smith & Mc Cray, 2007 [46])**

According to this model (see Fig. 4.5), which is based on the model of Falk & Arnett (1974, 1977) [12, 13]), the supernova light is produced by diffusion of thermal energy released by the passage of the SN shock wave through a shell of $10M_\odot$ of material extending to 160 AU, that was ejected by the progenitor in the decade preceding the explosion. The shell is supposed to be initially optically thick ($\tau > 300$) and acts as a pseudo-photosphere, so that the long duration of the peak and the weakness of X-rays emission are explained in terms of a long diffusion time and a very large optical depth.

The SN appears suddenly as soon as the blast wave reaches the surface of the shell, delayed by a few weeks after the actual explosion occurs because during that time the blast wave was expanding through the opaque shell.

By day ∼70, when the maximum R luminosity is reached, the radius of the emitting photosphere reaches R=320 AU. Afterwards, the decline in luminosity is determined by thermal diffusion.

The interaction features typical of type IIn SNe are supposed to arise in the observed spectra as soon as the shock wave breaks out of the opaque

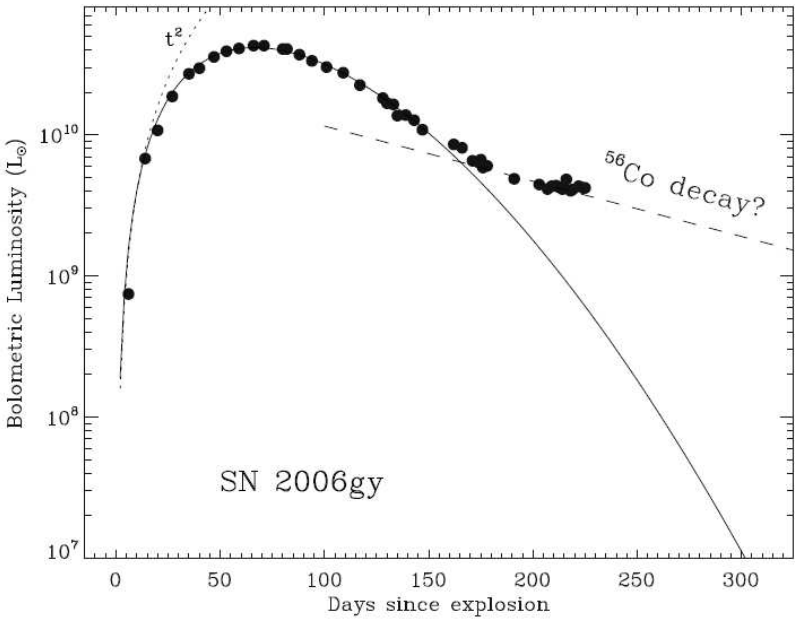

Figure 4.5— Model of the light curve of SN 2006gy by Smith & Mc Cray [46]. The rise to the maximum is modeled as the constant expansion of a black-body, so that $L \propto t^2$. After maximum the light curve evolution is modeled as the diffusion of internal radiation through a homogeneous expanding sphere as done by Falk & Arnet [12, 13]. The dashed line shows the hypothetical ^{56}Co decay luminosity expected for 8 $M_\odot$ of ^{56}Ni .

shell into the surrounding, lower-density wind. The light curve of SN 2006gy observed up to about day 170 comes entirely from energy deposited by the initial blast and does not require any source of radioactive energy or ongoing CSM interaction. However, after ∼170 days the model fails to reproduce the light curve. Instead of fading rapidly as it were expected after the opacity decreases and the radiative diffusion time-scale gets shorter and shorter, the light curve experiences a phase of steady luminosity decline, until day ∼240. This requires an additional energy source. Assuming that the radioactive decay is responsible to power the optical luminosity at this phase, the authors calculate that 8 $M_\odot$ of ^{56}Ni are required. Alternatively, a possible source could be continued shock interaction with the transparent CSM external to the opaque shell.

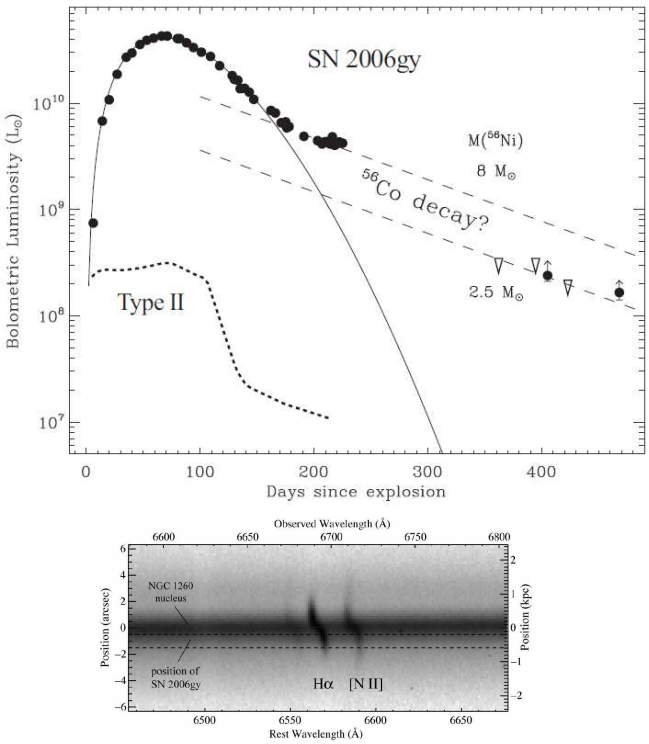

Figure 4.6— *Top:* Bolometric luminosity light curve of SN 2006gy, including the lower limits to the late-time luminosity [44]. Also plotted along with the light curve is the photon-diffusion model from Smith & McCray [46]. The two late-time data points are lower limits to the luminosity derived from the observed K'-band magnitudes, where the SED is supposed to peak. Dashed lines show the expected energy deposition rate for representative masses of ^{56}Ni . *Bottom:* Observed spectrum of SN 2006gy at 364 days after explosion. Continuum from the nucleus of NGC 1260 is seen clearly, as is the narrow Hα and [N II] emission from H ii regions that follow the galaxys rotation curve. No broad or intermediate-width Hα emission from SN 2006gy is detected.

4.4 The fading of SN 2006gy

The debate about the nature of the brightest event became even more intriguing when, after the observation following the period of Solar occultation (∼1 year from discovery), it was reported to be undetected in deep optical images [44]. Instead, it turned out to be visible in the K' band on day 405 and 468. Upper limits were derived in the R, J and H bands (Fig.4.6). An optical, LRIS low-resolution spectrum was also acquired on day 364.

The bolometric luminosity could be computed until late phases by Smith et al. [44] supposing that the black-body energy distribution peaks in the K' band. Indeed, the late-times brightness resulted to be much higher than the predicted decay from photon diffusion in the shell-shocked model of Smith & McCray [46]. The authors discussed this additional luminosity in terms of (*i*) *continued CSM interaction* as the shock runs into an extended, dense CSM created by a progenitor with $\dot{M} \sim 10^{-2}\,M_{\odot}\,yr^{-1}$, (*ii*) *radioactive decay* from ∼2.5 $M_{\odot}$ of ^{56}Ni , or (*iii*) *an IR echo*, as light from the time of peak luminosity is now heating dust in another massive shell at a radius of 1 light year from the SN, ejected by the progenitor star 1500 yr earlier.

Regarding the first hypothesis, the CSM interaction is supposed to occur as the blast wave encounters additional dense material outside of the LBV-like ejecta shell required in the shell shocked models of Smith & Mc Cray [46]. However, after an analysis of the Hαprofile and intensity in the optical spectrum, the authors concluded that both the absence of a broad or intermediate emission and the weakness of the detected flux made the CSM-interaction hypothesis unlikely. Also the weakness of the X-ray emission observed on December 2007 confirmed that CSM could not be the main engine of the late-times brightness.

Concerning the radioactive decay hypothesis, the late-times luminosity measurements set a new lower limit to the ejected ^{56}Ni mass as 2.5 $M_{\odot}$. However, the NIR emission could also be explained in terms of newly-formed dust in the ejecta which is absorbing optical radiation and re-emitting it in the NIR. As a consequence, the true emitted flux could be much larger, and therefore also the true ejected ^{56}Ni mass. This would gave credit to the pair instability scenario.

The last suggestion was the presence of an IR echo, produced when the UV and visual radiation from the SN at peak light has reached a dust shell at large radii; the dust gets heated and reradiates the absorbed energy in the IR [11]. With standard assumptions about dust grains and temperatures at a radius of 0.5-1 light year, the authors calculated that the dust mass near the lightcone needed to account for that IR luminosity is at least 0.05-0.1 $M_{\odot}$. With a normal gas-to-dust ratio, this requires the existence of a pre-existing shell of at least 5-10 $M_{\odot}$. Given the wind velocity derived by Smith et al. [45], i.e. 200 km s^{-1} ,

this shell must have been ejected by the progenitor star roughly 1,500 yr before the explosion. According to the authors, this scenario reinforces the hypothesis of the explosion of a giant star like η Carinae, since these kind of stars are the most subjected to multiple eruptions and are most frequently surrounded by multiple massive shells.

4.5 Was it really extraordinary?

The Padova-Asiago Supernova Group, in collaboration with other European institutions, was also active in the observations of SN 2006gy since the early phases. Given the difficulties encountered with the data reduction -complicated by the strong background-contaminated explosion site- and the proliferating of studies and theories about its nature, the work on SN 2006gy took most of the time of my PhD.

However, the analysis of data both from the observational and from the theoretical point of view has lead to very interesting results.

In **Agnoletto et al. (2009)** [1] we have presented new data, which include observations at all relevant phases, from discovery to more than 1 year later. Multi-band light curves were presented for the first time. An extended spectral sequence was shown and discussed. By comparison with other SNe and by means of modeling, the study on SN 2006gy aimed at verifying to which extent this SN is really extra-ordinary, as other authors has suggested, and to provide new constraints for the progenitor and the explosion.

4.6 Observations

Optical (*BVRI*) and near–infrared (*JHK'*) images of SN 2006gy were acquired at TNG, NOT (La Palma, Spain) and the Copernico 1.82m Telescope on Mt. Ekar (Asiago, Italy) over a period spanning more than 500 days from discovery. Optical spectroscopy was also performed, up to ∼389 days (see Table 4.1 for a complete log of the observations).

Since the SN is located very close to the nucleus of the host galaxy, template subtraction was required for photometry. We used archival B-, R- and I-band images of NGC 1260 acquired at the Jakobus Kapteyn Telescope[2] (La Palma, Spain), and a V-band image taken at the Schmidt Telescope at Kiso Observatory[3] (Japan). Additional information about the template images is given in Table 4.2.

All images were debiased and flat–field-corrected. A local sequence of stars in the SN field was calibrated using observations of standard stars obtained during photometric nights. Template subtraction was performed using ISIS Alard & Lupton (1998) [2], and the SN magnitudes were measured on the subtracted

[2]web archive http://archive.ast.cam.ac.uk/ingarch/ingarchold.html
[3]web archive http://www.ioa.s.u-tokyo.ac.jp/kisohp/

UT Date	Telescope	Equipment	Bands	Grisms	Range [Å]	Resolution [Å]	Pixelscale ["/pix.]
06/09/25	TNG	DOLORES	-	LR-B, LR-R	3200-9000	18, 17	0.25
06/09/30	NOT	ALFOSC	*BVRI*	4	3400-8800	21	0.19
06/10/29	Ekar1.82m	AFOSC	*BVRI*	-	-	-	0.46
06/12/19	Ekar1.82m	AFOSC	*BVRI*	4	3500-7500	24	0.46
07/02/10	NOT	ALFOSC	*BVRI*	4, 5	3500-9800	21,'20	0.19
07/03/10	Ekar1.82m	AFOSC	*BVRI*	-	-	-	0.46
07/03/12	Ekar1.82m	AFOSC	-	2, 4	3400-7600	38, 24	0.46
07/04/13	Ekar1.82m	AFOSC	*VRI*	-	-	-	0.46
07/09/14	Ekar1.82m	AFOSC	R	4	3400-7600	24	0.46
07/10/05	TNG	NICS	*JHK'*	-	-	-	0.25
07/10/17	TNG	DOLORES	*BRI*	-	-	-	0.25
08/01/12	TNG	NICS	*K'*	-	-	-	0.25

Table 4.1— Journal of photometric and spectroscopic observations of SN 2006gy.

UT Date	Telescope	Equipment	Bands	Exp.time	Seeing ["]	Pixelscale ["/pix.]
91/12/01	JKT	AGBX	*B*	600	1	0.33
91/12/01	JKT	AGBX	*R*	300	1.15	0.33
96/01/13	JKT	AGBX	*I*	360	1.5	0.33
03/02/12	Schmidt T.		*V*	300	3.7	1.46

Table 4.2— Main data on the archive images used for the photometric template subtraction.

image with a point-spread function (PSF) fitting technique, as explained in Sect. 3.4 and 3.5.

For spectroscopy, all scientific exposures were acquired at low airmass and positioned the slit along the parallactic angle, as described in Sect. 3.5.4. Wavelength calibration was accomplished with arc-lamp exposures and checked against the night-sky lines. The flux was calibrated using instrumental sensitivity functions obtained from observations of spectrophotometric standard stars. These were used also to remove telluric absorptions from the spectra. In order to improve the signal-to-noise ratio, separate spectra taken during the same nights were combined. Finally, flux calibration was checked against photometry. If necessary, a constant multiplicative factor was applied to correct for flux losses caused by slit miscentering or non–photometric sky conditions.

The spectrum acquired on 2006 December 19th with the Ekar 1.82m telescope required further adjustments because of the poor seeing conditions and the residual contamination from the galaxy background. The latter was removed using the spectrum at 389 days, where the SN is not detected, as a background template.

For the sake of simplicity, the *phase* cited in the next Sections refers to the same *reference epoch* as in Smith et al. [45], JD=2453967 (2006 August 19.5 UT). This was derived from a backward extrapolation of the rising branch of the light curve. Smith et al. (2007) [45] refer to this date as the explosion epoch, but this term may be misleading in view of some of the proposed scenarios[4].

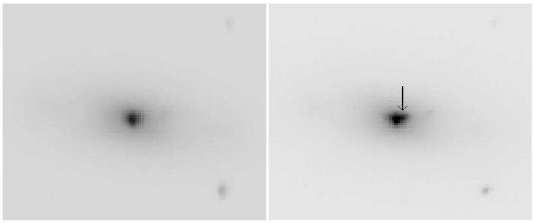

Figure 4.7— Images aquired with NICS at TNG with filter J (left panel) and K' (right panel) on October 5th, 2007 (JD 2454378.5). SN 2006gy is still clearly visible near the host galaxy nucleus in the K' band image, whereas there is no detectable source at that position in the J band frame.

[4]In the shocked-shell diffusion model (Smith & Mc Cray, (2007) [46]) the detection of the SN emission occurs a few weeks after the real explosion. In the scenario suggested by citetwoos07 there is not even a SN explosion, but only an outburst release of matter.

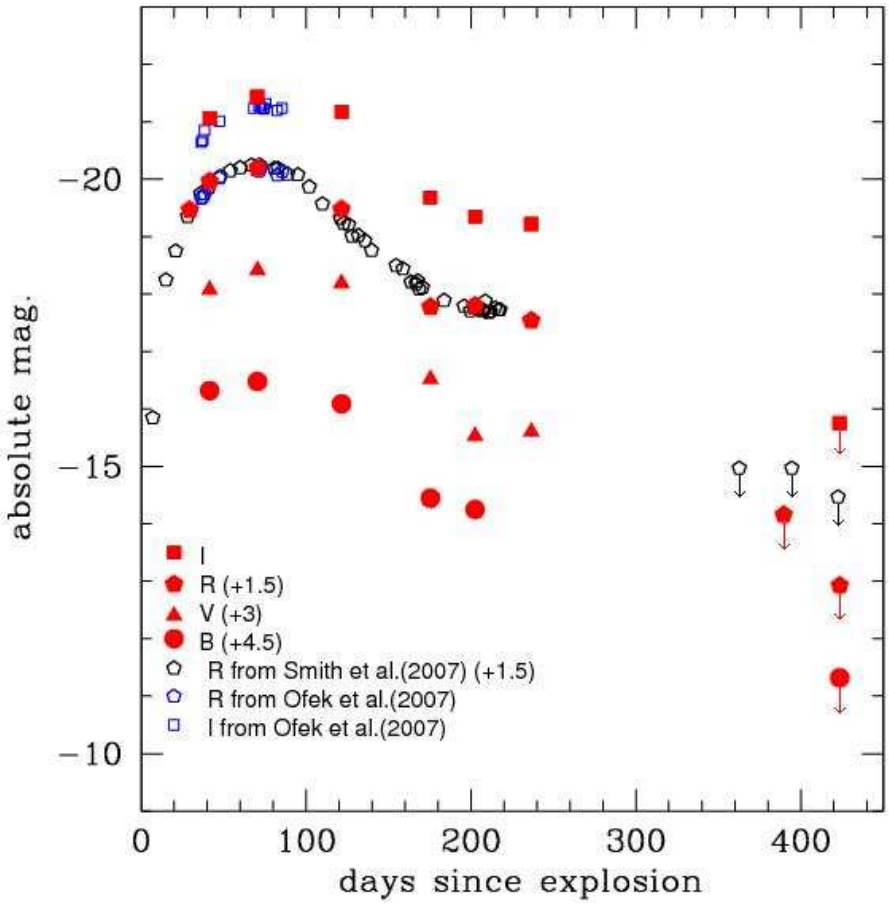

Figure 4.8— BVRI absolute light curves of SN 2006gy, obtained with the distance and extinction reported in the text. Late phase (>300 days) detection limits are marked with an arrow. R data from Smith et al. (2007) [**?**] and Smith et al. 2008 [**?**], as well as R and I data from citetof07 are also reported.

UT Date	JD - 2,400,000	Phase [days]	*B*	*Berr*	*V*	*Verr*	*R*	*Rerr*	*I*	*Ierr*
06/09/18	53996.5	29.5	-	-	-	-	15	-	-	-
06/09/30	54008.5	41.5	16.00	.08	15.19	.22	14.51	.10	14.48	.07
06/10/29	54037.5	70.5	15.84	.06	14.85	.13	14.28	.04	14.10	.06
06/12/19	54088.5	121.5	16.23	.06	15.08	.15	14.99	.04	14.37	.06
07/02/10	54142.4	174.5	17.87	.08	16.75	.22	16.69	.10	15.86	.07
07/03/10	54169.5	204.5	18.07	.06	17.74	.15	16.67	.04	16.19	.06
07/04/13	54203.5	236.5	-	-	17.66	.15	16.93	.04	16.32	.06
07/09/14	54356.5	389.5	-	-	-	-	>20.30	-	-	-
07/10/17	54390.6	423.5	>21	-	-	-	>21.55	-	>19.75	-

Table 4.3— Optical photometry of SN 2006gy. The phase is reported with respect to JD=2453967.0.

4.7 Photometry

To compute the absolute magnitudes of SN 2006gy some assumptions regarding the host galaxy distance and SN extinction are needed.

Lacking other indicators, the distance to NGC 1260 was estimated from the Hubble law, $d = v_{rec}/H_0$, where $v_{rec} = 5822 kms^{-1}$ is the host galaxy recession velocity corrected for Virgo cluster infall (from *HyperLEDA*[5]) and $H_0 = 72 \pm 8$ $km\,s^{-1}\,Mpc^{-1}$ Freedman et al. (2001) [15]. These values imply a distance modulus $\mu = 34.53$, equivalent to a distance of 80.86 Mpc.

We adopted a Galactic extinction towards NGC 1260 of $E(B-V)_{gal} = 0.16$ ($A_{B,gal} = 0.69$, Schlegel et al. (1998) [42]). An estimate of the extinction in the host galaxy was obtained comparing the spectra of SN 2006gy to those of SN II 2007bw, another peculiar and bright SN IIn, photometrically similar to SN 2006gy (cf. Chapter 5). This yields $E(B-V)_{host} \simeq 0.4$, assuming little or no extinction for SN 2007bw. It is interesting to note that on the 42 days spectrum the EWs of NaID due to the galactic and interstellar absorption are 2.2Å and 5.5Å, respectively. Assuming for NGC 1260 a gas-to-dust ratio along the line of sight as in our Galaxy and adopting the extinction of Schlegel et al. (1998) [42], the internal absorption derived is fully in agreement with that derived by comparison with SN 2007bw.

Therefore the total color excess is $E_{tot}(B-V) \simeq 0.56$. This is comparable to the estimate of Smith et al. (2007) [45], i.e. $E_{tot}(B-V) \simeq 0.48$, which was also obtained by comparison with SNe IIn, and slightly smaller than the value

[5] http://leda.univ-lyon1.fr/

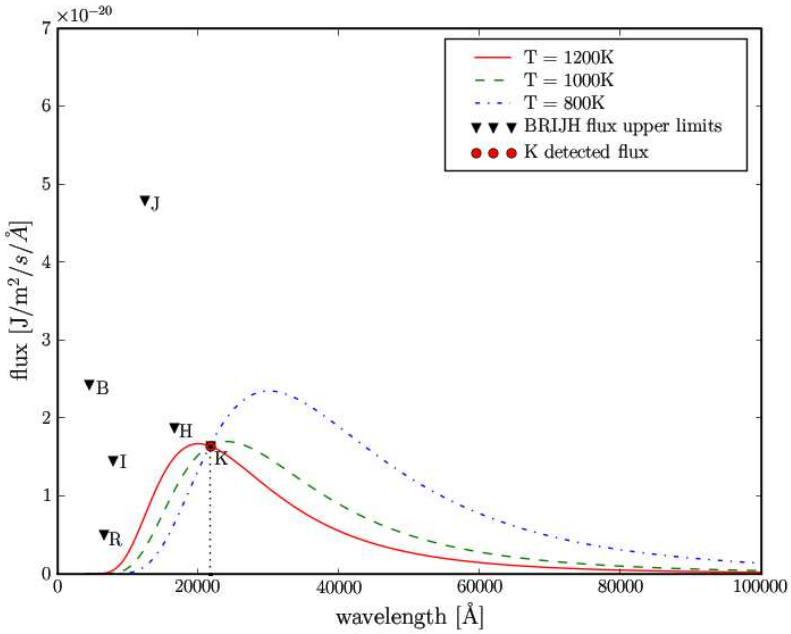

Figure 4.9— Comparison between the optical (day 423) and near–infrared (day 411) flux measured for SN 2006gy. We also show the expected emission from dust at different temperatures, normalized to the K band magnitude.

adopted by Ofek et al. (2007) [32], $E_{tot}(B-V) \simeq 0.7$.

The *BVRI* absolute light curves of SN 2006gy are plotted in Fig.4.8. Instead, the light curves in apparent magnitudes, and the (B-V) color evolution are shown in Fig.4.10,4.11,4.12 and 4.13.

In all bands the light curve exhibits a slow increase to maximum, which is reached ~ 70 days after the reference epoch. The peak magnitudes are $B \sim -21$, $V \sim -21.4$, $R \sim -21.7$ and $I \sim -21.5$. Such an extended, plateau-like peak was noted for a type IIn SN only in the case of SN 2005kd (Tsvetkov et al. [50]).

Between day ~ 100 and day ~ 170, the light curve declined relatively rapidly ($\gamma_B \sim 3.0\text{mag}\,(100\,\text{d})^{-1}$, $\gamma_V \sim 3.1$, $\gamma_R \sim 3.2$, $\gamma_I \sim 2.8$). Then, from day ~ 170 onwards the light curve evolution suddenly flattened: in the following ~ 70 days the decline was only $\gamma_R \sim 0.4\text{mag}\,(100\,\text{d})^{-1}$. When the SN could be observed again after solar occultation, its luminosity was below the detection limit in the optical bands. A limit was obtained placing artificial stars of different

magnitudes at the SN position. Despite the long exposure times, only relatively bright upper limits were derived because the SN is very close to the nucleus of the galaxy (cf. [45], Figure 1). The derived apparent magnitude limit on day 389 is $\gtrsim 20.3$ in R. Optical upper limits were obtained also at 423 days, when we derive $B \gtrsim 21.0$, $R \gtrsim 21.5$ and $I \gtrsim 19.75$. These measurements imply a new steepening in the luminosity decline after day 237.

Guided by the evolution of other SNe (e.g., SN 1998S, [36] or SN 2006jc, [9, 25, 44, 49]), we considered the possibility that at late epochs a significant fraction of the bolometric luminosity could be emitted at IR wavelengths. To test whether this was the case, late observations of SN 2006gy were obtained with NICS at the TNG, on 2007, October 5 (*JHK'* bands) and on 2008, January 12 (*K'* band only). We could not apply the template subtraction technique in the near-infrared because the available pre-discovery images of the host galaxy retrieved from the 2MASS archive are not deep enough to be compared to the TNG images. Therefore, we had to rely on the PSF fitting technique which, given the SN position, has a large uncertainty. Photometric calibration was performed adopting field star magnitudes as listed in the 2MASS Point Source Catalogue[6].

The SN was not detected in the J and H bands, for which we could only estimate upper limits, $J \gtrsim 17.0$ and $H \gtrsim 16.5$. Instead, a point source was detected in the *K'* band at the SN position (Figure4.7). The SN was measured at $K \sim 16.0 \pm 0.5$ on day 411 and $K \sim 16.3 \pm 0.5$ on day 510. These values are ~ 1 mag fainter than those measured by Smith et al.(2008) [44] at similar epochs (K=15.1 $\pm$ 0.1 and K=15.4 $\pm$ 0.1 on day 405 and 468, respectively). Even allowing for the large error bars, the two sets of measurements do not agree, probably because of a different calibration.

[6] http://tdc-www.harvard.edu/software/catalogs/tmpsc.html

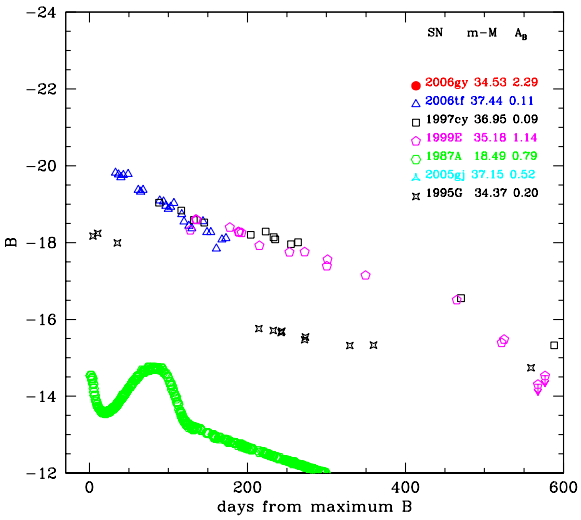

Figure 4.10— B absolute magnitude of SN 2006gy compared to a sample of IIn SNe and SN 1987A.

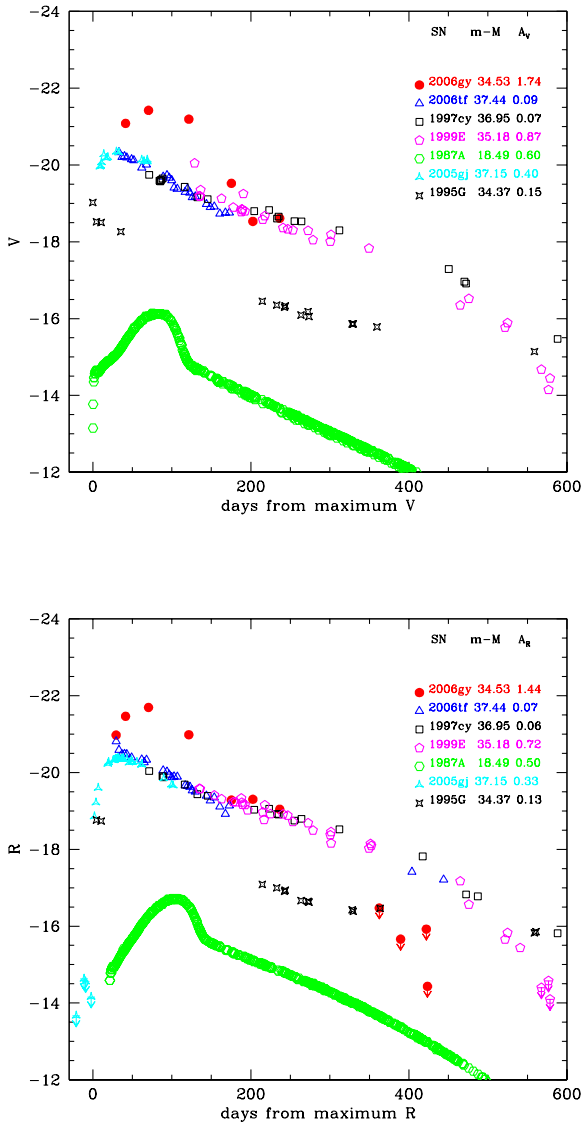

Figure 4.11— V and R absolute magnitude of SN 2006gy compared to a sample of IIn SNe and SN 1987A.

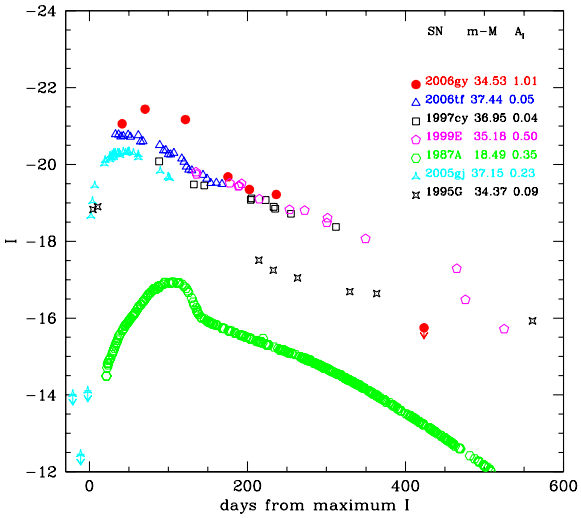

Figure 4.12— I absolute magnitude of SN 2006gy compared to a sample of IIn SNe and SN 1987A.

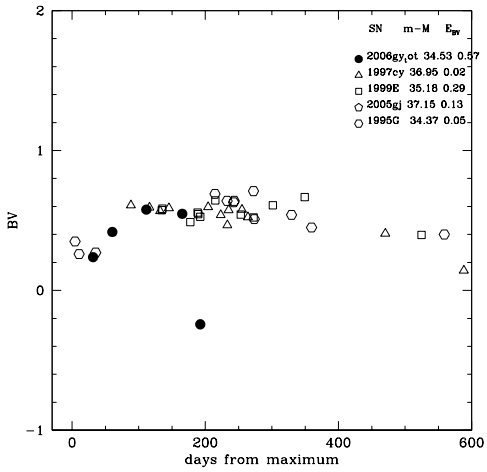

Figure 4.13— (B − V) color evolution of SN 2006gy compared to a sample of IIn SNe.

4.7.1 Infrared emission and bolometric luminosity

Given the *K'*-band detection of the SN at 411 and 510 days, it cannot be excluded that at late phases a considerable amount of flux is emitted in the near-infrared.

Smith et al. [44] suggested two possible sources of the late *K'*-band luminosity. The *K'*-band emission could be associated with an IR light echo from circumstellar dust, for which the input energy is the light emitted by the SN near maximum. In this case the IR flux should not be considered when computing the late-time bolometric light curve. Alternatively, the IR flux may originate from circumstellar dust heated by an instantaneous energy supply (radioactive decay or on-going CSM-ejecta interaction), as was suggested by Pozzo et al. [36] to explain the late phase photometric data of SN 1998S.

In order to get some constraints on the total emission from dust at $\sim$ 411-423 days we assumed a black body energy distribution multiplied to a factor $1/\lambda$, as an approximation of what reported in Spitzer et al. (2008), and normalized it to the observed K-band flux. Given that we have no constraints on the dust temperature, we adopted three values including T=1200K, the dust temperature in the ejecta of SN 1998S derived by Pozzo et al. [36]. For each value we plotted the spectral energy distribution (SED) of the associated emission (Fig. 4.9) and integrated over the entire wavelength range from $\lambda_{\rm K} = 2.16\,\mu$m to $\lambda = \infty$.

It is interesting to note that the K-band luminosity of SN 1998S measured at similar epochs (K=13.8 at $\sim$464 days) would differ from that of SN 2006gy by a factor 1-5 (adopting for SN 2006gy K=16.3 from this work or K=15.4 from S08) if scaled at the same distance. Therefore, given that the two fluxes are of the same order, it is plausible that any mechanism explaining the IR emission of SN 1998S can work also for SN 2006gy.

From our multiwavelength photometry we can derive the pseudo-bolometric luminosity evolution of SN 2006gy integrating the flux in the optical bands ($BVRI$). The pseudo-bolometric light curve is shown in Fig.5.12, compared to those of the type II SNe 1987A, 1995G, 1997cy, 1999E and 2005gj. The pseudo-bolometric luminosities which include the dust contribution in the near IR are represented with plus symbols. It is remarkable that, at about 6 to 8 months, the luminosity and decay rate of SN 2006gy become comparable to those of other events, in particular to SNe 1997cy and SN 1999E. We will come back to this issue in the Sections 4.9.1 and 4.9.3.

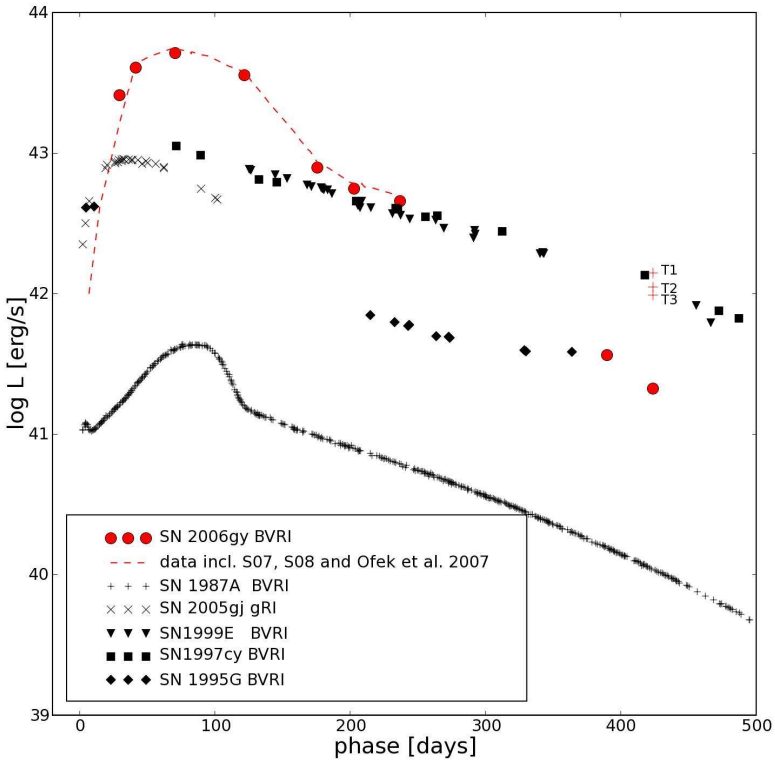

Figure 4.14— Pseudo-bolometric light curve of SN 2006gy compared to those of type IIP SN 1987A [56], type IIn SN 2005gj [38], SN 1999E [40], SN 1997cy [16, 51] and SN 1995G [33], all integrated in the same wavelength range. Red crosses at late times include the near-IR contribution due to a possible cold dusty region in SN 2006gy ejecta, based on the K-band detection and on three possible dust temperatures (T1=800K, T2=1000K and T3=1200K). For SN 1997cy and SN 1999E the epochs of the associated GRB explosions (GRB 970514 and GRB 980919) are adopted as phase reference epochs.

4.8 Spectroscopy

The spectral evolution of SN 2006gy from day 37 to day 389 is presented in Figure 4.15. The spectra have been de-redshifted and corrected for extinction.

The early spectra (days 37 and 42) show the typical features of SNe IIn, namely a blue continuum and strong Hα and Hβ emission lines, without broad P-Cygni absorptions.

Using *GELATO* [19], the automatical spectra comparison tool applied to the Asiago Supernova Archive (ASA), the best match for the earliest available SN 2006gy spectrum (phase 37) is found with SN 1995G (∼36 days since discovery, [33]), which is generally considered a typical SN IIn, although there are differences in the strength of the lines emission.

Three months after discovery, the spectrum of SN 2006gy became similar to those of other well-studied SNe II. In the high resolution spectrum taken on day 96 by S07 (their Figure 4) narrow absorption lines of Fe II (multiplets 42, 48, and 49 at 5000-5400 Å and multiplet 74 in the region 6100-6500 Å) are evident. A similar narrow line forest was identified in the spectra of SN 1999el [10], SN 1995G [33] and SN 1994W [6, 47]. In all cases these lines are associated with slowly expanding, unperturbed material surrounding the star.

Despite the lower resolution and S/N ratio, our spectrum at phase 122 days is broadly consistent with the features discussed by S08. At this phase the Hα flux has decreased by a factor of 2 with respect to the first spectrum, while Hβ emission almost disappeared.

At a phase of 174 days the near-IR Ca II triplet is strong in emission. For this epoch a good spectral match is obtained with SNe 1997cy, 1999E (Fig.4.17), 2002ic and 2005gj.

The Hα flux continues to decrease with time: on day 174 it is ∼3 times fainter than on day 37 and on day 204 even 5 times. Finally, the last spectrum (day 389) shows no evidence of the typical lines of SNe II; at this epoch, the narrow Hα emission should be attributed to the host galaxy. This is consistent with S08 and with the upper limit in the optical luminosity that was deduced from the photometry.

The emission peak of Hα remains at the rest frame wavelength at all phases, exhibiting a three–component profile (Fig.5.18). For the intermediate Hα component we measured a FWHM$\sim$ 2100 km s^{-1} at a phase of 42 days, and FWHM $\sim$ 3200 km s^{-1} at 174 days. Smith et al. [45] pointed out an asymmetry of the line at early times (also evident in our day 42 spectrum), likely caused by a blueshifted P-Cygni absorption, which vanishes with time. For this reason we can admit that the true unabsorbed profile Hα remained roughly constant during the SN evolution. A roughly constant FWHM $\sim$ 9100km s^{-1} is measured

for the broad component of Hα.

The physical interpretation of the intermediate and broad components is still a matter of debate. Smith et al. 2007 [45] and Smith et al. 2008 [44] assumed that the intermediate component ($v \sim 4000\,km\,s^{-1}$) traces the kinematics of the SN shock wave, while the broader one is related to the SN ejecta ($v \sim 6000\,km\,s^{-1}$, a value significantly lower than what we obtain, $v \sim 9100 km\,s^{-1}$). The *intermediate* velocity component was used to compute the luminosity expected from CSM interaction. On the other hand, according to Chevalier et al. [5] and to Zampieri et al. [59], the luminosity originating from the reverse shock during ejecta-CSM interaction is proportional to the ejecta velocity, i.e. to the width of the *broadest* Hα component. There is still no consensus on this issue. Because of these ambiguities, one should be careful before assigning physical velocities to various regions from just line widths, especially for objects with peculiar individual features as are SNe IIn.

4.9 Discussion

As discussed in Sect. 4.7, the light curve of SN 2006gy shows three distinct phases: *i)* a very broad, exceptionally high luminosity peak (day 0 to ∼170), *ii)* an intermediate phase of slow decline (day ∼170 to ∼237) and *iii)* a late phase in which the optical luminosity drops below the detection limit and IR emission dominates (day >389). As we will show, the first phase requires a specific star+CSM configuration. The other two phases have been observed in other SNe.

In the following, we rewind the movie of the event and use the late observations to constrain the possible scenario. Starting from the late phases, we discuss the role of dust and ^{56}Ni in the ejecta, stressing that a very large amount of ^{56}Ni is not required. We then consider the evolution of the SN at intermediate phases and explain that, independently of the source that powered the luminosity at peak, interaction dominates between days ∼ 170 and ∼ 237. Finally, we discuss the light curve models for the first ∼5 months obtained with a semi-analytical code Zampieri et al. [60]. Based on these results, we propose a new evolutionary scenario for SN 2006gy.

4.9.1 Nickel mass and dust emission

The late light curve of most SNe is powered by the radioactive decay of ^{56}Ni into ^{56}Co and ^{56}Fe via γ and e^+ deposition.

Thermonuclear SNe Ia eject a large ^{56}Ni mass ($0.1M_\odot < M_{^{56}Ni} < 1.1M_\odot$, Cappellaro et al. [4], Mazzali et al. [27]), but become rapidly transparent to the γ-rays from the radioactive decay because of the small ejected mass and the

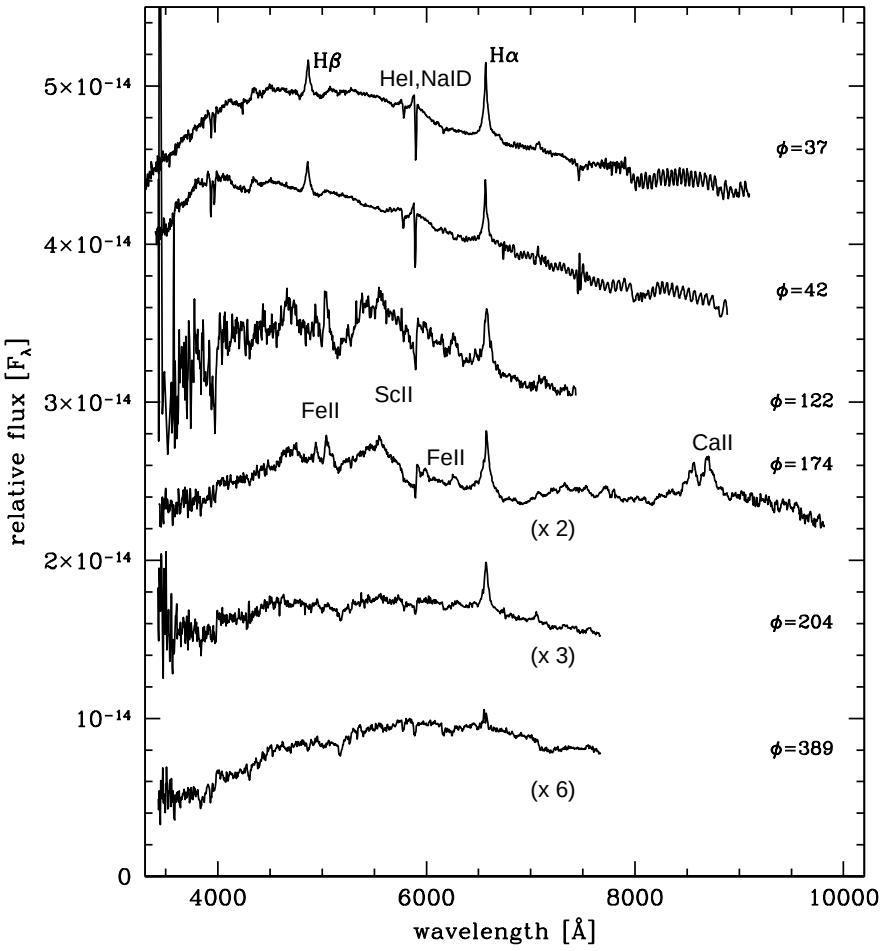

Figure 4.15— Spectroscopic evolution of SN 2006gy from 37 days to 389 days since explosion in the host galaxy rest-frame, corrected for extinction assuming E(B−V)=0.56. The spectra at phase 174, 204 and 389 were multiplied by a factor 2, 3 and 6 respectively.

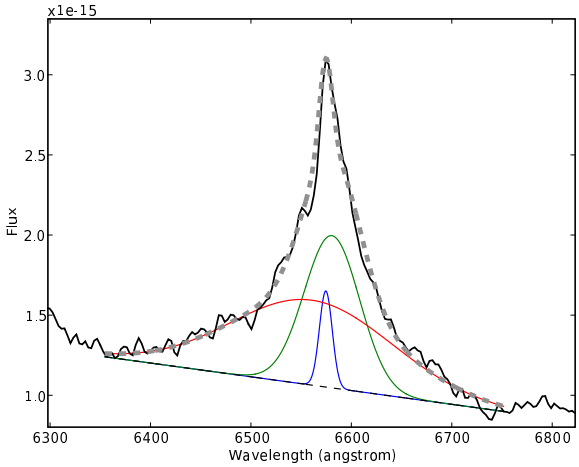

Figure 4.16— Detail of the Hα profle in the spectrum obtained at NOT on February 10th, 2007. The line is decomposed into three gaussian profiles, having FWHM = 685 (unresolved), 3200 and 9000 km s^{-1}.

high expansion velocity. As a consequence, at $t \sim 100$ days after explosion the luminosity declines at a rate $\sim$1.5mag (100 d)$^{-1}$, higher than the ^{56}Co decay input ($\sim$ 0.98mag (100 d)$^{-1}$). A similar behavior was found for most type Ib/c SNe [7].

In the case of H-rich, core-collapse SNe the ejecta remain almost opaque to γ-rays for more than a year, and the late-time luminosity decline tracks the radioactive decay. In this case, if the date of the explosion is known, the late-time luminosity provides a direct estimate of the ejected ^{56}Ni mass. This spans a wide range of values ($0.005 < M_{^{56}Ni} < 0.3 M_\odot$; L. Zampieri et al., in preparation), but is typically smaller than in SNe Ia and Ib/c.

For SN 2006gy, in the optical bands only upper limits to the luminosity at very late phases (411 days) can be obtained. In the near infrared, the K-band detection reported in S08 and discussed in the previous section may be suggestive of the presence of low-temperature dust emitting in the far IR. This makes a precise estimate of the ejected ^{56}Ni mass difficult. The bolometric luminosity including the emission from dust (plus symbols in Fig.5.12) imply ejected ^{56}Ni masses up to $\sim 15 M_\odot$ for T=800K. However, given the uncertainty on the nature of dust and its temperature, a more significant estimate of M(^{56}Ni) can be obtained adopting the bolometric luminosity at earlier epochs, i.e. at

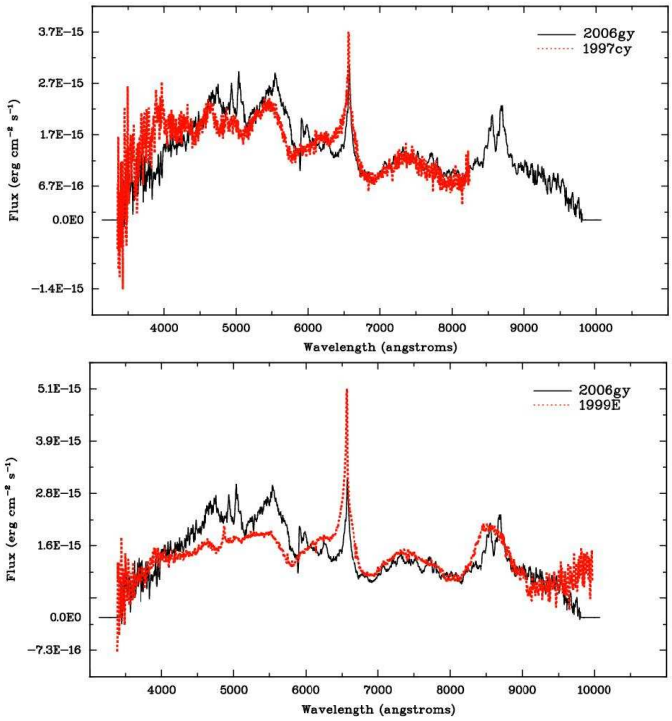

Figure 4.17— GELATO comparison between the spectrum of SN 2006gy at phase ∼174 days, SN 1997cy (*top*, [51]) and SN 1999E (*bottom*, [40]) at similar phases. Although the comparison SNe have broader lines, (e.g., $\mathrm{FWHM_{H\alpha}}$=12800 km s^{-1} in SN 1997cy according to [51]), the objects show an overall remarkable similarity.

$\sim$ 180 days. At this phase the relation $\mathrm{L} = 1.4 \cdot 10^{43} \mathrm{M_{Ni}} \cdot \exp(-\mathrm{t}/113.6)\,\mathrm{erg\,s^{-1}}$ provides $\mathrm{M_{Ni}} \sim 3\mathrm{M_\odot}$ assuming complete γ-ray trapping. This value is in disagreement with the value obtained by Smith & McCray [46] with the same relation ($\mathrm{M_{^{56}Ni}} \sim 8\mathrm{M_\odot}$). A possible explanation may reside in a different estimate of the bolometric luminosity, which is about a factor 3 higher in Smith & McCray [46].

Of course, we expect the bolometric flux - and therefore the ^{56}Ni mass - to increase if the IR/longer wavelength emission contribution is taken into account. On the other hand, the luminosity decay at phase 170-137 days is much slower than what is expected from ^{56}Co decay. This suggests that an energy source additional to radioactive decay of ^{56}Ni has to be present. Compared to those measured for other SNe, an amount of $3\mathrm{M_\odot}$ of ^{56}Ni may not appear

unreasonably large (see for example SN 1999as, [8]).

4.9.2 Evidence of strong, late-time ejecta-CSM interaction

We mentioned in Sect. 4.7.1 that at 170-237 days SN 2006gy shares several properties with SNe 1997cy, 1999E, 2005gj and 2002ic. Although some authors regard some of these SNe as thermonuclear explosions (see Hamuy et al. [18] for SN 2002ic and Prieto et al. [38] for SN 2005gj, but see also Benetti et al. [3] and S. Benetti et al. 2009, in preparation, for an alternative scenario) there is unanimous consensus on the fact that interaction dominates their emission at late phases. Despite the brighter magnitude at maximum, SN 2006gy has luminosity and luminosity decline rate comparable to the SNe mentioned above at 170-237 days (Fig.4.17), which is when they also show similar spectra.

Therefore, it is natural to assume that at this phase ejecta-CSM *interaction plays a dominant role also in SN 2006gy.* Although the low X-ray flux at this phase (cf. §6.2) might appear to be in contradiction with the ejecta/CSM interaction scenario, this may not be a problem, because for sufficiently high densities ($\rho \sim 10^8 \mathrm{g\,cm^{-3}}$) the X-rays that are produced in the shock are immediately absorbed [51].

In the context of interaction, the luminosity L arising from the shock is proportional to the progenitor mass loss rate $\dot{\mathrm{M}}$, to the ejecta velocity $\mathrm{V_{ej}}$ and to the unshocked CSM wind velocity $\mathrm{V_{CSM}}$, as follows: $\mathrm{L} \propto \mathrm{V_{ej}^3 \dot{M} V_{CSM}^{-1}}$. Unfortunately, because of the ambiguity in the interpretation of emission line profiles, we cannot precisely measure the velocities in the different circumstellar regions and thus derive a reliable estimate of the CSM density from the observational data. However, the emission lines in SNe 1997cy and 1999E are generally broader than in SN 2006gy (i.e., their ejecta are probably faster), but their luminosity is comparable. In view of the former relation, we expect that the shock wave of SN 2006gy encounters a higher CSM density at 170-237 days.

4.9.3 A highly energetic supernova impinging on massive gaseous clumps

The SN evolution during the first 170 days is explained reasonably well by the scenario proposed by Smith & McCray [46]. In the shocked-shell diffusion model the supernova light is produced by diffusion of thermal energy after the passage of the SN shock wave through a shell of $10\mathrm{M_\odot}$ of material, ejected in the decade preceding the explosion. The shell is supposed to be initially optically thick and acts as a pseudo-photosphere, so that the long duration of the peak and the weakness of X-rays emission are explained in terms of a long diffusion time and a very large optical depth. The interaction features typical of type

IIn SNe are supposed to arise in the observed spectra as soon as the blast wave breaks out of the opaque shell into the surrounding, lower-density wind.

However, in Smith & McCray [46] a number of items have not been considered. A first inconsistency concerns the model assumptions. According to the model of Falk & Arnett [12, 13] which is adopted in Smith & McCray [46], in order to reproduce the observed luminosity rise to maximum, the initial radius of the shocked shell has to be much smaller than the radius at peak luminosity. However, in the model of Smith & McCray [46] the initial and final radius differ only by a factor of 2. Thus the model of Falk & Arnett [12, 13]is not applicable: the simple assumption of the existence of a single shell at a large radius surrounding the exploding star can not explain the properties of the light curve of SN 2006gy, in particular the slow rise to maximum.

Secondly, in the model of Smith & McCray [46] the important role of ^{56}Ni is overlooked. No attempt has been made to estimate the amount of ^{56}Ni deposited by the SN and to determine its effect on the light curve during the diffusive phase[7].

The third problem concerns recombination, whose effects can not be neglected as soon as the decreasing photospheric temperature reaches the gas recombination temperature during the post-diffusive phase.

With these shortcomings in mind, we have developed an alternative, comprehensive scenario that attempts to take all these aspects into account. First of all, we divided the evolution of SN 2006gy into two distinct phases, before and after maximum luminosity. Each phase was modeled independently. The earlier phase (i.e., the rising branch of the light curve) was modeled as the explosion of a core-collapse SN originating from a compact progenitor. For the peak phase we adopted a scenario similar to that of Smith & McCray [46], in which the ejecta impact on very massive ($> 6M_{\odot}$, see Table 5) clumps of previously ejected material and deposit their kinetic energy. Because the density is very high, the energy of the shock produced by the ejecta-clump interaction is completely thermalized. A photosphere forms, so that the evolution of the shocked clumps can be modeled as if it was another SN with very large radius and little ejected ^{56}Ni.

A fundamental difference with respect to the model of Smith & McCray [46] is that, in our scenario, the true SN explosion is not completely hidden by the circumstellar material which is therefore not homogeneously distributed around the star. Rather, it is fragmented into big clumps which may be distributed symmetrically with respect to the centre of the star. This is motivated by

[7]The estimate of $8M_{\odot}$ of ^{56}Ni reported in their paper derives from the extrapolation of the light curve luminosity after day 170.

the assumption that the progenitor of SN 2006gy may have undergone mass-loss episodes similar to those observed in η Carinae. The rise to maximum corresponds to the early emission of the SN ejecta during the initial phase in which the radius is rapidly expanding, similarly to the case of SN 1987A (Woosley et al. [58]). In our model the peak luminosity is sustained by the *combined contribution* of the early SN explosion and the energy from the ejecta-clump interaction. Unfortunately, no early spectra are available to verify this claim. The first available spectrum (37 days) already shows signs of interaction, mainly in the Hα profile, probably caused by flux arising directly from the interaction, being not thermalized by the dense clumps. Therefore we can reasonably assume that at this phase the ejecta-clump collision had already started. Another assumption of our model is that the impact is instantaneous, i.e. that all material is reached by the ejecta at the same radial distance from the star.

Our semi-analytical code (see Zampieri et al. [60] for more details) was used to estimate the parameters of the ejected envelope from a simultaneous comparison of the observed and computed light curve, photospheric gas velocity and continuum temperature. The radius of the star at the explosion, the mass and velocity of the ejecta and the explosion energy are fitting parameters, whereas the ejected ^{56}Ni mass is an input fixed parameter, which is based on the late-time light curve. The fitting parameters are estimated by means of a χ^2 minimization procedure for both evolutionary phases (i.e. the SN explosion and the ejecta-clumps impact).

The parameters of the models for each phase are listed in Table 4.4 and 4.5. Models of the earlier phase (*e1*, *e2*, *e3* and *e4*) refer to different values of the input parameters M_{Ni} and T_{rec}, while models of the later phase (*c1* and *c2*) refer to different χ^2 minima.

Critical parameters for the earlier phase are the initial radius and the mass of ^{56}Ni. As discussed before, the large increase in luminosity in the pre-maximum phase calls for small initial radii ($< 10^{13}$cm), which are not compatible with RSG stars but are consistent with BSG or Wolf Rayet stars. The amount of ^{56}Ni determines the peak luminosity. The adopted upper limit is $M_{Ni} \sim 2M_{\odot}$, considering that $\sim 3M_{\odot}$ were estimated at ~ 180 days neglecting the contribution of interaction, which instead *is* already active at that phase, as explained above (according to the model the γ-rays trapping is always more than 80% effective at a phase 170-237 days, given the large ejecta masses). A minimum ^{56}Ni yield of 0.75 $M_{\odot}$ was required to fit the early rise of the light curve, assuming no contribution from interaction (i.e., the CSM is supposed to be rarified in the vicinity of the exploding star).

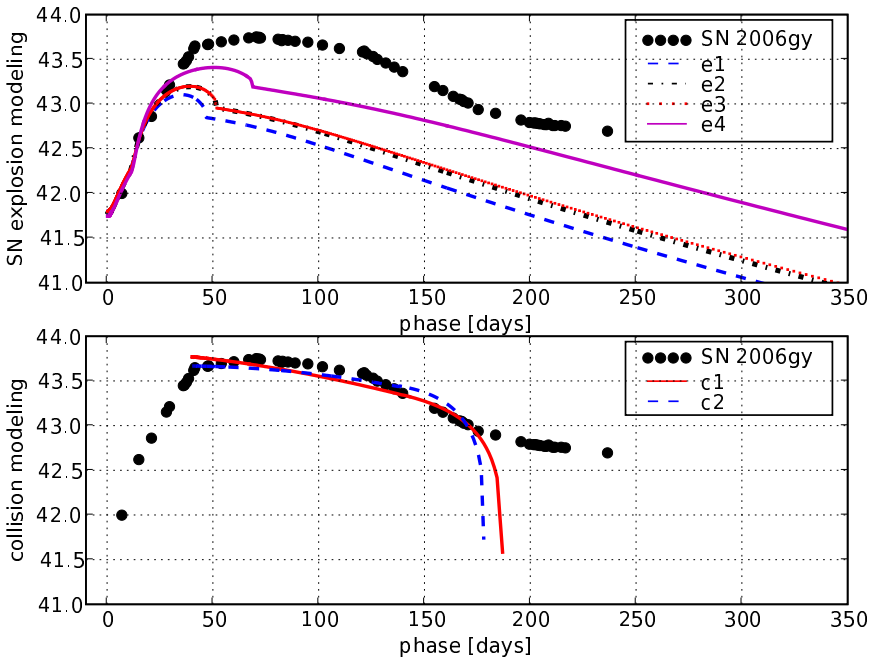

Figure 4.18— Best fits of the light curve of SN 2006gy obtained with the semianalytical model [60] showed separately for the rising branch and maximum/postmaximum phase. The code in the legenda refers to the models summarized in Tables 4.4 and 4.5.

Table 4.4 lists the best-fit-parameters for the initial radius of the star, for the ejecta mass and for the velocity and SN explosion energy, given the adopted ^{56}Ni masses and recombination temperatures. It should be noted that the radius estimated by the code is actually an upper limit: the initial part of the light curve is not very sensitive as long as it remains below the reported values. The SN parameters are not exceptionally high for a core-collapse SN. For example, the explosion energy is only $\sim 3-4.5$ times larger than that of SN 1987A. The explosion energy increases with increasing ^{56}Ni mass, as one may naively expect from the fact that larger amounts of ^{56}Ni may be synthetized in more energetics events. On the other hand, for a constant ^{56}Ni mass a smaller recombination temperature implies an increase in the ejecta velocity and mass, and therefore

model	$R_{star}[\cdot 10^{12}cm]$	$M_{ej}[M_\odot]$	V_{ej}[km/s]	$M_{Ni}[M_\odot]$	T_{rec}[K]	$E_{expl}[10^{51}erg]$
(*e1*)	8.4	5.3	7700	0.75	7000	3.8
(*e2*)	5.9	8.3	8900	1.0	6500	7.9
(*e3*)	8.4	6.9	7700	1.0	7000	4.9
(*e4*)	8.4	14.4	7300	2.0	7000	9.2

Table 4.4— Model output parameters of the semi-analytical code for the first evolutionary phase.

model	$R_{cl}[\cdot 10^{12}cm]$	$M_{cl}[M_\odot]$	V_{cl}[km/s]	$M_{Ni}[M_\odot]$	T_{rec}[K]	$E_{imp}[10^{51}erg]$	Diff. time [days]
(*c1*)	1339.9	6.5	1900	0.1	6500	0.3	100
(*c2*)	290.6	10.0	3600	0.1	6500	1.6	10

Table 4.5— Model output parameters of the semi-analytical code for the second evolutionary phase.

in the explosion energy.

The later phase is not powered by ^{56}Ni alone. The main source of energy is in fact the transformation of the kinetic energy of the ejecta into thermal energy and radiation inside the dense clumps, which form a photosphere. The duration and shape of the luminosity peak depends on the radius and mass of the clumps and on their expansion velocity. The parameters listed in Table 6 are the clump radius, mass and velocity, the amount of ^{56}Ni in the clumps, the recombination temperature, the energy released by the ejecta-clumps interaction and the diffusion time. The recombination temperature adopted is $T = 6500 \pm 1000$K, as measured from the 37-day spectrum. For both models reported (*c1* and *c2*) the energy deposited by the ejecta in the CSM is about a factor ∼2-30 smaller than the SN explosion energy. This value may result naturally, considering that the clumps cover a solid angle not larger than 2π as seen from the center of the star. In the two models the radius of the clump is significantly different. For an ejecta velocity of 8000 km s^{-1}, and assuming that the ejecta-clump impact occurs at ∼30-40 days, the distance of the clumps is $\sim 10^{15}$ cm s^{-1}. Adopting a characteristic sound speed of $\sim 10^8$cm^{-1}, the shock wave produced by the impact takes ~ 100 days to cross the clump in model *c1* and ~ 10 days in model *c2*. On these grounds, model *c2* seems to be favored, as the optical display of the shocked clumps is fully developed by ~ 40 days after explosion. The values obtained for the clump distance and mass are roughly consistent with those derived by Smith & McCray [46].

Our simple model gives a satisfactory fit for both the explosion and collision phase (Fig. 4.18). We did not attempt to fit the light curve in the transition

phase. The parameters that characterize the explosion of SN 2006gy are actually not particularly remarkable. An extra-ordinary amount of ^{56}Ni in the ejecta is not necessary to fit the light curve. The estimated amount of ^{56}Ni is 2 to 6 times larger than that derived for other well studied, bright core-collapse events [26, 51]. It should be noted that an high amount of ^{56}Ni is even not to relate to the huge brightness of the recently discovered SN 2008es, the second most luminous SN known, according to Gezari et al. [17] and to Miller et al. [29] (cf. Chapters 5 and 6). SN 2006gy was certainly a highly energetic event compared to other normal CC-SNe, perhaps comparable to the class of *hypernovae* (e.g., SN 2003dh, [24]; SN 2003jd, [52]; SN 1998bw, [20]). The combined mass of the ejecta and of the clumps is $\sim 20 M_{\odot}$, indicating an originally very massive progenitor, likely much more massive than $\sim 30 M_{\odot}$ if account is taken of the likely large mass loss in the pre-SN stage. These values are significantly smaller than those claimed in some of the previously proposed scenarios ($> 100 M_{\odot}$). Still, LBV-like mass-loss phenomena are required to produce massive clumps around the star. Given the radius at explosion derived by the model, a star in a LBV or early Wolf-Rayet phase might be good candidates for the progenitor of SN 2006gy.

4.10 New insights on SN 2006gy from recent works

In 2009, more data regarding the nebular phase of SN 2006gy were published, reinforcing once again the debate on its origin.

Nomoto et al. (2009) computed a bolometric light curve and showed that the model with M(^{56}Ni) = 15M$_\odot$, M$_{ej}$ = 53 M$_\odot$, and E$_k$in = 64×10^{51}erg could explain the observed light curve in the first 200 days. However, this model failed to reproduce the late-times observation of **Kawabata et al. (2009)** [21]. The latter observed SN 2006gy with the SUBARU telescope on day 27, 157 and 394 both in photometry and in spectroscopy. Contrary to Smith et al. [44] and Agnoletto et al. [1] they detected the SN in the V and R band on day 394, and attributed the successful detection to a better seeing condition. We note that the reported V and R magnitude R = 19.77 ± 0.14 is not consistent, even within the error bars, to the deeper magnitude measured by Agnoletto et al. [1] at a very similar epoch. This is puzzling and difficult to understand, and could possibly result from a different background subtraction.

Anyway, the new optical photometric epoch on day 394 did not add much more information on the nature of the event. Assuming that its luminosity was powered by radioactive decay, Kawabata et al. [21] found a lower limit to the ^{56}Ni mass equal to 3M$_\odot$. Interestingly, this is consistent to the upper limit on the ^{56}Ni measured by Agnoletto et al. [1] from the luminosity at phase 180-230 days.

Concerning spectroscopy, the appearance of the spectrum at 394 days presented by Kawabata et al. (2009) [21] turned out to be unique (Fig.4.19, upper panel). They showed that it was dominated by lines with intermediate width ($< 2000\,\mathrm{km\,s^{-1}}$), and several unusual emission lines at $7400 - 8800$ Å, some of which were attributed to Ti or Ni. The emission of Ca II IR triplet was considered much narrower than in ordinary Type IIn/IIa SNe, suggestive of a slow SN ejecta. Furthermore, no emission of O I, generally strong in Type II and Ib/c, was detected at $\lambda\lambda$ 6300, 6364. The weakness of the flux at the Hα wavelength, implying a flux luminosity of $\sim 1 \times 10^{39}\mathrm{erg\,s^{-1}}$, definitely ruled out the hypothesis of CSM interaction sustaining the luminosity at late times.

The authors found no evident similarity between the spectrum of SN 2006gy on day 394 and the typical nebular spectra of the most common SNe (see Figures 10 and 11 of Kawabata et al. [21]). However, a fairly good spectral match was found with SN 2005hk (Fig.4.19, lower panel, green line). Though SN 2005hk is labeled as peculiar Ia SN in the Figure, in a recent paper Valenti et al. [53] showed that this SN belongs to the group of the hydrogen-poor supernovae which are misclassified as thermonuclear events (sometimes labeled

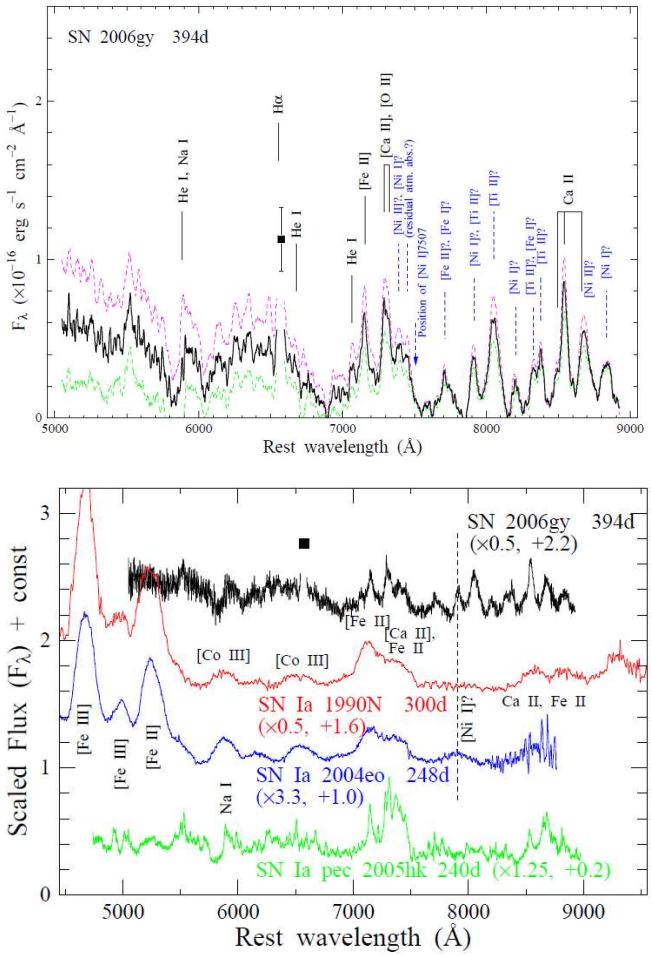

Figure 4.19— *Upper panel*: low resolution spectrum of SN 2006gy at t = 394 days (black line). The dashed line represent the uncertainties in the flux, due to the difficult subtraction of the flux from an HII region. There are several identified and unidentified emission lines at 7000 − 8800Å, mostly attributed to the Ti or Ni [21].

as SN "2002cx-like" events). They could be the outcome of the explosion of massive stars that end up their life as black holes, and whose explosions produce ejecta of low kinetic energy, a faint optical luminosity and a small mass fraction of ^{56}Ni (MacFadyen et al. [23]). Alternatively, the collapse of the O-Ne core of a star of 79 $M_{\odot}$ was also proposed to explain their origin (Nomoto [31]). In any case, the spectral agreement between the two events can represent *another clue pointing towards the core-collapse origin of SN 2006gy*, in agreement with what proposed by Smith et al. [44, 45], Woosley et al. [57] and Agnoletto et al. [1]. This is not in contrast with the different spectral appearance at early phases, assuming that the early spectroscopy of SN 2006gy is supposed to be completely dominated by the collision with the clumpy, H-rich medium.

In 2009 the group of **Miller et al. (2009)** [30] also presented new early-times NIR observations of SN 2006gy, as well as optical and NIR late-times imaging extending until more than two years since explosion (Fig.4.20). In this work the authors interpreted the NIR excess detected after day 100, the slow luminosity decay rate measured after day ∼400 and the blue color measured on day 825 as the evidence of the presence of *warm dust* near the explosion site. The model described by Dwek et al. [11], predicting a fast rise in the IR followed by an extended plateau before the IR luminosity starts a rapid decline, is indeed consistent with what observed in SN 2006gy by Miller et al. (2009) [30]. The NIR plateau after day ∼400 occurs because the hottest dust, lying at the edge of a dust-free cavity, dominates the emission. For a distant observer, the emitting volume is a series of paraboloid light fronts that expand throughout the dust-free cavity [34]. The emission from the dust is dominated by the UV/optical radiation produced by the SN at peak. Once this radiation sweeps past the back edge of the cavity the IR luminosity begins to rapidly decline. Assuming that the slight NIR excess seen at day ∼100 is the rise of an IR echo, Miller et al. [30] calculated that the radius of the dust-free cavity is $\sim 8 \times 10^{17}$cm. Then, assuming the properties of dust as in Dwek [11], and deriving the optical depth of dust from the ratio $E_{IR}/(E + E_{IR}) \sim 0.16$, they obtained a dust mass of 0.1 $M_{\odot}$. In a typical for the dust-to-gas ratio, 1:100, this corresponds to a mass of the circumstellar shell of ∼10 $M_{\odot}$ [30].

However, an optical counter-part of the echo is also expected. In fact, when successive paraboloids sweep out to progressively larger radii, dust in the circumstellar environment can scatter that light toward the observer, creating a plateau in the optical light curve of the SN. Scattering preferentially selects shorter wavelengths, which results in a spectrum that is bluer than that of the SN at peak. Indeed, the SED derived from the HST photometry on day 825 spectrum by Miller et al. (2009) [30] perfectly matches the spectrum acquired on day 71 by Smith et al. (2009) [43] (Fig. 4.21), assuming a scattering law of

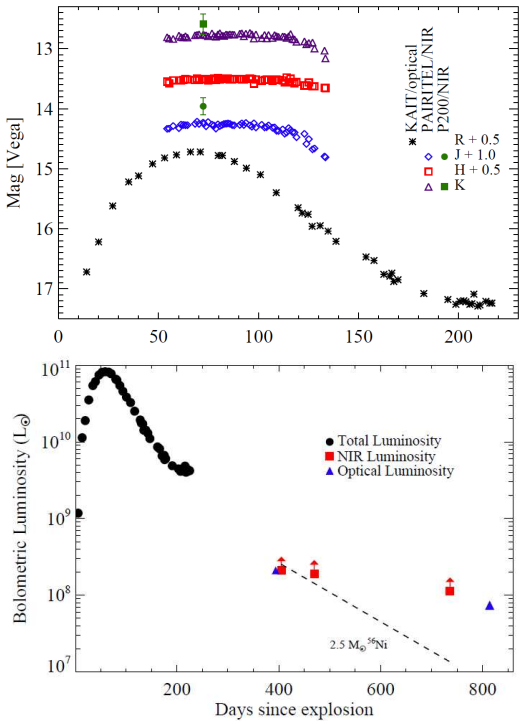

Figure 4.20— *Top*: Early photometric evolution of SN 2006gy, including the unfiltered observations are from Smith et al. [45], the PAIRITEL J, H, and Ks from Miller et al. [30] and Palomar AO photometry from Ofek et al. [32]. *Bottom*: bolometric luminosity of SN 2006gy during the first 800 day after explosion Miller et al. [30].

$\lambda^{-\alpha}$ with $\alpha = 1.2 \pm 0.15$.

In any case, both assuming that the scattering light echo is due to the same shell that gives rise to the NIR-echo, or supposing another shell of dust inside NGC 1260 at a distance of 20 pc (as calculated by Miller et al. (2009) [30]), the dusty environment of SN 2006gy requires a massive progenitor. Indeed, thanks to the work of Miller et al. [30] the hypothesis of an extremely large amount of ^{56}Ni synthesized in the explosion had to be rejected by the slow NIR luminosity decay. Therefore, the suggestion of SN 2006gy as PISN could be also definitely ruled out.

Finally, very recently **Smith et al. (2009)** [43] published on the astro-ph a fourth study on SN 2006gy, presenting a very detailed analysis of a previously-unpublished spectral sequence regarding the phase 36-237 days, (Fig. 4.22) and

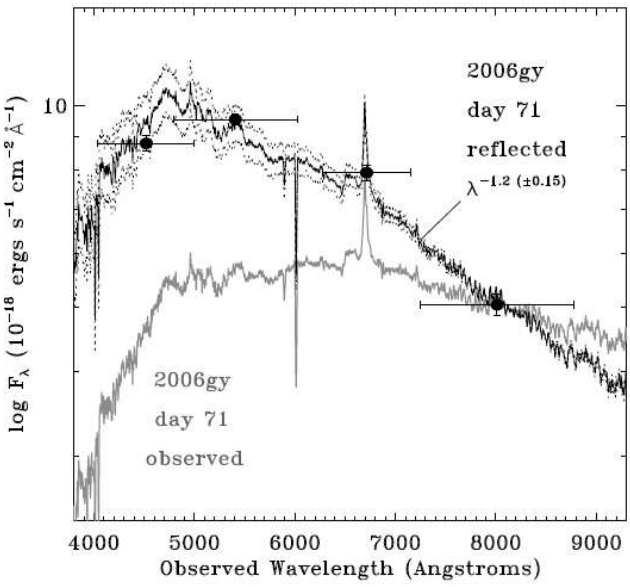

Figure 4.21— HST/WFPC2 photometry of SN 2006gy (black dots) compared to the observed and reflected spectra (Miller et al. [30]).

a discussion on an evolution scenario which reviews some aspects of the work of Smith & McCray [46].

Though the work presents excellent data, the interpretation is not always straightforward, and it sometimes requires an ad-hoc scenario which involves specific values for the properties of the circumstellar medium (density, velocity, ionization state etc.). However, an interesting insight to explain the appearance of the spectral lines is the suggestion that at early phases (before and up to the time of maximum luminosity), the photosphere lays *outside* the forward shock. The authors state that at this epochs the spectrum is supposed to be generated in the pre-shock CSM, from a ionizing radiation that diffuses out an opaque shell. Consequently, the post-shock cold dense shell and the SN ejecta cannot be seen. Starting from the phase of maximum luminosity the photosphere is supposed to recede past the forward shock and into the cold dense shell, which becomes progressively transparent. This allows the formation of broad lines in the spectra. Finally, starting from day ∼150, the decrease in luminosity of cooling-diagnostic lines as H, Fe II, and Ca II lines is supposed to be a sign that the interaction is ceasing and that the forward shock has reached the outer

boundary of the dense pre-SN shell.

However, this scenario can not explain the flattening of the light curve at phase 180-230 days. Contrary to what suggested by Agnoletto et al. [1], in Smith et al. [44] the CSM interaction is not considered as an explanation, given the observed decrease in the luminosity of lines as H, Fe II, and Ca II, as mentioned above. Neither the possible energy from the ^{56}Ni decay is taken into consideration (likely because the higher estimate in the bolometric luminosity calculated by Smith et al. 2008 [44] would imply an amount $\geq$8 $M_{\odot}$, inconsistent with the late-times observations).

Another fundamental difference is that Smith et al. [43] do not find any evidence of spectral lines broader than 5000 km s^{-1} . On the other hand, in Agnoletto et al. [1] broad lines at 9000 km s^{-1} are the evidence that the fast SN ejecta can be seen throughout the clumps even before the maximum luminosity.

It should be also stressed that the bolometric luminosity in Smith et al. 2009 [43] is calculated adding a bolometric correction to the unfiltered light curve luminosity, and results to be by a factor 5 higher than in Agnoletto et al. [1], who had a BVRI-light curve. Given this inconsistencies, the reader should be careful in considering the parameters like the mass-loss rate, the black-body radius of the expanding photosphere and the mass of the ejecta, which are calculated from the bolometric luminosity in the work of Smith et al. [43].

4.11 Final remarks

In this chapter we have reviewed the scenarios that were suggested to explain the peculiar evolution of SN 2006gy. Though some hypothesis have been ruled out due to the recent observational data (e.g., the PISN scenario), a tight constraint on the nature of the transient does not exist yet. The suggestions by Woosley et al. [57], Smith & McCray [46], Agnoletto et al. (2009) [1] or Smith et al. [43] to explain the early light curve of SN 2006gy may be all considered valid.

However, from the comprehensive properties of the data collected up to now it seems likely that the nature of this enigmatic transient deals with the explosion of a very massive star in a particularly CSM-rich and dusty environment. Given the strong mass-loss rates inferred, a star in a late LBV or WG stage might be a good candidate for the progenitor of SN 2006gy.

However, there are not enough clues to precisely estimate the mass of the progenitor of SN 2006gy. In Agnoletto et al. [1] we have shown that the light curve can be reproduced by the explosion of a $\sim$30 $M_{\odot}$ star. Fundamental requirements are a SN energetic explosion and a collision with a clumpy shell of

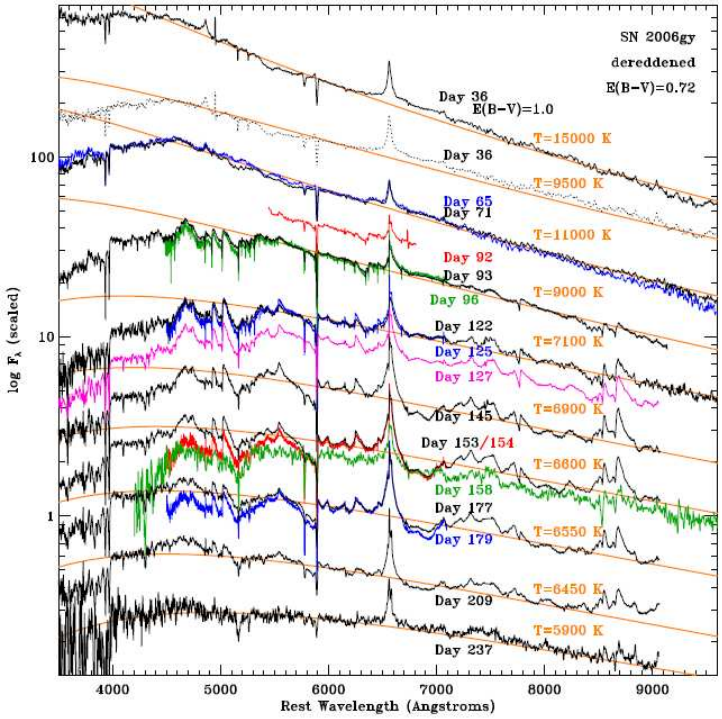

Figure 4.22— Spectral sequence presented by Smith et al. [43].

matter. This does not differs much from the main point of Woosley et al. [57], though they consider a different mechanism for the outburst and much more massive star.

Bibliography

[1] I. Agnoletto, S. Benetti, E. Cappellaro, L. Zampieri, M. Turatto, P. Mazzali, A. Pastorello, M. D. Valle, F. Bufano, A. Harutyunyan, H. Navasardyan, N. Elias-Rosa, S. Taubenberger, S. Spiro, and S. Valenti. SN 2006gy: Was it Really Extraordinary? *Apj*, 691:1348–1359, February 2009.

[2] C. Alard and R. H. Lupton. A Method for Optimal Image Subtraction. *Apj*, 503:325–+, August 1998.

[3] S. Benetti, E. Cappellaro, M. Turatto, S. Taubenberger, A. Harutyunyan, and S. Valenti. Supernova 2002ic: The Collapse of a Stripped-Envelope, Massive Star in a Dense Medium? *Apjl*, 653:L129–L132, December 2006.

[4] E. Cappellaro, P. A. Mazzali, S. Benetti, I. J. Danziger, M. Turatto, M. della Valle, and F. Patat. SN IA light curves and radioactive decay. *Aap*, 328:203–210, December 1997.

[5] R. A. Chevalier and C. Fransson. Supernova Interaction with a Circumstellar Medium. *ArXiv Astrophysics e-prints*, October 2001.

[6] N. N. Chugai, S. I. Blinnikov, R. J. Cumming, P. Lundqvist, A. Bragaglia, A. V. Filippenko, D. C. Leonard, T. Matheson, and J. Sollerman. The Type IIn supernova 1994W: evidence for the explosive ejection of a circumstellar envelope. *Mnras*, 352:1213–1231, August 2004.

[7] A. Clocchiatti, J. C. Wheeler, M. M. Phillips, N. B. Suntzeff, S. Cristiani, A. Phillips, R. P. Harkness, M. A. Dopita, K. Beuermann, M. Rosa, P. Grosbol, P. O. Lindblad, and A. V. Filippenko. SN 1983V in NGC 1365 and the Nature of Stripped Envelope Core-Collapse Supernovae. *Apj*, 483:675–+, July 1997.

[8] J. S. Deng, K. Hatano, T. Nakamura, K. Maeda, K. Nomoto, P. Nugent, G. Aldering, and D. Branch. Luminous SN 1999as: Hypernova with $4M_{\odot}$ of Ni Ejected? In H. Inoue & H. Kunieda, editor, *New Century of X-ray Astronomy*, volume 251 of *Astronomical Society of the Pacific Conference Series*, pages 238–+, 2001.

[9] E. Di Carlo, C. Corsi, A. A. Arkharov, F. Massi, V. M. Larionov, N. V. Efimova, M. Dolci, N. Napoleone, and A. Di Paola. Near-Infrared Observations of the Type Ib Supernova SN 2006jc: Evidence of Interactions with Dust. *Apj*, 684:471–480, September 2008.

[10] E. Di Carlo, F. Massi, G. Valentini, A. Di Paola, F. D'Alessio, E. Brocato, D. Guidubaldi, M. Dolci, F. Pedichini, R. Speziali, G. Li Causi, A. Caratti o Garatti, E. Cappellaro, M. Turatto, A. A. Arkharov, Y. Gnedin, V. M. Larionov, S. Benetti, A. Pastorello, I. Aretxaga, V. Chavushyan, O. Vega, I. J. Danziger, and A. Tornambé. Optical and Infrared Observations of the Supernova SN 1999el. *Apj*, 573:144–156, July 2002.

[11] E. Dwek, M. F. A'Hearn, E. E. Becklin, R. H. Brown, R. W. Capps, H. L. Dinerstein, I. Gatley, D. Morrison, C. M. Telesco, A. T. Tokunaga, M. W. Werner, and C. G. Wynn-Williams. The evolution of the infrared emission from the Type II supernova 1980k in NGC 6946 - The dust formation model. *Apj*, 274:168–174, November 1983.

[12] S. W. Falk and W. D. Arnett. A Theoretical Model for Type II Supernovae. *Apjl*, 180:L65+, March 1973.

[13] S. W. Falk and W. D. Arnett. Radiation Dynamics, Envelope Ejection, and Supernova Light Curves. *Apjs*, 33:515–+, April 1977.

[14] R. J. Foley, W. Li, M. Moore, D. S. Wong, D. Pooley, and A. V. Filippenko. Supernova 2006gy in NGC 1260. *Central Bureau Electronic Telegrams*, 695:1–+, October 2006.

[15] W. L. Freedman, B. F. Madore, B. K. Gibson, L. Ferrarese, D. D. Kelson, S. Sakai, J. R. Mould, R. C. Kennicutt, Jr., H. C. Ford, J. A. Graham, J. P. Huchra, S. M. G. Hughes, G. D. Illingworth, L. M. Macri, and P. B. Stetson. Final Results from the Hubble Space Telescope Key Project to Measure the Hubble Constant. *Apj*, 553:47–72, May 2001.

[16] L. M. Germany, D. J. Reiss, E. M. Sadler, B. P. Schmidt, and C. W. Stubbs. SN 1997CY/GRB 970514: A New Piece in the Gamma-Ray Burst Puzzle? *Apj*, 533:320–328, April 2000.

[17] S. Gezari, J. P. Halpern, D. Grupe, F. Yuan, R. Quimby, T. McKay, D. Chamarro, M. D. Sisson, C. Akerlof, J. C. Wheeler, P. J. Brown, S. B. Cenko, A. Rau, J. O. Djordjevic, and D. M. Terndrup. Discovery of the Ultra-Bright Type II-L Supernova 2008es. *Apj*, 690:1313–1321, January 2009.

[18] M. Hamuy, M. M. Phillips, N. B. Suntzeff, J. Maza, L. E. González, M. Roth, K. Krisciunas, N. Morrell, E. M. Green, S. E. Persson, and P. J. McCarthy. An asymptotic-giant-branch star in the progenitor system of a type Ia supernova. *Nature*, 424:651–654, August 2003.

[19] A. Harutyunyan, S. Benetti, M. Turatto, E. Cappellaro, N. Elias-Rosa, and G. Andreuzzi. Supernova 2006gy in NGC 1260. *Central Bureau Electronic Telegrams*, 647:1–+, September 2006.

[20] K. Iwamoto, P. A. Mazzali, K. Nomoto, H. Umeda, T. Nakamura, F. Patat, I. J. Danziger, T. R. Young, T. Suzuki, T. Shigeyama, T. Augusteijn, V. Doublier, J.-F. Gonzalez, H. Boehnhardt, J. Brewer, O. R. Hainaut, C. Lidman, B. Leibundgut, E. Cappellaro, M. Turatto, T. J. Galama, P. M. Vreeswijk, C. Kouveliotou, J. van Paradijs, E. Pian, E. Palazzi, and F. Frontera. A hypernova model for the supernova associated with the γ-ray burst of 25 April 1998. *Nature*, 395:672–674, October 1998.

[21] K. S. Kawabata, M. Tanaka, K. Maeda, T. Hattori, K. Nomoto, N. Tominaga, and M. Yamanaka. Extremely Luminous Supernova 2006gy at Late Phase: Detection of Optical Emission from Supernova. *Apj*, 697:747–757, May 2009.

[22] R. Kennicutt, S. Sakai, C. Moss, and M. Whittle. A Deep Survey of Star Formation in Nearby Galaxy Clusters. In *NOAO Proposal ID #2000B-0223*, pages 223–+, August 2000.

[23] A. I. MacFadyen, S. E. Woosley, and A. Heger. Supernovae, Jets, and Collapsars. *Apj*, 550:410–425, March 2001.

[24] T. Matheson, P. M. Garnavich, K. Z. Stanek, D. Bersier, S. T. Holland, K. Krisciunas, N. Caldwell, P. Berlind, J. S. Bloom, M. Bolte, A. Z. Bonanos, M. J. I. Brown, W. R. Brown, M. L. Calkins, P. Challis, R. Chornock, L. Echevarria, D. J. Eisenstein, M. E. Everett, A. V. Filippenko, K. Flint, R. J. Foley, D. L. Freedman, M. Hamuy, P. Harding, N. P. Hathi, M. Hicken, C. Hoopes, C. Impey, B. T. Jannuzi, R. A. Jansen, S. Jha, J. Kaluzny, S. Kannappan, R. P. Kirshner, D. W. Latham, J. C. Lee, D. C. Leonard, W. Li, K. L. Luhman, P. Martini, H. Mathis, J. Maza, S. T. Megeath, L. R. Miller, D. Minniti, E. W. Olszewski, M. Papenkova, M. M. Phillips, B. Pindor, D. D. Sasselov, R. Schild, H. Schweiker, T. Spahr, J. Thomas-Osip, I. Thompson, D. Weisz, R. Windhorst, and D. Zaritsky. Photometry and Spectroscopy of GRB 030329 and Its As-

sociated Supernova 2003dh: The First Two Months. *Apj*, 599:394–407, December 2003.

[25] S. Mattila, W. P. S. Meikle, P. Lundqvist, A. Pastorello, R. Kotak, J. Eldridge, S. Smartt, A. Adamson, C. L. Gerardy, L. Rizzi, A. W. Stephens, and S. D. van Dyk. Massive stars exploding in a He-rich circumstellar medium - III. SN 2006jc: infrared echoes from new and old dust in the progenitor CSM. *Mnras*, 389:141–155, September 2008.

[26] P. A. Mazzali and P. Podsiadlowski. The $(^{54}Fe +^{58} Ni)/^{56}Ni$ ratio as a second parameter for Type Ia supernova properties. *Mnras*, 369:L19–L22, June 2006.

[27] P. A. Mazzali, F. K. Röpke, S. Benetti, and W. Hillebrandt. A Common Explosion Mechanism for Type Ia Supernovae. *Science*, 315:825–, February 2007.

[28] H. Meusinger, J. Brunzendorf, and R. Krieg. IRAS galaxies in the Perseus cluster. *Aap*, 363:933–946, November 2000.

[29] A. A. Miller, R. Chornock, D. A. Perley, M. Ganeshalingam, W. Li, N. R. Butler, J. S. Bloom, N. Smith, M. Modjaz, D. Poznanski, A. V. Filippenko, C. V. Griffith, J. H. Shiode, and J. M. Silverman. The Exceptionally Luminous Type II-Linear Supernova 2008es. *Apj*, 690:1303–1312, January 2009.

[30] A. A. Miller, N. Smith, W. Li, J. S. Bloom, R. Chornock, A. V. Filippenko, and J. X. Prochaska. New Observations of the Very Luminous Supernova 2006gy: Evidence for Echoes. *ArXiv e-prints*, June 2009.

[31] K. Nomoto. Evolution of 8-10 solar mass stars toward electron capture supernovae. I - Formation of electron-degenerate O + NE + MG cores. *Apj*, 277:791–805, February 1984.

[32] E. O. Ofek, P. B. Cameron, M. M. Kasliwal, A. Gal-Yam, A. Rau, S. R. Kulkarni, D. A. Frail, P. Chandra, S. B. Cenko, A. M. Soderberg, and S. Immler. SN 2006gy: An Extremely Luminous Supernova in the Galaxy NGC 1260. *Apjl*, 659:L13–L16, April 2007.

[33] A. Pastorello, M. Turatto, S. Benetti, E. Cappellaro, I. J. Danziger, P. A. Mazzali, F. Patat, A. V. Filippenko, D. J. Schlegel, and T. Matheson. The type IIn supernova 1995G: interaction with the circumstellar medium. *Mnras*, 333:27–38, June 2002.

[34] F. Patat, S. Benetti, E. Cappellaro, and M. Turatto. Reflections on reflexions - II. Effects of light echoes on the luminosity and spectra of Type Ia supernovae. *Mnras*, 369:1949–1960, July 2006.

[35] S. F. Portegies Zwart and E. P. J. van den Heuvel. A runaway collision in a young star cluster as the origin of the brightest supernova. *Nature*, 450:388–389, November 2007.

[36] M. Pozzo, W. P. S. Meikle, A. Fassia, T. Geballe, P. Lundqvist, N. N. Chugai, and J. Sollerman. On the source of the late-time infrared luminosity of SN 1998S and other Type II supernovae. *Mnras*, 352:457–477, August 2004.

[37] J. L. Prieto, P. Garnavich, A. Chronister, and P. Connick. 2006gy in NGC 1260. *Central Bureau Electronic Telegrams*, 648:1–+, September 2006.

[38] J. L. Prieto, P. M. Garnavich, M. M. Phillips, D. L. DePoy, J. Parrent, D. Pooley, V. V. Dwarkadas, E. Baron, B. Bassett, A. Becker, D. Cinabro, F. DeJongh, B. Dilday, M. Doi, J. A. Frieman, C. J. Hogan, J. Holtzman, S. Jha, R. Kessler, K. Konishi, H. Lampeitl, J. Marriner, J. L. Marshall, G. Miknaitis, R. C. Nichol, A. G. Riess, M. W. Richmond, R. Romani, M. Sako, D. P. Schneider, M. Smith, N. Takanashi, K. Tokita, K. van der Heyden, N. Yasuda, C. Zheng, J. C. Wheeler, J. Barentine, J. Dembicky, J. Eastman, S. Frank, W. Ketzeback, R. J. McMillan, N. Morrell, G. Folatelli, C. Contreras, C. R. Burns, W. L. Freedman, S. Gonzalez, M. Hamuy, W. Krzeminski, B. F. Madore, D. Murphy, S. E. Persson, M. Roth, and N. B. Suntzeff. A Study of the Type Ia/IIn Supernova 2005gj from X-ray to the Infrared: Paper I. *ArXiv e-prints*, June 2007.

[39] R. Quimby. Supernova 2006gy in NGC 1260. *Central Bureau Electronic Telegrams*, 644:1–+, September 2006.

[40] L. Rigon, M. Turatto, S. Benetti, A. Pastorello, E. Cappellaro, I. Aretxaga, O. Vega, V. Chavushyan, F. Patat, I. J. Danziger, and M. Salvo. SN 1999E: another piece in the supernova-gamma-ray burst connection puzzle. *Mnras*, 340:191–196, March 2003.

[41] E. Scannapieco, P. Madau, S. Woosley, A. Heger, and A. Ferrara. The Detectability of Pair-Production Supernovae at z = 6. *Apj*, 633:1031–1041, November 2005.

[42] D. J. Schlegel, D. P. Finkbeiner, and M. Davis. Maps of Dust Infrared Emission for Use in Estimation of Reddening and Cosmic Microwave Background Radiation Foregrounds. *Apj*, 500:525–+, June 1998.

[43] N. Smith, R. Chornock, J. M. Silverman, A. V. Filippenko, and R. J. Foley. Spectral Evolution of the Extraordinary Type IIn Supernova 2006gy. *ArXiv e-prints*, June 2009.

[44] N. Smith, R. J. Foley, J. S. Bloom, W. Li, A. V. Filippenko, R. Gavazzi, A. Ghez, Q. Konopacky, M. A. Malkan, P. J. Marshall, D. Pooley, T. Treu, and J.-H. Woo. Late-Time Observations of SN 2006gy: Still Going Strong. *Apj*, 686:485–491, October 2008.

[45] N. Smith, W. Li, R. J. Foley, J. C. Wheeler, D. Pooley, R. Chornock, A. V. Filippenko, J. M. Silverman, R. Quimby, J. S. Bloom, and C. Hansen. SN 2006gy: Discovery of the Most Luminous Supernova Ever Recorded, Powered by the Death of an Extremely Massive Star like η Carinae. *Apj*, 666:1116–1128, September 2007.

[46] N. Smith and R. McCray. Shell-shocked Diffusion Model for the Light Curve of SN 2006gy. *Apjl*, 671:L17–L20, December 2007.

[47] J. Sollerman, S. T. Holland, P. Challis, C. Fransson, P. Garnavich, R. P. Kirshner, C. Kozma, B. Leibundgut, P. Lundqvist, F. Patat, A. V. Filippenko, N. Panagia, and J. C. Wheeler. Supernova 1998bw - the final phases. *Aap*, 386:944–956, May 2002.

[48] R. E. Taam and P. M. Ricker. Common Envelope Evolution. *ArXiv Astrophysics e-prints*, November 2006.

[49] N. Tominaga, M. Limongi, T. Suzuki, M. Tanaka, K. Nomoto, K. Maeda, A. Chieffi, A. Tornambe, T. Minezaki, Y. Yoshii, I. Sakon, T. Wada, Y. Ohyama, T. Tanabé, H. Kaneda, T. Onaka, T. Nozawa, T. Kozasa, K. S. Kawabata, G. C. Anupama, D. K. Sahu, U. K. Gurugubelli, T. P. Prabhu, and J. Deng. The Peculiar Type Ib Supernova 2006jc: A WCO Wolf-Rayet Star Explosion. *Apj*, 687:1208–1219, November 2008.

[50] D. Y. Tsvetkov. SN 2005kd: Another Very Luminous, Slowly Declining Type IIn Supernova. *Peremennye Zvezdy*, 28:6–+, April 2008.

[51] M. Turatto, T. Suzuki, P. A. Mazzali, S. Benetti, E. Cappellaro, I. J. Danziger, K. Nomoto, T. Nakamura, T. R. Young, and F. Patat. The Properties of Supernova 1997CY Associated with GRB 970514. *Apjl*, 534:L57–L61, May 2000.

[52] S. Valenti, S. Benetti, E. Cappellaro, F. Patat, P. Mazzali, M. Turatto, K. Hurley, K. Maeda, A. Gal-Yam, R. J. Foley, A. V. Filippenko, A. Pastorello, P. Challis, F. Frontera, A. Harutyunyan, M. Iye, K. Kawabata, R. P. Kirshner, W. Li, Y. M. Lipkin, T. Matheson, K. Nomoto, E. O. Ofek, Y. Ohyama, E. Pian, D. Poznanski, M. Salvo, D. N. Sauer, B. P. Schmidt, A. Soderberg, and L. Zampieri. The broad-lined Type Ic supernova 2003jd. *Mnras*, 383:1485–1500, February 2008.

[53] S. Valenti, A. Pastorello, E. Cappellaro, S. Benetti, P. A. Mazzali, J. Manteca, S. Taubenberger, N. Elias-Rosa, R. Ferrando, A. Harutyunyan, V. P. Hentunen, M. Nissinen, E. Pian, M. Turatto, L. Zampieri, and S. J. Smartt. A low-energy core-collapse supernova without a hydrogen envelope. *Nature*, 459:674–677, June 2009.

[54] A. Vazdekis. Evolutionary Stellar Population Synthesis at 2 Å Spectral Resolution. *Apj*, 513:224–241, March 1999.

[55] G. Wegner, M. Bernardi, C. N. A. Willmer, L. N. da Costa, M. V. Alonso, P. S. Pellegrini, M. A. G. Maia, O. L. Chaves, and C. Rité. Redshift-Distance Survey of Early-Type Galaxies: Spectroscopic Data. *Aj*, 126:2268–2280, November 2003.

[56] G. L. White and D. Malin. Astrometry of the LMC supernova SN 1987A and the probability that the progenitor is a line-of-sight coincidence with Sk-69 deg 202. In I. J. Danziger, editor, *European Southern Observatory Astrophysics Symposia*, volume 26 of *European Southern Observatory Astrophysics Symposia*, pages 11–17, 1987.

[57] S. E. Woosley, S. Blinnikov, and A. Heger. Pulsational pair instability as an explanation for the most luminous supernovae. *Nature*, 450:390–392, November 2007.

[58] S. E. Woosley and W. C. Haxton. Supernova neutrinos, neutral currents and the origin of fluorine. *Nature*, 334:45–47, July 1988.

[59] L. Zampieri, P. Mucciarelli, A. Pastorello, M. Turatto, E. Cappellaro, and S. Benetti. Simultaneous XMM-Newton and ESO VLT observations of supernova 1995N: probing the wind-ejecta interaction. *Mnras*, 364:1419–1428, December 2005.

[60] L. Zampieri, M. Ramina, and A. Pastorello. Understanding Type II Supernovae. *ArXiv Astrophysics e-prints*, October 2003.

CHAPTER 5

A photometric and spectroscopic study of three very luminous core-collapse supernovae

In this chapter I will present a photometric and spectroscopic study of three core-collapse supernovae, i.e. SNe 2007bt, 2007bw, and 2008fz. Reaching an absolute R magnitude of -20.66, -21.22 and -21.79, respectively, these three events are among the brightest SNe ever discovered. After having discussed the assumption for extinction, distance and explosion epoch, I will present their photometric evolution and discuss their spectral properties. Then I will highlight the similarities and differences among the three events and discuss some possible scenarios which can explain the observational data of the three peculiar transients.

5.1 Enlarging the sample of Very Luminous Supernovae (VLSNe)

After SN 2006gy, thanks to efficient supernova surveys and the capabilities of modern robotic telescopes, several Very Luminous Supernovae (VLSNe, [23]) have been discovered during the last four years. Their intrinsic brightness, $M_V < -20$ or even $M_V < -22$, is significantly higher than any previously-observed core-collapse or thermonuclear event.

The current sample of VLSNe includes SNe 2005ap [27], 2006tf [31], 2007bi [13, 42], 2008es [14, 22] and 2008fz [9] (cf. Table 6.1 in Chapter 6 for an up-to-date list). Further to this, very recently three new bright transients with a peculiar spectroscopic evolution have been discovered at high redshift [28].

As SN 2006gy, these events are characterized by a very high luminosity at

maximum light and by broad spectroscopic emission lines (up to v $\sim$ 12000 km s^{-1}), implying high kinetic energies. Given the additional large and long-lasting energy emitted as radiation, these ultra-bright transient might be the outcome of remarkably high energetic explosions. Interestingly, these energetic explosions are mostly found in low-luminosity galaxies and seem to be little affected by extinction from the host [9]. Due to the natural association of the VLSN to the collapse of the most rare and massive stars (M $\gg$ 20 M$_{\odot}$), large efforts have recently been made to unveil their origin [17, 31, 40].

Given their peak brightness, the supernovae 2007bt, 2007bw and 2008fz also belong to the sample of VLSNe. The Padova-Asiago Supernova Group, in collaboration with other European institutions, was active in the observation of these three peculiar targets. *UBVRI* magnitude and low-resolution spectra were acquired until late phases. This is very interesting since - with the exception of SN 2006gy-no other study of any other VLSN yet exist that extends up to the nebular phase. As it will be shown in the next sections, the evolution of the three transients cannot be considered very different from that of SN 2006gy.

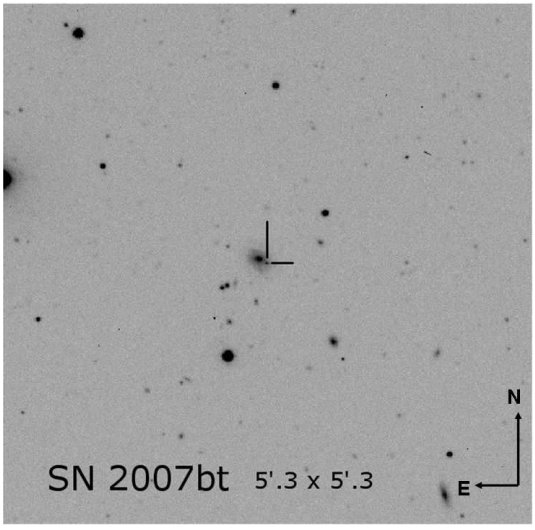

Figure 5.1— R-band images centered on the SN 2007bt acquired near maximum.

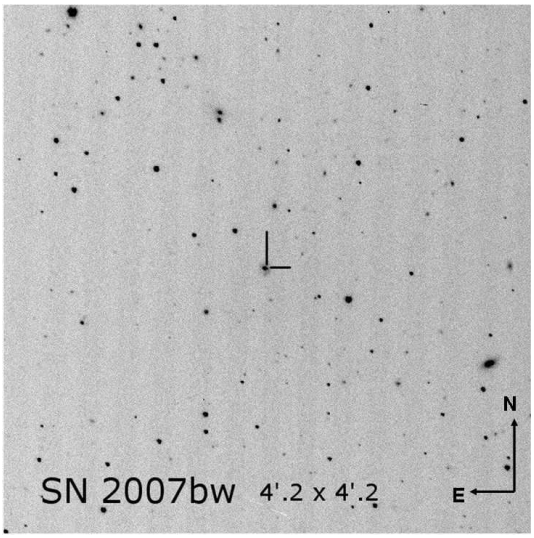

Figure 5.2— R-band images centered on the SN 2007bw acquired near maximum.

5.2 Observations and data reduction

Optical $UBVRI$ photometry and low-resolution spectroscopy were acquired for SNe 2007bt, 2007bw and 2008fz (Fig.5.1, 5.2 and 5.3) at the Telescopio Nazionale Galileo (TNG), the 2.6-m Nordic Optical Telescope (NOT), Calar Alto (CA), New Technology Telescope (NTT), Ekar 1.8m and Pennar 1.2 telescopes. Additional imaging and spectra were obtained with the robotic Palomar 60" telescope, William Herschel Telescope (WHT) and LT (Liverpool Telescope).

Finally, some VRI and unfiltered images of SN 2008fz were acquired by amateur astronomers at the Observatorio de Cantabria[1] (OC, Spain) and at Taurus Hill Observatory[2] (THO, Finland), respectively. A complete log of the observations of the three SNe is provided in Tables 5.1, 5.2 and 5.3.

The photometric data were reduced using routines within IRAF and the photometry measured with standard point-spread-function (PSF) fitting techniques (cf. Chapter 3). In the case SN 2007bw, the faintness of the SN in the high galactic-background made the subtraction with a template before the PSF-fitting necessary for the last photometric epoch. $BVRI$ images acquired

[1] http://www.observatorioastronomicocantabria.com/
[2] http://www.taurushill.net/

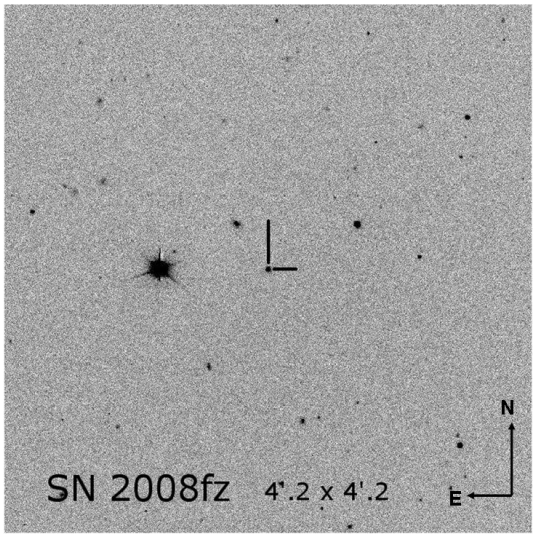

Figure 5.3— R-band images centered on SN 2008fz acquired near maximum.

at NTT (+EFOSC2) on July, 16.12 UT 2009 of the field of SN 2007bw were used as templates.

The photometric zero-points were measured using standard fields from the Landolt (1990) [19] catalogue observed during several photometric nights. The SN magnitudes were then measured differentially with respect to the magnitudes of reference stars in the fields of the three SNe. Magnitudes acquired with SLOAN filters at the LT were also calibrated using Landolt standard stars and thus reported to the standard system. Given the large recession velocities of the parent galaxies, the photometry of the SNe 2007bw and 2008fz was corrected for the K-correction. Because of the limited wavelength and temporal extension of the spectra, only K-correction in the BVR filters was calculated for the available spectral epochs; the results were fitted with a third-order function in order to derive its temporal evolution and to correct all the photometric epochs. The standard deviations of the associated to the K-correction reach K_B, K_V, $K_R \sim 0.02$, 0.04, and 0.03 for SN 2007bw and K_B, K_V, $K_R \sim$0.06, 0.06 and 0.03 for SN 2008fz, respectively. For the U and I filters the absence of the spectral coverage made any attempt of estimating the K-correction worthless. In fact, a calculation for a sample of 5-6 II and IIn SNe from the ASA archive showed that the K-correction in the U band at the distance of z$\sim$0.13 and z$\sim$0.14 may be very different for each considered object and may change con-

siderably with time, varying between $K_U \sim 0$ and $K_U \sim 0.5$. In the I band the K-correction has turned out to be more stable, but it is still affected by significant scatter, i.e. $K_U \sim 0.4 \pm 0.2$. The lack of a proper K-correction will introduce an uncertainty when comparing our U and I-band photometry of the SNe 2007bw and 2008fz to other objects.

The resulting optical photometry for the three SNe is reported in Tables 5.1, 5.2 and 5.3. The errors associated with the magnitudes are estimated as the rms of the error associated to the PSF-fitting and of the error due to the calibration with the local stars sequence.

Concerning spectroscopy, the spectra of the supernovae were acquired at low airmass, with the slit oriented along the parallactic angle. All raw frames were first bias and flat-field corrected, and then the SN spectra were optimally extracted. Wavelength calibration was obtained with the help of comparison lamp exposures, while the spectra were flux calibrated using standard star spectra obtained on the same night as the SN observations. When no spectrophotometric standard star was observed, a sensitivity function derived on a different night (close in time) was used. Telluric features were removed from the SN spectra, again using spectrophotometric standard stars spectra. However, in the case of SN 2007bw some residuals of the strong telluric band at 7570-7750 Å are still present. Given that an imperfect removal would affect the red wing of the Hα I have tried to remove the telluric absorptions as much as possible, without altering the red wing.

All spectra were checked against the photometry and, where discrepancies occurred (especially during low-transparency or bad-seeing nights), the photometric data were used to derive a scaling factor to apply to the SN spectrum. The relative, final flux calibration was good, and the agreement with photometry within 10%. Finally, the spectra were corrected for Galactic extinction and redshift.

5.2.1 SN 2007bt and SN 2007bw

Both SN 2007bt and SN 2007bw were discovered and classified by the Nearby Supernova Factory in two different, anonymous galaxies on 2007 April 17.5 UT and 18.5 UT, respectively [2].

The distances to these events were calculated using the redshift of the host-galaxy emission-lines. A redshift of $z = 0.140 \pm 0.001$ was derived for

UT Date	Telescope	Instrument	Bands	Grisms	Spec. range [Å]	Resolution [Å]	Pixelscale ["/pix.]
2007 May 04	LT	RATCam	*UBVr'i'*	...	...	...	0.13
2007 May 08	Pennar	B&C	...	200tr/mm	3410 − 7925	25	0.6
2007 May 12	LT	RATCam	*UBVr'i'*	...	...	...	0.13
2007 May 26	LT	RATCam	*UBVr'i'*	...	...	...	0.13
2007 Jun 01	LT	RATCam	*UBVr'i'*	...	...	...	0.13
2007 Jun 12	LT	RATCam	*UBVr'i'*	...	...	...	0.13
2007 Jun 15	WHT	ISIS	...	R300B, R158R	3700 − 9920	7,10	0.19
2007 Jun 23	LT	RATCam	*UBVr'i'*	...	...	...	0.13
2007 Jul 01	LT	RATCam	*UBVr'i'*	...	...	...	0.13
2007 Jul 21	WHT	ISIS	....	R300B, R158R	3700 − 10790	7,10	0.19
2007 Jul 25	LT	RATCam	*BVr'i'*	...	...	...	0.13
2007 Aug 02	LT	RATCam	*BVr'i'*	...	...	...	0.13
2007 Aug 12	WHT	ISIS	...	R300B, R158R	3065 − 9565	7,10	0.19
2007 Aug 13	LT	RATCam	*BVr'i'*	...	...	...	0.13
2007 Aug 20	LT	RATCam	*BVr'i'*	...	...	...	0.13
2008 Mar 30	NOT	ALFOSC	*VRI*	...	...	...	0.19
2008 May 05	TNG	DOLORES	*BVRI*	...	...	...	0.25
2008 Jul 05	CA	CAFOS	*BVRI*	...	...	...	0.53
2008 Aug 08	TNG	DOLORES	...	LR-R	4900 − 8900	18,17	0.25

Table 5.1— Journal of photometric and spectroscopic observations of SN 2007bt. The names of the telescopes are written with acronyms, as specified in the text.

UT Date	Telescope	Instrument	Bands	Grisms	Spec. range [Å]	Resolution [Å]	Pixelscale ["/pix.]
2007 May 04	LT	RATCam	*UBVr'i'*	...	...	...	0.13
2007 May 13	LT	RATCam	*UBVr'i'*	...	...	...	0.13
2007 May 20	TNG	DOLORES	...	LR-B,LR-R	3420 – 8000	18, 17	0.25
2007 May 26	LT	RATCam	*UBVr'i'*	...	...	...	0.13
2007 Jun 01	LT	RATCam	*UBVr'i'*	...	...	...	0.13
2007 Jun 12	LT	RATCam	*UBVr'i'*	...	...	...	0.13
2007 Jun 21	LT	RATCam	*UBVr'i'*	...	...	...	0.13
2007 Jul 01	LT	RATCam	*UBVr'i'*	...	...	...	0.13
2007 Jul 07	Ekar	AFOSC	...	gm2,gm4	3210 – 6860	38,24	0.46
2007 Jul 21	WHT	ISIS	...	R158B, R158R	2805 – 8985	11,10	0.24
2007 Jul 22	LT	RATCam	*UBVr'i'*	...	...	...	0.13
2007 Jul 31	LT	RATCam	*UBVr'i'*	...	...	...	0.13
2007 Aug 12	LT	RATCam	*UBVr'i'*	...	...	...	0.13
2007 Aug 15	TNG	DOLORES	*BVRI*	LR-R	4420 – 8170	17	0.25
2007 Aug 21	LT	RATCam	*UBVr'i'*	...	...	...	0.13
2007 Sep 10	WHT	ISIS	...	R158R -R300B	3000 – 9000	10, 7	0.24
2008 May 10	TNG	DOLORES	*BVRI*	...	...	...	0.25
2008 Jul 11	TNG	DOLORES	...	LR-R	4440 – 8960	17	0.25

Table 5.2— Journal of photometric and spectroscopic observations of SN 2007bw. The names of the telescopes are written with acronyms, as specified in the text.

UT Date	Telescope	Instrument	Bands	Grisms	Spec. range [Å]	Resolution [Å]	Pixelscale ["/pix.]
2008 Oct 09	TNG	DOLORES	*UBVRI*	LR-B,LR-R	3529 – 8100	18,17	0.25
2008 Oct 14	P60	CCDCam	*BVRI*	...	...	...	0.37
2008 Oct 15	CA	CAFOS	*UBVRI*	...	...	...	0.53
2008 Oct 15	P60	CCDCam	*BVRI*	...	...	...	0.37
2008 Oct 17	P60	CCDCam	*BVRI*	...	...	...	0.37
2008 Oct 19	OC	CCD-ST-8 XME	*VRI*	...	...	...	0.46
2008 Oct 19	P60	CCDCam	*BVRI*	...	...	...	0.37
2008 Oct 21	P60	CCDCam	*BVRI*	...	...	...	0.37
2008 Oct 27	P60	CCDCam	*BVRI*	...	...	...	0.37
2000 Oct 29	P60	CCDCam	*BVRI*	...	...	...	0.37
2000 Oct 31	P60	CCDCam	*BVRI*	...	...	...	0.37
2008 Nov 01	P60	CCDCam	*BVRI*	...	...	...	0.37
2008 Nov 06	TNG	DOLORES	*UBVRI*	LR-B, LR-R	3984 – 8136	18,17	0.25
2008 Nov 16	NOT	ALFOSC	*UB*	gm4	3125 – 8000	19	0.19
2008 Nov 23	TNG	DOLORES	*UBVRI*	LR-B, LR-R	4553 – 8224	18,17	0.25
2008 Nov 27	Ekar	AFOSC	*BVRI*	...	...	...	0.46
2008 Nov 28	NOT	ALFOSC	*UB*	gm4	3553 – 8342	19	0.19
2008 Nov 28	THO	...	*Unf.*	...	...	...	0.61
2008 Dec 20	NOT	ALFOSC	*UB*	gm4	3078 – 7960	19	0.19
2008 Dec 21	TNG	DOLORES	*BVRI*	LR-R	4536 – 9062	17	0.25
2008 Dec 23	Ekar	AFOSC	*BVRI*	...	...	...	0.46
2009 Jan 23	NOT	ALFOSC	*R*	gm4	3533 – 7997	19	0.19
2009 May 17	NTT	EFOSC2	*R*	...	...	...	0.16
2009 Jun 04	CA	CAFOS	*R*	...	...	...	0.53
2009 Oct 22	NTT	EFOSC2	*VRI*	...	...	...	0.16
2009 Nov 22	NTT	EFOSC2	*I*	...	...	...	0.16

Table 5.3— Journal of photometric and spectroscopic observations of SN 2008fz. The names of the telescopes are written with acronyms, as specified in the text.

Date UT	JD -2,400,000	Phase [days]	U	Uerr	B	Berr	V	Verr	R	Rerr	I	Ierr
2007 Apr 17	54209.0	18	...	...	...	...	...	...	17.30	0.30	...	...
2007 May 04	54225.6	34.6	18.51	0.06	18.66	0.06	18.06	0.04	17.74	0.04	17.25	0.01
2007 May 13	54233.7	42.7	18.59	0.05	18.84	0.02	18.16	0.02	17.83	0.02	17.39	0.02
2007 May 26	54247.6	56.6	18.84	0.06	19.02	0.03	18.33	0.04	17.93	0.05	17.51	0.02
2007 Jun 01	54253.4	62.4	19.01	0.06	19.08	0.03	18.42	0.04	17.98	0.05	17.58	0.02
2007 Jun 12	54264.6	73.6	...	...	19.35	0.03	18.47	0.02	18.29	0.04	17.76	0.024
2007 Jun 21	54273.7	82.7	19.24	0.05	19.28	0.04	18.58	0.03	18.24	0.03	17.80	0.026
2007 Jul 01	54283.5	92.5	19.33	0.08	19.45	0.06	18.63	0.02	18.34	0.05	17.83	0.04
2007 Jul 22	54304.5	113.5	19.54	0.09	19.66	0.04	18.89	0.07	18.65	0.04	18.14	0.04
2007 Jul 31	54313.5	122.5	19.59	0.17	19.57	0.08	18.99	0.05	18.67	0.04	18.15	0.02
2007 Aug 12	54325.5	134.5	19.85	0.07	19.90	0.04	19.03	0.03	18.88	0.03	18.14	0.02
2007 Aug 15	54328.4	137.4	...	...	19.84	0.05	19.10	0.03	18.81	0.03	...	...
2007 Aug 21	54334.5	143.5	19.97	0.12	19.76	0.05	19.14	0.05	18.91	0.07	18.16	0.08
2008 May 10	54596.5	405.5	...	...	21.39	0.07	20.51	0.09	20.40	0.11	19.97	0.28
2008 Jul 05	54653.4	462.4	...	...	20.85	0.03	20.56	0.05	20.16	0.05	19.72	0.04

Table 5.4— Optical Photometry of SN 2007bt.

Date UT	JD -2,400,000	Phase [days]	U	Uerr	B	Berr	V	Verr	R	Rerr	I	Ierr
2007 Apr 17	54209.0	18	...	...	...	...	...	...	17.30	0.30	...	...
2007 May 04	54225.6	34.6	18.51	0.05	18.66	0.06	18.06	0.03	17.74	0.03	17.25	0.01
2007 May 13	54233.7	42.7	18.59	0.04	18.84	0.02	18.16	0.02	17.83	0.02	17.39	0.02
2007 May 26	54247.6	56.6	18.84	0.05	19.02	0.03	18.33	0.04	17.93	0.05	17.51	0.02
2007 Jun 01	54253.4	62.4	19.01	0.06	19.08	0.03	18.42	0.04	17.98	0.05	17.58	0.02
2007 Jun 12	54264.6	73.6	...	...	19.35	0.03	18.47	0.02	18.29	0.04	17.76	0.02
2007 Jun 21	54273.7	82.7	19.24	0.05	19.28	0.03	18.58	0.03	18.24	0.03	17.80	0.03
2007 Jul 01	54283.5	92.5	19.33	0.07	19.45	0.06	18.63	0.02	18.34	0.05	17.83	0.04
2007 Jul 22	54304.5	113.5	19.54	0.09	19.66	0.04	18.89	0.07	18.65	0.04	18.14	0.04
2007 Jul 31	54313.5	122.5	19.59	0.17	19.57	0.08	18.99	0.05	18.67	0.04	18.15	0.02
2007 Aug 12	54325.5	134.5	19.85	0.07	19.90	0.04	19.03	0.03	18.88	0.03	18.14	0.02
2007 Aug 15	54328.4	137.4	...	...	19.84	0.05	19.10	0.03	18.81	0.04	...	...
2007 Aug 21	54334.5	143.5	19.97	0.11	19.76	0.05	19.14	0.04	18.91	0.07	18.16	0.07
2008 May 10	54596.5	405.5	...	...	21.39	0.07	20.51	0.09	20.40	0.11	19.97	0.28
2008 Jul 05	54653.4	462.4	...	...	20.85	0.02	20.56	0.05	20.16	0.05	19.72	0.04

Table 5.5— Optical Photometry of SN 2007bw.

Date UT	JD -2,400,000	Phase [days]	U	Uerr	B	Berr	V	Verr	R	Rerr	I	Ierr
2008 Jun 13	54630.9	-89.1	...	...	...	...	...	...	20.0	...	...	...
2008 Sep 22	54731.8	11.8	...	...	...	...	...	...	17.1	...	...	...
2008 Sep 23	54732.6	22.6	...	...	...	...	...	...	17.3	...	17.4	...
2008 Sep 24	54733.6	23.6	...	...	...	...	...	...	17.2	...	...	...
2008 Sep 28	54737.9	27.9	...	...	...	...	...	...	17.0	...	...	...
2008 Oct 09	54748.6	28.6	16.35	0.01	17.10	0.01	16.93	0.01	16.91	0.01	16.80	0.01
2008 Oct 15	54754.6	34.6	...	...	17.26	0.02	17.07	0.02	16.90	0.01	16.85	0.02
2008 Oct 15	54755.3	35.3	16.51	0.02	17.36	0.02	17.06	0.01	17.10	0.01	16.92	0.01
2008 Oct 17	54756.6	36.6	...	...	17.29	0.002	17.09	0.02	16.96	0.03	16.77	0.02
2008 Oct 19	54758.5	38.5	...	0.000	17.39	0.03	17.14	0.03	16.96	0.02	16.80	0.02
2008 Oct 19	54758.6	38.6	...	...	...	...	17.21	0.03	16.97	0.03	...	...
2008 Oct 21	54760.6	40.6	...	...	17.32	0.04	17.17	0.02	17.00	0.02	16.80	0.03
2008 Oct 26	54766.6	46.6	...	...	17.43	0.03	17.26	0.03	17.06	0.03	16.84	0.03
2000 Oct 29	54768.5	48.5	...	...	17.51	0.05	17.29	0.05	17.07	0.04	16.84	0.04
2000 Nov 01	54771.6	51.6	...	...	17.61	0.04	...	...	17.11	0.03	...	...
2008 Nov 06	54777.4	57.4	17.34	0.02	17.88	0.03	17.44	0.02	17.17	0.02	16.92	0.02
2008 Nov 16	54787.4	67.4	17.79	0.03	18.26	0.03	...	...	...	...	...	...
2008 Nov 23	54793.5	73.5	17.80	0.02	18.44	0.02	17.89	0.02	17.73	0.02	17.30	0.02
2008 Nov 27	54798.3	78.3	...	...	18.63	0.04	17.98	0.02	17.70	0.04	17.10	0.03
2008 Nov 27	54799.4	79.4	18.43	0.05	18.68	0.01	...	...	...	...	...	...
2008 Nov 28	54799.4	79.4	...	...	...	...	...	...	17.68	.0	...	...
2008 Dec 20	54821.3	101.3	19.48	0.04	19.51	0.03	...	...	...	...	...	...
2008 Dec 21	54822.3	102.3	...	...	19.52	0.01	18.59	0.02	18.26	0.02	...	...
2008 Dec 23	54824.0	104.0	...	...	19.54	0.03	18.61	0.02	18.25	0.06	...	...
2009 Jan 23	54855.3	135.3	...	...	...	...	19.45	0.04	...	...	...	...
2009 Jun 04	54987.0	267.0	...	...	...	...	...	...	21.53	0.20	....	...
2009 Oct 22	55126.5		...	...	...	...	24.55	0.40	23.89	0.20	22.70	0.16
2009 Nov 11	55157.5		...	...	...	...	...	...	...	...	24.00	0.30

Table 5.6— Optical Photometry of SN 2008fz.

SN 2007bw, and $z = 0.044 \pm 0.002$ for SN 2007bt, in good agreement with the values reported by Antilogus et al. [2]. The error associated to these estimates is mainly due to the standard deviation of the fitting function with which the wavelength calibration was performed. Using a cosmological model with $\Omega_M = 0.28$, $\Omega_\Lambda = 0.72$ and $H_0 = 72$ km s^{-1} Mpc^{-1} [12], I derived a distance modulus of $\mu = 36.39$ mag ($D_L = 189.5$ Mpc) for SN 2007bt, and $\mu = 39.04$ mag ($D_L = 644.4$ Mpc) for SN 2007bw. I adopted the map of Schlegel et al. [30] to evaluate the color excess due to the extinction in the Milky Way, which gives $E(B-V)_{Gal} = 0.05$ and 0.03 mag (assuming $R_V = 3.1$) for SN 2007bt and SN 2007bw, respectively.

Deducing the amount of host galaxy extinction for these SNe was non-trivial. For SN 2007bt, the absorption of Na I D may be tentatively identified in the high-resolution spectra. Its Equivalent Width (EW) is supposed to be related to the color excess due to internal absorption according to the relation of Turatto et al. [38]. However, Elias-Rosa et al. [10] and Blondin et al. [5] showed that this relation suffers a non-negligible scatter especially for EWs<1 Å. For SN 2007bt, the estimated EW of ∼0.4 would imply $0 < E(B-V)_{Int} < 0.35$ mag, and most likely less than 0.2 mag. For SN 2007bw there is no evidence of an Na I D absorption in the spectra, albeit this could be due to the low S/N. Given the lack of evidence for substantial host galaxy extinction, I have neglected any such contribution for both SNe. Note that any additional extinction would make these already very luminous supernovae even brighter. It can be further noted that the absence of extinction seems to be a common feature of VLSNe (Table 6.1 in Chapter 6).

Pinning down the explosion date also represents a challenging task for SNe 2007bt and 2007bw, as it was for the VLSN SN 2006tf [33]. No hints about their age are given in the discovery circular [2]. Images of their field were acquired by the Nearby Supernova Factory Search about 167/8 days before discovery, which is likely much earlier than both SN explosions. This does not allow me to constrain the SN age and will be a cause of concern throughout the discussion, for example when comparing with other SNe. Considering the spectral appearance (Sec. 5.4.1, 5.4.2) the SNe were probably not caught very early. This is indicated by the slow spectral and color evolution. A simple black-body argument, assuming spherical emission, indicates that SN 2007bw had a radius of $R_{BB} \sim 337$ AU at the epoch of our first spectrum, 21 days past discovery. Even at a velocity as high as 10,000 km s^{-1} this implies that the SN exploded about two weeks before discovery for a progenitor radius of $\sim 10^{15}$ cm, and about one month before discovery for a progenitor radius of $\sim 10^{14}$ cm. Given these uncertainties, I will simply postulate an explosion date for these two events. I will fix the explosion date to April 1, 2007 (JD=2454191.0) for

both SNe, which is consistent with the explosion of a progenitor with a radius of $\sim 10^{15}$ cm. I will allow a temporal uncertainty of ± 18 days on this epoch.

Optical images were collected using several telescopes until day $\sim$489 for SN 2007bt and until day $\sim$462 for SN 2007bw. The spectral sequence extends to 496 days for SN 2007bt and to 468 days for SN 2007bw.

5.2.2 SN 2008fz

SN 2008fz was discovered by Drake et al. [8] in the course of the Catalina Real Time Transient Survey (CRTS) on September 22.34 UT, 2008. About one day later, Hsiao et al. [15] noted some spectroscopic analogies with SN 1998bw and classified SN 2008fz as a Type Ic.

On October 9.16 UT, Benetti et al. [3] reclassified SN 2008fz as a Type IIn on the basis of its spectroscopic similarity with SNe 1990K and 2005gj. Benetti et al. [3] furthermore suggested an origin similar to the very luminous SN 2006gy. Mahabal et al. [21] reported that a spectrum of SN 2008fz taken on October 1 was consistent with that of a Type II SN near maximum light, and that the spectrum acquired on September 27 exhibited no strong features.

According to Drake et al. [9], the anonymous host galaxy is not visible in the CSS co-added, pre-discovery images up to an apparent magnitude 22[3] and absolute magnitude $M_R = -16.7$. Nevertheless, Hsiao et al. [15] noted a faint extended object at the position of the transient on a digitized plate of the second Palomar Sky Survey. Unfortunately, the PSF of the SN completely obscures the host galaxy emission, which is therefore included in my photometry measurements.

As for SNe 2007bt and 2007bw, because of the absence of any Na I D absorption in the spectra, I only corrected for the Galactic extinction as given by Schlegel et al. [30], i.e. $A_{B,Gal} = 0.22$ mag.

Adopting the same cosmological parameters as for SN 2007bw, the estimated redshift of SN 2008fz as calculated from the host-galaxy emission lines, is $z = 0.133 \pm 0.002$. This is in agreement with what estimated by Drake et al. [9].

To pin down the explosion date for SN 2008fz the photometric and spectroscopic similarity of SN 2008fz to SN 2008es (Sect. 5.4.3) and to SN 2006gy (Fig.5.4) can be helpful. The comparison to SN 2008es is simplified by the presence of an evident peak of the light curve (Fig. 5.5 and inset of Fig.5.9). However, for SN 2008fz the two early unfiltered, pre-peak data from the CRTS make rise to the light curve maximum slower than in SN 2008es, which is supposed to reach the peak brightness in only $\sim$7 days from explosion.

[3] http://voeventnet.org/feeds/Catalina.shtml

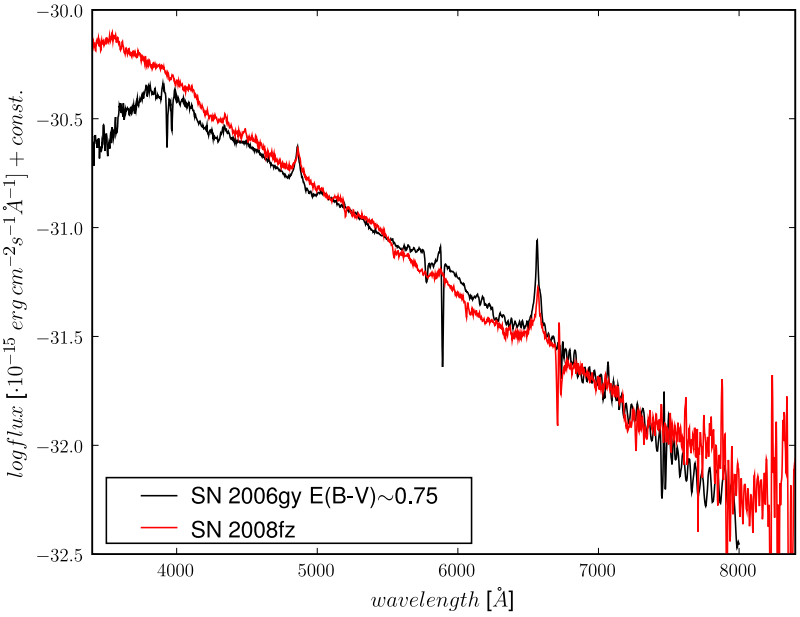

Figure 5.4— Spectral comparison between SN 2008fz and SN 2006gy, normalized to photometry and corrected for an extinction E(B − V) ∼ 0.75.

Also, the first spectrum of SN 2008fz matches very well the spectrum of SN 2006gy (Fig.5.4), if we assume for the latter an extinction of E(B − V) ∼ 0.75, i.e. 0.20 mag higher than what is assumed in Chapter 4. Assuming that the similarity of the two spectra implies that the spectra of both events were formed after a SN ejecta collision on a massive CSM (as it will be explained in Section 6.5), it is reasonable that the epoch of these spectra is not very close to the explosion. Indeed, though with a slightly faster decay, the evolution of the early light curve of SN 2008fz matches reasonably well that of SN 2006gy; this is true also for SN 2008es, if the phase is increased by +25 days, as it is shown in Fig.5.5. It should be noted that, despite of the large distance (z=0.231, [23]), for SN 2008es the K-correction and the time-dilation correction were not taken into account by Miller et al. [22] nor by Gezari et al. [14]. However, I have estimated that for a type II SN at this distance the K-correction in the R-band would change between -0.4 and +0.3 in the early ∼80 days (Fig.5.6), with the effect that the light curve pre-peak/peak would be significantly fainter,

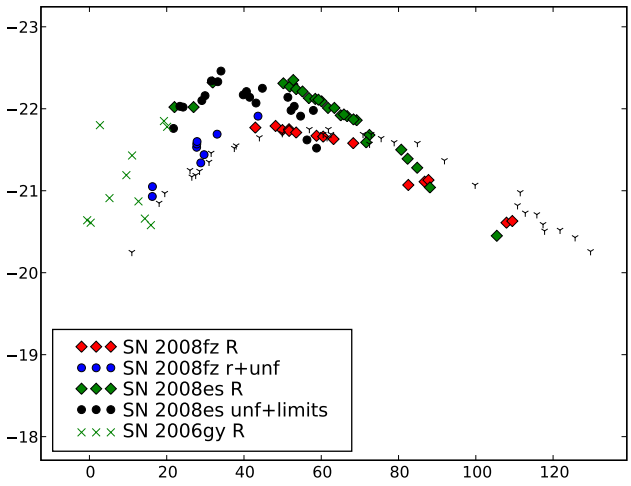

Figure 5.5— Early light curve evolution of SNe 2006gy [1, 34], 2008es [14, 22], 2008fz (data from this thesis). The light curve of SN 2008es has been shifted of +25 days in phase with respect to the explosion date estimated by Gezari et al. [14], in order to match the light curves of SNe 2008 The black dots and diamond represent unfiltered magnitudes or upper limits. Given the large distances, the light curves of SNe 2008fz and 2008es have been corrected for stretch-factor; the light curve of SN 2008fz has been also corrected for K-correction.

whereas it would be slightly brighter thereafter. The light curve evolution would become therefore more similar to SN 2006gy. Since the K-correction changes significantly with time and the explosion date of SN 2008es is not well constrained, I did not K-corrected the magnitudes reported in Fig.5.5.

The adopted explosion epoch for SN 2008fz is $\mathrm{JD_{expl}} = 2454700.0 \pm 10$ (August 22, 2008). This transient was well-monitored in the $UBVRI$ bands for about 124 days. In addition, a late V-band image was obtained on day ∼155 an additional R-band images was acquired on day ∼287 at NTT with EFOSC. With the same telescope and equipment deep VRI images and an I image were collected on day 426.55 and 457, respectively. The sequence of spectra extends until day ∼155.

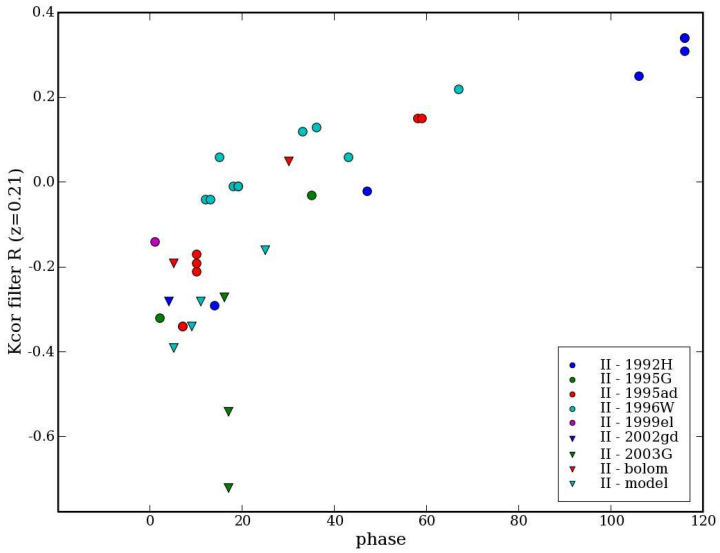

Figure 5.6— Estimate of the K-correction for a sample of type II SNe at z=0.21 from the ASA archive.

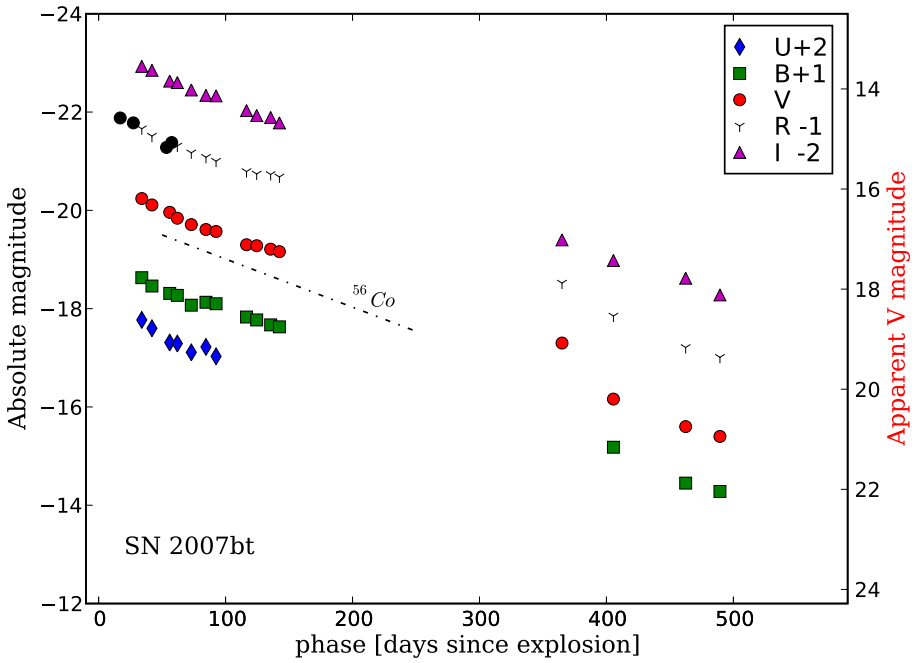

Figure 5.7— Photometric evolution in the $UBVRI$ absolute magnitudes of SN 2007bt. The right hand scale reports the apparent V-band magnitudes. The early times, black circles refer to unfiltered or CR magnitude from http://www.astrosurf.com/snweb2/2007/07bt/07btMeas.htm.

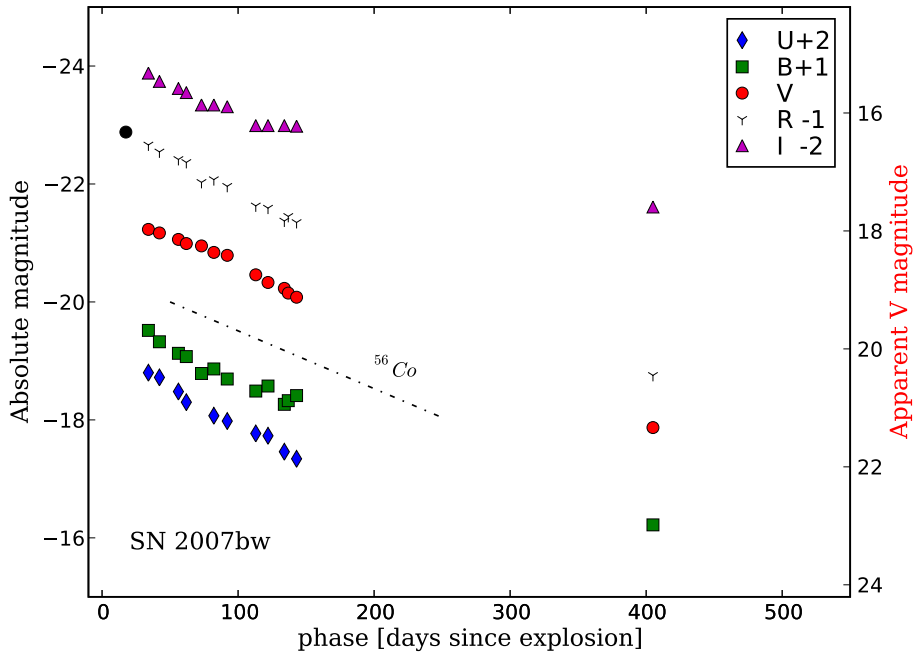

Figure 5.8— Photometric evolution in the $UBVRI$ absolute magnitudes of SN 2007bw. To account for the large distance, a K-correction was applied to the the B, V, R light curves. The early times, black circle refer to the unfiltered magnitude reported in the circular.

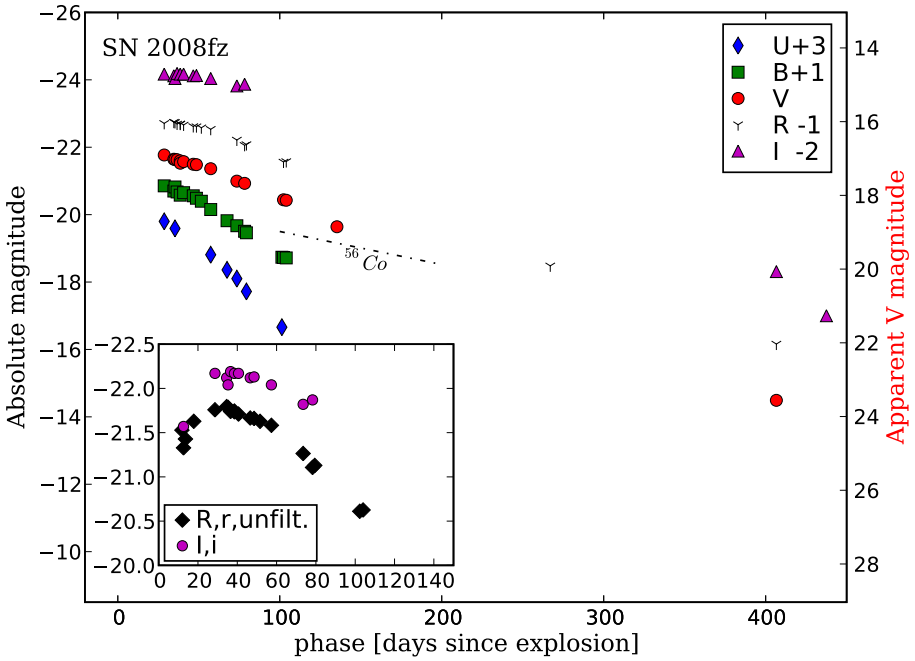

Figure 5.9— Photometric evolution in the $UBVRI$ absolute magnitudes of SN 2008fz. To account for the large distance, a K-correction was applied to the the B, V, R light curves. In the lower-left inset the R- and I-band light-curves include also the unfiltered and Sloan-filtered magnitudes.

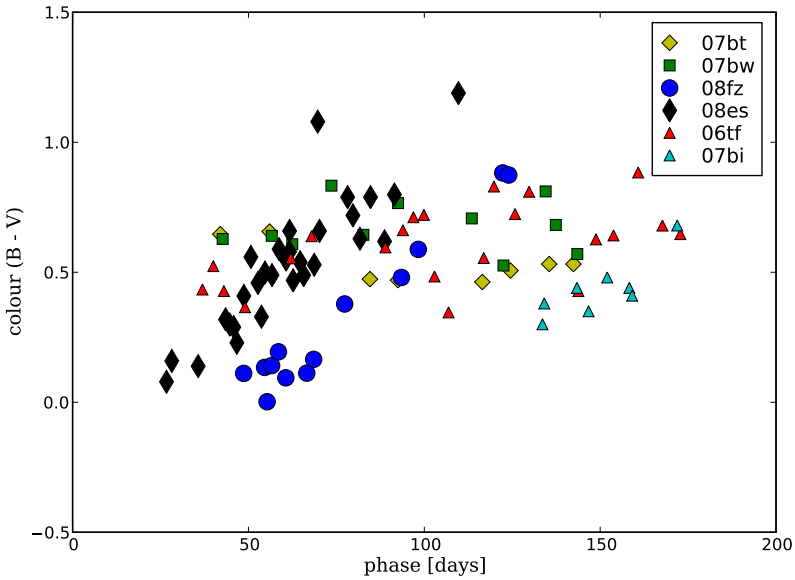

Figure 5.10— Time evolution of $B - V$ colour for the three SNe, compared with the SNe 2006tf [31], 2007bi [13, 42] and 2008es [14, 22].

5.3 Photometry

The $UBVRI$ light curves of SNe 2007bt, 2007bw and 2008fz are plotted in absolute magnitudes with respect to their estimated dates of explosion in Figs.5.7, 5.8 and 5.9, respectively.

With an absolute R-band magnitude of -21.79, SN 2008fz is the third brightest SN ever discovered, after SN 2005ap, which reached $M_{unf.} \sim -22.7$ [27], and SN 2008es, with a peak at $M_R \sim -22.31$ [14, 22];. However, the K-correction was not computed for the SNe 2008es and 2005ap. Therefore, these SNe could be fainter at peak by a factor $K_R \leq -0.4$ during the first $\sim$50 days.

The measured brightest magnitude of SN 2007bw is $M_R \sim -21.22$, whereas it is $M_R \sim -20.66$ for SN 2007bt, but the peaks may have been reached earlier.

A plot presenting the early R-band light curve evolution of the brightest known SNe is presented in Fig.5.11.

It is evident that SNe 2007bt and 2007bw follow a common luminosity decay rate, which is linear in all bands until late phases. Both events display a decay rate close to one magnitude per 100 days in all bands during the first $\sim$150 days. In particular, γ= 1.14, 0.85, 0.98, 0.95 and 1.04 mag (100 days)$^{-1}$ for the U, B, V, R and I bands, respectively, for SN 2007bt, whereas γ= 1.29, 0.99, 0.97, 1.18 and 0.82 mag (100 days)$^{-1}$ for the U, B, V, R and I bands, respectively, for SN 2007bw. Thereafter, the optical observations were interrupted while the two transients passed behind the Sun. This luminosity decrease rate matches that from the decay of ^{56}Co, $\gamma \sim 0.98$ mag (100 days)$^{-1}$. It can be noted that the same decay rate was found for SN 2006tf for days $<$173 [33].

At late phases ($>$ 300 days) the estimated magnitudes of SNe 2007bt and 2007bw are attached with larger error bars, mainly due to the faintness of the objects and their apparent proximity to their host-galaxy nuclei.

Though less bright, the light curves of 2007bt have the same decline rate at days $\gtrsim$400 in the $BVRI$ bands maintain the same decline rate as in the early phases, with an uncertainty of $\pm$0.4.

Also in the case of SN 2007bw the early decline rate is consistent with the supposed decay rate during Solar occultation within 10%.

For SN 2008fz the $UBVRI$ light curves are presented until phase $\sim$457 days (Fig.5.9). The light curve evolution is significantly different from that of the linearly-decaying SNe 2007bt and 2007bw. If the early unfiltered and SDSS-filter r and i magnitudes from Drake et al. [8] are taken into account, a rather smooth light-curve peak emerges. The light curve reaches a maximum at an epoch very close to our first Johnson-Cousin-filtered data point,

i. e. at about day ∼50 in both R and I (see inset in Fig.5.9). The very slow luminosity decrease in the early light curve also for the bluer pass-bands ($\gamma_B \sim 0.59\,\mathrm{mag}$ $(100\ \mathrm{days})^{-1}$ between day 30 and 50) is consistent with a scenario where also these pass-bands reached a maximum close to that deduced for R and I. After day ∼70 the light curve sets on a faster decline in all bands, γ= 4.9, 3.6, 2.5, 1.8 and 0.78 mag $(100\ \mathrm{days})^{-1}$ for the U, B, V, R and I bands, respectively. The two R-band epochs at late-times are consistent with the early decline within $\gamma \sim \pm 0.05$. Instead, the I luminosity seems to drop faster after 400 days, though the error bars at these phases are larger. In general, given the steep evolution of the light curve it can be claimed that the host-galaxy contribution to the SN luminosity is negligible, especially at earlier times, being its magnitude ≤24, in agreement with what suggested by Drake et al. [9].

The early color evolution (Fig.5.10) of SN 2008fz differs from the two other VLSNe reported on in this paper. SN 2008fz is significantly bluer and evolves much faster, very similar to SN 2008es. On the contrary, the sample composed of SNe 2006tf, 2007bt and 2007bw shows almost no color evolution, staying at (B − V)∼0.5 mag for the first 5 months.

Finally, the pseudo-bolometric evolution in $(U)BVRI$ for the three SNe is presented in Fig.5.12, compared to SNe 2006tf, 2008es, 2006gy and 2007bi.

These bolometric light curves of the presented SNe underline some of the afore-mentioned properties on the magnitude and color evolution, in which SNe 2007bt and 2007bw follow the evolution of e.g., SN 2006tf, while SN 2008fz is very similar to SN 2008es. Note that much of the emission for SN 2008es emerges at even shorter wavelengths at early times, but the measured SWIFT/UVOT magnitudes were not included in this plot to allow comparison to the other SNe.

The pseudo-bolometric luminosity can also be a valuable indicator of the amount of radioactive ^{56}Ni ejected in the SN explosion, under the assumption that radioactive decay of ^{56}Co into ^{56}Fe is the main source of radiative energy. In that case, the mass of ^{56}Ni can be approximated by a simple comparison with the luminosity of SN 1987A, i.e. $\mathrm{M}_{^{56}\mathrm{Ni,SN}}\,[\mathrm{M}_\odot] \sim 0.075 \cdot \mathrm{L_{SN}}/\mathrm{L_{SN87A}}$.

Neglecting any interaction with the circumstellar medium, I would thus derive a Nickel mass of $\sim 3 \pm 0.5$ $\mathrm{M}_\odot$ for SN 2007bt and $\sim 10 \pm 2$ $\mathrm{M}_\odot$ for SN 2007bw.[4]. In the extreme case of considering the discovery epoch as the explosion date, these values would decrease to $\sim 2.6 \pm 0.5$ $\mathrm{M}_\odot$ and $\sim 9.5 \pm 0.5$ $\mathrm{M}_\odot$, respectively. I will therefore consider such values as lower limits to the amount of ejected ^{56}Ni .

[4]The relatively large uncertainty is due to the offset in luminosity between the early and the late-times luminosity of the bolometric light curve

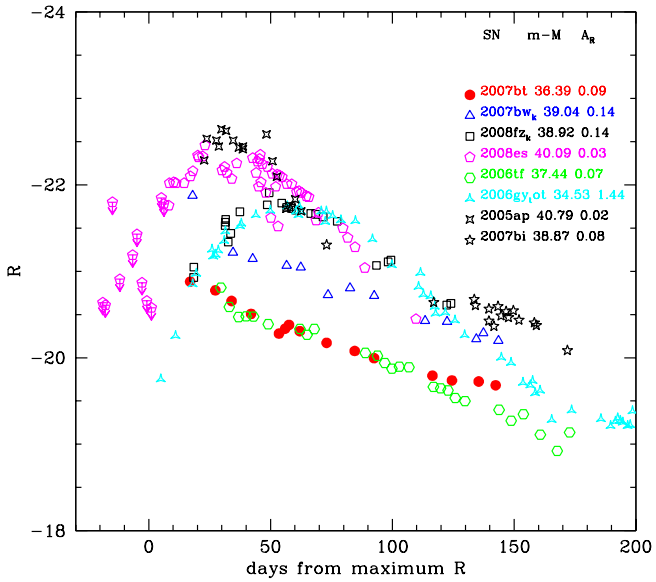

Figure 5.11— Absolute R-band light-curves of SNe 2007bt, 2007bw and 2008fz compared with SNe 2005gj [26], 2006tf [31], 2008es [14, 22], SN 2005ap ([27], unfiltered magnitudes) and 2007bi [13, 42].

Although such high amounts of Nickel has never before been unequivocally measured for any core-collapse supernova, they can not a priori be excluded. However, for these SNe other feasible source of radiative energy should be considered.

For SN 2008fz the light curve declines more steeply than ^{56}Co, which make the hypothesis of radioactive decay sustaining the light curve peak less feasible than in the two other cases. However, it cannot be excluded the assumption of dust formation in the ejecta, which, as in the case of SN 2006gy, would absorb the optical radiation and re-emit in the NIR range. This would increase the late-times luminosity and consequently the amount of ejected ^{56}Ni . Note that a ^{56}Co-like decay of the nebular luminosity has been frequently observed in IIL SNe (e.g., SN 1979C, [11]). Therefore, I am forced to consider the estimate of the ^{56}Ni mass calculated from the last epoch, i.e. ~ 1 M$_\odot$ as a lower limit.

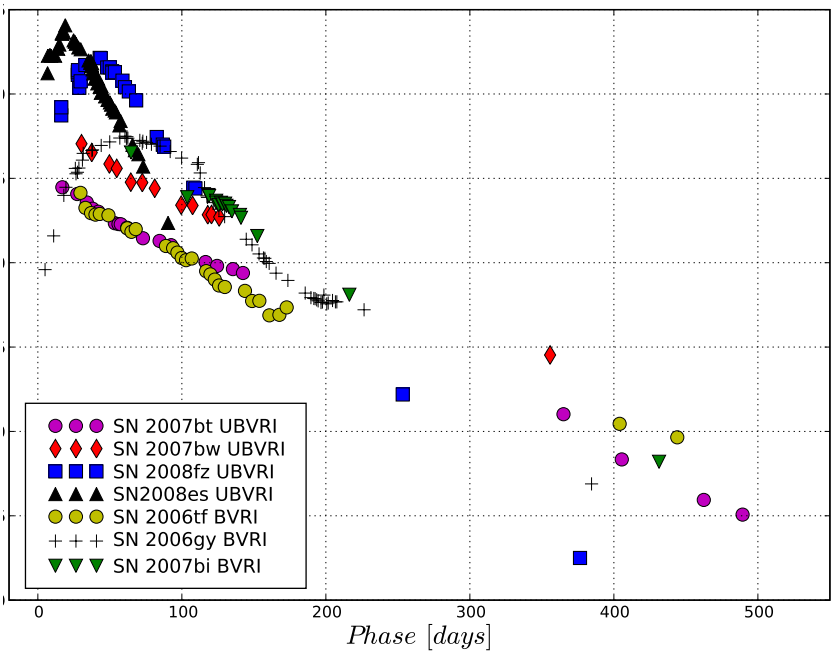

Figure 5.12— The $UBVRI$ pseudo-bolometric evolution of SNe 2007bt (purple circles), 2007bw (red diamonds) and 2008fz (blue squares, including also unfiltered magnitudes) compared to pseudo-bolometric light-curves SNe 2008es ($UBVRI$+unfiltered magnitudes and upper limits, from [22] and [14]) 2006tf ($BVRI$ from [31]) and SN 2006gy ($BVRI$ from [34] [1] and [18]), 2007bi (($BVRI$ from [13, 42] plotted since explosion epoch. For SN 2006gy the point at 364 days has been computed with the magnitudes measured by Kawabata et al. [18]. The light curves of SNe 2007bw, 2008es, 2008fz and 2007bi have been corrected for cosmological time-dilation effect.

5.4 Spectroscopy

The spectral sequences of SNe 2007bt, 2007bw and 2008fz are shown in Figs.5.13, 5.15 and 5.19. The displayed spectra are all flux-calibrated using the photometry, and have been corrected for (Galactic) extinction and redshift. For each SN, the evolution of the velocities at zero intensity of the Hα and Hβ lines are also presented in Figs 5.14, 5.16 and 5.20.

5.4.1 SN 2007bt

The spectra of SN 2007bt are characterized by a slow evolution both of the continuum and of the emission lines. This is consistent with the very slow color evolution as derived from the photometry. A black-body fit of the continuum gives T$\sim$6450$\pm$400 K for the spectrum on day 101. The temperature can be considered nearly constant, within the error bars, from the first to the fourth spectrum (day 134).

Generally, the sequence resemble the spectra of normal Type II SNe, showing broad emission of Balmer lines, hints of He I at λ5876 and λ7065 and an intense Ca II triplet at $\lambda\lambda\lambda$8498-8542-8662, likely blended with O I at λ8446. Unlike for most Type IIn SNe, faint narrow lines are visible only on top of the Hα and Hβ lines (Fig.5.14). In particular, the profile of Hα shows a narrow component with a velocity FWHM of $\sim 320\,\mathrm{km\,s^{-1}}$, which however is at the limit of the resolution on the WHT-R158R spectrum and therefore cannot be indicative.

The emission line profile of Hα is clearly asymmetric at the first epoch, showing a more intense emission in the blue wing than on the red side. The latter, however, extends to larger velocities, i.e. $v_{zi} \sim 13000\,\mathrm{km\,s^{-1}}$ at zero intensity. With time the contrast between the amplitude of the blue and red wing becomes less pronounced and the line turns into a more symmetrical profile.

By day $\sim$134 the velocity at zero intensity on the red wing of Hα is -$v_{zi} \sim 12000\,\mathrm{km\,s^{-1}}$. This is a bit higher than what was measured in SN 2006tf for the broadest Hα component by Smith et al. (2008b) [31], i.e. $\sim 7500\,\mathrm{km\,s^{-1}}$ which however was measured on the *blue* wing of the line. It is also larger than the velocity inferred for H$\alpha$for the luminous SN 2008es, for which $v_{zi} \sim 9000\,\mathrm{km\,s^{-1}}$ [22].

The same profile and velocity evolution as for Hα can be inferred for the Hβ line. The Hα/Hβ flux-ratio is $\sim$1.3 during the first $\sim$140 days, meaning that the collisional process are likely dominating in the formation of the line [24]. Furthermore, the profile of Hβ is characterized by a narrow component showing a P-Cygni, already visible in the day 38 spectrum. Its velocity deduced by the minimum resolved in the WHT-R300B spectra, being $\sim 330\,\mathrm{km\,s^{-1}}$. This is

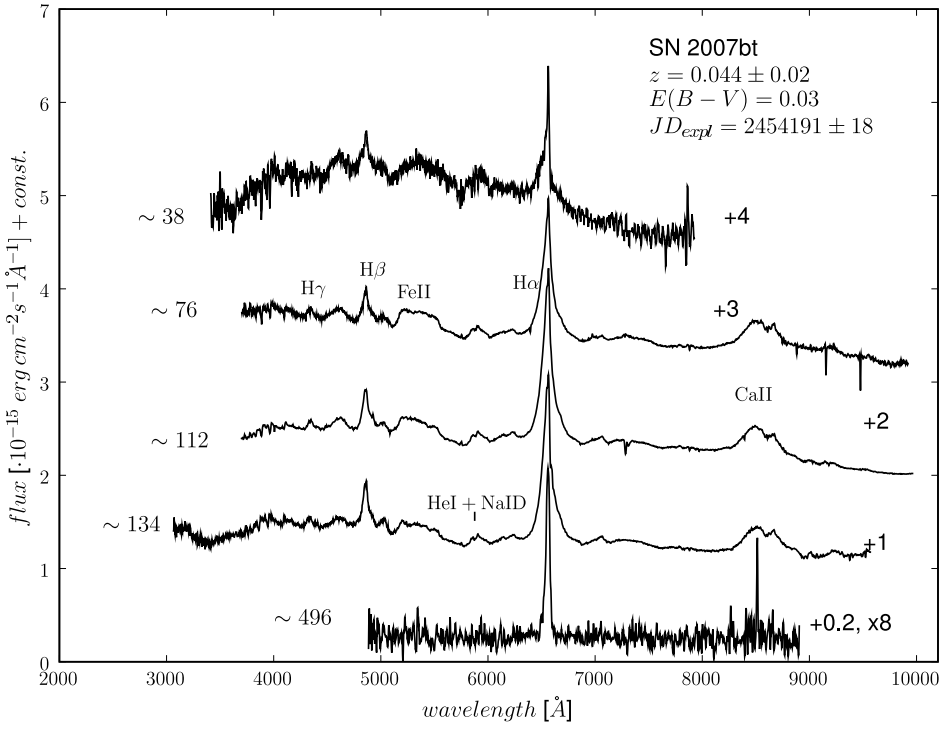

Figure 5.13— *Top:* Spectroscopic evolution of SN 2007bt from ∼38 to ∼496 past explosion. The spectra are in the host galaxy rest-frame, and are corrected for extinction assuming E(B−V)=0.03 mag. On the left side of the spectra are indicated the phases since explosion; on the right side, the numbers refer to the flux shift.

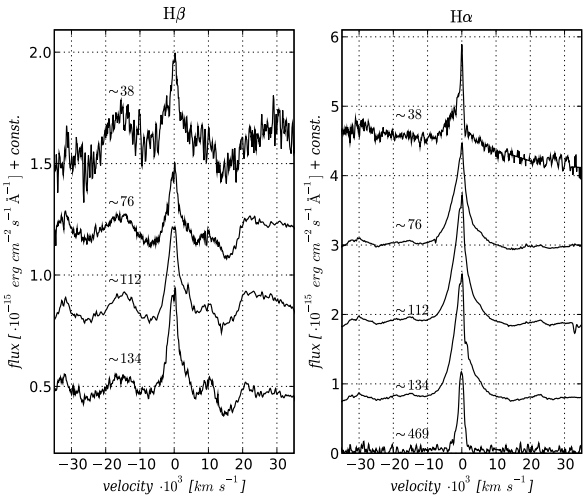

Figure 5.14— Velocity time-evolution of Hα and Hβ for SN 2007bt.

the same velocity as the FWHM of the narrow emission atop of Hα, and can be interpreted as the velocity of the unshocked, slow-moving wind around the exploding star.

The last spectrum (day ∼496) reports only a weak (i.e., about 1/20 of the flux on day 134) Hα line with $v_{zi} \sim 3300\,\mathrm{km\,s^{-1}}$.

In general, the form and evolution of the continuum, as well the relative intensity of the emission lines of SN 2007bt is remarkably similar to that of SN 2006tf; though the latter apparent showed much more prominent narrow Balmer lines, the absolute luminosity of H$\alpha$is about 1/2 of SN 2007bt (Fig.5.17, lower panel).

5.4.2 SN 2007bw

The spectral sequence of SN 2007bw is shown in Fig.5.15. The larger distance and a strong background make the signal-to-noise ratio somewhat lower for the spectra of this supernova. There are strong signs of host-galaxy contamination, as evident from the narrow emission lines of [O II] λ3727 and [O III] $\lambda\lambda$4959, 5007. Given the proximity to the host galaxy nucleus, it is likely that the narrow Balmer lines may also be partially due to the emission from an HII region. Differences in the seeing or in the centering of the slit could cause some of the extemporal variation of the flux in the narrow Hα and in the [O II] line.

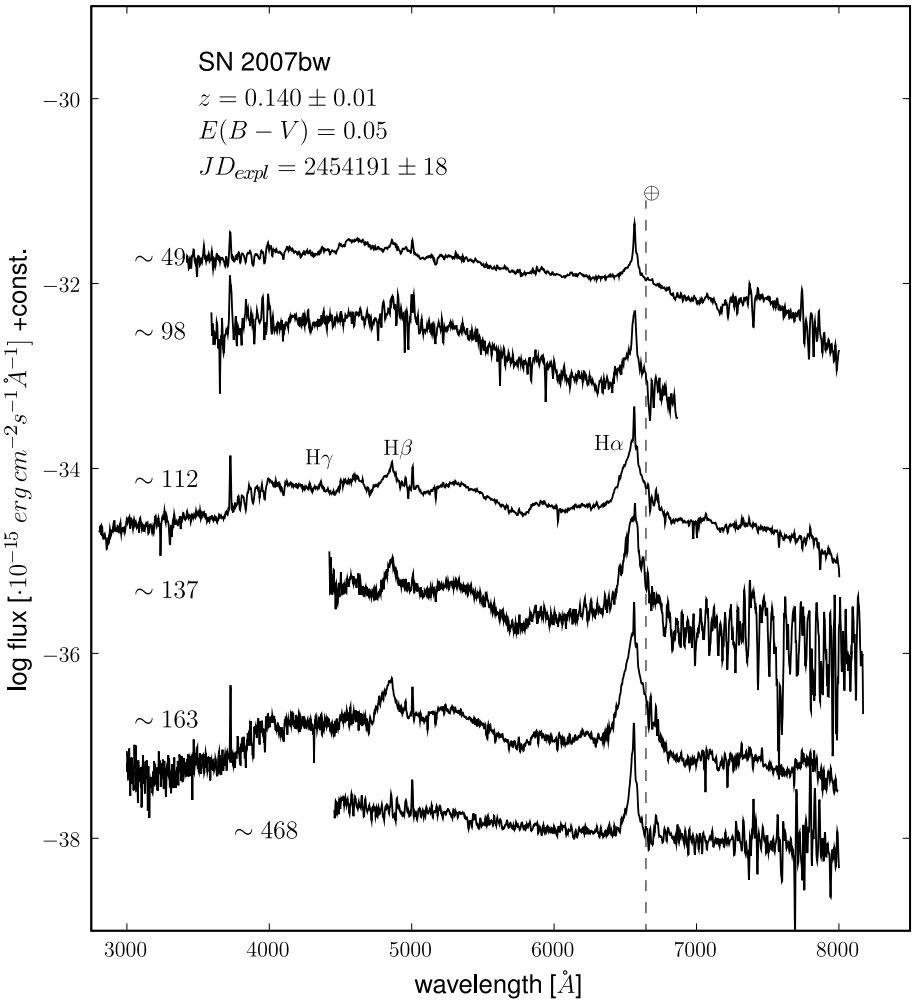

Figure 5.15— Spectroscopic evolution of SN 2007bw from day ∼49 until day∼468 since explosion, in the host galaxy rest-frame, corrected for extinction assuming E(B−V)=0.05 and normalized to the photometry. On the left side of the spectra are indicated the phases since explosion.

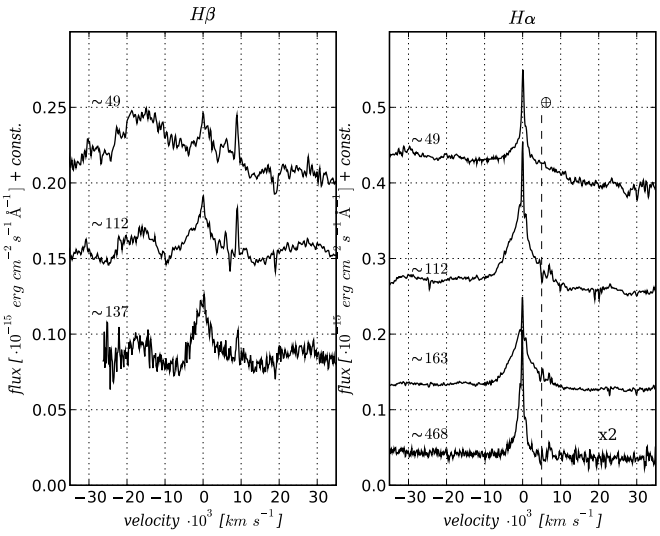

Figure 5.16— Velocity time-evolution of Hα and Hβ for SN 2007bw at four representative phases.

The narrow Hα component is unfortunately unresolved. Unlike SN 2007bt, the narrow component is not present on Hβ, and the Hα/Hβ flux-ratio is much higher at the first epochs, being $\sim$8 at day 49 and decreasing to $\sim$6 by day 112.

The black-body temperature decreases slowly as in SN 2007bt, though starting from a slightly higher value, i.e. T= 7000$\pm$300 K by day 49. Differently from SN 2007bt there is neither hint of Ca II at late times, nor evident signs of He. Lines of the Fe group are likely dominating the blue side of the spectral sequence.

A velocity at zero intensity of $\sim 12000\,\mathrm{km\,s^{-1}}$ is measured on red end of the Hα emission, showing no evident deceleration between day 49 and day 163. Interestingly, the asymmetric structure of the early line profile of Hα found for SN 2007bt is evident also in SN 2007bw: the intermediate-velocity red wing is much less intense than the blue one, but the red wing of the broadest component reaches higher velocities at zero-intensity ($\mathrm{v_{zi,red}} \sim 13000\,\mathrm{km\,s^{-1}}$) This is evident especially on day 49 (Fig. 5.18) after which the line becomes more and more symmetric with time. The spectrum on day 468 still do show this peculiarity, even though the velocity has slowed down to $\mathrm{v_{zi}} \sim 5000\,\mathrm{km\,s^{-1}}$, but given the residual of the telluric absorption it is difficult to estimate the

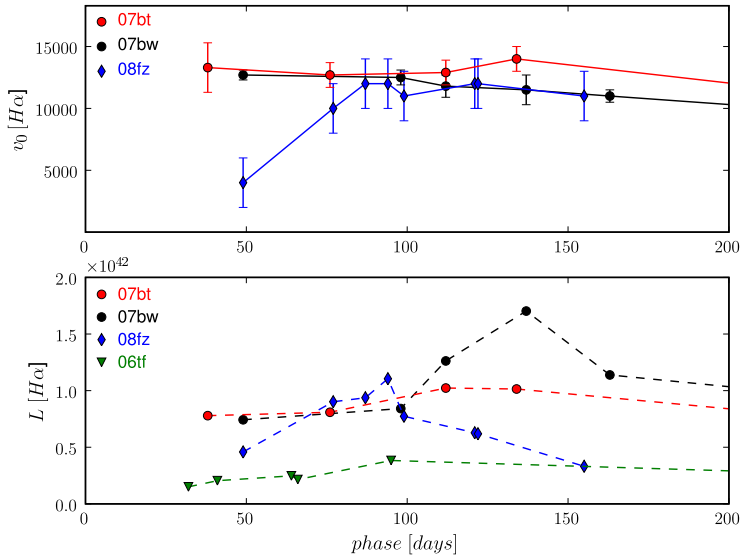

Figure 5.17— Evolution of the velocity (upper panel) and of the luminosity (lower panel) of Hα during the first ∼150 days. The velocity has been calculated at the zero intensity of the red wing of the emission line.

exact extension of the broad red wing.

5.4.3 SN 2008fz

The spectral sequence of SN 2008fz from day ∼49 until day ∼155 is shown in Fig.5.19.

Also shown is the newly-extracted and calibrated spectrum acquired by the group of Eric Hsiao on September 23rd, 2008 that was claimed to belong to type Ic SN [15]. Evidently this spectrum does not show any typical feature of a stripped-envelope SN, and it is rather consistent with the early spectra of IIn SNe, presenting a blue continuum on which a weak Hβ line emerges. This is in agreement with the description of the spectrum of Mahabal et al. [21] acquired about one week later. It is interesting to note that a featureless, blue continuum is shown also in the earliest spectrum of the VLSN 2008fz [22].

In general the spectral evolution of SN 2008fz are substantially different compared to those of the other two luminous SNe. At early times ($<$ 100 days) the spectra are characterized by a very blue continuum with a rapidly decreas-

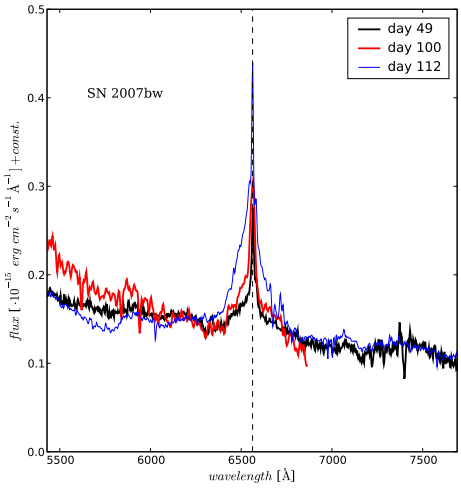

Figure 5.18— Zoom on the Hα profile, centered at λ 6562.8, at three representative phases.

ing black-body temperature, starting from $T_{BB} \sim 14000$ K on day ∼33. By day ∼49 the spectrum displays only the Balmer serie emission lines, including Hα, Hβ, Hγ and Hδ. As shown in Fig.5.20, the red wing of the Hα line extends to $v_{zi} \sim 4800\,km\,s^{-1}$ on the first epoch, reaching a nearly constant value $v_{zi} \sim 12000\,km\,s^{-1}$ in the following epochs. However, given the steepness of the continuum it is difficult to clearly isolate the profile of the line. It is interesting to note that in the spectrum by day ∼329 presented by Drake et al. [9] still does not show any significant deceleration.

The steepness of the blue continuum decreases rapidly with time and and very broad lines develop in the blue, mostly belonging to the Fe group. They could be responsible for the early blue excess, as pointed out by Immler et al. [16] for SN 2006bo. As in SN 2007bw, no hints of Ca or O are detected in the spectra. Also the Hβ line remains very intense during the second and third month, with a flux-ratio Hα/H$\beta \sim 1.5$, consistently with the ratio predicted by the H recombination. Concerning he luminosity of Hα , the lower panel of Fig. 5.17 shows that it nearly doubles its values between the first and the second epoch (day 49 and day 77), reaching SNe 2007bt and 2007bw; however, contrary to these, it also appears to decline fast after day ∼99.

For the overall spectral appearance I can also note a remarkable similar-

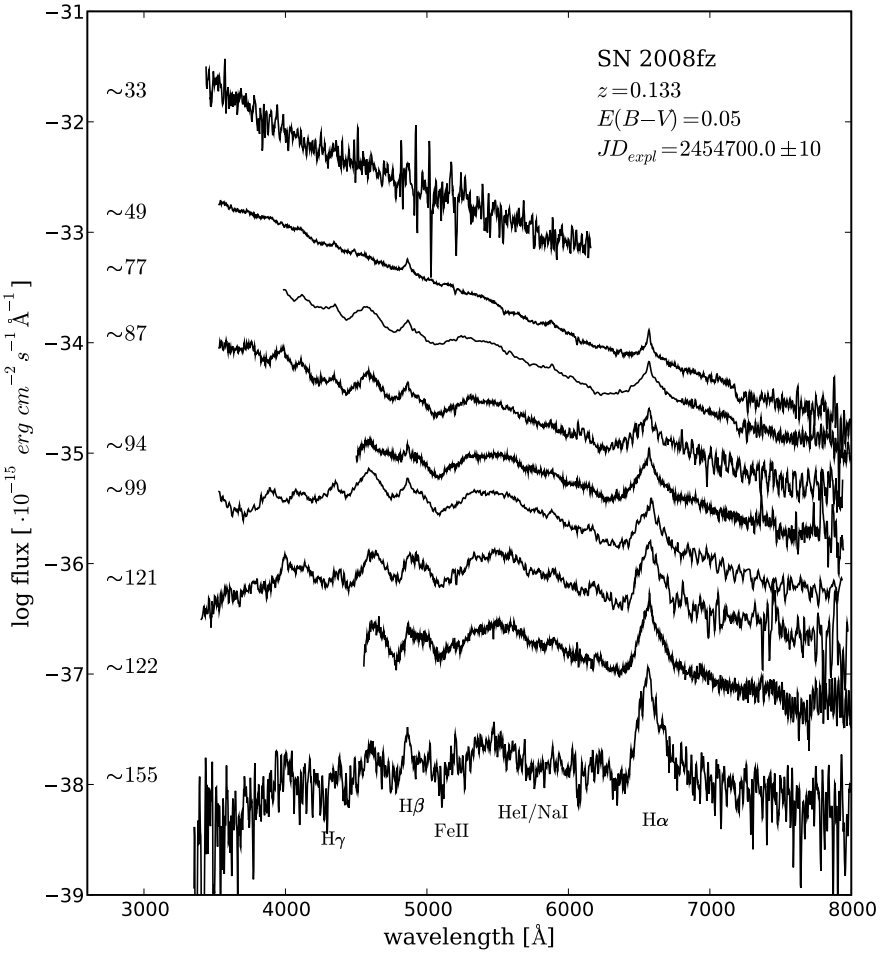

Figure 5.19— Spectroscopic evolution of SN 2008fz from ∼49 days to ∼155 days since explosion in the host galaxy rest-frame, corrected for extinction assuming E(B−V)=0.05. On the left side of the spectra the phases since explosion are indicated.

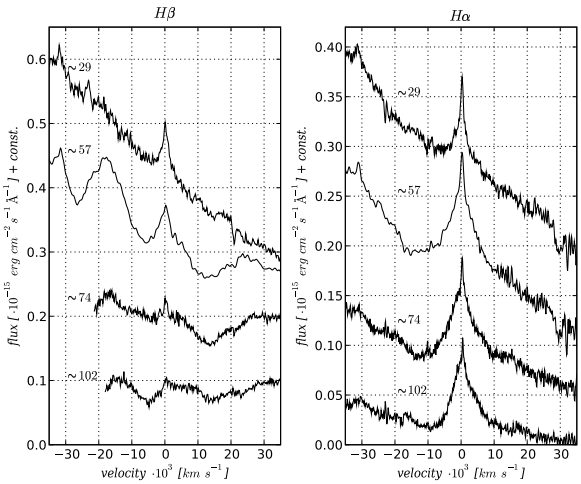

Figure 5.20— Velocity time-evolution of Hα and Hβ for SN 2008fz at some representative phases.

ity with SN 2008es (see also Fig.5.22). Though the latter was less H-rich at discovery and early phases (cf. [22]), the two events are similar in terms of the form of the continuum, the composition and strength of the emission lines. However, SN 2008fz evolved more slowly at early times, maintaining a blue continuum for a longer time. This is in accordance with the similarity found for the photometric evolution.

5.5 Discussion

I have presented a photometric and spectroscopic study of three core-collapse supernovae, that are among the most luminous supernovae ever discovered. I have highlighted analogies and differences among each other and with respect to some SNe from the sample of VLSNe from the literature.

Photometrically, I have shown that the light curves of SNe 2007bt and 2007bw are substantially different from that of SN 2008fz, evolving more slowly, being redder at the earlier phases and decaying with a rate consistent with that predicted by the radioactive decay of ^{56}Co. Interestingly, a similar luminosity decay was measured also for type IIn SN 2006tf [31] and for type Ic SN 2007bi, that was claimed to be the first pair-instability SN [13]. Also the spectral appearance of SNe 2007bt, 2007bw and 2006tf presents many common features,

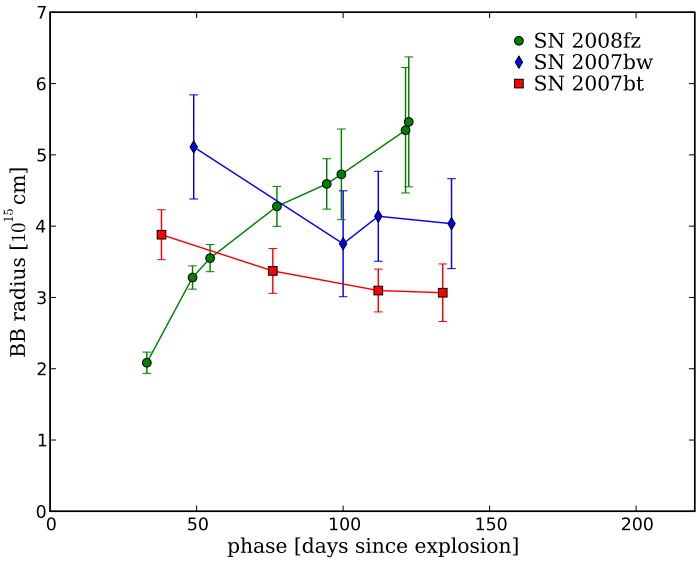

Figure 5.21— Temporal evolution of the black-body radius for the three VLSNe derived with the black-body temperature measured from the spectra.

being characterized by a slow evolution, dominated by Balmer lines.

On the other hand SN 2008fz is very similar to SN 2008es [14, 22]. Indeed the fast luminosity decrease of SN 2008fz is not typical of SNe Type IIn (as it was classified), for which the interaction with a relatively dense circumstellar medium is supposed to sustain the luminosity of the SN up to late phases, making the luminosity decay rate much slower than the radioactive ^{56}Co decay (e.g., SN 1988Z, [39], but see also events like SN 1994W, [36]). Its fast early decline is rather more reminiscent of SNe Type IIL, such as SN 1990K [6] or SN 1979C [25]. We note that among the VLSNe, also SN 2008es and the most luminous SN 2005ap can be considered Type IIL events. As it is expected from IIL SNe, the spectral evolution changes very rapidly, both in the continuum and in the emission lines, starting from high temperatures ($T \sim 12000$ K for SN 2008fz). However, SN 2008fz was classified as a IIn on the basis of the presence of a narrow line atop Hα. Though it is not resolved, it is evident that a narrow line is present on this line also at later phases, implying the presence of an undisturbed, emitting CSM around the progenitor star.

Spectroscopically the three events are characterized by high-velocity, slowly-

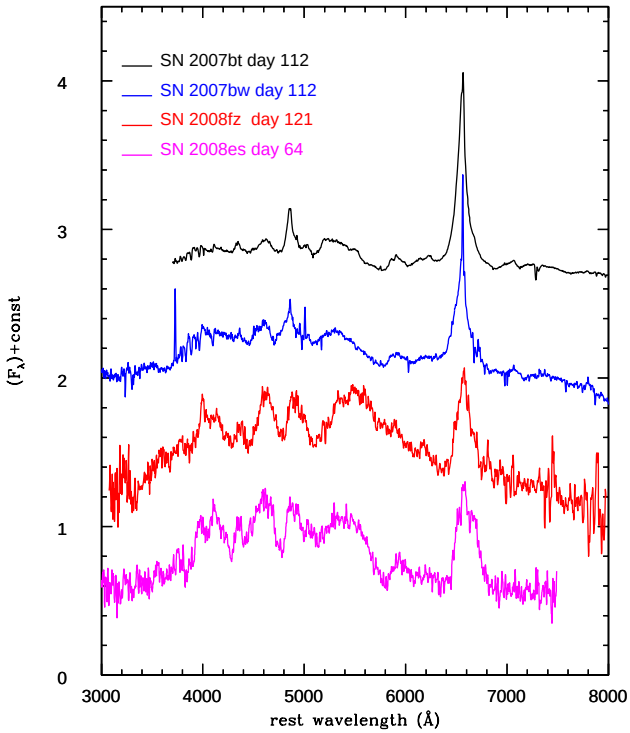

Figure 5.22— Comparison between spectra of the SNe 2007bt, 2007bw, and 2008fz at similar phases. The latest available spectrum of SN 2008es at phase ∼64 days (kindly provided by Miller et al. [22]) is also shown.

decelerating emission lines, which can be as large as $\sim 12000\,\mathrm{km\,s^{-1}}$. For SNe 2007bt and 2007bw the Balmer lines are dominating over the continuum. Moreover, both events share a common asymmetry in the profile of Hα, which slowly weakens with time. Such a complexity in the line profile was also seen in the spectra of SN 2007rt, a Type IIn SN [37]. The spectra of the latter are supposed to be at a later phase (> 100 days) than SNe 2007bt and 2007bw, but there are significant uncertainties in the estimate of the explosion epoch. Also for SN 2007rt the line profile became progressively more symmetric with time, and showed no signs of asymmetry by day 475. Trundle et al. [37] interpreted the line asymmetry in that supernova as either due to dust formation in the expanding ejecta or to the presence of an asymmetric/bipolar outflow. In SN 2008fz the Hα emission has a rather triangular profile, presenting quite broad, flat wings. It is interesting to note that these can be well-fitted by a Lorentzian profile of FWHM$\sim 7100\,\mathrm{km\,s^{-1}}$ as was done by Smith et al. (2009) [33] for the earliest spectrum of SN 2006gy, as well as by Leonard et al. [20] and Chugai [7] for SN 1998S. Such a profile was interpreted by these authors in terms of an intrinsically narrow emission line, broadened by thermal electron-scattering phenomena in an opaque shell.

In the Sections 5.2.1 and 5.2.2. I have also pointed out the uncertainties related to the age of the three SNe, which hamper our data interpretation, especially for the two slowly evolving SNe from 2007. Unfortunately, the time interval between pre-discovery and discovery is too large to put a tight constrain on the explosion epoch. As a consequence, the absolute luminosity at a given phase and the ejected ^{56}Ni quantity could have been much larger. The values for the ^{56}Ni mass that were derived in Section 6.3 are only lower limits. We note that the problem of the aging was also addressed by Smith et al. [31] for SN 2006tf.

For SN 2008fz the aging was accomplished thanks to an evident photometric and spectroscopic similarity with SNe 2008es and SN 2006gy (5.4). As previously mentioned, this can provide us a precious link on the data interpretation. For this event the hypothesis of radioactive decay sustaining the luminosity at maximum seems unlikely, given the steep decaying light curve. A much lower quantity, in the order of 1 $\mathrm{M_\odot}$ would be required to explain the late-times data, excluding the presence of dust formation absorbing the optical emission. In general, the emission of the internal energy which is produced by the shock in a typical core-collapse SN produce a maximum luminosity which lower than that of SN 2008fz by a factor 2. Therefore, *the only plausible way to explain the brightness of the peak of SN 2008fz is to admit the presence of interaction phenomena.*

On this issue the early evolution of the black-body radius can be helpful. In

Fig. 5.21 we show the evolution of the black-body radius in the first ∼5 months for the three discussed supernovae. As expected, in all cases the high luminosity and the evolution of the black body temperature derived from the spectra favor a scenario with an initial radius $R_0 > 10^{15}$cm, i.e. much larger than a standard RSG radius. Interestingly, the black-body radius of SN 2008fz seems to be increasing up rapidly, contrary to SNe 2007bt and 2007bw. A qualitatively and quantitatively similar evolution has been derived also by Gezari et al. [14] for SN 2008es. Given the extremely large values, it is natural to consider such radii as the radii of an unbound, emitting shell of dense CSM rather than those of the ejecta. We can also assume that the shell is moving fast, at about $\sim 12000\,\mathrm{km\,s^{-1}}$, as the highest velocity derived from the spectra. This is possible if we admit that *(i)* the shell has been efficiently accelerated, likely by the impact of a SN ejecta; *(ii)* the mass of the shell was not extremely high. Indeed, both the spectral appearance, the velocity and radius evolution and the derived light curve are consistent with this hypothesis; a further confirm is represented by the evident spectroscopic similarity between SN 2006gy and SN 2008fz, as pointed out by Drake et al. [9]. In fact, we expect the shell to emit thanks to the conversion of kinetic energy into radiation produced after the collision by an energetic SN ejecta, just as it was supposed for SN 2006gy.

Soon after the collision, the shell is efficiently warmed up and accelerated by the high-velocity SN ejecta. Given the moderately small mass, the shell is brought to high temperatures - higher than in SN 2006gy - and the H is completely ionized. The spectrum is therefore a blue, featureless continuum. This is consistent with the early spectrum of SN 2008es [22]. As soon as the temperature decreases the H in the shell starts to recombine, so that the Balmer lines appear. Also, the shell suffers an acceleration by the ejecta, and by day ∼49 it moves at $\sim 4300\,\mathrm{km\,s^{-1}}$. At this phase the spectrum of SN 2008fz clearly resembles that of SN 2006gy, which also illustrates a scenario in which a shell has just been hit by an energetic SN ejecta (cf. Chapter 4). With time the velocity of the shell increases until it reaches a nearly constant value $v\sim 12000\,\mathrm{km\,s^{-1}}$. Given the yet high opacity of the shell, the SN core with the heavier elements are obscured. Besides the Balmer lines, only the easily-ionized Fe lines are formed. Because of the relatively small mass in the shell, the photon diffusion time is smaller than that calculated for SN 2006gy, and the radiated energy plummets rapidly, before recombination takes place. At late times (day ∼329) the velocity at zero intensity of the Hα emission line is still comparable to the early phases (spectrum by Drake et al. 2009 [9]). However, no other emission is present. This may indicate that the SN is interacting with a dense, H-rich CSM, which obscures the emission by other lines.

For a shell of mass M_{shell}, radius $R \sim 2 \times 10^{15}$cm, thickness ΔR, and op-

tical depth τ, the maximum light will occur when the diffusion time, $t_{diff} \sim 3\Delta R\tau/c$, is comparable to the dynamical time, $t_{dyn} \sim \Delta R/v$. This gives the optical depth at maximum light, $\tau_{max} \sim c/3v_{ph} \sim 8.3$, neglecting any differences between the photospheric velocity and the mean ejecta velocity. Since $M_{sh} \sim 4\pi R^2\tau_{max}/k$, the mass of the shell would be about 0.5 $M_\odot$, with $k = 0.4$ absorption coefficient for the electron scattering. The peak luminosity would be $L \sim M_{shell}v^2_{phot}/t_{max} \sim 3.5 \times 10^{44}$erg for $t_{max} \sim 4.3 \times 10^6$s, with t_{max} the time of maximum luminosity, i.e. 4.3×10^6s. The result is roughly consistent with the observations.

Note that, in our opinion, a fundamental difference with SN 2006gy lies in the interpretation of the high-velocity features in the spectra. Also for SN 2006gy we detected constant, broad lines at FWHM $\sim 9000\,km\,s^{-1}$. However, as discussed in the previous chapter, such velocities have to be attributed to the SN ejecta, which are not obscured by the massive clumps around the exploding star. This allows us to interpret the long, rising branch of the light curve of SN 2006gy as the expansion of a compact progenitor. Instead, in the case of SN 2008fz the spectroscopic fast-velocity lines are attributed to the shell which can be promptly accelerated given its modest mass. The ejecta are obscured because they lie behind the clumps; for this reason we can never detect the emission produced by the intermediate elements. Moreover, an evident, isolated broad component of the Hα emission line is never observed in SN 2008fz, as it is instead, in SN 2006gy.

A very similar scenario has been proposed also by Miller et al. [22] for SN 2008es and by Quimby et al. [27] for SN 2005ap even, if the latter did not detect any narrow lines in the spectra as a proof for the high-velocity CSM surrounding the star. Miller et al. (2009) calculate that a shocked-shell with a mass in the order of 5 $M_\odot$ can account for the SN luminosity. This is roughly consistent with what was found for SN 2008fz.

Instead, Gezari et al. [14] favor for SN 2008es the model of Blinnikov & Bartunov [4] for linear decaying supernovae, which predicts that a RSG star with an extended structure ($\sim 6000\,R_\odot$), a small H mass and a dense superwind (up to $10^{-3}M_\odot\,yr^{-1}$) can reproduce a linearly decaying light curve with a peak up to -22. However, this model fails to explain the derived expansion of the black-body radius, as well as the presence of high-velocity emission lines.

For the SNe 2007bt and 2007bw the data interpretation is complicated by the uncertainty on the SN age. In Figure 5.22 we compare the spectra of SNe 2007bt, 2007bw, 2008es and 2008fz at a similar phase. This comparison shows that, though with a different apparent intensity in the Hα , these SNe present some features in common, like the form of the continuum, the velocity of the

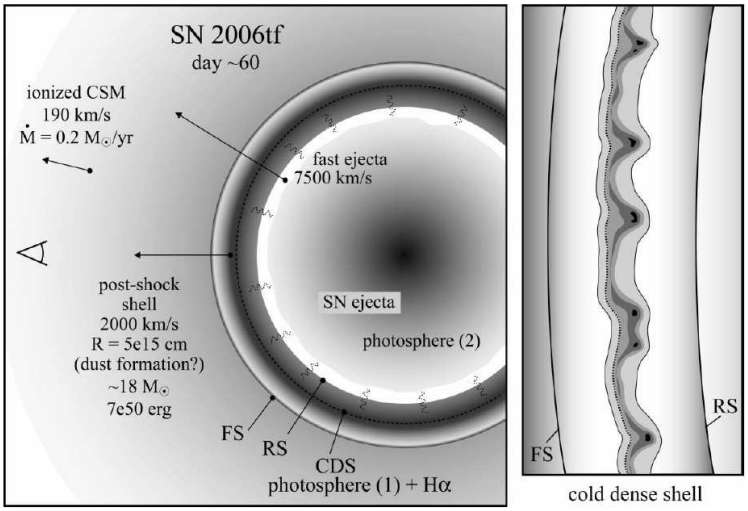

Figure 5.23— Illustration of the components of SN 2006tf at about 60 days after discovery, during the decline from the main light-curve peak (Figure from [31]). The primary feature is the massive post-shock shell of gas, composed of the swept-up opaque pre-SN envelope around the star ejected in the decade before core collapse. Most of the mass is in the cold dense shell (CDS), bounded by the forward shock (FS) and the reverse shock (RS). This shell expands at constant speed into the preshock CSM. The interior of the shell is filled by freely expanding SN ejecta. A second photosphere, marked with "2", is in the SN ejecta; it is fainter than the main photosphere and can only be seen if the main shell thins or develops clumps as time proceeds

Hα line and the emissions in the blue. This may hint to a similar kinematic and composition of the expanding layers. These similarities may indicate that also the two 2007 SNe may have an origin similar to SN 2008fz. On the other hand, we have to remind that their luminosity remains higher than SN 2008fz for a longer time; furthermore, spectroscopically they nearly show any other emission lines besides the Balmer lines, even at ∼160 days, when SN 2008fz and SN 2006gy did show the presence of broad lines in the bluer part of the spectra, mainly attributed to Fe and Sc [32].

Excluding for a moment the role of the ejected ^{56}Ni for these two SNe, we can invoke a similar luminosity powering mechanism as in SN 2008fz, e.g., an emission by a shocked shell, reviewing some aspects. In the case of SN 2007bt and 2007bw we expect that the mass of the shocked shell is higher than in SN 2008fz and in SN 2006gy because of slower luminosity decline. Indeed, with the model proposed by Smith & Mc Cray [35], Smith et al. [31] explain the

data of SN 2006tf assuming an ejecta-interaction with a H-rich, clumpy shell of about 18 $M_{\odot}$ of H, ejected 4-8 years before the explosion. The shell is supposed to be moving at $\sim 2000\,\mathrm{km\,s^{-1}}$, as the velocity inferred from the intermediate component of the Hα line. The high velocity features at FWHM $\sim 7500\,\mathrm{km\,s^{-1}}$ are supposed to originate in the SN ejecta behind the shell that have been not reached by the reverse shock, and that are visible to us through the clumps that compose the shell (Fig.6.1). The clumps also allow a gradual radiation emission leakage, so that the SN shock exits the shell into a less dense medium with a certain distribution of timescales.

Given the photometric and spectroscopic strong similarities that we have highlighted in Section 5.3, 5.4.1 and 5.4.2, this scenario could explain reasonably well the observational data of the SNe 2007bt and 2007bw. However, the stressed asymmetry in the early profile of Hα (Fig.5.18) lead us to favor an *asymmetric distribution* of the CSM, not covering the whole SN solid angle, but likely only half of it. In Fig. 5.24 we show a geometric configuration of the SN+CSM which could possibly explain the peculiar line profile. Most of the CSM is located in a massive , clumpy CSM which lies directly on the line of sight of the observer. After the SN explosion, the CSM is reached by the SN ejecta and, after a photon-diffusion time-scale it starts to emit. Contrary to SN 2008fz, for the SN 2007bt and 2007bw the massive CSM is not set into a high-velocity motion because of its much larger mass. Moreover, since the CSM is clumpy, at early times the observer can detect both the emission caused by the approaching shell and by the underlying approaching ejecta, which have been decelerated by the impact on the massive CSM. These 2 components are seen in the intermediate and large component on the blue wing of the Hα line. On the contrary, in our scenario the ejecta which are *receding* from the observer have not been efficiently decelerated, likely because the CSM in that region is less dense. This produces a broad emission on the red wing of the Hα line, which is broader than that on the blue wing. Instead, the emission produced by the receding shocked region at early times is not detected by the observer. This is probably to be attributed to the high opacity of the intra-clumpy medium which lies in front of him; only when the latter expands and becomes more rarified the emission produced by the receding shocked region starts to be visible. The decrement of the Hα measured for the late times spectra could be explained in terms of a deceleration of the slow expanding CSM, as a result of a strong increase of swept-up CSM mass during the expansion. Moreover, the absence of other strong emission lines besides the Balmer lines in the spectra could be prevented by the high opacity of the intra-clumps region.

Note that, though it may initially appear "ad-hoc", the configuration with a massive ejection only on one side of the SN could be more than reasonable

if we consider the effect of binarity in massive stars, that ware introduced in Chapter 2, Sec.2.5. In fact, the massive clump could result from the mass-loss on the SN-progenitor induced by a companion star, or it could be directly shed by the companion star itself. In the latter case we do expect that from a certain view angle the observer could detect the SN emission throughout the CSM of the companion.

Of course, the luminosity Co-like decay observed for the three slow evolving SNe 2006tf, 2007bt and 2007bw is highly remarkable. For this reason we can not exclude that these events are mainly powered by the radioactive decay. Interestingly, for a very large ejected ^{56}Ni quantity (e.g., $> 10\,M_{\odot}$) it may be possible that the ejecta are at least in part ionized by radioactive heating and that they would then be opaque even in the optical bands at late phases. In fact, for a very extended star the dynamical time would be larger than the decay time of Co, which, in turn, would make the radioactive decay the dominant process, determining the shape of the light curve. This could explain the absence of emission by any other element besides H in the spectra. Moreover, the continuum observed in the spectrum at phase ∼38 days of SN 2007bt would be interpreted as a consequence of a phase of recombination of the ejecta.

However, to produce >10 $M_{\odot}$ of ^{56}Ni we had to require a non-standard explosion mechanism, as the explosion via pair-production. Such an explosion is predicted to produce a short luminosity peak, followed by a Co-like decay [29], as it is observed in SN 2007bi by Gal-Yam et al (2009) [13] and by Young et al. (2009) [42]. The fact that we did not observe any peak in the light curves of the SNe 2007bt, 2007bw and 2006tf may simply mean that we have observed them too late.

5.6 Conclusions

Though some uncertainty still exists, we have explained the observational data of the three VLSNe in terms of a scenario which presents some analogies to that proposed for SN 2006gy (being supported by a spectroscopic match, cf. Fig.5.4). It is based on the conversion of kinetic energy into radiation inside an opaque CSM, which is reached by an energetic SN shock. The emission mechanism is therefore photon diffusion in a massive CSM, rather than optically thin emission in a standard ejecta-CSM interaction. In fact, narrow lines are nearly (always) present (cf. SN 2008es). The emission originates in an over-heated, accelerated shell whose main component, H, is initially ionized. The emission time-scale follows the photon diffusion time-scale, which increases proportionally to the mass of the shell. The (clumpy) structure and the geometric configuration of

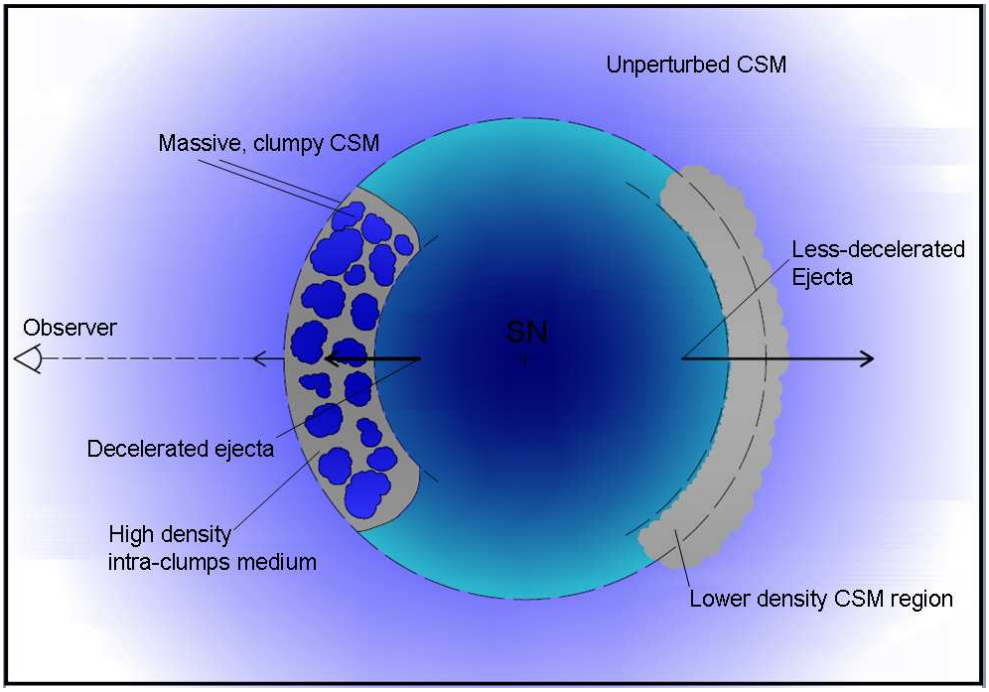

Figure 5.24— Schematic cartoon of the SN+CSM configuration which may explain the asymmetry of the profile of Hα identified in the early spectra of SNe 2007bt and 2007bw: an intermediate component on the blue wing which has no counterpart on the red side, and a blue broad component which is *less broad* than its counterpart on the red side. In this scenario, a massive, clumpy medium is located on the line of sight of the observer. This is responsible for the decelerations of the approaching ejecta; the observer can detect the ejecta because the medium is clumpy. On the contrary the receding ejecta, which are still well detectable, are not (or to a less extent) decelerated, likely because they encounter a less dense medium (the black arrows denote the *vectors* of the velocity). At early phases the approaching emission by the shocked CSM is well visible; instead, the high opacity of the massive CSM prevents the detection of the photons emitted by the shocked, lower density CSM, which are receding from the observer. However, with the expansion and rarefaction of the CSM this effect decreases and the Hα line becomes more and more symmetric.

the CSM have turned out to be important parameters, which we have linked to the spectral composition of the ejecta and to the lines' profiles.

Concerning the progenitor, we have some arguments to claim that the explosions of SNe 2007bt, 2007bw and 2008fz must originate from massive stars, which likely experience strong mass-loss before they explode. These arguments include: *(i)* the fast CSM-wind derived for SN 2007bt (Section 5.4.1); *(ii)* the energetic of these events, much higher than that of a standard SN values. In the massive star+shell, one further argument regards the energy which has to be transferred to the SN ejecta to be able to accelerate a massive, compact CSM to $\sim$12000 km s^{-1} .

Indeed, a luminous stellar outburst because of ejecta+opaque shell impact may originate in many different ways from the late time evolution of massive stars [32, 41, 43]. A discussion about the possible progenitors of VLSNe will be addressed in the next Chapter.

Bibliography

[1] I. Agnoletto, S. Benetti, E. Cappellaro, L. Zampieri, M. Turatto, P. Mazzali, A. Pastorello, M. D. Valle, F. Bufano, A. Harutyunyan, H. Navasardyan, N. Elias-Rosa, S. Taubenberger, S. Spiro, and S. Valenti. SN 2006gy: Was it Really Extraordinary? *Apj*, 691:1348–1359, February 2009.

[2] P. Antilogus, J. Li, R. Pain, R. Pereira, C. Wu, C. Buton, Y. Copin, E. Gangler, G. Smadja, G. Aldering, C. Aragon, S. Bailey, S. Bongard, M. Childress, S. Loken, P. Nugent, S. Perlmutter, K. Runge, R. C. Thomas, B. A. Weaver, E. Pecontal, G. Rigaudier, R. Kessler, C. Baltay, A. Bauer, N. Ellman, D. Herrera, D. Rabinowitz, and R. Scalzo. Supernovae 2007bo-2007bz. *Central Bureau Electronic Telegrams*, 941:1–+, April 2007.

[3] S. Benetti, A. Harutyunyan, I. Agnoletto, S. Valenti, A. Pastorello, and V. Lorenzi. Supernova 2008fz. *Central Bureau Electronic Telegrams*, 1533:1–+, October 2008.

[4] S. I. Blinnikov and O. S. Bartunov. Non-Equilibrium Radiative Transfer in Supernova Theory - Models of Linear Type-II Supernovae. *Aap*, 273:106–+, June 1993.

[5] S. Blondin, J. L. Prieto, F. Patat, P. Challis, M. Hicken, R. P. Kirshner, T. Matheson, and M. Modjaz. A Second Case of Variable NaI D Lines in a Highly Reddened Type Ia Supernova. *Apj*, 693:207–215, March 2009.

[6] E. Cappellaro, I. J. Danziger, M. della Valle, C. Gouiffes, and M. Turatto. The bright linear type II SN 1990K. *Aap*, 293:723–732, January 1995.

[7] N. N. Chugai, S. I. Blinnikov, A. Fassia, P. Lundqvist, W. P. S. Meikle, and E. I. Sorokina. The origin of the high-velocity circumstellar gas around SN 1998S. *Mnras*, 330:473–480, February 2002.

[8] A. J. Drake, S. G. Djorgovski, A. Mahabal, M. J. Graham, R. Williams, E. C. Beshore, S. M. Larson, R. Hill, and E. Christensen. Supernova 2008fz. *Central Bureau Electronic Telegrams*, 1524:1–+, October 2008.

[9] A. J. Drake, S. G. Djorgovski, J. L. Prieto, A. Mahabal, D. Balam, R. Williams, M. J. Graham, M. Catelan, E. Beshore, and S. Larson. Discovery of the Extremely Energetic Supernova 2008fz. *ArXiv e-prints*, August 2009.

[10] N. Elias-Rosa, S. Benetti, M. Turatto, E. Cappellaro, S. Valenti, A. A. Arkharov, J. E. Beckman, A. di Paola, M. Dolci, A. V. Filippenko, R. J. Foley, K. Krisciunas, V. M. Larionov, W. Li, W. P. S. Meikle, A. Pastorello, G. Valentini, and W. Hillebrandt. SN 2002cv: a heavily obscured Type Ia supernova. *Mnras*, 384:107–122, February 2008.

[11] R. A. Fesen and D. M. Matonick. The optical recovery of SN 1979C in NGC 4321 (M100). *Apj*, 407:110–114, April 1993.

[12] W. L. Freedman, B. F. Madore, B. K. Gibson, L. Ferrarese, D. D. Kelson, S. Sakai, J. R. Mould, R. C. Kennicutt, Jr., H. C. Ford, J. A. Graham, J. P. Huchra, S. M. G. Hughes, G. D. Illingworth, L. M. Macri, and P. B. Stetson. Final Results from the Hubble Space Telescope Key Project to Measure the Hubble Constant. *Apj*, 553:47–72, May 2001.

[13] A. Gal-Yam, P. Mazzali, E. O. Ofek, P. E. Nugent, S. R. Kulkarni, M. M. Kasliwal, R. M. Quimby, A. V. Filippenko, S. B. Cenko, R. Chornock, R. Waldman, D. Kasen, M. Sullivan, E. C. Beshore, A. J. Drake, R. C. Thomas, J. S. Bloom, D. Poznanski, A. A. Miller, R. J. Foley, J. M. Silverman, I. Arcavi, R. S. Ellis, and J. Deng. Supernova 2007bi as a pair-instability explosion. *Nature*, 462:624–627, December 2009.

[14] S. Gezari, J. P. Halpern, D. Grupe, F. Yuan, R. Quimby, T. McKay, D. Chamarro, M. D. Sisson, C. Akerlof, J. C. Wheeler, P. J. Brown, S. B. Cenko, A. Rau, J. O. Djordjevic, and D. M. Terndrup. Discovery of the Ultra-Bright Type II-L Supernova 2008es. *Apj*, 690:1313–1321, January 2009.

[15] E. Y. Hsiao, M. L. Graham, C. J. Pritchet, and D. Balam. Supernova 2008fz. *Central Bureau Electronic Telegrams*, 1524:2–+, October 2008.

[16] S. Immler, P. J. Brown, P. Milne, L. Dessart, P. A. Mazzali, W. Landsman, N. Gehrels, R. Petre, D. N. Burrows, J. A. Nousek, R. A. Chevalier, C. L. Williams, M. Koss, C. J. Stockdale, M. T. Kelley, K. W. Weiler, S. T. Holland, E. Pian, P. W. A. Roming, D. Pooley, K. Nomoto, J. Greiner, S. Campana, and A. M. Soderberg. X-Ray, UV, and Optical Observations of Supernova 2006bp with Swift: Detection of Early X-Ray Emission. *Apj*, 664:435–442, July 2007.

[17] D. Kasen and L. Bildsten. Supernova Light Curves Powered by Young Magnetars. *ArXiv e-prints*, November 2009.

[18] K. S. Kawabata, M. Tanaka, K. Maeda, T. Hattori, K. Nomoto, N. Tominaga, and M. Yamanaka. Extremely Luminous Supernova 2006gy at Late Phase: Detection of Optical Emission from Supernova. *Apj*, 697:747–757, May 2009.

[19] A. U. Landolt. Broadband UBVRI photometry of the Baldwin-Stone Southern Hemisphere spectrophotometric standards. *Aj*, 104:372–376, July 1992.

[20] D. C. Leonard, A. V. Filippenko, A. J. Barth, and T. Matheson. Evidence for Asphericity in the Type IIN Supernova SN 1998S. *Apj*, 536:239–254, June 2000.

[21] A. Mahabal, A. J. Drake, S. G. Djorgovski, M. Catelan, M. J. Graham, E. Glikman, C. Donalek, R. Williams, E. C. Beshore, S. M. Larson, E. Christensen, C. Baltay, D. Rabinowitz, R. Scalzo, and PQ Team. Discovery and Confirmation of Supernovae from PQ and CRTS. *The Astronomer's Telegram*, 1778:1–+, October 2008.

[22] A. A. Miller, R. Chornock, D. A. Perley, M. Ganeshalingam, W. Li, N. R. Butler, J. S. Bloom, N. Smith, M. Modjaz, D. Poznanski, A. V. Filippenko, C. V. Griffith, J. H. Shiode, and J. M. Silverman. The Exceptionally Luminous Type II-Linear Supernova 2008es. *Apj*, 690:1303–1312, January 2009.

[23] A. A. Miller, N. Smith, W. Li, J. S. Bloom, R. Chornock, A. V. Filippenko, and J. X. Prochaska. New Observations of the Very Luminous Supernova 2006gy: Evidence for Echoes. *ArXiv e-prints*, June 2009.

[24] D. E. Osterbrock and N. G. Bochkarev. Book-Review - Astrophysics of Gaseous Nebulae and Active Galactic Nuclei. *Soviet Astronomy*, 33:694–+, November 1989.

[25] N. Panagia, G. Vettolani, A. Boksenberg, F. Ciatti, S. Ortolani, P. Rafanelli, L. Rosino, C. Gordon, D. Reimers, K. Hempe, P. Benvenuti, J. Clavel, A. Heck, M. V. Penston, F. Macchetto, D. J. Stickland, J. Bergeron, M. Tarenghi, B. Marano, G. G. C. Palumbo, A. N. Parmar, G. S. W. Pollard, P. W. Sanford, W. L. W. Sargent, R. A. Sramek, K. W. Weiler, and P. Matzik. Coordinated optical, ultraviolet, radio and X-ray observations of supernova 1979c in M 100. *Mnras*, 192:861–879, September 1980.

[26] J. L. Prieto, P. M. Garnavich, M. M. Phillips, D. L. DePoy, J. Parrent, D. Pooley, V. V. Dwarkadas, E. Baron, B. Bassett, A. Becker, D. Cinabro, F. DeJongh, B. Dilday, M. Doi, J. A. Frieman, C. J. Hogan, J. Holtzman, S. Jha, R. Kessler, K. Konishi, H. Lampeitl, J. Marriner, J. L. Marshall, G. Miknaitis, R. C. Nichol, A. G. Riess, M. W. Richmond, R. Romani, M. Sako, D. P. Schneider, M. Smith, N. Takanashi, K. Tokita, K. van der Heyden, N. Yasuda, C. Zheng, J. C. Wheeler, J. Barentine, J. Dembicky, J. Eastman, S. Frank, W. Ketzeback, R. J. McMillan, N. Morrell, G. Folatelli, C. Contreras, C. R. Burns, W. L. Freedman, S. Gonzalez, M. Hamuy, W. Krzeminski, B. F. Madore, D. Murphy, S. E. Persson, M. Roth, and N. B. Suntzeff. A Study of the Type Ia/IIn Supernova 2005gj from X-ray to the Infrared: Paper I. *ArXiv e-prints*, June 2007.

[27] R. M. Quimby, G. Aldering, J. C. Wheeler, P. Höflich, C. W. Akerlof, and E. S. Rykoff. SN 2005ap: A Most Brilliant Explosion. *Apjl*, 668:L99–L102, October 2007.

[28] R. M. Quimby, S. R. Kulkarni, M. M. Kasliwal, A. Gal-Yam, I. Arcavi, M. Sullivan, P. Nugent, R. Thomas, D. A. Howell, L. Bildsten, J. S. Bloom, C. Theissen, N. Law, R. Dekany, G. Rahmer, D. Hale, R. Smith, E. O. Ofek, J. Zolkower, V. Velur, R. Walters, J. Henning, K. Bui, D. McKenna, D. Poznanski, S. B. Cenko, and D. Levitan. Mysterious transients unmasked as the bright blue death throes of massive stars. *ArXiv e-prints*, September 2009.

[29] E. Scannapieco, P. Madau, S. Woosley, A. Heger, and A. Ferrara. The Detectability of Pair-Production Supernovae at z = 6. *Apj*, 633:1031–1041, November 2005.

[30] D. J. Schlegel, D. P. Finkbeiner, and M. Davis. Maps of Dust Infrared Emission for Use in Estimation of Reddening and Cosmic Microwave Background Radiation Foregrounds. *Apj*, 500:525–+, June 1998.

[31] N. Smith, R. Chornock, W. Li, M. Ganeshalingam, J. M. Silverman, R. J. Foley, A. V. Filippenko, and A. J. Barth. SN 2006tf: Precursor Eruptions and the Optically Thick Regime of Extremely Luminous Type IIn Supernovae. *Apj*, 686:467–484, October 2008.

[32] N. Smith, R. Chornock, J. M. Silverman, A. V. Filippenko, and R. J. Foley. Spectral Evolution of the Extraordinary Type IIn Supernova 2006gy. *ArXiv e-prints*, June 2009.

[33] N. Smith, R. J. Foley, J. S. Bloom, W. Li, A. V. Filippenko, R. Gavazzi, A. Ghez, Q. Konopacky, M. A. Malkan, P. J. Marshall, D. Pooley, T. Treu, and J.-H. Woo. Late-Time Observations of SN 2006gy: Still Going Strong. *Apj*, 686:485–491, October 2008.

[34] N. Smith, W. Li, R. J. Foley, J. C. Wheeler, D. Pooley, R. Chornock, A. V. Filippenko, J. M. Silverman, R. Quimby, J. S. Bloom, and C. Hansen. SN 2006gy: Discovery of the Most Luminous Supernova Ever Recorded, Powered by the Death of an Extremely Massive Star like η Carinae. *Apj*, 666:1116–1128, September 2007.

[35] N. Smith and R. McCray. Shell-shocked Diffusion Model for the Light Curve of SN 2006gy. *Apjl*, 671:L17–L20, December 2007.

[36] J. Sollerman, R. J. Cumming, and P. Lundqvist. A Very Low Mass of 56Ni in the Ejecta of SN 1994W. *Apj*, 493:933–+, January 1998.

[37] C. Trundle, A. Pastorello, S. Benetti, R. Kotak, S. Valenti, I. Agnoletto, F. Bufano, M. Dolci, N. Elias-Rosa, T. Greiner, D. Hunter, F. P. Keenan, V. Lorenzi, K. Maguire, and S. Taubenberger. Possible evidence of asymmetry in SN 2007rt, a type IIn supernova. *Aap*, 504:945–958, September 2009.

[38] M. Turatto, S. Benetti, and E. Cappellaro. Variety in Supernovae. In W. Hillebrandt & B. Leibundgut, editor, *From Twilight to Highlight: The Physics of Supernovae*, pages 200–+, 2003.

[39] M. Turatto, E. Cappellaro, I. J. Danziger, S. Benetti, C. Gouiffes, and M. della Valle. The Type II supernova 1988Z in MCG + 03-28-022 - Increasing evidence of interaction of supernova ejecta with a circumstellar wind. *Mnras*, 262:128–140, May 1993.

[40] S. E. Woosley. Bright Supernovae from Magnetar Birth. *ArXiv e-prints*, November 2009.

[41] S. E. Woosley, S. Blinnikov, and A. Heger. Pulsational pair instability as an explanation for the most luminous supernovae. *Nature*, 450:390–392, November 2007.

[42] D. R. Young, S. J. Smartt, S. Valenti, A. Pastorello, S. Benetti, C. R. Benn, D. Bersier, M. T. Botticella, R. L. M. Corradi, A. H. Harutyunyan, M. Hrudkova, I. Hunter, S. Mattila, E. J. W. de Mooij, H. Navasardyan, I. A. G. Snellen, N. R. Tanvir, and L. Zampieri. Two Type Ic supernovae in low-metallicity, dwarf galaxies: diversity of explosions. *ArXiv e-prints*, October 2009.

[43] T. R. Young, D. Smith, and T. A. Johnson. An Optical Afterglow Model for Bright Linear Type II Supernovae. *Apjl*, 625:L87–L90, June 2005.

CHAPTER 6

Conclusions

In this last Chapter I will extend the discussion to the whole sample of known VLSNe. I will first discuss their general properties; secondly I will review the feautures characterizing every single object and summarize the evolution scenario that was proposed for it by the different authors. Finally I will present the hypothesis that were suggested to explain the nature of VLSNe, discussing which aspects are more/less likely. In the last Section I will draw the conclusions.

6.1 General properties of VLSNe

As mentioned in the previous Chapter, the number of detections of SN events with exceptional high luminosity at maximum has remarkably increased in the last 4 years. A complete, current list of known VLSNe is reported in Table 6.1. The most frequent SN type is evidently IIn and Ic; however, included in the list are also the transients discovered by the PTF (Palomar Transient Factory) whose SN type has not been clarified yet. Also a number of very recent objects with high brightness at discovery or at maximum[1], for which no detailed study yet exists, can be treated as VLSNe and have been also included in the list.

By looking at the general properties listed in the Table, some interesting features emerge.

[1]The light curves of the transients discovered by the Catalina Transient Survey are public and accessible online at http://nesssi.cacr.caltech.edu/catalina/AllSN.html.

First, as found for SNe 2007bt and 2007bw (cf. Chapter 5), the VLSNe *apparently do not suffer of internal extinction.* An exception is SN 2006gy which, instead, is highly reddened, being E(B-V)∼0.55 (or even E(B-V)∼0.75 from the comparison with SN 2008fz). On this issue, in order to homogenize the sample Drake et al. [13] suggested the possibility that SN 2006gy may have originated in an orbiting, low-metalicity dwarf galaxy lying *behind* NGC 1260. This would make the absolute luminosity of SN 2006gy even higher.

Secondly, VLSNe *are mostly discovered in low-luminosity galaxies.* This could be partially due to a selection effect of the SN searches, which are more efficient at discovering supernovae that are more luminous than their hosts; therefore, the detection is biased toward the brightest SNe and SNe in very faint galaxies.

Concerning their environment, for many cases the relatively high distance of VLSNe has prevented to derive constraints on the the host-galaxy morphology and characterization. For the PTF transients and for SN 2008fz the host-galaxy has been not even detected.

However, on the basis of the available information it could be claimed that the explosion sites of VLSNe are preferably *irregular* or *dwarf* galaxies. This is interesting as such low-mass galaxies tend to have *low metallicity* [17, 50] which may lead to more massive envelopes at the time of explosion, and are also the preferred environment in which hypernovae are found [18, 25, 43].

6.2 Discovery, rate & future of the VLSNe

The relatively high number of detections in the last 4-5 years naturally raises the questions "*Why did the number of VLSNe suddenly increased*", and "*How have these events gone undetected until now*?"

To answer these questions we must account for the different strategies and aims with which past surveys have observed the sky. Past surveys have been mainly concentrated on areas of tens to hundreds of square degrees and have typically searched for *specific types* of astronomical transients such as microlensing (MACHO, [3]; OGLE, [52]; EROS, [6]), gamma-ray burst afterglows (ROTSE, [2]), and SNe (LOSS & SDSS for type Ia SNe). Deep surveys for variability have been carried out over *small areas* (< 25 deg^2) by the Subaru/XMM-Newton Deep Survey (SXDS, [36]), the Deep Lensing Survey (DLS, [7]), and the Faint Sky Variability Survey (FSVS, [28]) whereas large-area surveys, such as the Sloan Digital Sky Survey (SDSS, [56]), the Two Micron All Sky Survey (2MASS, [45]), and the Galaxy Evolution Explorer Survey (GALEX, [33]) have generally *not been synoptic.* In the SN field, the search has been focused on

nearby objects. Projects like the LOSS ([16]), the Nearly SN Factory [4], or the Chilean Automatic Supernova Search (CHASE) [38] have mostly looked for low-z SNe clearly associated with *large, bright, galaxies*.

Only in the last few years the search area has been enlarged to cover wider regions of sky. Current wide-field transient surveys include the Robotic Optical Transient Search Experiment (ROTSE-III; daily covering 1260 deg^2 to R $<$ 17.5, [2]), and the All Sky Automated Survey (ASAS-3; covering 30,000 deg^2 to V $<$ 13.5 during the year, [39]). Furthermore, modern surveys like the *Catalina Real Time Survey* (CRTS, Drake et al. 2009a, 26000 deg^2) have covered the sky irrespective of potential transient targets. As a consequence, the detection of bright events, especially in faint galaxies, has been favored. The large volume monitored (roughly matching the total, past narrow-field, CCD surveys which targeted known galaxies), the high completeness of the sample resulting from a tight cadence and ability to work in the cores of galaxies, along with prompt high S/N spectroscopic follow-up, have made these surveys succesful in discoverying VLSNe.

According to the Padova Asiago SN Catalogue about 722 core-collapse supernovae have been discovered in the last 5 years (2005-2009). Among these, $\sim$14 are VLSNe of the Ic, IIn or IIL (from Table 6.1, excluding the transients discovered by PTF). This means that $\sim$2 % of CCSNe are VLSNe. The brightness of VLSNe is about 10 times higher than a typical CCSN. Being on average a factor of 10 brighter implies that in a magnitude-limited search they would be detectable in a volume larger by a factor of $10^{3/2} \sim 32$ (since volume $\propto r^3$, distance $\propto r^{-2}$). This result suggests that there is a large population of SNe missed by many current SN surveys because they sample a much smaller area. Concerning the absence of detections of VLSNe in the past, it may well be possible that there have been prior detections, but they have remained unpublished mysteries. Quimby et al. [41] note that the blue colors, high peak luminosity, and slow photometric evolution of the transient called PALS-1 [**?**], appears to fit well with the sample.

Indeed, several future large experiments such as the Large Synoptical Survey Telescope (LSST; Ivezic et al. 2008), the Panoramic Survey Telescope and Rapid Response System (PanSTARRS; Hodapp et al. 2004), and SkyMapper (Keller et al. 2007), are set to make a major impact in the near future by covering thousands of square degrees with targets ranging from distant SNe to near-Earth asteroids. VLSNe will represent prime targets for high redshift studies, where their broad light curve at maximum and their UV brightness will make them visible for months to years in the observer frame, strongly interacting with the surrounding environment and thus providing also an opportunity to study the most primitive galaxies, independently from the current GRBs

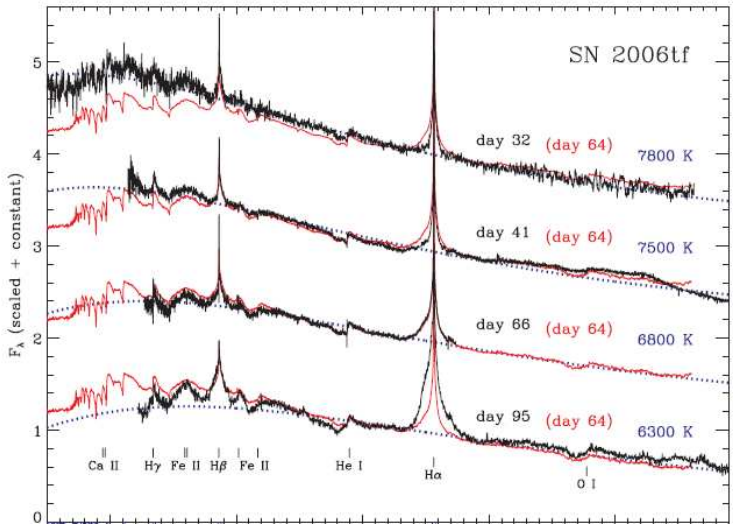

Figure 6.1— Visual-wavelength spectra of SN 2006tf on days 32, 41, 66, and 95, from Smith et al. [46]. The day 64 spectrum (obtained for spectropolarimetry) is plotted in red several times for comparison with the other epochs.

studies.

6.3 On the origin of VLSNe

In order to extend the discussion to a more general interpretation of the data and possibly to shed light on the nature of the VLSNe it is helpful to review the observational properties of the most studied VLSNe, as well as the scenarios that were proposed by the different authors. I will exclude from the review SNe 2006gy, 2007bw and 2007bw, which have been deeply discussed in Chapters 4 and 5.

- **SN 2005ap** is currently the most luminous supernova recorded. The spectra taken by Quimby et al. [40] about 3 days before and 6 days after maximum light show narrow emission lines and absorption lines at a redshift of z = 0.2832 (Fig.6.2), which leads to a peak unfiltered magnitude of -22.7 ± 0.1. Broad P Cygni features corresponding to Ha, C III, N III, and O III are detected with a photospheric velocity of 20000 km s^{-1} . The light curve indicates a 13 week rise to peak followed by a relatively rapid decay, consistent with that of a IIL SN. The host galaxy is a dwarf

SN	Host & Absorption	Type	z	Abs.mag	Notes	Discovery	Reference
SN 2005ap	anon., dwarf galaxy, unextincted	IIL	0.283	−22.7 (unfilt.)	similar to PTF transients	ROTSE-III	[40]
SN 2006gy	NGC 1260, S0/Sa, heavily extincted	IIn	0.019	−22.09 (R)	X-ray and radio faint	ROTSE-III	[48]
SN 2006tf	anon., faint, unextincted	IIn	0.074	−21.01 (R)	weak polarized	ROTSE-III	[46]
SN 2007bi	anon., faint, extincted	Ic	0.128	−21.3 (R)		SN Factory	[21, 57]
SN 2007bt	anon., unextincted	IIn	0.044	−20.66 (R)	in the host outskirts	SN Factory	this thesis, CBET 941
SN 2007bw	anon., faint, unextincted	IIn	0.140	−21.22 (R)		SN Factory	this thesis, CBET 941
SN 2008es	anon., dwarf, faint, unextincted	IIL	0.0202	−21.96 (R)	X-ray faint (XRT)		[35]
SN 2008fz	anon., faint, unextincted	IIn	0.133	−21.79 (R)			[13], this thesis
	PTF transients						
SCP06F6	anon., faint	?	1.189	−23 (u)		PTF	[41]
PTF09atu	unresolved	?	0.501	−22.5 (u)	X-ray faint	PTF	[41]
PTF09cnd	unresolved	?	0.258	−22.7 (u)	X-ray faint	PTF	[41]
PTF09cwl	anon., faint	?	0.349	−22.7 (u)	X-ray faint	PTF	[41]
	CTRS transients						
SN 2008iu	unknown	Ic	?			CRTS	[14]
SN 2009de	unknown	Ic	0.14	−20.1 (unfilt.)		CRTS	[12]
SN 2009mb	unknown	IIn	0.15	−20 (unfilt.)		CRTS	[9]
SN 2009nm	unknown	IIn	0.21	−20.9 (unfilt.)		CRTS	[10]
SN 2008am	anonymous	IIn	0.23	−21.7 (unfilt.)	X-ray and radio faint		[37]

Table 6.1— Updated list of VLSNe.

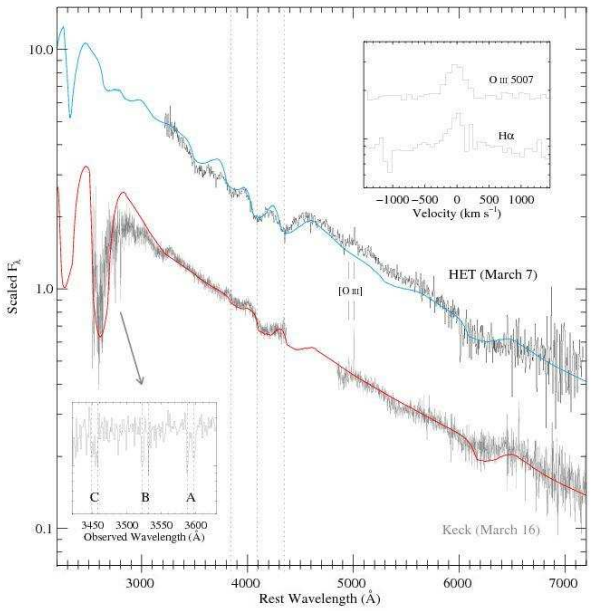

Figure 6.2— Spectrum of SN 2005ap obtained with HET+LRS taken 3 days before maximum light (black curve) and spectrum Keck LRIS data from 6 days after maximum light (gray curve), both from Quimby et al. [40]. The left inset is a detail from the Keck spectra showing three narrow absorption doublets that are identified as intervening Mg II λ2796, 2804 systems. The upper inset shows the narrow Hα and [O III] λ5007 from the Keck data plotted in velocity space.

galaxy 5 magnitudes fainter than the SN at maximum. To account for the brightness of the event, Quimby et al. [40] discuss (for the first time for a VLSN) the possibility that the luminosity arises in the collision of the ejecta with a surrounding, perhaps dense, shell of circumstellar matter (with mass $\sim$1.3 $M_\odot$) shed by a wind or a process like an LBV mass ejection. The hypothesis of a rapid spin-down of a magnetar [32] is also discussed.

- **SN 2006tf** is a IIn supernova and, like SNe 2007bt and 2007bw, it is characterized by prominent Balmer lines on a relatively flat continuum at $\sim$7000 K [46] (Fig.6.1). It is characterized by a slow photometric evolution, which declines by $\sim$1 mag 100^{-1}days. Narrow lines on Hα confirm the presence of a high-velocity CSM ($v \sim 190$ km s^{-1}). Trough a very detailed analysis of line profiles Smith et al. [46] describe SN 2006tf as a

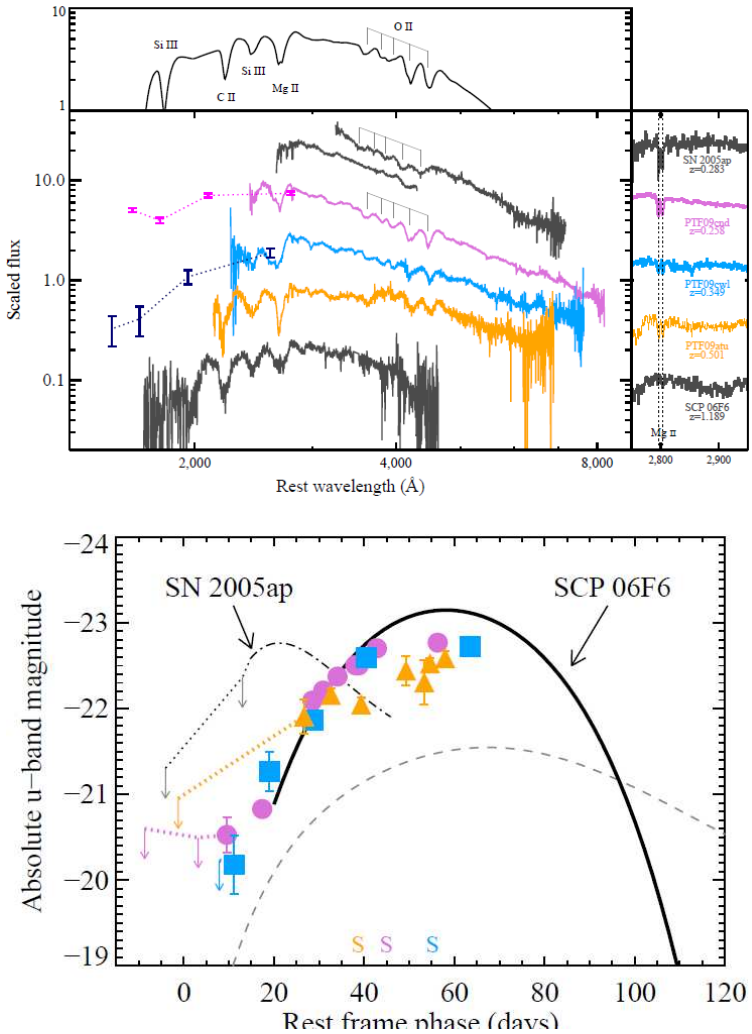

Figure 6.3— *Upper panel*: Spectra of the 2005ap-like sample. From top to bottom: SN2005ap on March 7 and again on March 16 (grey), PTF09cnd on August 25 (purple), PTF09cwl on August 25 (blue), PTF09atu on July 20 (orange), and an average of all three SCP06F6 spectra presented in ref. 9 (grey). Lower panel: luminosity evolution, in the rest frame u-band of the SN2005ap-like sample. Shown are the SCP06F6 transient (solid line), SN2005ap (dash-dot line), PTF09atu (orange triangles), PTF09cnd (purple dots), and PTF09cwl (blue squares) [41].

transition supernova between two regimes: *(1)* a luminous Type IIn supernova powered by emission directly from interaction with circumstellar material, like SN 1994W [11] and *(2)* a more extreme luminous SN where the CSM interaction is so optically thick that energy must diffuse out from an opaque shocked shell [1, 47, 49]. With time the SN evolves from the second to the first regime. The bulk of this luminosity is supposed to originate from the thermalization of the ejecta impinging on a ∼18 $M_\odot$ shell of CSM that was emetted in the ∼4-8 years before core collapse; other 2-6 $M_\odot$ are supposed to be emitted in the decade before that, and are responsible of the presence of the narrow lines.

- **SN 2008es** is defined a IIL SN [24, 35] because of the fast-evolving light curves and the spectroscopic features which are common to SN 1979C [15]. The light curve and the spectral appearance of this SN have been discussed in the previous Chapter in terms of the similarities with SN 2008fz. Concerning the nature of this event, Miller et al. [35] favor the hypothesis that the luminosity is powered by the interaction of the SN blast-wave with a massive circumstellar shell (∼5 $M_\odot$) that was ejected in an episodic eruption [49]. However on this issue Gezari et al. [24] argue that the intermediate-width P-Cygni lines (at a few thousand $\mathrm{km\,s^{-1}}$) which should be produced from the dense post-shock gas and the slow escape of radiation due to photon diffusion of the thermal energy through the opaque shell are not consistent with the broad, symmetric Hα line emission, and relatively fast rise time of SN 2008es. They prefer a model in which the large peak brightness is a consequence of the core collapse of a progenitor star with a low-mass extended hydrogen envelope and a stellar wind of $10^{-3}M_\odot yr^{-1}$, close to the upper limit of the mass-loss rate measured from the lack of an X-ray detection by the Swift X-ray Telescope.

- for **SN 2008fz** a study has already been published by Drake et al. [13]. A light curve in V-magnitudes (converted from unfiltered magnitudes) and three spectra are presented. The authors compare with the light curve and the spectra of SN 2008fz to SN 2006gy; however, they take no preferred position concerning the cause of the SN brightness.

- **SN 2007bi** presents the spectroscopical features of type Ic SNe, with an exceptional brightness at maximum and an unusual slow evolution [21, 57] (Fig.6.4). The reason for this is still controversial; Gal Yam et al. [21] calculate that the light curve of SN 2007bi fits well the evolution expected for the explosion of a star with a He core mass of 100 $M_\odot$.

From the modeling of the nebular spectra they also show that of $> 3\,M_\odot$ of radioactive ^{56}Ni was synthesized during the explosion. They argue that the observations are well fitted by models of pair-instability supernovae, and suggest for SN 2007bi a progenitor with a initial mass in the order of 200 $M_\odot$. Instead, Young et al. [57] consider both a PISN model and an interpretation in terms of a massive (40-60 $M_\odot$) iron-core-collapse supernova of a C+O star [53], slightly favoring the latter.

- **PTF09atu, PTF09cnd, and PTF09cw** are three unexplained, optical transients discovered by PTF [41], whose distance has been estimated thanks to the narrow absorption features of the Mg II $\lambda\lambda$2796, 2803 doublet in the spectra; together with **SCP 06F6** [22] they are currently the most distant VLSNe known. They are characterized by an unprecedented ultra-violet peak luminosity (-23) and by broad ($\sim$ 100 days), bell-like light curves. Spectroscopically they present broad absorption dips toward the blue end of the spectra, which are tentatively identified as O II, Mg II and C II lines. Such absorptions had been found also in SN 2005ap. Lacking any explanation for their exceptional brightness, Quimby et al. [41] argue that both SN 2005ap and the four peculiar transients (i.e., the three PTF transients and SCP 06F6 reveal the death throes of the most massive stars, likely pulsational pair-instability outbursts.

In general, though some evident analogies exist, a unifying scenario which can explain the observational diversity of all VLSNe seems unlikely.

An appealing, simplifying hypothesis is that all VLSNe are linked to the explosion of PISNe (cf. Chapter 3) and that the peak luminosity is mainly sustained by ^{56}Ni . This is also the most natural way to explain the remarkable Co-like luminosity decay found for both the type Ic and IIn SNe, as well as the lack of evidence of CSM in some cases (e.g. SN 2008es). However, the explosion via pair-production is difficult to reconcile with the observed high-velocities spectroscopic lines, which are not expected for extremely massive SN ejecta, and are instead observed in the VLSNe sample, including SN 2007bi. Furthermore, the broad peak which is expected in the light curves of PISNe [44] is not observed for the ^{56}Co-like-decaying VLSNe. This could be due to the late observation of these targets, with respect to their explosion. However the relatively high number of the objects with this features (i.e. 3) make this assumption less likely. On the other hand, the VLSNe which do show a peak in the light curve do not fade consistently with the decay of ^{56}Co.

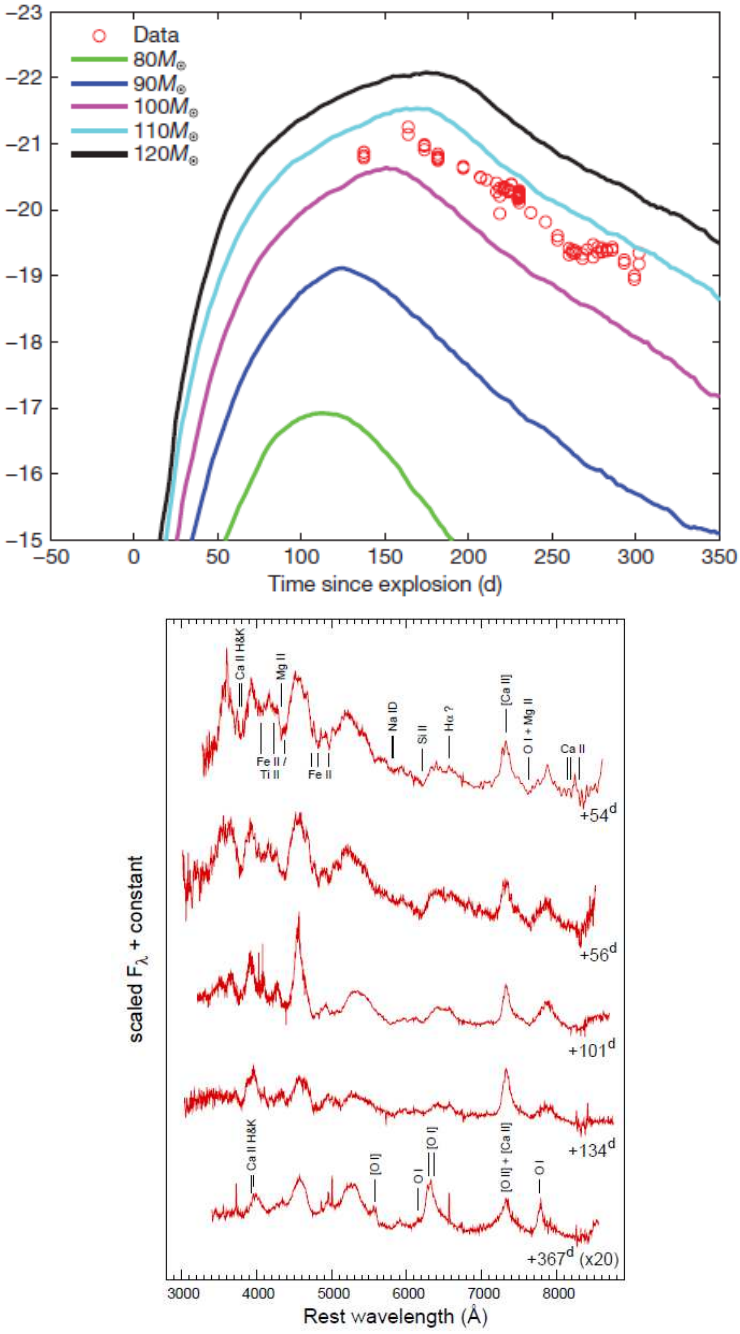

Figure 6.4— *Top:* Comparison of the observations of SN 2007bi with models calculated by Heger & Woosley [26] and Kasen et al. (2008) [30] before the SN discovery. The curves presented are for various helium cores exploding as PISNs. The data are well fitted by 100−110 $M_{\odot}$ models. *Bottom*: Spectral sequence of SN 2007bi, with some elements identified [57].

Another argument against the PISN hypothesis concerns metallicity: the models calculation of Langer et al. [31] allow slowly rotating, H-rich, massive (120-140 $M_\odot$) yellow supergiants with massive He cores to produce PISNe if the metallicity is low enough, i.e. about $Z \sim Z_\odot/3$. For most of the VLSNe in Table 6.1 no information is available in literature about the environment and the hosts. I have mentioned above that the low-luminosity of the hosts-galaxies can be treated as an indicator of low-metallicity. However, there is at least one exception. Among the three VLSNe which have been discussed in Chapter 5, an example of an high luminosity/metallicity galaxy is the host of SN 2007bt. In fact, a rough estimate on the metallicity of the environment can be obtained through the B luminosity, using the relation of Garnett [23] $\log[O/H] = -0.16 M_B - 6.4$, where O and H respectively denote the number densities of atomic O and H. Measuring the B magnitude in a deep image with the SN subtracted provides the *lower limit* $12 + \log\frac{O}{H} \sim 8.37$, which is ∼97% of the Solar metallicity [5], clearly too high to maintain an intact H envelope atop of extremely massive stars as the precursors of PISNe. Note also that Young et al. [57] argue that even for SN 2007bi the metallicity $12 + \log\frac{O}{H} \sim 8.25$ deduced from the host-galaxy absolute luminosity is low, but *not exceptionally low* (such as $Z \sim Z_\odot/1000$), as it is predicted for fast-rotating, H-depleted massive star (∼80 $M_\odot$) which should end their life as PISNe, according to Langer et al. [31].

It should be also stressed that the PISN scenario which is claimed by Gal-Yam et al. [21] for SN 2007bi presents other inconsistencies. First, in the abundances derived from the modeling of the ejecta, the mass of the light elements (Ca, O, Mg) seems to be over-estimated. By adopting the theoretical model output for elements that do not have strong nebular emission in the optical (mostly Si and S, and some Ne and Ar), Gal-Yam et al. [21] calculate an ejected mass of >50 $M_\odot$, which is far too low for an exploding star of with an He-core of 100 $M_\odot$, as derived from the light curve. Also, the estimate of the explosion date is done by fitting the early photometric data, but the uncertainty associated to this estimate is fairly large, in the order of ∼30 days. As a consequence, the late-times luminosity and the ^{56}Ni mass, which is claimed to be even >7 $M_\odot$, could be lower.

Alternatively, a simple Fe-collapse of a massive star could be invoked to produce large quantities of ^{56}Ni , for very energetic explosions. Umeda & Nomoto [53] have calculated the evolution of several very massive stars with the initial masses of M<100 $M_\odot$, $Z \sim Z_\odot/200$ from the main sequence to just before the Fe core collapse. They have found that the >80 $M_\odot$ stars pulsate during the central Si-burning stages. The existence of this stage makes the lifetime

of the stars longer and makes the Fe core grow; this result in a larger ejected ^{56}Ni mass. This effect is highly dependent on the mass and it is larger for the most massive stars, because the density profile of the progenitor is steeper; despite being very high, the explosion energy is instead only a secondary factor. They calculate that for an explosion energy of E$\sim 30 \times 10^{51}$, M(^{56}Ni)$\sim$2.2, 2.3, 5.0, and 6.6 $M_\odot$ can be produced for M$\sim$ 30, 50, 80, and 100 $M_\odot$ stars with a C+O core of 11.4, 19.3, 34.0 and 42.6 $M_\odot$. Therefore, as a byproduct, a large O and C mass is expected in the SN ejecta. Indeed, very intense C and O lines are detected in the spectra of SN 2007bi. This is not true for the IIn and IIL VLSNe, whose emission is dominated by Balmer lines at late epochs. Therefore, this model could not explain the spectra of SNe 2006gy, 200bt, 2007bw and 2008fz (for which we have observed their late-times spectra), unless we require an extremely opaque medium, which prevents the formation of O lines. This is less likely for the most massive C-O cores stars.

Another valid model to explain the luminosity of the VLSNe is the one proposed by Blinnikov & Bartunov [8] for IIL supernovae. The model predicts that a RSG star with an extended structure ($\sim 6000\,R_\odot$), a small H mass and a dense superwind (up to $10^{-3} M_\odot\,yr^{-1}$) can reproduce a linearly decaying light curve with a peak up to -22 (Fig. 6.5). The unusual brightness is naturally explained as the reradiation of ultraviolet photons, created at the shock breakout, in the superwind shell surrouding the exploding star; no large ejected ^{56}Ni quantity is required. The model predicts a steep drop in the luminosity after day 50, when the recombination reaches the Si core. After that the light curve is powered by radioactive decay or eventually by CSM interaction.

This scenario explains the absence of the absorption component in Hα , which is due to the fact that at late stages the temperature inside the dense envelope is lower than the shock wave temperature. However, as mentioned in Chapter 4, the model fails to explain the expansion of the radius which is measured for the SNe 2008fz and 2008es. It also predicts a *rapid* rise prior to maximum, which depends on the central condensation of the supernova envelope; it may be as short as 5 days for centrally condensed models and about 20-30 days for more uniform supergiant envelopes. Such time-scales are shorter than what was estimated for SN 2008fz and than what was observed for SN 2006gy.

For the SNe 2006tf, 2007bt and 2007bw no peak was detected. Even if the rise to maximum was extremely short as predicted by the Blinnikov & Bartunov [8] model, we must account for another energy source to explain the slow-luminosity decay of their light curves.

Young et al. find the values for the radius and superwind of the Blinnikov & Bartunov [8] model unrealistic, and prefer for SN 1979C a scenario in which a hydrogen-rich massive star core collapses, via jet explosion that punctures through the star and initiates a shock that ejects the hydrogen-rich envelope. The jet is supposed to be responsible for a low-density high-energy ejecta; it contains enough energy to create an asymmetric shock wave that ejects the He core and the overlying H envelope. The authors also suggest that the energy of the jet could be dissipated by the hydrogen envelope and thus not cause the ejecta to expand with the high velocities typically seen in Type Ic supernovae associated with GRBs.

This scenario could link the VLSNe to the hypernovae without any associated GRB, and thus explain the common environment in which both energetic transients are mostly found. Note that the association of luminous IIn SNe to GRBs is not unprecented (cf. SNe 1997cy and 1999E, [42, 51]). However, the ^{56}Ni quantities that are inferred to VLSNe 2006tf, 2007bt, 2007bw are sensibly higher than the highest quantities that were measured in hypernovae [34].

Gezari et al. [24] also argue that, in this scenario, the optical afterglow emission produced from the external shocks created by the interaction of the relativistic jet with the H envelope will emit non-thermal synchotron radiation, which is in contraddiction with the cooling blackbody spectral energy distribution measured for SN 2008es. However, this is not true if we let the jet interact with *an extremely opaque, H-rich CSM*, rather than a H envelope, as supposed for the IIn VLSNe in Chapter 5. In that case we do expect that the thermalization of the jet produces a black-body emission.

Another reasonable way to produce a luminous burst occurs via *pulsational pair instability* inside the core, as suggested by Woosley, Blinnikov and Heger [55]. As already explained in Chapter 4, the collision between shells produced during different outbursts can energize a variety of explosive phenomena with a SN display (of the type I or II, but also SN impostors) with characteristic timescales ranging from days to centuries. Contrary to PISNe, for such stars the low metallicity environment is not a tight requirement, which turns out to be consistent with the values found for some of the VLSNe.

In general, the heavy ejections of matter via pair-instability could explain the brightness of the H-rich VLSNe. An eventual detection of a past or future heavy outburst in one VLSN could likely prove this scenario. The photometric and spectroscopic analogies that we have highlighted in this thesis would favor the existence of a limited range of parameters (CSM mass, distance and configuration) to produce the observed data.

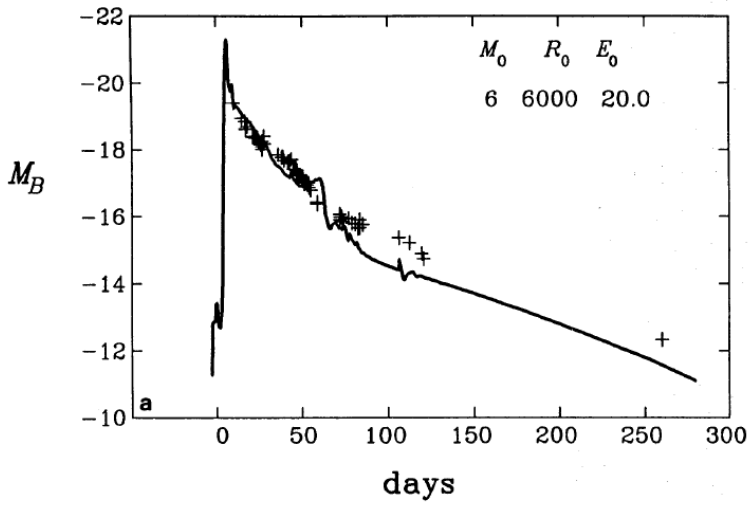

Figure 6.5— Modeling for the light curve resulting from the explosion of a star with radius $R_0 \sim 6000\,R_\odot$, explosion energy 2×10^{51}erg, $M_0 \sim 6\,M_\odot$, $M_H \sim 3.1\,M_\odot$ and $M_{Ni} \sim 0.2\,M_\odot$ [8]. Also plotted is the light curve from SN 1979C.

Finally, Kasen et al. [29] and Woosley et al. [54] find an excellent agreement (Fig.6.6) between the light curves of SNe 2008es and 2007bi and the modeled light curve which would be produced by the energy deposited into an expanding supernova remnant by a highly magnetic ($B \sim 5 \times 10^{14}$G), rapidly rotating (i.e. magnetar spin < 5 ms) neutron star (or *rapidly rotating magnetar*). Through numerical radiation hydrodynamical calculations they show that the magnetar input also produces a central bubble which sweeps the ejecta into an internal dense shell, resulting in a prolonged period of nearly constant photospheric velocity in the observed spectra. This is indeed consistent with the nearly constant velocities detected for the VLSNe sample. Kasen et al. [29] also claims that the predicted statistics of magnetars, i.e. a few percent of all core collapse supernovae, is in agreement with the statistics of the brightest events with $L \sim 10^{44}\mathrm{erg\,s^{-1}}$. But in this thesis we have enlarged the sample of VLSNe and listed the new recent discoveries (Table 6.1), showing that such brightest events are more frequent than what was thought, apparently more than the predicted frequency of magnetars.

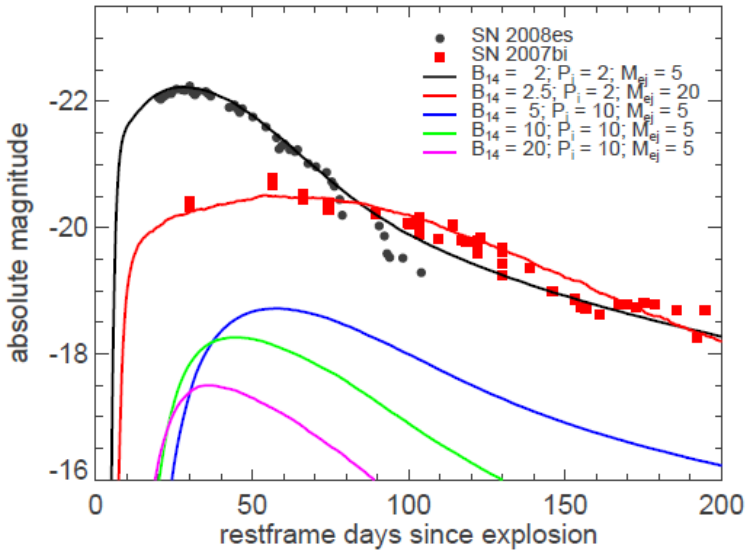

Figure 6.6— Bolometric light curve calculations of magnetar energized supernovae compared to observed events [29]. Black circles show V-band observations of the luminous Type IIL SN2008es [24] with an assumed rise time of 25 days. Red squares show R-band observations of the Type Ic SN 2007bi [21] with an assumed rise time of 50 days.

6.4 Final remarks

In this thesis I have tried to explain the evolution of the light curve and spectra of a sample of 4 VLSNe through a similar star+CSM configuration, mainly varying the H mass, and possibly, the clumpiness in the CSM. Combining the energy of an energetic SN to that produced by the impact with a CSM has the advantage of not requiring any exotic explosion mechanism, a supermassive star (M >>100 $M_{\odot}$) nor an extremely large quantity of ^{56}Ni .

Concerning the SN progenitor, only in the case of SN 2006gy the early photometric evolution could be explained with the expansion of a compact star, whose radius and mass have been derived through the modeling. For SNe 2007bt and 2007bw the remarkable emission profile of the Hα line has been interpreted with an asymmetric configuration of the CSM, i.e. a massive clump lying in the direction of the observer. This is also in agreement with what was derived by the semi-analytical code for the impact energy in SN 2006gy: the results have shown that the clumps likely do not cover the whole solid angle around the SN, but only a limited fraction of it. Indeed the role of winds around

massive stars in the local universe are poorly known. The wind velocity that we have measured for SN 200bt is -as in SNe 2006gy and 2006tf- consistent with the wind velocities of Lumimous Blue Variable stars like ηCarinae. Multiband observations of ηCarinae have proved that the distribution of the mass ejected in the star's frequent outbursts is all but homogeneous [**?**]. Though stellar evolution theory do not allow the explosion of massive stars with the H envelope intact, recent observations seem to favor the contrary [20, 27]. Recently, the progenitor of IIn SN 2005gl has been serendipitously identified for the first time by Gal-Yam et al. [19].

Regarding the energy powering the ejecta, more than one among the afore-discussed hypothesis is possible (i.e., pulsation via pair production, GRB jet, magnetar, simple core-collapse etc.). Given the theoretical uncertainties on the evolutionary paths of massive stars and the practical difficulties in the reproducing a SN display dominated by a CSM with an unknown geometry and complex physical configuration, a deeper study and much more time would be required to clarify these issues.

Anyway, it is interesting to note that an energetic SN like SN 2007bi would perfecty match the progenitor of SN 2006gy, acting like the "engine" of luminosity which powers the event.

In general, what is common to the H-dominated VLSNe sample is that a *strong mass-loss rate*, and a *short time between last outburst and explosion* are crucial requirements to explain their brightness and spectral features.

Instead, for SN 2007bi and the transients detected by Quimby et al. [41] the lack of evidence of CSM in the spectra forces to consider an energetic SN, and this leads to look for non-ordinary explosion mechanisms. This field has been explored only very recently, and we are still far from finding a unique solution which is able to explain the diversity of the considered cases. Nevertheless, determining the main observational properties of these peculiar transients represents an important step in the right direction.

Neglecting for a moment the issues of the explosion mechanism and of the source of the peak brightness, we can try to build subgroups of VLSNe with similar observational properties, using the H mass of the CSM as a discriminating parameter:

A The slow evolution found for the group composed by SNe 2006gy, 2006tf, 2007bt and 2007bw points towards a massive H-rich medium (*in the order of* $\sim$*10* $M_{\odot}$), that could be either fragmented into big, massive clumps covering a limited angle around the star (cf. SN 2006gy [1]), or homoge-

neously distributed in a shell all around the star (cf. SN 2006tf [46]). For a sufficiently large mass and photon diffusion time, the dense H-rich CSM would enable a slow luminosity decline at late times. For these events the velocities extend in the range 7500-12000 $\mathrm{km\,s^{-1}}$;

B The fast evolving spectra and the steep light curves of SNe 2008es and 2008fz favor a progenitor which has ejected a lower amount of H (*in the order of* $\sim$*1* $\mathrm{M_\odot}$) and -though lower limits are uncertain- a modest amount of ^{56}Ni . Also in this case the H could be uniformly distributed in a dense clumpy medium even obscuring the SN behind;

C Both the VLSN 2007bi, 2005ap and the group of transients detected by Quimby et al. (2009) [41] are evidently associated with a progenitor that was depleted by its H envelope long before the explosion. The spectra of SN 2007bi show high velocities (12000 $\mathrm{km\,s^{-1}}$) [21] which, however, are not as fast as hypernovae. For the PTF transients the highest velocities are $\sim$7000 $\mathrm{km\,s^{-1}}$ [41].

Currently, radioactive decay of ^{56}Ni seems to be the most plausible hypothesis for both kind of events.

In general, the number of VLSNe is rapidly growing at low and intermediate redshift, which may indicate that we are not dealing with extremely exotic events. Moreover, the evident analogies that I have emphasized in this work are encouraging. These extreme transients represent a precious opportunity to understand the final evolutionary stages of very massive stars, which are still poorly known. Despite the theoretical uncertainties, tight constraints can be derived through the observations. Understanding the role of interaction and how it makes itself visible on the light curves and spectra will be a primary concern.

Bibliography

[1] I. Agnoletto, S. Benetti, E. Cappellaro, L. Zampieri, M. Turatto, P. Mazzali, A. Pastorello, M. D. Valle, F. Bufano, A. Harutyunyan, H. Navasardyan, N. Elias-Rosa, S. Taubenberger, S. Spiro, and S. Valenti. SN 2006gy: Was it Really Extraordinary? *Apj*, 691:1348–1359, February 2009.

[2] C. Akerlof, S. Amrose, R. Balsano, J. Bloch, D. Casperson, S. Fletcher, G. Gisler, J. Hills, R. Kehoe, B. Lee, S. Marshall, T. McKay, A. Pawl, J. Schaefer, J. Szymanski, and J. Wren. ROTSE All-Sky Surveys for Variable Stars. I. Test Fields. *Aj*, 119:1901–1913, April 2000.

[3] C. Alcock, R. A. Allsman, D. R. Alves, T. S. Axelrod, A. C. Becker, D. P. Bennett, K. H. Cook, A. J. Drake, K. C. Freeman, M. Geha, K. Griest, M. J. Lehner, S. L. Marshall, D. Minniti, C. A. Nelson, B. A. Peterson, P. Popowski, M. R. Pratt, P. J. Quinn, C. W. Stubbs, W. Sutherland, A. B. Tomaney, T. Vandehei, and D. L. Welch. The MACHO Project: Microlensing Optical Depth toward the Galactic Bulge from Difference Image Analysis. *Apj*, 541:734–766, October 2000.

[4] G. Aldering, G. Adam, P. Antilogus, P. Astier, R. Bacon, S. Bongard, C. Bonnaud, Y. Copin, D. Hardin, F. Henault, D. A. Howell, J.-P. Lemonnier, J.-M. Levy, S. C. Loken, P. E. Nugent, R. Pain, A. Pecontal, E. Pecontal, S. Perlmutter, R. M. Quimby, K. Schahmaneche, G. Smadja, and W. M. Wood-Vasey. Overview of the Nearby Supernova Factory. In J. A. Tyson & S. Wolff, editor, *Society of Photo-Optical Instrumentation Engineers (SPIE) Conference Series*, volume 4836 of *Presented at the Society of Photo-Optical Instrumentation Engineers (SPIE) Conference*, pages 61–72, December 2002.

[5] M. Asplund, N. Grevesse, A. J. Sauval, C. Allende Prieto, and D. Kiselman. Line formation in solar granulation. IV. [O I], O I and OH lines and the photospheric O abundance. *Aap*, 417:751–768, April 2004.

[6] E. Aubourg, P. Bareyre, S. Brehin, M. Gros, J. de Kat, M. Lachieze-Rey, B. Laurent, E. Lesquoy, C. Magneville, A. Milsztajn, L. Moscoso, F. Queinnec, C. Renault, J. Rich, M. Spiro, L. Vigroux, S. Zylberajch, R. Ansari, F. Cavalier, M. Moniez, J.-P. Beaulieu, R. Ferlet, P. Grison, A. Vidal-Madjar, J. Guibert, O. Moreau, F. Tajahmady, E. Maurice, L. Prevot, and C. Gry. Search for very low-mass objects in the Galactic Halo. *Aap*, 301:1–+, September 1995.

[7] A. C. Becker, A. Rest, G. Miknaitis, R. C. Smith, and C. Stubbs. LSST : Image Subtraction Transient Detection Techniques. In *Bulletin of the American Astronomical Society*, volume 36 of *Bulletin of the American Astronomical Society*, pages 1529–+, December 2004.

[8] S. I. Blinnikov and O. S. Bartunov. Non-Equilibrium Radiative Transfer in Supernova Theory - Models of Linear Type-II Supernovae. *Aap*, 273:106–+, June 1993.

[9] E. Christensen, A. J. Drake, S. G. Djorgovski, A. Mahabal, M. J. Graham, R. Williams, M. Catelan, E. C. Beshore, and S. M. Larson. Super-

novae 2009lz, 2009ma, and 2009mb. *Central Bureau Electronic Telegrams*, 2059:1–+, November 2009.

[10] E. Christensen, A. J. Drake, S. G. Djorgovski, A. Mahabal, M. J. Graham, R. Williams, M. Catelan, E. C. Beshore, and S. M. Larson. Supernovae 2009nl and 2009nm. *Central Bureau Electronic Telegrams*, 2106:1–+, December 2009.

[11] N. N. Chugai, S. I. Blinnikov, R. J. Cumming, P. Lundqvist, A. Bragaglia, A. V. Filippenko, D. C. Leonard, T. Matheson, and J. Sollerman. The Type IIn supernova 1994W: evidence for the explosive ejection of a circumstellar envelope. *Mnras*, 352:1213–1231, August 2004.

[12] A. J. Drake, S. G. Djorgovski, A. Mahabal, R. Williams, M. J. Graham, M. Catelan, E. C. Beshore, S. M. Larson, and E. Christensen. Supernovae 2008iw, 2008ix, 2009bx, and 2009de-2009dk. *Central Bureau Electronic Telegrams*, 1766:1–+, April 2009.

[13] A. J. Drake, S. G. Djorgovski, J. L. Prieto, A. Mahabal, D. Balam, R. Williams, M. J. Graham, M. Catelan, E. Beshore, and S. Larson. Discovery of the Extremely Energetic Supernova 2008fz. *ArXiv e-prints*, August 2009.

[14] A. J. Drake, S. G. Djorgovski, R. Williams, A. Mahabal, M. J. Graham, M. Catelan, E. C. Beshore, and S. M. Larson. Supernovae 2008iu and 2008iv. *Central Bureau Electronic Telegrams*, 1681:1–+, February 2009.

[15] R. A. Fesen and D. M. Matonick. The optical recovery of SN 1979C in NGC 4321 (M100). *Apj*, 407:110–114, April 1993.

[16] A. V. Filippenko, W. D. Li, R. R. Treffers, and M. Modjaz. The Lick Observatory Supernova Search with the Katzman Automatic Imaging Telescope. In B. Paczynski, W.-P. Chen, & C. Lemme, editor, *IAU Colloq. 183: Small Telescope Astronomy on Global Scales*, volume 246 of *Astronomical Society of the Pacific Conference Series*, pages 121–+, 2001.

[17] D. A. Forbes, P. Sánchez-Blázquez, and R. Proctor. The correlation of metallicity gradient with galaxy mass. *Mnras*, 361:L6–L9, July 2005.

[18] A. S. Fruchter, A. J. Levan, L. Strolger, P. M. Vreeswijk, S. E. Thorsett, D. Bersier, I. Burud, J. M. Castro Cerón, A. J. Castro-Tirado, C. Conselice, T. Dahlen, H. C. Ferguson, J. P. U. Fynbo, P. M. Garnavich, R. A.

Gibbons, J. Gorosabel, T. R. Gull, J. Hjorth, S. T. Holland, C. Kouveliotou, Z. Levay, M. Livio, M. R. Metzger, P. E. Nugent, L. Petro, E. Pian, J. E. Rhoads, A. G. Riess, K. C. Sahu, A. Smette, N. R. Tanvir, R. A. M. J. Wijers, and S. E. Woosley. Long γ-ray bursts and core-collapse supernovae have different environments. *Nature*, 441:463–468, May 2006.

[19] A. Gal-Yam and D. C. Leonard. A massive hypergiant star as the progenitor of the supernova SN 2005gl. *Nature*, 458:865–867, April 2009.

[20] A. Gal-Yam, D. C. Leonard, D. B. Fox, S. B. Cenko, A. M. Soderberg, D.-S. Moon, D. J. Sand, W. Li, A. V. Filippenko, G. Aldering, and Y. Copin. On the Progenitor of SN 2005gl and the Nature of Type IIn Supernovae. *Apj*, 656:372–381, February 2007.

[21] A. Gal-Yam, P. Mazzali, E. O. Ofek, P. E. Nugent, S. R. Kulkarni, M. M. Kasliwal, R. M. Quimby, A. V. Filippenko, S. B. Cenko, R. Chornock, R. Waldman, D. Kasen, M. Sullivan, E. C. Beshore, A. J. Drake, R. C. Thomas, J. S. Bloom, D. Poznanski, A. A. Miller, R. J. Foley, J. M. Silverman, I. Arcavi, R. S. Ellis, and J. Deng. Supernova 2007bi as a pair-instability explosion. *Nature*, 462:624–627, December 2009.

[22] B. T. Gänsicke, A. J. Levan, T. R. Marsh, and P. J. Wheatley. SCP 06F6: A Carbon-rich Extragalactic Transient at Redshift z sime 0.14? *Apjl*, 697:L129–L132, June 2009.

[23] D. R. Garnett. The Luminosity-Metallicity Relation, Effective Yields, and Metal Loss in Spiral and Irregular Galaxies. *Apj*, 581:1019–1031, December 2002.

[24] S. Gezari, J. P. Halpern, D. Grupe, F. Yuan, R. Quimby, T. McKay, D. Chamarro, M. D. Sisson, C. Akerlof, J. C. Wheeler, P. J. Brown, S. B. Cenko, A. Rau, J. O. Djordjevic, and D. M. Terndrup. Discovery of the Ultra-Bright Type II-L Supernova 2008es. *Apj*, 690:1313–1321, January 2009.

[25] A. Heger, C. L. Fryer, S. E. Woosley, N. Langer, and D. H. Hartmann. How Massive Single Stars End Their Life. *Apj*, 591:288–300, July 2003.

[26] A. Heger, S. Woosley, I. Baraffe, and T. Abel. Evolution and Explosion of Very Massive Primordial Stars. In M. Gilfanov, R. Sunyeav, & E. Churazov, editor, *Lighthouses of the Universe: The Most Luminous Celestial Objects and Their Use for Cosmology*, pages 369–+, 2002.

[27] J. L. Hoffman, D. C. Leonard, R. Chornock, A. V. Filippenko, A. J. Barth, and T. Matheson. The Dual-Axis Circumstellar Environment of the Type IIn Supernova 1997eg. *Apj*, 688:1186–1209, December 2008.

[28] M. E. Huber, M. E. Everett, and S. B. Howell. Color and Variability Characteristics of Point Sources in the Faint Sky Variability Survey. *Aj*, 132:633–649, August 2006.

[29] D. Kasen and L. Bildsten. Supernova Light Curves Powered by Young Magnetars. *ArXiv e-prints*, November 2009.

[30] D. Kasen, A. Heger, and S. Woosley. The First Stellar Explosions: Theoretical Light Curves and Spectra of Pair-Instability Supernovae. In B. W. O'Shea & A. Heger, editor, *First Stars III*, volume 990 of *American Institute of Physics Conference Series*, pages 263–267, March 2008.

[31] N. Langer, C. A. Norman, A. de Koter, J. S. Vink, M. Cantiello, and S.-C. Yoon. Pair creation supernovae at low and high redshift. *Aap*, 475:L19–L23, November 2007.

[32] K. Maeda, M. Tanaka, K. Nomoto, N. Tominaga, K. Kawabata, P. A. Mazzali, H. Umeda, T. Suzuki, and T. Hattori. The Unique Type Ib Supernova 2005bf at Nebular Phases: A Possible Birth Event of a Strongly Magnetized Neutron Star. *Apj*, 666:1069–1082, September 2007.

[33] C. Martin and GALEX Science Team. The Galaxy Evolution Explorer. In *Bulletin of the American Astronomical Society*, volume 33 of *Bulletin of the American Astronomical Society*, pages 889–+, May 2001.

[34] P. A. Mazzali, F. K. Röpke, S. Benetti, and W. Hillebrandt. A Common Explosion Mechanism for Type Ia Supernovae. *Science*, 315:825–, February 2007.

[35] A. A. Miller, R. Chornock, D. A. Perley, M. Ganeshalingam, W. Li, N. R. Butler, J. S. Bloom, N. Smith, M. Modjaz, D. Poznanski, A. V. Filippenko, C. V. Griffith, J. H. Shiode, and J. M. Silverman. The Exceptionally Luminous Type II-Linear Supernova 2008es. *Apj*, 690:1303–1312, January 2009.

[36] T. Morokuma, M. Doi, N. Yasuda, M. Akiyama, K. Sekiguchi, H. Furusawa, Y. Ueda, T. Totani, T. Oda, T. Nagao, N. Kashikawa, T. Murayama, M. Ouchi, M. G. Watson, M. W. Richmond, C. Lidman, S. Perlmutter, A. L. Spadafora, G. Aldering, L. Wang, I. M. Hook, and R. A. Knop. The

Subaru/XMM-Newton Deep Survey (SXDS). V. Optically Faint Variable Object Survey. *Apj*, 676:163–183, March 2008.

[37] E. Ofek, J. S. Bloom, R. J. Foley, M. Modjaz, and A. A. Miller. Supernova 2008am. *Central Bureau Electronic Telegrams*, 1262:3–+, February 2008.

[38] G. Pignata, J. Maza, R. Antezana, R. Cartier, G. Folatelli, F. Forster, L. Gonzalez, P. Gonzalez, M. Hamuy, D. Iturra, P. Lopez, S. Silva, B. Conuel, A. Crain, D. Foster, K. Ivarsen, A. Lacluyze, M. Nysewander, and D. Reichart. The CHilean Automatic Supernova sEarch (CHASE). In G. Giobbi, A. Tornambe, G. Raimondo, M. Limongi, L. A. Antonelli, N. Menci, & E. Brocato, editor, *American Institute of Physics Conference Series*, volume 1111 of *American Institute of Physics Conference Series*, pages 551–554, May 2009.

[39] G. Pojmański. The All Sky Automated Survey (ASAS-3) System - Its Operation and Preliminary Data. In B. Paczynski, W.-P. Chen, & C. Lemme, editor, *IAU Colloq. 183: Small Telescope Astronomy on Global Scales*, volume 246 of *Astronomical Society of the Pacific Conference Series*, pages 53–+, 2001.

[40] R. M. Quimby, G. Aldering, J. C. Wheeler, P. Höflich, C. W. Akerlof, and E. S. Rykoff. SN 2005ap: A Most Brilliant Explosion. *Apjl*, 668:L99–L102, October 2007.

[41] R. M. Quimby, S. R. Kulkarni, M. M. Kasliwal, A. Gal-Yam, I. Arcavi, M. Sullivan, P. Nugent, R. Thomas, D. A. Howell, L. Bildsten, J. S. Bloom, C. Theissen, N. Law, R. Dekany, G. Rahmer, D. Hale, R. Smith, E. O. Ofek, J. Zolkower, V. Velur, R. Walters, J. Henning, K. Bui, D. McKenna, D. Poznanski, S. B. Cenko, and D. Levitan. Mysterious transients unmasked as the bright blue death throes of massive stars. *ArXiv e-prints*, September 2009.

[42] L. Rigon, M. Turatto, S. Benetti, A. Pastorello, E. Cappellaro, I. Aretxaga, O. Vega, V. Chavushyan, F. Patat, I. J. Danziger, and M. Salvo. SN 1999E: another piece in the supernova-gamma-ray burst connection puzzle. *Mnras*, 340:191–196, March 2003.

[43] S. Savaglio. Low-Mass and Metal-Poor Gamma-Ray Burst Host Galaxies. In L. K. Hunt, S. Madden, & R. Schneider, editor, *IAU Symposium*, volume 255 of *IAU Symposium*, pages 204–211, December 2008.

[44] E. Scannapieco, P. Madau, S. Woosley, A. Heger, and A. Ferrara. The Detectability of Pair-Production Supernovae at z = 6. *Apj*, 633:1031–1041, November 2005.

[45] M. F. Skrutskie, R. M. Cutri, R. Stiening, M. D. Weinberg, S. Schneider, J. M. Carpenter, C. Beichman, R. Capps, T. Chester, J. Elias, J. Huchra, J. Liebert, C. Lonsdale, D. G. Monet, S. Price, P. Seitzer, T. Jarrett, J. D. Kirkpatrick, J. E. Gizis, E. Howard, T. Evans, J. Fowler, L. Fullmer, R. Hurt, R. Light, E. L. Kopan, K. A. Marsh, H. L. McCallon, R. Tam, S. Van Dyk, and S. Wheelock. The Two Micron All Sky Survey (2MASS). *Aj*, 131:1163–1183, February 2006.

[46] N. Smith, R. Chornock, W. Li, M. Ganeshalingam, J. M. Silverman, R. J. Foley, A. V. Filippenko, and A. J. Barth. SN 2006tf: Precursor Eruptions and the Optically Thick Regime of Extremely Luminous Type IIn Supernovae. *Apj*, 686:467–484, October 2008.

[47] N. Smith, R. Chornock, J. M. Silverman, A. V. Filippenko, and R. J. Foley. Spectral Evolution of the Extraordinary Type IIn Supernova 2006gy. *ArXiv e-prints*, June 2009.

[48] N. Smith, W. Li, R. J. Foley, J. C. Wheeler, D. Pooley, R. Chornock, A. V. Filippenko, J. M. Silverman, R. Quimby, J. S. Bloom, and C. Hansen. SN 2006gy: Discovery of the Most Luminous Supernova Ever Recorded, Powered by the Death of an Extremely Massive Star like η Carinae. *Apj*, 666:1116–1128, September 2007.

[49] N. Smith and R. McCray. Shell-shocked Diffusion Model for the Light Curve of SN 2006gy. *Apjl*, 671:L17–L20, December 2007.

[50] M. Spolaor, R. N. Proctor, D. A. Forbes, and W. J. Couch. The Mass-Metallicity Gradient Relation of Early-Type Galaxies. *Apjl*, 691:L138–L141, February 2009.

[51] M. Turatto, T. Suzuki, P. A. Mazzali, S. Benetti, E. Cappellaro, I. J. Danziger, K. Nomoto, T. Nakamura, T. R. Young, and F. Patat. The Properties of Supernova 1997CY Associated with GRB 970514. *Apjl*, 534:L57–L61, May 2000.

[52] A. Udalski, M. Szymanski, J. Kaluzny, M. Kubiak, M. Mateo, and W. Krzeminski. The optical gravitational lensing experiment: The discovery of three further microlensing events in the direction of the galactic bulge. *Apjl*, 426:L69+, May 1994.

[53] H. Umeda and K. Nomoto. How Much Ni Can Be Produced in Core-Collapse Supernovae? Evolution and Explosions of 30-100 $M_{\odot}$ Stars. *Apj*, 673:1014–1022, February 2008.

[54] S. E. Woosley. Bright Supernovae from Magnetar Birth. *ArXiv e-prints*, November 2009.

[55] S. E. Woosley, S. Blinnikov, and A. Heger. Pulsational pair instability as an explanation for the most luminous supernovae. *Nature*, 450:390–392, November 2007.

[56] D. G. York, J. Adelman, J. E. Anderson, Jr., S. F. Anderson, J. Annis, N. A. Bahcall, J. A. Bakken, R. Barkhouser, S. Bastian, E. Berman, W. N. Boroski, S. Bracker, C. Briegel, J. W. Briggs, J. Brinkmann, R. Brunner, S. Burles, L. Carey, M. A. Carr, F. J. Castander, B. Chen, P. L. Colestock, A. J. Connolly, J. H. Crocker, I. Csabai, P. C. Czarapata, J. E. Davis, M. Doi, T. Dombeck, D. Eisenstein, N. Ellman, B. R. Elms, M. L. Evans, X. Fan, G. R. Federwitz, L. Fiscelli, S. Friedman, J. A. Frieman, M. Fukugita, B. Gillespie, J. E. Gunn, V. K. Gurbani, E. de Haas, M. Haldeman, F. H. Harris, J. Hayes, T. M. Heckman, G. S. Hennessy, R. B. Hindsley, S. Holm, D. J. Holmgren, C.-h. Huang, C. Hull, D. Husby, S.-I. Ichikawa, T. Ichikawa, Ž. Ivezić, S. Kent, R. S. J. Kim, E. Kinney, M. Klaene, A. N. Kleinman, S. Kleinman, G. R. Knapp, J. Korienek, R. G. Kron, P. Z. Kunszt, D. Q. Lamb, B. Lee, R. F. Leger, S. Limmongkol, C. Lindenmeyer, D. C. Long, C. Loomis, J. Loveday, R. Lucinio, R. H. Lupton, B. MacKinnon, E. J. Mannery, P. M. Mantsch, B. Margon, P. McGehee, T. A. McKay, A. Meiksin, A. Merelli, D. G. Monet, J. A. Munn, V. K. Narayanan, T. Nash, E. Neilsen, R. Neswold, H. J. Newberg, R. C. Nichol, T. Nicinski, M. Nonino, N. Okada, S. Okamura, J. P. Ostriker, R. Owen, A. G. Pauls, J. Peoples, R. L. Peterson, D. Petravick, J. R. Pier, A. Pope, R. Pordes, A. Prosapio, R. Rechenmacher, T. R. Quinn, G. T. Richards, M. W. Richmond, C. H. Rivetta, C. M. Rockosi, K. Ruthmansdorfer, D. Sandford, D. J. Schlegel, D. P. Schneider, M. Sekiguchi, G. Sergey, K. Shimasaku, W. A. Siegmund, S. Smee, J. A. Smith, S. Snedden, R. Stone, C. Stoughton, M. A. Strauss, C. Stubbs, M. SubbaRao, A. S. Szalay, I. Szapudi, G. P. Szokoly, A. R. Thakar, C. Tremonti, D. L. Tucker, A. Uomoto, D. Vanden Berk, M. S. Vogeley, P. Waddell, S.-i. Wang, M. Watanabe, D. H. Weinberg, B. Yanny, and N. Yasuda. The Sloan Digital Sky Survey: Technical Summary. *Aj*, 120:1579–1587, September 2000.

[57] D. R. Young, S. J. Smartt, S. Valenti, A. Pastorello, S. Benetti, C. R. Benn, D. Bersier, M. T. Botticella, R. L. M. Corradi, A. H. Harutyunyan, M. Hrudkova, I. Hunter, S. Mattila, E. J. W. de Mooij, H. Navasardyan, I. A. G. Snellen, N. R. Tanvir, and L. Zampieri. Two Type Ic supernovae in low-metallicity, dwarf galaxies: diversity of explosions. *ArXiv e-prints*, October 2009.